PLATELET SIGNALING IN HEMOSTASIS AND VASCULAR INFLAMMATION

By

Anh Tran Phuong Ngo

A DISSERTATION

Presented to the Department of Biomedical Engineering

Of the Oregon Health & Science University

School of Medicine

In partial fulfillment of the requirements for the degree of

Doctor of Philosophy

In Biomedical Engineering

October 2020

Department of Biomedical Engineering
School of Medicine
Oregon Health & Science University

CERTIFICATE OF APPROVAL

This is to certify that the Ph.D. Dissertation of

Anh Tran Phuong Ngo

"Platelet Signaling in Hemostasis and Vascular Inflammation"

has been approved

Mentor: Owen J. T. McCarty, Ph.D.
Professor of Biomedical Engineering

Member/Chair: David H. Farrell, Ph.D.
Professor of Surgery

Member: Show-Ling Shyng, Ph.D.
Professor of Chemical Physiology and Biochemistry

Member: Anthony P. Barnes, Ph.D.
Assistant Professor of Medicine

Member: David Zonies, M.D.
Professor of Surgery

Dành cho Ngoại và Mẹ…

…Những người luôn yêu thương con hơn chính bản thân mình

Acknowledgements

Special thanks to Dr. Owen J.T. McCarty for being a mentor and a friend. Thank you for teaching me the patience that comes with science as well as long-distance hiking. Thank you for encouraging me to reach new limits and to never settle for anything less than superb! Most importantly, thank you for always having my back.

Thank you, Dr. Joseph E. Aslan, for introducing me to the intricate world of platelets, and for always making time for me when I needed help the most. I will miss your “see ya!” at the end of every lab day.

I thank Dr. Cristina Puy for her wisdom and patience in showing me how fascinating the coagulation system is. Thank you for teaching me work-life balance and how to be confident in myself. I will miss how I can just turn around at my desk and Cristina is always there for me.

I thank Stéphanie Reitsma for being an awesome colleague, a sister, a friend and for making me a better person. Together we have climbed mountains (literally and figuratively), and I thank Stéphanie for the companionship.

I thank Alexander Melrose for the technical support as a colleague and for always cheering me on as a friend. I will miss all our coffee runs and gym time together.

I thank Jiaqing Pang for all of his technical support in the lab. It has been a pleasure and a privilege to work with JP and to share common Asian traditions with him.

Special thanks to Kelley Jordan for being there with me through very difficult, transitional times in the lab, and for working extra hours to get things done before COVID-19 lab shutdown. I would not have made it without the technical and emotional support. Thank you for believing in me.

I thank Hari Lakshmanan, Dr. Ivan Parra-Izquierdo, Tia Kohs and Tony Zheng for being supportive and cheering me on throughout my graduate school journey.

I thank the entire Biomedical Engineering Department, especially the Hinds Lab, Yantasee Lab, Maloyan Lab, Dr. Joseph Shatzel, Dr. Sven Olson and the entire BME administrative staff for providing me with endless resources and support throughout my time at OHSU.

Special thanks to my Dissertation Advisory Committee: Drs. David Farrell, Owen McCarty, Show-Ling Shyng, Anthony Barnes and David Zonies for mentoring and guiding me through my projects and career goals,… and for approving my graduation!

Special thanks to previous lab members: Daniel Sallee, Drs. Jevgenia Zilberman-Rudenko, Laura Healy, Sandra Baker, Annachiara Mitrugno, Joanna Sylman, Rachel Rigg, Toshiaki Shirai and Anne Rocheleau for welcoming me into the lab with open

arms, guiding me through the early years of graduate school, being my friends and support group, and for loving me till this day.

I thank my undergraduate mentees: Marisa Thierheimer, Anna-Liisa Sepp, Kendra Jones, Zhoe Rub and Tiffany Chu for the opportunity to inspire and spread scientific knowledge among a younger generation of scientists. Thank you for helping me realize my love for teaching!

I thank my collaborators at OHSU, particularly the Computational Biology Program, the Knight Cardiovascular Institute, Department of Biochemistry and Molecular Biology, Division of Hematology and Oncology and Division of Vascular Surgery. Special thanks to my collaborators at Aronora Inc., IONIS Pharmaceuticals, Stony Brook University and Vanderbilt University. Thank you for the opportunity to do great science with you all.

I thank Dr. Elizabeth DuPriest at Warner Pacific University and Dr. Susan Bagby at OHSU for introducing me to the world of scientific research, which has led me to my current career passion.

I thank my partner, Kyle T. Gustafson (soon to be Dr. Gustafson), for his patience, wisdom, caring and love for me throughout my journey together in life and in graduate school. Kyle has made me a better person, and I thank him for being there to cheer me on at my best, and for embracing me at my worst.

Con chân thành cảm ơn Ba, Mẹ vì đã sinh con ra và tạo đủ điều kiện cho con thực hiện ước mơ của mình. Con cảm ơn Bà Ngoại luôn yêu thương con và cổ vũ cho con. Con cảm ơn cô chú, dì dượng, cậu mợ hai bên gia đình lúc nào cũng nhớ tới con và chờ mong con trở về. Cảm ơn đất nước Việt Nam là nơi con được sinh ra, lớn lên và là nơi con luôn muốn giới thiệu đến bạn bè năm châu với niềm tự hào. Cảm ơn gia đình vì tất cả những sự hi sinh và cống hiến để cho con có được ngày hôm nay.

Con nợ gia đình cả cuộc đời.

Table of Contents

List of Figures and Tables

List of Abbreviations

ACD	acid citrate dextrose
ADAM	a disintegrin and metalloprotease
ADP	adenosine diphosphate
AMP	adenosine monophosphate
APC	allophycocyanin
APGAR	appearance, pulse, grimace, activity and respiration
aPTT	activated partial thromboplastin time
ASK	apoptosis signal-regulating kinase
ASO	antisense oligonucleotide
ATP	adenosine triphosphate
AU	arbitrary unit
BAPTA	1,2-bis(o-aminophenoxy)ethane-N,N,N’,N’-tetraacetic acid
BSA	bovine serum albumin
BTK	Bruton's tyrosine kinase
BV	brilliant violet
CD	cluster of differentiation
CHO	Chinese hamster ovary
CIP4	Cdc42-interacting protein 4
CLEC-2	C-type lectin-like receptor
CRP	collagen-related peptide

CXCL-12	CXC motif chemokine ligand 12
CXCR	chemokine receptor
DAG	diacylglycerol
DIC	differential interference contrast
DMSO	dimethyl sulfoxide
DNA	deoxyribonucleic acid
DOAC	direct-acting oral anticoagulant
DOCK	dedicator of cytokinesis
DTBP	dimethyl dithiobispropionimidate
DTS	dense tubular system
EC	endothelial cell
ECM	extracellular matrix
EDTA	Ethylenediaminetetraacetic acid
ER	endoplasmic reticulum
ERK	extracellular signal-regulated kinase
F	factor
FACS	fluorescence-activated cell sorting
FAK	focal adhesion kinase
FITC	fluorescein isothiocyanate
FLNA	filamin
FPLC	fast performance liquid chromatography
FSC	forward scatter

GAP	GTPase-activating proteins
GDI	guanine nucleotide dissociation inhibitor
GDP	guanosine diphosphate
GEF	guanine nucleotide exchange factors
GFP	gel-filtered platelets
GIT	ARF GTPase-activating protein
GMP	cyclic guanosine monophosphate
GP	glycoprotein
GPCR	G protein-coupled receptor
GSK	glycogen synthase kinase
GST	glutathione S-transferase
GTP	guanine triphosphate
HCT	hematocrit
HDAC	histone deacetylase
HDL	high-density lipoprotein
HFD	high-fat diet
HGB	hemoglobin
HRP	horseradish peroxidase
HSD	hemodynamic shearing device
HUVEC	human umbilical vein endothelial cells
ICAM-1	intercellular adhesion molecule 1
IL	interleukin

IP	immunoprecipitation
IP_3	inositol trisphosphate
IRB	Internal Review Board
IRS	insulin receptor substrate
ITAM	immunoreceptor tyrosine-based activation motif
JNK	c-Jun N-terminal kinase
LARGE	glycosyltransferase-like protein
LAT	linker for activation of T cells
LDL	low-density lipoprotein
LRP1	low-density lipoprotein receptor-related protein 1
MAPK	mitogen-activated protein kinase
MAPKAPK	MAP kinase activated protein kinase (MK2)
MCH	mean corpuscular hemoglobin
MCHC	mean corpuscular hemoglobin concentration
MCP-1	monocyte chemoattractant protein-1
MCV	mean corpuscular volume
MEK	mitogen-activated protein kinase kinase (MAP2K/MAPKK)
MFI	mean fluorescence intensity
MI	myocardial infarction
MLC	myosin light chain
MPV	mean platelet volume
MSN	moesin

MW	molecular weight
MYLK	myosin light chain kinase
NA	numerical aperture
NADPH	nicotinamide adenine dinucleotide phosphate
NF2	merlin
NO	nitric oxide
ORO	Oil-red-O
PAK	p21-activated kinase
PAR	protease-activated receptor
PAS	platelet activation state
PBS	phosphate-buffered saline
PDI	protein disulfide isomerase
PE	phycoerythrin
PECAM	platelet/ endothelial cell adhesion molecule
PFA	paraformaldehyde
PGI_2	prostacyclin
PI3K	phosphoinositide 3-kinase
PIP_2	phosphatidylinositol 4,5-bisphosphate
PKA	protein kinase A
PKC	protein kinase C
PKG	protein kinase G
PLA	phospholipase A

PLC	phospholipase C
PLT	platelet
PPACK	D-Phenylalanyl-L-prolyl-L-arginine chloromethyl ketone
PPI	protein-protein interaction
PPP	platelet-poor plasma
PRP	platelet-rich plasma
PS	phosphatidylserine
PSGL	P-selectin glycoprotein ligand-1
PTFE	polytetrafluoroethylene
RANTES	regulated upon activation, normal T cell expressed and secreted
RBC	red blood cell
RDW	red cell distribution
RGD	Arg-Gly-Asp
RNA	ribonucleic acid
ROCE	receptor-operated calcium entry
ROCK	Rho-associated protein kinase
ROS	reactive oxygen species
RT	room temperature
RTN4	reticulon-4
SC	subcutaneous
SDF-1	stromal cell-derived factor 1
SDS-PAGE	sodium dodecyl sulfate-polyacrylamide gel electrophoresis

SEM	standard error of the mean
SFK	Src family kinase
SFM	serum-free media
SIF	Simple Interaction Format
SIM	structure-illumination microscopy
SIRT	sirtuin
SNARE	soluble N-ethylmaleimide-sensitive factor attachment protein receptor
SLP-76	lymphocyte cytosolic protein 2
SNAP	synaptosome associated protein
SR	superresolution
SOCE	store-operated calcium entry
SSC	side scatter
STIM1	stromal interaction molecule 1
TBXA2R	thromboxane A2 receptor
TF	tissue factor
TFPI	tissue factor pathway inhibitor
TGA	thrombin generation assay
TLR	Toll-like receptor
TRAP	thrombin receptor activator peptide
TRITC	tetramethylrhodamine
TRPC	transient receptor potential channel
TSP	thrombospondin

TXA2	thromboxane A2
VAMP	vesicle associated membrane protein
VCAM-1	vascular cell adhesion molecule 1
VEGF	vascular endothelial growth factor
VLDL	very-low-density lipoprotein
VWD	von Willebrand disease
VWF	von Willebrand factor
WASP	Wiskott-Aldrich syndrome protein
WAVE	WASP-family verprolin-homologous protein
WB	Western blot
WBC	white blood cell
WT	wild-type
ZYX	zyxin

Abstract

Platelet Signaling in Hemostasis and Vascular Inflammation

Anh Tran Phuong Ngo

Department of Biomedical Engineering

School of Medicine

Oregon Health & Science University

October 2020

Thesis Advisor: Owen J. T. McCarty, Ph.D.

Formation of a hemostatic clot is essential for minimizing blood loss upon injury and is mediated, in part, by tightly regulated activity of and crosstalk between platelets and plasma proteases of blood coagulation. Dysregulation of this otherwise protective clotting mechanism provokes thrombosis, which is caused by pathologic intravascular progression of some hemostatic mechanisms, and manifests as the common underlying pathology of major cardiovascular diseases. Pathological communication between platelets and coagulation proteases exerts inflammatory effects on the vascular endothelium. Chronic inflammation defines the development and progression of atherosclerotic plaques, from the early stages to plaque rupture and atherothrombosis, the main cause of mortality associated with cardiovascular diseases. Unfortunately,

current antithrombotic strategies increase bleeding risk; thus, there remains an unmet clinical need for safer therapeutics that are effective while also preserving hemostasis. The present research defines signaling mechanisms underlying the role of platelet and coagulation proteases in hemostasis and vascular inflammation.

Driven by Rho GTPases and their regulators, Rho-specific guanine nucleotide dissociation inhibitors (RhoGDIs), platelets undergo cytoskeletal reorganization essential to hemostasis at sites of vascular injury. In this thesis I first investigate the roles for RhoGDIs in platelet function by determining the spatial organization of RhoGDIs relative to Rho GTPases and identifying molecular signaling pathways in regulating RhoGDI functions. I demonstrate that protein kinase C (PKC) phosphorylates RhoGDIs to spatially anchor Rho GTPases at specific intracellular locations within platelets and fine tune Rho GTPase-driven hemostatic function. As many Rho GTPase regulatory proteins remain uncharacterized, this study provides mechanistic insights into RhoGDIs as master regulators of the platelet cytoskeletal dynamics underlying hemostatic plug formation.

Next, this thesis delves further into signaling pathways around PKC and mitogen-activated protein kinase (MAPK) associated with platelet cytoskeletal dynamics, procoagulant activity and inflammatory responses. Roles for MAPK p38 has been implicated in thrombosis and inflammation, yet little is known regarding mechanistic p38 targets in the platelet activation program. Utilizing causal pathway tools to map protein phosphorylation events upon platelet activation, I discover the p38-MK2-RNT4-Bcl-xl

signaling axis as a crucial mediator of platelet procoagulant phenotype, whose signaling mechanism was unknown prior to my study. As omics tools and informatics databases continue to mature, this study demonstrates utility of causal pathway tools in modeling, organizing and discovering signaling routes and therapeutic targets in platelets and other cell and tissue systems.

Over the last decade, it has become clear that neonatal and adult megakaryocytes produce platelets with distinct functionality due to ontogenic changes in the megakaryocyte-platelet linage. However, drug dosing of antiplatelet agents for neonates still relies on data extrapolated from adult clinical trials. To further investigate neonatal platelet hemostatic response, I focus on platelet functions downstream of G-protein-coupled receptors (GPCRs), as the thrombin receptors protease-activated receptors (PARs) and ADP receptors $P2Y_1$/$P2Y_{12}$ are major targets of antiplatelet therapies. I observe blunted granule secretion and integrin activation in neonatal compared to adult platelets, attributed in part to the lower expression of PARs. Interestingly, I find neonatal platelet responses downstream of $P2Y_1$/$P2Y_{12}$ to be robust, perhaps as a compensatory mechanism for the hyporeactivity downstream of PARs in order to maintain neonatal hemostasis. In light of such distinct functional neonatal platelet phenotypes, this study provides new considerations for the management of bleeding complications through transfusion of adult platelets into neonates.

Finally, due to the pathologic involvement of coagulation factor (F) XI of the intrinsic pathway in thrombosis and inflammation, I describe a role for FXI in potentiating

atherosclerosis, a chronic inflammatory disease driven by platelets, coagulation and endothelial dysfunction. While the link between coagulation and atherothrombosis is well known, contribution of coagulation in the early steps of atherosclerosis remains unclear. I investigated whether FXI promotes atherogenesis and already established atherosclerosis in $Ldlr^{-/-}$ mice by pharmacological targeting of FXI with antibody 14E11 or FXI-antisense oligonucleotide. Inhibition of FXI reduces atherogenesis without affecting plasma cholesterol levels, inflammatory monocyte levels, platelet activation or monocyte infiltration into the plaque. I find that exposure of cultured endothelium to activated FXI disrupts VE-cadherin expression at the endothelial cell junctions, enhancing the traverse of lipoproteins through the endothelium. Such inflammatory effects on endothelial VE-cadherin, exerted by FXI, is also observed *in vivo.* This study demonstrates therapeutic potential for targeting FXI in atherosclerosis, perhaps along with the use of cholesterol-lowering drugs and antiplatelet therapy.

Overall, these studies explore new signaling mechanisms for platelets and coagulation in hemostasis and vascular inflammation and provide insights into the rational design and development of safer antiplatelet and anticoagulant agents.

Chapter 1. Introduction to key vascular components in hemostasis, thrombosis and inflammatory diseases

1.1 Overview

Platelets are anucleate cell fragments of megakaryocytes and the smallest cellular elements of circulating blood. As the primary cellular mediators of hemostasis, upon detection of vessel damage, platelets tether and adhere to the exposed extracellular matrix proteins, organize their cytoskeleton to undergo drastic morphological changes and aggregate with other platelets to protect vascular integrity. Concomitantly, the blood coagulation cascade is activated upon exposure of tissue factor present in the subendothelial space, culminating in the generation of thrombin. The platelet procoagulant surface and granule releasate upon platelet activation facilitate and enhance activation of coagulation enzymes; vice versa, thrombin directly activates platelets and facilitates fibrin formation that allows platelet-platelet interaction into a tightly-packed hemostatic plug. In the following sections, I will explore various cellular and acellular components of the vasculature and appreciate their synergistic actions in regulating hemostasis, a crucial physiological response to restore blood flow and prevent further damage in the case of injury. Furthermore, I will examine the role of platelets and coagulation proteases in diseased settings such as in thrombosis and vascular inflammation (Fig. 1.1).

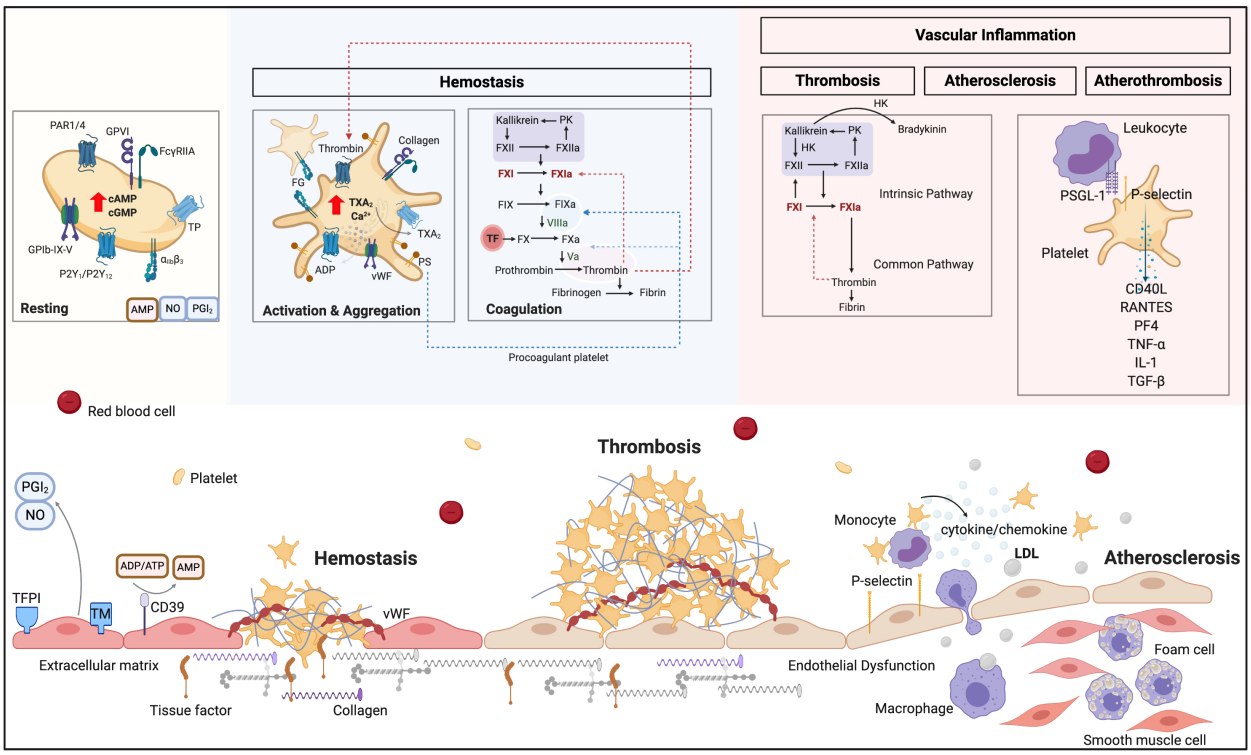

Figure 1.1. Roles of platelets and coagulation in hemostasis, thrombosis and vascular inflammation. Healthy endothelium expresses and secretes antiplatelet (prostacyclin-PGI_2, nitric oxide-NO, CD39) and anticoagulant (tissue factor pathway inhibitor-TFPI, thrombomodulin-TM) agents. Exposure of the extracellular matrix (ECM) proteins (collagen, von Willebrand factor-VWF, tissue factor-TF) to blood upon injury activates platelet adhesion receptors (GPIb, GPVI, CLEC-2) and allows TF binding to FVII/FVIIa to initiate the TF (extrinsic) pathway. Signaling downstream of platelet adhesion receptors triggers platelet secretion of soluble agonists, amplifying platelet activation via G-protein-coupled receptors (protease-activated receptors-PARs, thromboxane A2 receptor-TP, $P2Y_{1/12}$) and integrin $\alpha_{IIb}\beta_3$. Calcium signaling downstream of receptor-mediated platelet signaling facilitates integrin inside-out activation, cytoskeletal reorganization driving spreading and platelet aggregation. Sustained cytosolic calcium flux leads to membrane phosphatidylserine (PS) exposure, enhancing thrombin formation via assembly of the tenase and prothrombinase complex on the platelet procoagulant surface. TF:FVIIa complex activates FX into activated FX (FXa). FXa:Va (cofactor) prothrombinase complex induces thrombin generation. Thrombin cleaves fibrinogen into fibrin, stabilizing platelet aggregate under shear. Thrombosis, the main cause of mortality due to cardiovascular disease, occurs when vascular inflammation induces dysregulated clotting that can occlude vessels. The intrinsic pathway is implicated in thrombosis, initiated by activation of FXII, leading to FXI, FIX activation and thrombin generation. FXI can also activate FXII, promoting inflammation through bradykinin formation by FXIIa cleavage of kallikrein. Platelets also express and secretes various ligands, cytokine and chemokines that facilitates vascular inflammation, leukocyte recruitment and thrombosis.

1.2 The unmet clinical need

Atherosclerosis-associated cardiovascular complications remain the leading cause of morbidity and mortality in the Western world. According to the Global Burden of Disease Study 2010, ischemic heart disease and stroke caused 1 in 4 deaths worldwide, with thrombosis being the common underlying pathology.[1] The link between platelets, coagulation and atherothrombosis has been demonstrated in numerous animal and clinical studies;[2-8] however, despite tremendous efforts in thrombosis prevention and intervention, the burden from this epidemic continues to represent a challenging public health problem. Currently used antiplatelet and anticoagulation therapies, although are effective, increase bleeding risks.[9,10] Understanding platelet signaling mechanisms and their cross-talk with other components of the vasculature such as coagulation and the endothelium in regulating hemostasis, thrombosis and inflammation would aid in the development of safer antithrombotic that still preserves hemostasis while effectively target thrombosis and inflammatory processes.

1.3 Platelet adhesion to extracellular matrix proteins

Platelets are anucleate, discoid fragments of bone marrow megakaryocytes that circulate in blood as sentinels of vascular integrity, a protective mechanism of clotting to prevent further bleeding and restore blood flow upon endothelial damage. Circulating at 150-400 $\times$ 10^9/L of blood with a lifespan of 8-10 days, platelets adhere to the damaged endothelium when endothelial cells are altered or extracellular matrix (ECM) proteins

are exposed as a critical initial step in hemostasis, thrombosis, inflammation and immunopathogenic responses.[11] Platelets then undergo numerous receptor-mediated signaling events driving platelet activation, cytoskeletal reorganization - namely the formation of actin-rich filopodia and lamellipodia, granule secretion and recruitment of other platelets and leukocytes that participate in fibrinogen-dependent platelet aggregation, hemostatic plug formation and set off host defense responses.[12,13] Selective adhesion and recruitment of more platelets and leukocytes (aggregation) to the site of vascular injury is orchestrated by adhesive interactions of platelets to the extracellular matrix proteins, local soluble agonists being released from platelets, leukocytes and endothelial cells and the expression of adhesive molecules on the platelet surface capable of attracting surrounding circulating cells.[14]

The extracellular matrix components that are exposed during vessel injury include multiple types of collagen, von Willebrand Factor (VWF), fibronectin, laminin, fibulin, nidogen and thrombospondin that are synthesized by vascular wall cells, and those that become immobilized onto the ECM upon injury or introduction to foreign materials (medical devices) such as fibrinogen/fibrin and vitronectin.[14] Static adhesion experiments with purified ECM proteins as performed in Chapters 3-5 are essential for establishing specific mechanisms of platelet action, although relative contribution of several adhesive interactions to platelet adhesion and spreading remains to be explored further, as ECM proteins may differ in their structure and conformation when assembled into complex matrices compared to when circulating in soluble forms in plasma.

1.3.1 von Willebrand factor

Platelets adhere to VWF by tethering of glycoprotein (GP) Ibα, part of the platelet membrane GPIb-IX-V complex [15,16] to the A1 domain of immobilized VWF. Subendothelial VWF associates with collagen type VI as constitutive components of endothelial cell matrix and can support platelet adhesion directly. Hemostasis is still preserved in the absence of endogenous endothelial VWF if plasma VWF is present, as plasma VWF can become immobilized by binding ECM proteins.[14,17-19] Platelets have no measurable interaction with soluble VWF but adhere promptly to immobilized VWF, and VWF molecules appear as elongated filament under high shear stress rather than loosely coiled structures as seen under static or low shear conditions. Ultra-large multimers of soluble VWF are released from endothelial cells and platelet granules, which can function locally but do not accumulate in circulating blood due to the presence of protease ADAMTS-13.[20,21] When VWF is bound to collagen, transition from rolling to adhesion occurs more rapidly at high shear rates than on collagen without VWF, highlighting the synergistic function of the VWF-collagen complex.[22] Platelets have two main binding sites for VWF, namely GPIbα and the integrin $\alpha_{IIb}\beta_3$ (GPIIb/IIIa).[23] Integrin $\alpha_V\beta_3$ may contribute to platelet adhesion to VWF through the ligand Arg-Gly-Asp (RGD) sequence as shown on endothelial cells,[24] although $\alpha_V\beta_3$ is present at much lower density than $\alpha_{IIb}\beta_3$.[23] Approximately 25,000 copies of GPIb-IX and 12,000 copies of GPV are expressed on resting platelets, with the ligand-binding site for VWF located within the 45 kDa N-terminal region of GPIbα. GPIbα interacts with

thrombin,[25,26] high molecular weight kininogen,[27] coagulation factor (F) XI, FXII [28,29] and thrombospondin-1.[30] The GPIb-V-IX complex also facilitates the interaction of resting platelets with activated leukocytes through Mac-1 binding [31] and activated endothelial cells through P-selectin binding,[32] contributing more to platelet inflammatory responses.

Deficiency in the platelet GPIb-V-IX complex results in a strong bleeding diathesis found in Bernard-Soulier Syndrome (Giant Platelet Syndrome), characterized by macrothrombocytopenia and absent ristocetin-induced platelet agglutination. VWF deficiency or defective VWF results in von Willebrand disease (VWD), the most common bleeding disorder affecting up to 1% of the United States population.

1.3.2 Collagen

The platelet membrane expresses several collagen receptors, including integrin $\alpha_2\beta_1$, GPVI, GPIV (CD36) and p65 specifically for type I collagen.[33-37] Only $\alpha_2\beta_1$ and GPVI have defined roles in platelet-collagen interactions. Integrin $\alpha_2\beta_1$ requires activation and divalent cations to engage its ligand with high affinity, although this may not be necessary for initial collagen contact. Even in the low affinity state, $\alpha_2\beta_1$ can still mediate platelet adhesion to collagen preceding GPVI-induced activation, similarly to non-activated $\alpha_{IIb}\beta_3$ mediating adhesion to fibrinogen.[17,38] GPVI plays a major role in collagen-induced platelet activation, specifically recognizing the sequence Gly-Pro-Hyp

(collagen-related peptide) and is considered indispensable for platelet-collagen interactions.[39-41] Mouse GPVI$^{-/-}$ platelets exhibit normal adhesion onto insoluble type I collagen, but activation-dependent platelet spreading is abolished, resulting in defective platelet aggregation.[41] Perhaps GPVI-deficient platelets can still bind collagen via $\alpha_2\beta_1$ or through GPIbα binding VWF that forms a functional unit with collagen. Regardless, collagen-induced platelet activation is blocked in the absence of GPVI, although congenital deficiency of either $\alpha_2\beta_1$ or GPVI in humans only results in a mild bleeding diathesis.[42,43] This indicates that GPVI may be an ideal antiplatelet therapy because of the receptor's narrowly-defined thrombotic role, in addition to a mild bleeding phenotype manifested by GPVI deficiency.

1.3.3 Fibronectin

Platelets express two main receptors for fibronectin, $\alpha_5\beta_1$ and $\alpha_{IIb}\beta_3$.[22,44] Soluble plasma fibronectin can assemble into fibrillar networks on the surface of fibroblasts, platelets and other cells to support platelet initial adhesion by association with collagen and/or VWF and platelet aggregate stabilization.[45,46] Mice with a conditional depletion of plasma fibronectin exhibit delayed thrombus growth and decreased aggregate stability.[47] Interestingly, in *ex vivo* experiments, purified fibronectin does not cause platelet adhesion, suggesting that supramolecular assembly with other ligands is necessary for fibronectin to exert a synergistic adhesive function to platelets.

1.3.4 Fibrinogen/fibrin

Fibrinogen facilitates platelet aggregation and is a substrate for platelet arrest under shear flow. Adherent platelets become activated and spread on surfaces coated with immobilized fibrinogen/fibrin, mediated by $\alpha_{IIb}\beta_3$.[48] Fibrin, the cross-linked polymer of fibrinogen can also support platelet adhesion by synergizing with immobilized VWF.[49]

1.3.5 Laminin and nidogen

Laminin is highly expressed in the subendothelial ECM and facilitates platelet adhesion at sites of vascular injury. Platelets contain and secrete laminins 8, 10 and 11 (α4β1γ1, α5β1γ1 and α5β2γ1, respectively), while subendothelial forms are laminins 8 and 10.[50] Laminin induces platelet adhesion, filopodia and lamellipodia formation via integrin $\alpha_6\beta_1$ and GPVI, suggesting synergistic roles for $\alpha_6\beta_1$ and GPVI as laminin receptors.[51]

Nidogen is a sulfated monomeric glycoprotein that acts as a bridging adapter protein for the association of collagen and laminin in the ECM. My group has demonstrated that recombinant human nidogen-1 supported platelet adhesion and activation dependent on GPVI and $\alpha_6\beta_1$. Nidogen may play a redundant hemostatic role by activating platelets downstream of GPVI.[52]

1.3.6 Other adhesive proteins

Thrombospondin-1 (TSP-1) is a glycoprotein contained in platelet α granules and is secreted upon activation, which then binds to the platelet membrane and mediates platelet adhesion.[53] Although the significance of TSP-1 in thrombus formation is unclear, it is noteworthy that TSP-1 is abundant in atherosclerotic plaques.

Thrombospondin-2 (TSP-2) is a constituent of the ECM and not present in platelets. TSP-2 deficiency has been associated with congenital hemostatic defect in mice,[54] although the extent to which such abnormality is related to adhesion remains unclear. TSP-2 is required for mouse megakaryocytes to produce platelets that can be fully activated by agonists.[55]

Vitronectin is present in the plasma, ECM and platelet α granules and binds integrin $\alpha_V\beta_3$. Vitronectin and fibrin co-distribute in fibrin clots [56] and a role for vitronectin in the stabilization of thrombi has been demonstrated *in vivo*.[57] Vitronectin mediates platelet-clot interactions through association between platelet-bound vitronectin and fibrin-incorporated vitronectin.[58] Interactions between adhesive proteins, soluble agonists and platelet receptors facilitate initial platelet recruitment and further platelet deposition to the site of injury prior to platelet activation signaling.

1.4 Platelet aggregation, spreading and procoagulant phenotype

1.4.1 Aggregation

Aggregation is a multistep adhesion process by which platelet adhere to each other at sites of vascular injury and involves distinct receptors and adhesive ligands whose interactions are highly dependent on shear flow conditions. Fibrinogen binding to $\alpha_{IIb}\beta_3$ is not the only relevant interaction for platelet aggregation. High shear stress alone can lead to VWF-mediated platelet aggregation via GPIbα and $\alpha_{IIb}\beta_3$.[59] However, without fibrinogen, thrombi grow rapidly but are unstable, detaching from the surface and embolize causing vascular occlusion downstream of the lesion in mice. In VWF-deficient mice, stable platelet aggregates eventually develop although were markedly delayed.[60] Therefore, both VWF and fibrinogen are required for functional and stable platelet aggregation (Fig. 1.2).

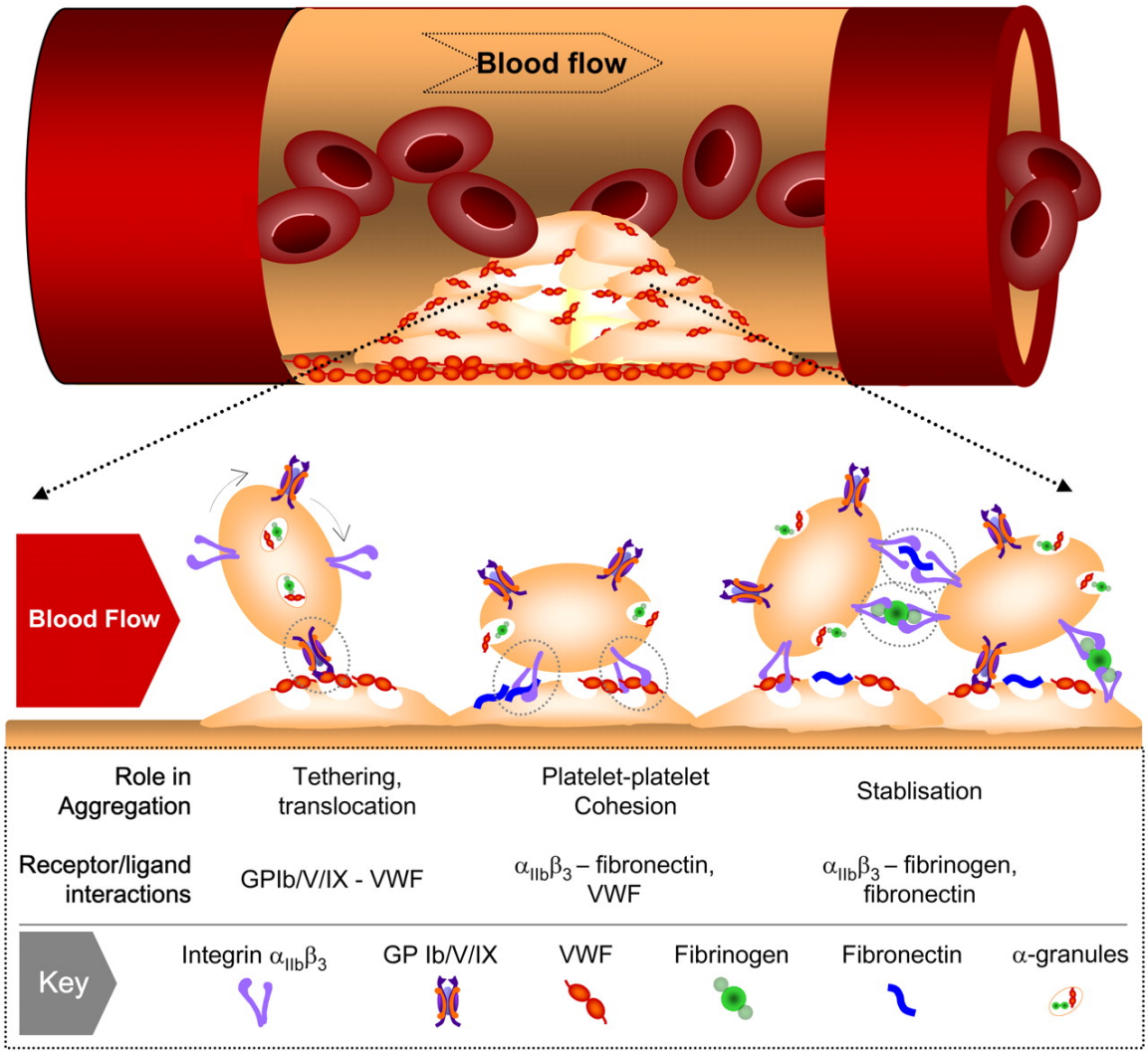

Figure 1.2. Multiple adhesion receptor-ligand interactions culminate in platelet aggregation under high shear flow. Initial tethering of platelets to the immobilized platelet surface involves VWF-GPIb interaction, although this interaction does not readily support platelet-platelet adhesion, resulting in translocation of platelet across the thrombus surface. Platelet stimulation by secreted soluble agonists during translocation promotes binding of VWF and fibronectin to integrin $\alpha_{IIb}\beta_3$, allowing sustained platelet-platelet adhesion. At elevated shear rates, fibrin(ogen)- $\alpha_{IIb}\beta_3$ interaction stabilizes platelet aggregates. Figure adapted from Jackson, *Blood* 2007; 109(12):5087-5095. Reprinted with permission.

1.4.2 Shape change and spreading

Platelet activation is associated with rapid changes in the actin cytoskeleton following adhesion to increase contact area at the site of injury. Spreading occurs when platelets are stimulated and is dependent on Gq-mediated calcium elevation or G13 that couples to small GTPase Rho. Reorganization of actin cytoskeleton is characterized by uncapping, severing and nucleation of actin filaments and their interaction with myosin II.[61] Rho mediates cytoskeletal reorganization through activation of myosin light chain kinase, enabling the reorganization of granules and organelles within platelets and formation of filopodia and lamellipodia that enable platelet secretion and spreading, along with other regulators such as Rac, Cdc42, VASP and protein kinase C.[12,61,62] Spreading is dependent on the activity of phospholipase C, calcium mobilization, generation of phosphoinositide and activation of platelet integrin $\alpha_{IIb}\beta_3$ (Fig. 1.3).[63-65]

1.4.3 Procoagulant phenotype

Even after strong activation, not all stimulated platelets become procoagulant. There exists heterogeneity in platelet response to agonists, manifesting in two distinct phenotypes discernible in the literature: 1) a procoagulant phenotype that externalizes phosphatidylserine, binds tenase and prothrombinase complex and accelerates coagulation and 2) an aggregating and contractile phenotype characterized by active integrin that binds fibrin to tighten the clot.[66-68] Procoagulant platelets show overlapping features such as ballooning or mitochondrial permeability transition pore

phenotypes, achieved by sustained calcium rise from mobilization from intracellular stores.[69,70] Platelet age or level of oxidative stress may also prime platelets to aggregatory or procoagulant phenotypes.[71-73]

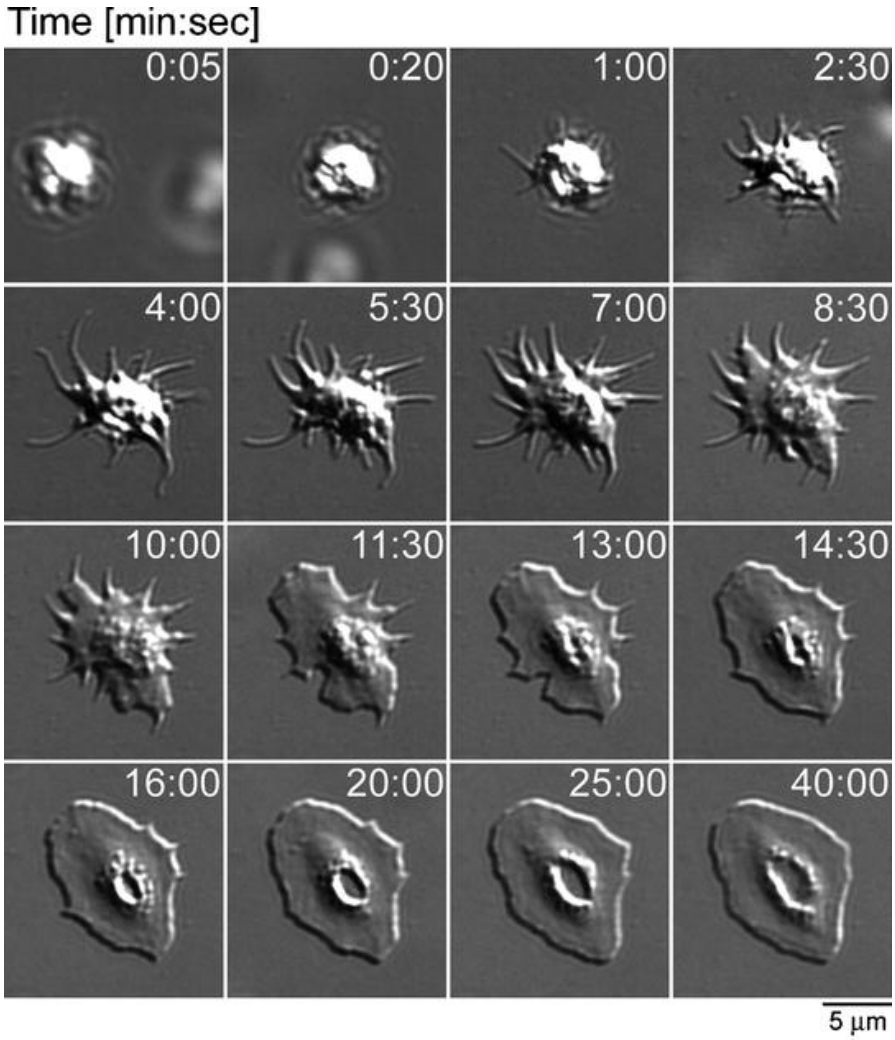

Figure 1.3. Real time imaging of platelet spreading on immobilized fibrinogen. Upon initial contact with fibrinogen, platelet undergo rounding before generating short filopodial protrusions. Sheet-like lamellipodia then proceed to fill in the gap between filopodia, resulting in a fully spread platelet at 25-min timepoint. Figure adapted from Aslan et al., *Methods in Molecular Biology: Platelets and Megakaryocytes* 2012; 788:91-100. Reprinted with permission.

1.5 Signaling during platelet activation

Signaling processes that occurs during platelet activation are classified into 3 stages: 1) early activation, 2) common signaling events (amplification) and 3) integrin inside-out activation and outside-in signaling.[74] Platelet adhesion at the site of vessel injury activates adhesion receptor-mediated signaling via the VWF receptor GPIbα, collagen receptor GPVI, podoplanin receptor CLEC-2 and fibrinogen receptor $\alpha_{IIb}\beta_3$. Soluble signaling molecules from damaged cells (ADP), coagulation activation (thrombin), atherosclerotic plaques (lysophosphatidic acid) and platelet secretome (ADP, thrombin, thromboxane A2, serotonin) bind G-protein-coupled receptors (GPCRs) on neighboring platelets to aid in early activation, act as endogenous amplification mechanisms and facilitates integrin outside-in signaling to achieve an appropriate level of response to vascular injury.

Adhesion receptor-mediated signaling (early activation)

Several major platelet adhesion receptors share similarities in their signal transduction mechanisms involving Src family kinases (SFKs - Fyn, Lyn), phosphoinositide 3-kinase (PI3K) and the immunoreceptor tyrosine-based activation motif (ITAM) signaling pathways.

1.5.1 GPIb-IX-V-mediated signaling

Platelet bind to VWF under high shear rate flow conditions present in arteries and arterioles via “catch bonds”, ultimately leading to integrin activation and integrin-dependent platelet adhesion and aggregation.[75,76] The cytoplasmic domain of the GPIbα interacts with SFK Lyn, PI3K and its downstream effector Akt, triggering intracellular calcium flux and integrin activation independent of other platelet receptors.[77-80] Downstream of Lyn/PI3K/Akt pathway, elevation of intracellular cGMP levels also occurs, resulting in the activation of protein kinase (PK) G, mitogen-activated protein kinase (MAPK) p38 and extracellular signal-regulated kinase (ERK) that activates nitric oxide (NO) synthase.[81-84] NO stimulates platelets at low concentrations while inhibiting platelets at high concentrations in addition to modulating vascular dilator tone, allowing robust hemostatic thrombus formation. Some studies suggest GPIb-IX is associated with the ITAM receptor FcγRIIA (FcRγ),[85,86] although loss of FcRγ,LAT and Syk does not affect GPIb-IX-dependent integrin activation and platelet adhesion to VWF under shear. [79,80,85] Deletion of ITAM signaling molecules FcRγ, Syk, LAT, SLP-76 and Btk abrogates secretion-dependent platelet aggregation,[87,88] suggesting that ITAM pathway rather functions as a signal amplification mechanism in GPIb-IX signaling. Overall, the Lyn-PI3K-Akt-cGMP-PKG-MAPK signaling axis plays a crucial role in VWF-GPIb-IX-mediated platelet activation (Fig. 1.4).

1.5.2 GPVI, CLEC-2 and FcγRIIa-mediated signaling

While integrin $\alpha_2\beta_1$ mediates platelet adhesion to collagen, GPVI is required for collagen-induced platelet activation.[89] GPVI is noncovalently coupled to FcRγ, and a conserved sequence (YxxL/I-X6 to 8-XXL/I) ITAM region within the FcRγ cytoplasmic domain is tyrosine phosphorylated by SKFs, mainly Lyn and Fyn bound to the cytoplasmic domain of GPVI.[90-93] ITAM phosphorylation leads to activation of Syk, which phosphorylates LAT and SLP-76 downstream, inducing the formation of the LAT signalosome complex consisting of LAT, SLP-76, Btk, Gads and phospholipase C (PLC)γ2. PLCγ2 also interacts with phosphatidylinositol 3,4,5-trisphosphate, a product of PI3K that facilitates PLCγ2 recruitment to the platelet plasma membrane and activation.[94-98] Overall, signaling events downstream of GPVI leads to thromboxane A2 (TXA_2) synthesis, granule secretion and integrin activation mediated by MAPK, PI3K and PKC.

C-type lectin-like receptor II-type (CLEC-2) is a more recently discovered platelet receptor, with the only confirmed endogenous ligand being podoplanin expressed by lymphatic endothelial cells, certain types of cancer cells, type I lung aveolar cells and kidney podocytes.[99,100] Other CLEC-2 agonists include snake venom protein rhodocytin and seaweed extract fucoidan.[101,102] Platelet responses to agonists via CLEC-2 has a slower onset of action, about 1- to 2-minute lag time before full activation.[102,103] CLEC-2 intracellular domain contains a unique single YxxL motif (hemITAM) that activates platelets through Syk, LAT and SLP-76 upon ligand engagement, leading to PI3K and PLCγ2 activation. CLEC-2 contributes to blood-

lymphatic separation during lymphatic vascular development, vessel integrity maintenance during inflammation, tumor metastasis and plays a role in thrombus formation and wound healing (Fig. 1.4).[104-108]

FcγRIIa (CD32a) is a low-affinity Fc receptor (FcR) for the constant region of IgGs that recognizes immune complexes and IgG-opsonized cells and is well-known to play a role in drug-induced thrombocytopenia.[109-111] Interestingly, FcγRIIa is not expressed in mice, and drug-induced prothrombotic events and thrombocytopenia can only be recapitulated in human FcγRIIa-transgenic mice.[112] FcγRIIa-mediated platelet activation and secretion facilitate direct antimicrobial function of platelets by means of amplifying integrin outside-in signaling. FcγRIIa becomes rapidly phosphorylated by tyrosine kinases upon crosslinking of the receptor.[113-115] Phosphorylated ITAM region provides a docking site for Syk and its tyrosine kinase activity,[114,116] which is required for downstream activation of PLCγ2 leading to inositol-1,4,5-trisphosphate (IP_3) and diacylglycerol (DAG) production, followed by calcium mobilization and activation of PKC (Fig. 1.4).[115,117]

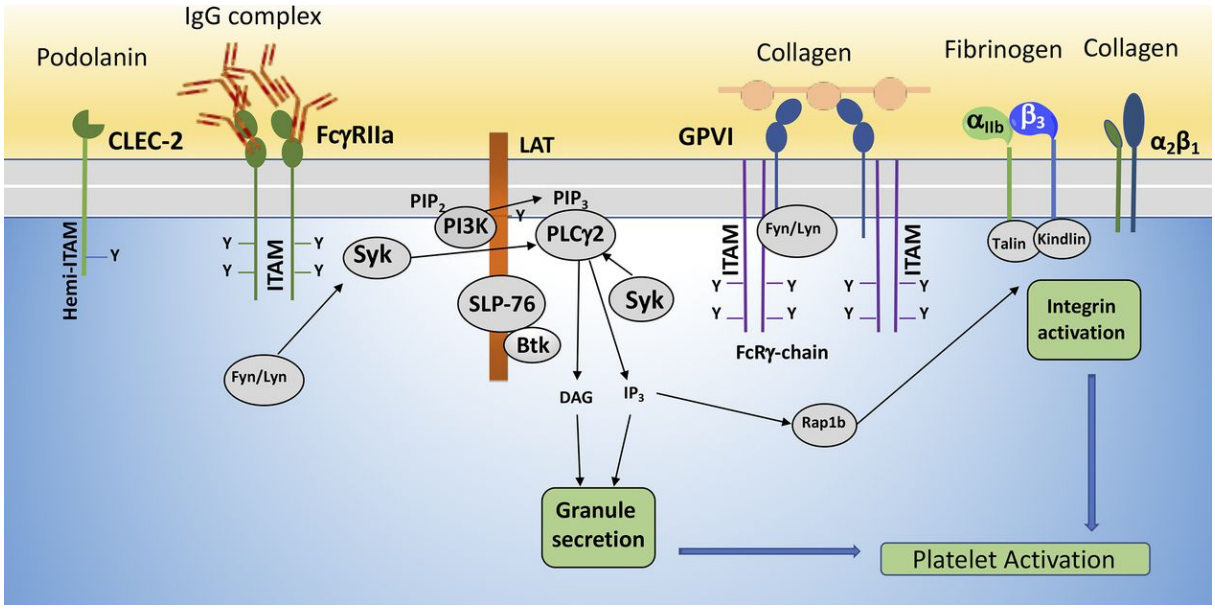

Figure 1.4. ITAM signaling in platelets. GPVI and $\alpha_2\beta_1$ are activated by collagen, while FcγRIIa recognizes IgG immune complexes to induce integrin activation. CLEC-2 contains a hemITAM that is activated by podoplanin. Ligand binding to GPVI or FcγRIIa results in Syk and PLCγ2 activation leading to platelet aggregation mediated by active integrin $\alpha_{IIb}\beta_3$. Figured adapted from Yeung et al., *Pharmacological Reviews* 2018; 70(3): 526-548. Reprinted with permission.

Soluble agonists-mediated signaling (early activation and amplification)

Soluble platelets agonists such as ADP and thrombin play a critical role in platelet activation and thrombus formation. In addition to soluble agonists, platelet secretome released from granules also interact with G-protein-coupled receptors (GPCRs) to amplify activation signals via integrin outside-in signaling.

1.5.3 G-protein-coupled receptor-mediated signaling

GPCRs are 7-transmembrane domain receptors that signal through heterotrimeric G proteins consisting of 3 subunits (α, β and γ) that bind to GPCRs to form a complex. The α subunit is converted from GDP- to GTP-bound active form upon receptor ligation, dissociating from the receptor and interact with downstream targets for signal transduction.[118] The β and γ complex can also interact with effectors including PI3Kγ.[119] platelets express Gq, G12/13, Gi/Gz and Gs. G proteins are coupled to agonist receptors (GPCRs) that stimulate platelet activation, except for Gs that is coupled to platelet inhibitors (prostacyclin and adenosine) to mediate inhibitory signals via cAMP synthesis (Fig. 1.5).

Thrombin, a product of coagulation, activates protease-activated receptor (PAR) 1 and 4 in human platelets, directly coupled to Gq and G12/13.[120] In mice, PAR3 sensitizes PAR4 to thrombin.[121] TXA_2, secreted from platelet dense granules, activates platelets via the TXA_2/prostaglandin H2 receptor (TP) that is coupled to Gq and G13.[122,123] Serotonin activates platelets via 5HT2A receptor that is coupled to Gq.[118] ADP

induces platelet activation via $P2Y_1$ (coupled to Gq) and $P2Y_{12}$ (coupled to Gi).[118,124] Epinephrine activates platelets via the epinephrine (α2) coupled to Gz, another Gi subtype.[125]

Gq transmits signals through interaction with and stimulation of PLCβ, and is important for GPCR-mediated platelet granule secretion, integrin activation and platelet aggregation. Furthermore, Gq is important in ADP-induced platelet shape change via the calcium/calmodulin- and RhoA-dependent platelet contractility.[126] Gi is also required for ADP-induced platelet activation and promotes TXA_2 and low dose thrombin-induced platelet activation in synergy with Gq.[127,128] $P2Y_{12}$-coupled Gi activates PI3K and subsequently small GTPase Rap1b critical for integrin activation.[129]

Platelet express both Gα12 and Gα13, although only Gα13 is important for thrombin- and TXA_2-induced platelet shape change, granule secretion and stable aggregation.[130,131] Gα13 interacts with and activates guanine nucleotide exchange factor (GEF) p115RhoGEF for the small GTPase RhoA, converting RhoA into the active GTP-bound form.[131] Activation of RhoA by GTP-bound Gα13 facilitates the activation of Rho kinase that enhances myosin light chain phosphorylation-dependent platelet contraction by inhibiting myosin light chain phosphatase, therefore stimulating platelet shape change and granule secretion.[132] Gα13 binds the cytoplasmic domain of integrin β_3 and plays a critical role in outside-in signaling.[133]

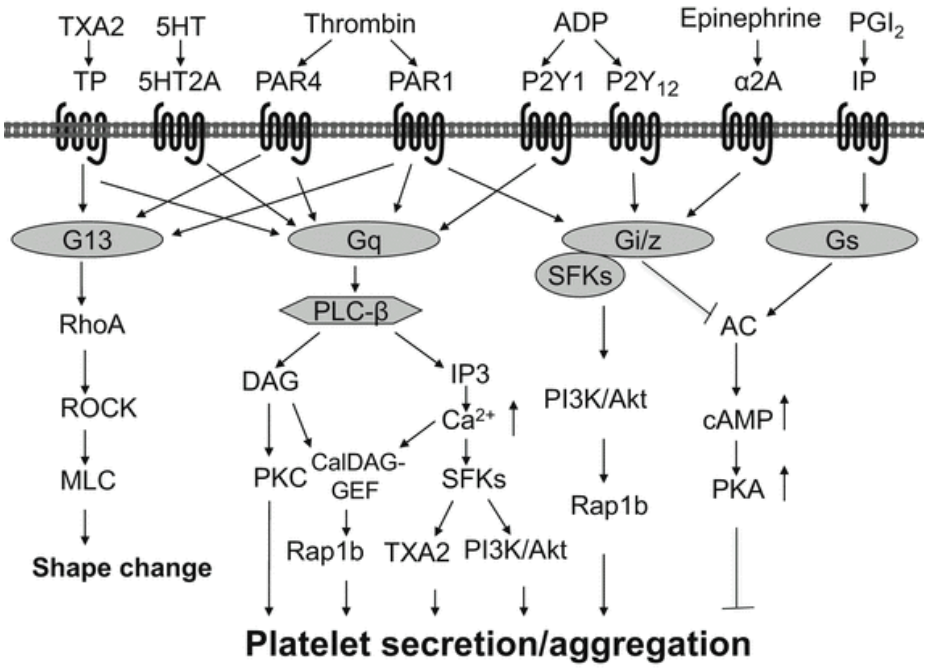

Figure 1.5. GPCR signaling in platelets. Upon agonist-induced platelet activation, release and activation of Gα subunits from of Gβγ subunits activate downstream targets to induce platelet granule secretion, TXA_2 synthesis and integrin activation. Figure adapted from Xiang et al., *Platelets in Thrombotic and Non-Thrombotic Disorders* 2017; 932-936. Reprinted with permission.

Major common signaling events (amplification pathways)

Although initial platelet signaling mechanisms differ between receptors, they ultimately merge into common signaling events driving calcium mobilization and granule secretion for signal amplification.

1.5.4 Calcium signaling

Originally identified as coagulation factor IV, calcium is now well established as a key cofactor in the formation of the tenase and prothrombinase complexes on the extracellular surfaces of procoagulant platelets to ultimately mediate fibrin generation and hemostasis.[134] Similarly, calcium has long been known to serve an important intracellular role in orchestrating the cell biological responses of platelets in hemostatic plug formation.[13,71,74,135] Changes in intracellular calcium concentrations that trigger the cellular responses driving platelet function are solicited downstream of a variety of receptors that differentially activate PLC family members (PLCγ2 and PLCβ3), resulting in IP_3 production and IP_3R (IP_3 receptor)-mediated release of calcium from intracellular stores (i.e., dense tubular system).[74,136-139] In addition to mobilization from internal stores after IP_3 generation, extracellular calcium also enters platelets via store- and receptor-operated calcium entry (SOCE and ROCE, respectively) routes involving more recently described players such as Orai1, STIM1 (stromal interaction

molecule 1), and transient receptor potential (TRP) family channels (Fig. 1.6).[71] Calcium and DAG activate actin-myosin interaction, PKC α and β, calmodulin, NO synthase, calcium-dependent proteases, small GTPases and their regulators and facilitates TXA_2 synthesis and granule secretion.

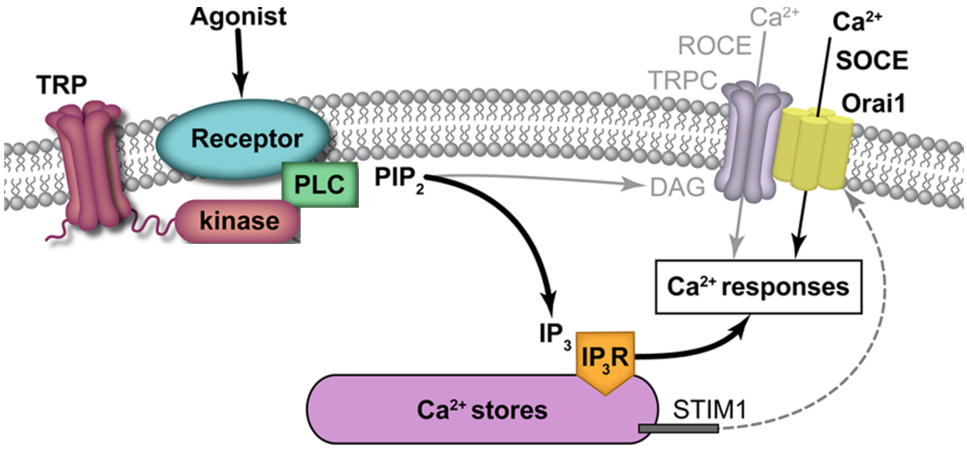

Figure 1.6. TRP kinase domain interacts with PLC family members to regulate intracellular calcium (Ca^{2+}) responses and platelet function. Platelet activation downstream of GPVI, CLEC-2, PARs and other receptors results in intracellular signaling events that upregulate PLC phosphorylation and activity to drive the metabolism of phosphatidylinositol 4,5-bisphosphate (PIP_2) on the cytosolic face of the platelet plasma membrane to produce inositol-1,4,5-trisphosphate (IP_3) and diacylglycerol (DAG). TRP channels (TRPC) and other associated processes serve as a constitutively active $Mg^{2+/}Ca^{2+}$ channel or regulating DAG-mediated receptor-operated calcium entry (ROCE), in addition to mediating Ca^{2+} mobilization and STIM1-Orai1–mediated store-operated calcium entry (SOCE), ultimately modulating intracellular Ca^{2+} concentrations and associated Ca^{2+} responses underlying platelet function. Illustration provided by Inky Mouse Studios ©2018—all rights reserved. Reprinted with permission.

1.5.5 Granule secretion

Platelets contain three major types of granules: α granules containing adhesion proteins, coagulation and fibrinolytic factors, cytokines, growth factors and adhesion receptors; dense granules containing nucleotides, serotonin, histamine and divalent cations; and lysozymes containing proteolytic enzymes.[140] Granule secretion is important in the amplification of platelet activation, recruitment of other platelets to form aggregates and thrombus stabilization. Furthermore, platelet secretome plays a plethora of roles in inflammation, atherosclerosis, immunity, wound healing, angiogenesis and cancer.[140-142] Granule secretion is culminated by numerous signaling events involving calcium mobilization, PKC-dependent phosphorylation of soluble N-ethylmaleimide-sensitive fusion protein attachment receptor (SNARE) complexes, integrin outside-in signaling, TXA_2 generation and small GTPases signaling.[143] In addition, SFK Lyn activates PI3K/Akt pathway and downstream NO/cGMP/PKG pathway, which activates MAPK (p38)/ERK/JNK axis to phosphorylate SNARE proteins leading to granule secretion.[144-150]

Integrin signaling

Platelet integrins $\alpha_{IIb}\beta_3$ (fibrinogen receptor), $\alpha_V\beta_3$ (vitronectin and collagen receptor), $\alpha_2\beta_1$ (collagen receptor), $\alpha_5\beta_1$ (fibronectin receptor) and $\alpha_6\beta_1$ (laminin receptor) share similar signal transduction mechanism, transforming from a resting low-affinity state into an activated high-affinity state following platelet activation. $\alpha_{IIb}\beta_3$ is the most abundant

integrin on the platelet surface and plays a crucial role in hemostasis. With over 80,000 copies on the platelet surface, together with an additional pool that can be trafficked to the membrane during platelet activation, $\alpha_{IIb}\beta_3$ is complexed from the calcium-dependent association of the α and β integrin subunits that require inside-out signaling events to modulate their function in a temporal and spatial manner.[94,151]

1.5.6 Integrin inside-out signaling

Section 1.5.6 is adapted from an editorial originally published by Ngo et al., *Platelets* 2020; 1-3. Permission is not required by the publisher for this type of use.

Intracellular signaling mechanisms that induce changes in the extracellular ligand-binding domain of integrins is commonly referred to as “inside-out” signaling. Platelet inside-out signaling is triggered by platelet agonists including ADP, thrombin, or extracellular matrix proteins ranging from major to minor constituents including collagen, laminin, and nidogen, respectively.[51,152] These agonists drive a cytosolic calcium flux resulting in a conformational change of the integrin from a low affinity state at rest to a high affinity state upon activation requisite for ligation of adhesive proteins including fibrinogen and fibronectin.[139] Upon ligation, $\alpha_{IIb}\beta_3$ then returns the favor by inciting outside-in signaling events to maintain or even further promote platelet activation.

$\alpha_{IIb}\beta_3$ inside-out signaling requires the binding of talin and kindlins to the cytoplasmic domain of β_3, disrupting the interaction between membrane proximal regions of

cytoplasmic domains of α_{IIb} and β_3 and subsequent conformational changes in $\alpha_{IIb}\beta_3$ that propagate the extracellular ligand-binding domain, transforming $\alpha_{IIb}\beta_3$ into the active conformation.[74,153] Conformational change in $\alpha_{IIb}\beta_3$ from a bent to an extended position activates the ligand-binding function of the integrin, allowing $\alpha_{IIb}\beta_3$ to bind the RGD sequence in their ligands.[154] Ras family of small GTPases signaling pathway has been demonstrated to play an important role in inside-out signaling. CalDAG-GEF1 activates Rap1, which interacts with the Rap1-GTP-interating adaptor molecule (RIAM) to partially promote $\alpha_{IIb}\beta_3$-talin interaction and integrin activation.[74,153] The procoagulant activity of platelets is dependent on the pattern, duration, and amplitude of calcium spikes,[155-157] and spatiotemporal pattern of $\alpha_{IIb}\beta_3$ activation is correlated to the direction of the transient calcium waves (Fig. 1.7).[94,151]

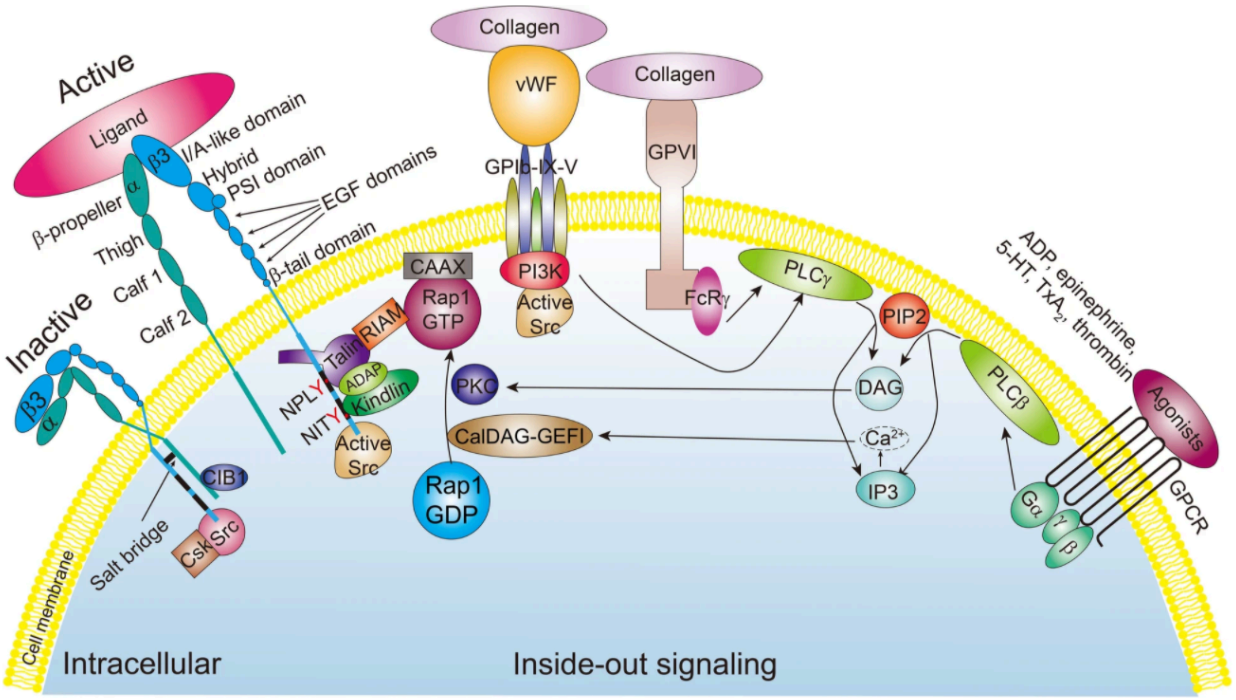

Figure 1.7. Integrin $\alpha_{IIb}\beta_3$ inside-out signaling. Adhesion and soluble agonist stimulation of GPIb, GPVI and GPCRs triggers PLC activation, generating diacylglycerol (DAG) and IP_3 leading to calcium release. DAG and calcium activate PKC, which allows activation of Rap1. Rap1-GTP and talin form the Rap1/RIAM/talin complex that interacts with β3 integrin, leading to integrin activation. Kindlin also binds the β3 tail, and ADAP serves as bridging molecule between kindlin and talin, promoting platelet integrin activation. Figure adapted from Huang et al., *Journal of Hematology & Oncology* 2019; 12, 26. Reprinted with permission.

1.5.7 Integrin outside-in signaling

Conversely, interactions between integrins and their ligands induces “outside-in” signaling across the platelet membrane that allows $\alpha_{IIb}\beta_3$ clustering during platelet aggregation.[158] In the propagation phase of platelet plug formation, calcium mobilization and accompanied secretion of ADP and TXA_2 form a coalition mediated by $P2Y_1$, $P2Y_{12}$, and thromboxane prostanoid receptors to recruit, activate, and form aggregates with other platelets. Tyrosine phosphorylation of specific substrates is one of the earliest events occurring during outside-in signaling. The G-protein subunit $G\alpha13$ interacts with the cytoplasmic domain of β_3, and upon ligand binding and subsequent integrin clustering, stimulates the activation of SFKs.[133,159] SFKs mediate outside-in signaling by phosphorylation of the two NXXY motifs in the cytoplasmic tail of β_3, regulating talin binding and protecting β_3 from calpain cleavage.[160-162] SFK c-Src phosphorylates and activates p190RhoGAP,[163] a major RhoA GTPase activating protein, which inactivates RhoA during the early phase of platelet spreading on fibrinogen that is critical for integrin outside-in signaling leading to platelet spreading.[164] Following thrombus formation, cleavage of c-Src-β_3 interacting site by calpain relieve the inhibitory effect on RhoA, leading to RhoA activation and clot retraction.[164] SFK also activates Syk via FcγRIIA-mediated Syk recruitment to the integrin signaling complex [165] and activation of downstream substrates include the RhoGEFs Vav1 and Vav3 and SLP-76. Syk activation facilitates the assembly of SLP-76/Btk/Vav complex that phosphorylates PLCγ2, focal-adhesion kinase (FAK) and

degranulation promoting adapter protein (ADAP).[153,166-168] Furthermore, signaling functions of PI3K are indispensable and complementary to PLC-mediated signaling in driving the cytosolic calcium flux crucial for maintaining $\alpha_{IIb}\beta_3$ activation. Altogether, SFK-mediated signals modulate activities of downstream Syk, PI3K and other small GTPases such as Ras, Rac and Rho in a manner analogous to the GPVI-mediated ITAM signaling (but without the involvement of LAT) to regulate platelet activation and spreading (Fig. 1.8).[165]

1.5.8 Crosstalk between GPCR and integrin signaling

Integrin outside-in signaling amplifies platelet responses to GPCR agonists; vice versa, GPCR signaling promotes outside-in signaling by inducing integrin activation. Sophisticated cross-talk between integrins and GPCRs orchestrates platelet cytoskeletal dynamics by regulating Rho GTPases-dependent cytoskeletal reorganization that is critical for platelet shape change, granule secretion, spreading and clot retraction (Fig. 1.9).

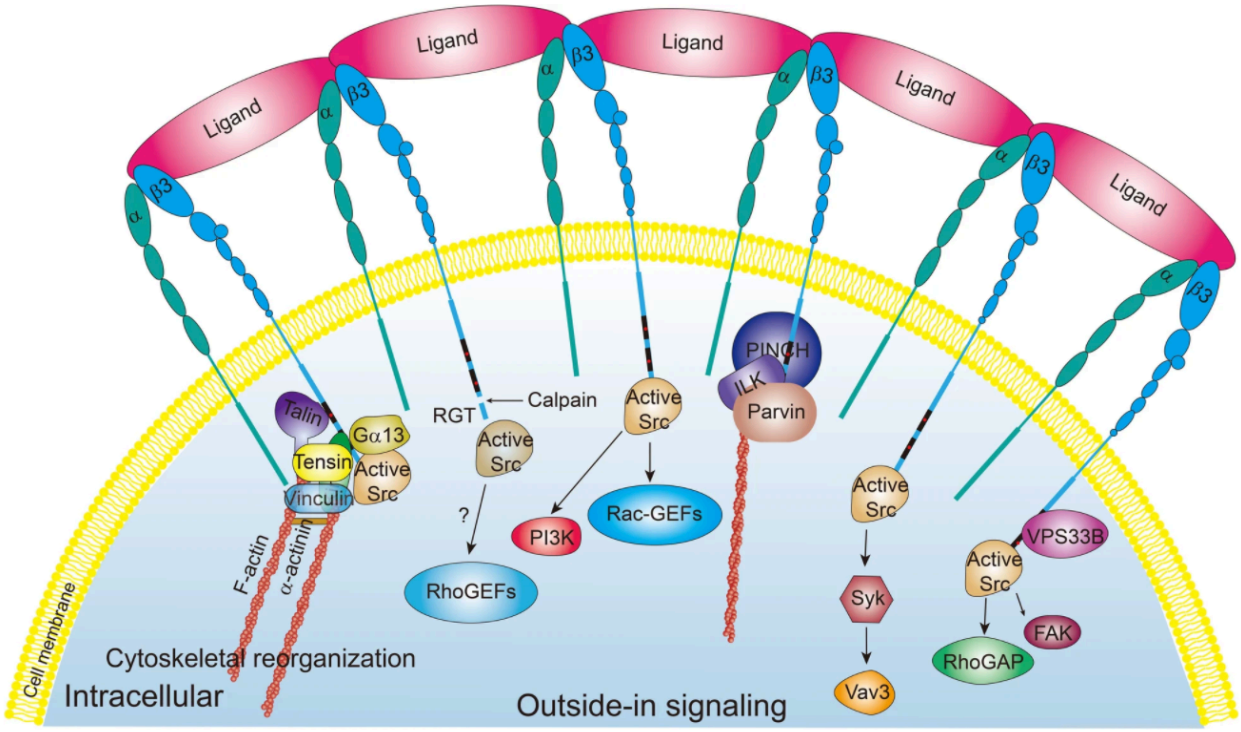

Figure 1.8. Integrin $\alpha_{IIb}\beta_3$ outside-in signaling. Following ligand binding to the extracellular domain of $\alpha_{IIb}\beta_3$, integrin clustering promotes Src activation by autophosphorylation. Calpain cleaves integrin β_3 tail and leads to dissociation of Src from the integrin. Src phosphorylates and supports the activation of multiple signaling proteins including FAK, Syk, RhoGAPs and GEFs and PI3K. Talin, kindling, tensin and vinculin links integrin signaling to actin dynamics to drive cytoskeletal reorganization. Figure adapted from Huang et al., *Journal of Hematology & Oncology* 2019; 12, 26. Reprinted with permission.

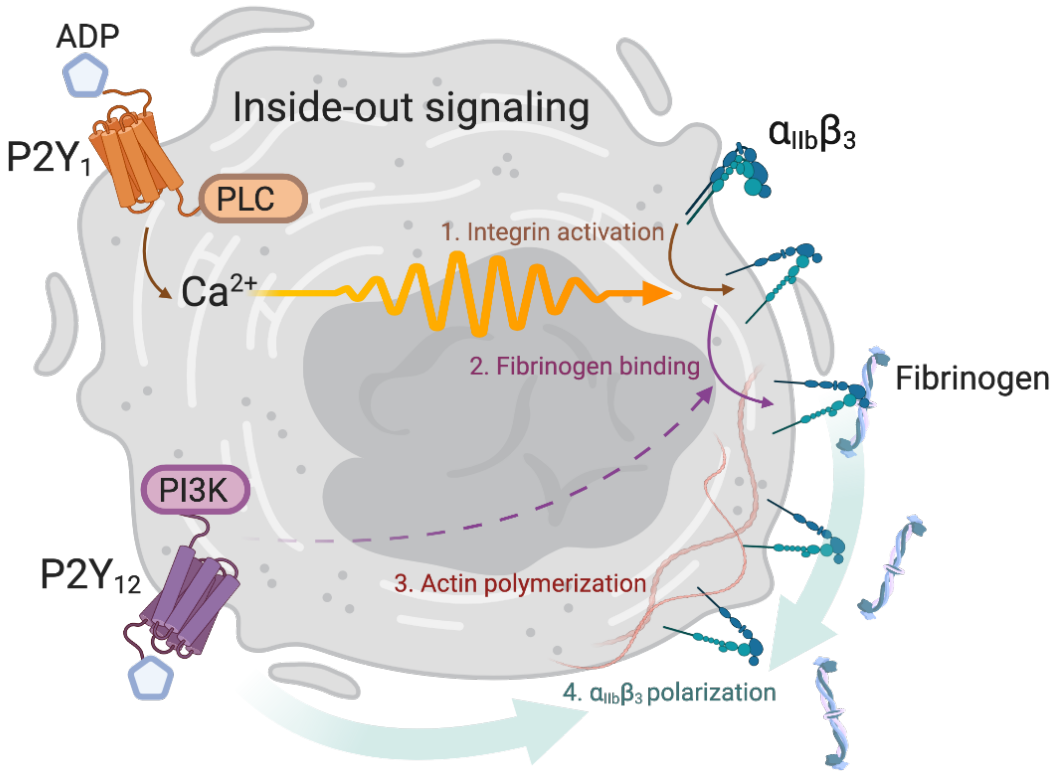

Figure 1.9. Synergy between $P2Y_1$ and $P2Y_{12}$ are required for integrin activation and fibrinogen binding. $P2Y_1$-mediated calcium transients downstream of PLC and $P2Y_{12}$-mediated PI3K activation synergize to facilitate $\alpha_{IIb}\beta_3$ activation and subsequent polarized fibrinogen binding in a manner correlating to the amplitude and frequency of calcium waves during platelet inside-out signaling. Reprinted with permission.

1.6 Rho GTPases regulate platelet secretion and spreading

Over several decades, numerous reports have highlighted the crucial role of the Rho family of GTPases members Rac1, Cdc42 and RhoA as major components of the intracellular signaling network leading to platelet cell shape change and motility, thus playing a major role in platelet spreading, secretion, aggregation and thrombus formation. Small GTP binding proteins of the Aplysia Ras Homologous (ARH), or Rho GTPase family play critical roles in platelet responses that ultimately orchestrate key features of platelet activation and thrombus formation.[12]

Rho GTPases and Rho-regulating proteins

The Rho GTPases family consists of small GTP-binding proteins that range from 20-40 kDa in size, and includes over 20 members divided into classic and atypical members.[12] Classic Rho GTPases such as RhoA, Rac1, and Cdc42 are regulated by Rho-specific guanine nucleotide exchange factors (GEFs), GTPases-activating proteins (GAPs), and guanine nucleotide dissociation inhibitors (GDIs). Rho GTPases themselves are not directly regulated by reversible phosphorylation mediating platelet activation; rather, a profound phosphorylation of GEFs, GAPs and other Rho regulators likely specify the activities of Rho GTPases in contexts of platelet activation.[169]

The Rho GTPases cycle between active GTP-bound state and inactive GDP-bound state, regulated by GEFs that activate GTPases by promoting exchange of GDP for GTP; GAPs that inactivate GTPases by promoting GTP hydrolysis; and, GDIs that

shuttle inactive GTPases throughout the cell.[170] Interactions between active GTP-bound GTPases and their effector molecules lead to activation of downstream signaling pathways that are crucial for regulating cellular functions including migration, secretion, and spreading. In platelets, the Rho GTPase family members Cdc42, Rac1 and RhoA are known to play critical roles in platelet hemostatic responses (Fig. 1.10).[12,171]

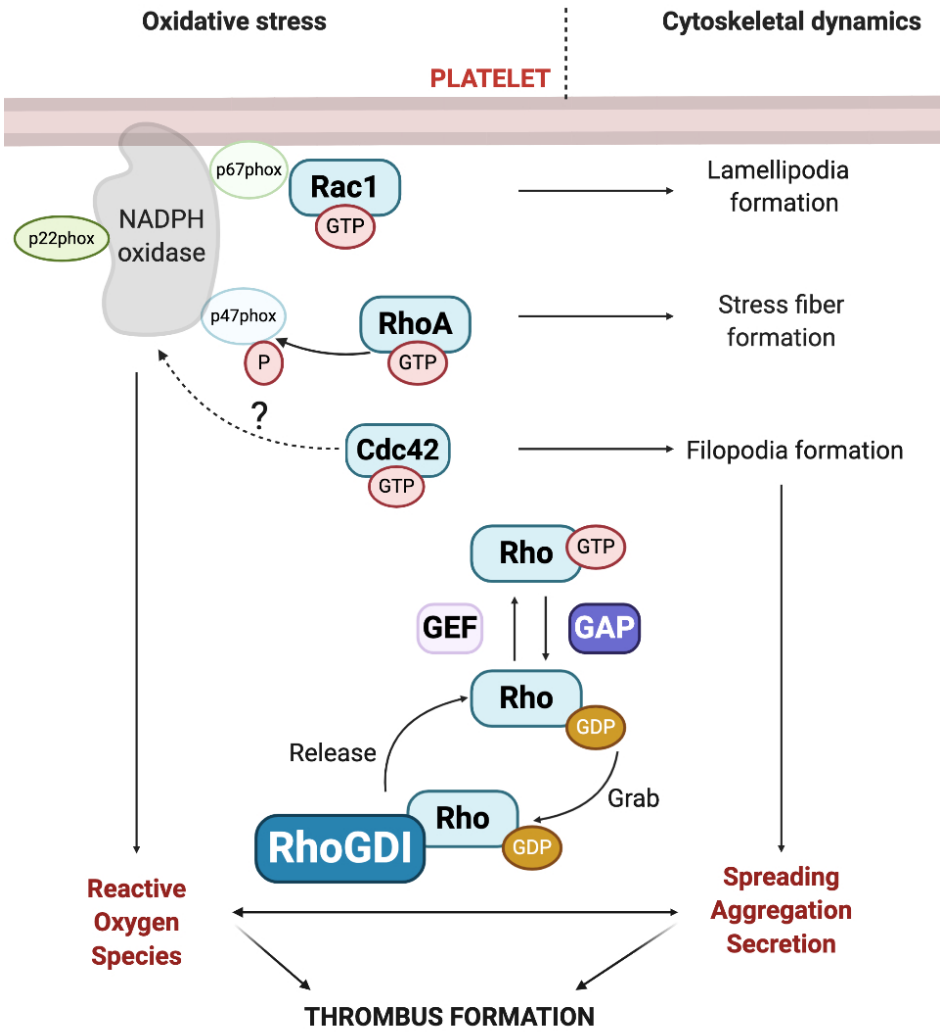

Figure 1.10. Rho GAPs, Rho GEFs and RhoGDIs regulate Rho GTPases function in mediating cytoskeletal dynamics underlying thrombus formation. Classic Rho GTPases such as RhoA, Rac1, and Cdc42 are regulated by Rho-specific guanine nucleotide exchange factors (GEFs), GTPases-activating proteins (GAPs), and guanine nucleotide dissociation inhibitors (GDIs). The Rho GTPases cycle between active GTP-bound state and inactive GDP-bound state, regulated by GEFs that activate GTPases by promoting exchange of GDP for GTP; GAPs that inactivate GTPases by promoting GTP hydrolysis; and, GDIs that shuttle inactive GTPases throughout the cell. Interactions between active GTP-bound GTPases and their effector molecules lead to activation of downstream signaling pathways that are crucial for platelet activation and thrombus formation.

1.6.1 Rac1

Rac1 has well established roles in actin assembly, lamellipodia formation and clot stability. Following the engagement of platelet receptor, intracellular signaling events through SFKs and the LAT signalosome as well as RhoG and other mediators support the activation of Rac1 GEFs (Vav1/3, P-Rex1, ARHGEF6 and Dock family members) that ultimately leads to the activation of Rac1.[171] GTP-bound active Rac contributes to PLCγ activation, supporting calcium signaling events that play important roles in CalDEG-GEF1 and Rap1 GTPase activation to facilitate “inside-out” integrin activation.[172,173] Rac1 and Cdc42 support the activation of downstream effectors including WASPs, WAVEs, Arp2/3, PAKs and their substrates in cytoskeletal organization. Rac1 also interacts with the NADPH oxidase $p67^{phox}$ to mediate platelet reactive oxygen species (ROS) production.[174]

1.6.2 RhoA

The subclass Rho of the Rho GTPases family is composed of three highly conserved proteins: RhoA, RhoB and RhoC. Among them, RhoA has been the most studied member. Although the three isoforms were discovered contemporarily, proteomic and transcriptomic studies revealed that RhoA is the dominant member expressed in human platelets as compared to RhoB and RhoC.[175,176] Whereas Rac1 and Cdc42 are critically involved in the regulation of lamellipodia and filopodia formation, RhoA regulates actomyosin contractility as well as actin-myosin stress fiber and focal

adhesion formation.[177] The signaling events leading to RhoA activation involve the activation of upstream G12 and G13 proteins and downstream Rho-associated coiled-coil containing protein kinase (ROCK) activation, subsequently promoting myosin light chain (MLC) phosphorylation, which is a major promoter of platelet shape change in both human and mouse platelets.[131,132] Activation of GPCRs by thrombin promotes Gαq and p115RhoGEF activation, which triggers the subsequent formation of a RhoA-GTP complex and promotes platelet contractile activity as well as granule secretion.[178]

In a secondary step of platelet activation, Gαq activates c-Src to promote a negative feedback loop that involves p190RhoGAP, stimulating the hydrolysis of RhoA-GTP to RhoA-GDP and therefore diminishing RhoA-induced contraction which in turn facilitates cell spreading.[179] RhoA-mediated signaling pathways downstream of GPCRs are also regulated though proline-rich tyrosine kinase (Pyk2) and scaffolding protein Disabled-2 (Dab2).[180,181] RhoA and Rac1-associated pathways are activated by integrin signaling via β_3-binding protein and Sec1/Munc18 family member VPS33B [182] to further link platelet integrin and Rho GTPase activation in mediating platelet function.[166] RhoA-mediated phosphorylation of the NADPH oxidase $p47^{phox}$ contributes to platelet ROS production along with Rac1.[174]

1.6.3 Cdc42

Cdc42 has less apparent roles in platelet function, most likely orchestrating with and mirroring Rac1 activities to control filopodia formation.[12] Rac and Cdc42 signaling converges on the p21-activated kinases (PAK) system including GIT1, βPIX and GEFH1 and downstream PAK effectors required for thrombin-mediated activation of the MEK/ERK pathway, Akt, calcium signaling and phosphatidylserine exposure critical for platelet hemostatic function.[183] Cdc42 also cooperates with Rac1 and their effectors WASP and WAVE in regulating actin assembly upstream of the Arp2/3 complex.[184]

Platelets Rho GTPases are regulated by a larger set of over 60 proteins that catalyze the exchange of GDP for GTP on Rho GTPases (GEFs) as well as over 70 proteins that promote GTP to GDP hydrolysis (GAPs) yet only two Rho dissociation inhibitor proteins (Rho GDIs) that sequester Rho GTPases in the cytoplasm. Quantitative proteomics studies of protein phosphorylation highlight the complexity in Rho GTPase regulation, with over 300 proteins found to change phosphorylation state upon ADP-mediated activation being Rho regulatory proteins.[185]

1.6.4 Rho GEFs

Rho GEFs such as ARHGEF1 (p115RhoGEF) and LARG regulate RhoA activity downstream of GPCRs.[12,186] Vav, a target of Src phosphorylation, regulates Rac1 downstream of GPVI and integrin signaling. Vav and P-Rex1 cooperate to regulate platelet neutrophil recruitment.[187] ARHGEF6 (Cool-2 or αPIX) is associated with the Rho GAP GIT1 (ArfGAP1) to regulate Rac activity. ARHGEF6 phosphorylation also

promotes binding with the Cdc42 interacting protein CIP4 to regulate platelet actin nucleation.[188] The fourteen GEFs identified as part of the platelet activating program include Vav3, KALRN, GEF1, ARHGEF7, ARHGEF10, LARG and DOCK proteins.[185]

1.6.5 Rho GAPs

ARHGAP17 (Nadrin or Rich1) inhibits Rac1 activation and platelet function following phosphorylation by PKA or PKG.[188] Oligophrenin (OPHN1) regulates Rac1, RhoA and Cdc42 downstream of GPVI and GPCRs.[189] The twenty-seven GAPs contributing to the platelet activation program include ARHGAP4, ARHGAP6, ARHGAP15, ARHGAP32, IQGAP and OPHN1.[185] These GEFs and GAPs phosphorylation events are largely uncharacterized and will require further investigation to determine their physiological roles.

1.6.6 Rho GDIs

Rho GDIs and their roles in regulating platelet activation and function have remained largely ignored. Platelets express two of the three Rho GDI family members, Rho GDI (ARHGDI1) and Ly-GDI (ARHGDI2).[171] Chapter 3 entails the characterization of Rho GDI regulation in human platelets.

1.6.7 Non-canonical Rho GTPases

Whereas the “classical” Rho GTPases are regulated by GDP/GTP cycling, noncanonical Rho GTPases are also regulated by other mechanisms such as transcriptional regulation (by microRNAs) and post-translational modifications and therefore may not require GEFs and GAPs.[190,191] Recent omics analyses also suggest other Rho GTPases may have roles in platelets such as the Rnd subfamily, RhoB, RhoC, RhoH, RhoQ, RhoBTB and mitochondrial Rho GTPases (MIRO2).[186,192]

1.7 Current and emerging antiplatelet therapies

Sections 1.7 and 1.9 are adapted from an editorial originally published by Ngo et al., *Journal of Thrombosis and Haemostasis* 2019; 17(2):247-249.

Permission is not required by the publisher for this type of use.

Research in the past couple decades has made remarkable progress in identifying fundamental mechanisms of platelet function and signaling pathways for platelet activation, aiding in the development of antiplatelet therapies for the treatment of thrombosis. Multiple drug classes currently exist to reduce platelet activity, including TXA_2 synthesis/ cyclooxygenase inhibitors (aspirin), phosphodiesterase inhibitors (dipyridamole), $\alpha_{IIb}\beta_3$ antagonists (abciximab, eptifibatide, tirofiban) and the $P2Y_{12}$ receptor antagonists (clopidogrel, ticagrelor and prasugrel).[193] Aspirin and $P2Y_{12}$ receptor antagonists are widely used in clinical practice in the acute treatment of

myocardial infarction (MI), secondary prevention of future MIs and as dual antiplatelet therapy (DAPT) when combined.[194]

Despite availability of antiplatelet and DAPT as a standard of care, high morbidity and mortality associated with acute coronary syndrome and recurrent thrombosis in coronary artery disease remain. Furthermore, drugs that block fundamental platelet functions such as integrin blockers cause bleeding in 0.5-1.5% of patients. Therapeutics involving platelet-directed antibodies run the risk of patients developing immune-mediated thrombocytopenia.[195,196] Aspirin and $P2Y_{12}$ receptor antagonists are also associated with drug resistance and bleeding. Emerging drug classes include targeting protease-activated receptor-1 (PAR1) and prevents cleavage of PAR1 by thrombin,[197,198] GPVI inhibitors (monoclonal antibodies) [199] and GPIa/IIa inhibitor (EMS16).[200] Small molecule inhibitors targeting Rho GTPases (Rac and RhoA) and their interaction with the NADPH oxidase complex to mediate cellular oxidative stress are also a recent topic of research as antithrombotic therapies.[201,202]

1.8 Platelets as mediators of inflammation

Increasing knowledge on platelets' role in the vasculature has yielded insights not only into how platelets interact with the vessel wall but also how they convey changes in the environment to other circulating cells. Platelets participate in the immune response against microbial organisms and foreign materials via specific receptors, granule release, RNA transfer and mitochondrial secretion.[203] When the endothelium is under

stress, platelet adhesion occurs through endothelial intercellular adhesion molecule 1 (ICAM-1) or through endothelial $\alpha V\beta 3$ and platelet $\alpha_{IIb}\beta_3$ in a fibrinogen-dependent manner. Platelet secretion of CD40 ligand (CD40L) or cytokines such as interleukin (IL)1β upregulates endothelial inflammation and endothelial expression of E-selectin, vascular cell adhesion molecule 1(VCAM-1) and ICAM-1 and secretion of monocyte chemoattractant protein (MCP-1) and IL-8.[204,205] IL-1β also enhances endothelial permeability and recruitment of leukocytes to the endothelium.[206]

Platelet CD40 and P-selectin are recognized by leukocyte PSGL-1 and CD154, leading to platelet-leukocyte aggregates, predominantly circulating with monocytes or neutrophils, contributing to innate immune response. Platelets also interact with and activate dendritic cells through CD40-CD154 interaction, causing dendritic cells to present antigen to T-cell, contributing to adaptive immunity. Platelet granule secretion releases serotonin and RANTEs that are known to mediate T-cell activation and differentiation. Platelets also express functional Toll-like receptors (TLRs), which can initiate thrombotic responses.[207-209] Platelet TLR4 and TLR2 can interact with neutrophils. Interestingly, platelet stimulation with TLR7 agonists results in smaller platelet groups, with fewer pseudopodia as compared to thrombin-mediated hemostatic response resulting in long filipodia and drastic shape change, indicating that platelet exhibit different levels of activation depending on the stimuli and functional response (Fig. 1.11).[203,207]

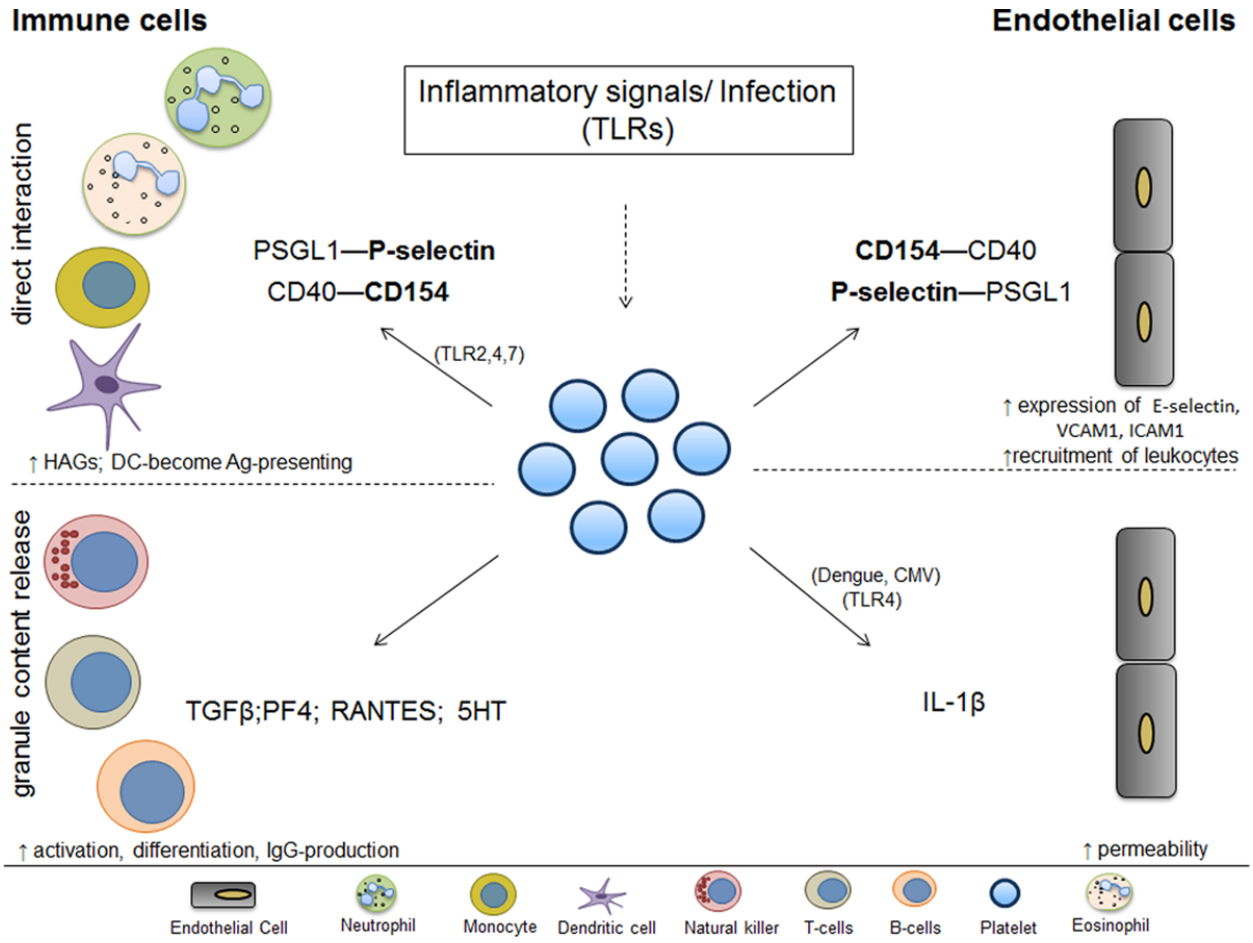

Figure 1.11. Platelet interactions with vascular and circulating cells. Platelets interact with endothelial and immune cells to orchestrate responses to microbes, inflammatory stimuli and vessel injury. Platelets engage immune cells by surface expression of TLRs and granule content release, interacting with dendritic cells, controlling T-cell function, enhancing endothelial permeability and mediating leukocyte trafficking. Proteins in bold represent changes of expression on the platelet surface. Continuous lines represent direct binding; dotted lines represent interaction through secretion. 5HT indicates serotonin; CMV-cytomegalovirus; ICAM-1-intercellular adhesion molecule 1; IL-interleukin; PF4-platelet factor 4; PSGL1-P-selectin glycoprotein ligand 1; RANTES-regulated on activation, normal T cell expressed and secreted; TGF-β-transforming growth factor-β; VCAM-1-vascular cell adhesion molecule 1. Figure adapted from Koupenova et al., *Circulation Research* 2018; 122:337-351. Reprinted with permission.

1.9 Coagulation

The vertebrate coagulation system is essential for the maintenance of a closed, high pressure circulatory system, responding to vascular injury by amplifying platelet activation and reinforcing the platelet plug through deposition of the insoluble fibrin network.[210] Activated platelets come in a procoagulant state after prolonged elevation in cytosolic calcium, exposing phosphatidylserine (PS) at their outer surface that strongly propagates coagulation by facilitating the assembly and activation of the tenase (FIXa-FVIIIa) and prothrombinase (FXa-FVa) complexes on the platelet surface.[211]

1.9.1 The extrinsic pathway

Coagulation can be initiated via the intrinsic and extrinsic pathways that converge at FX as part of the common pathway. The extrinsic pathway is rapidly activated when blood comes in contact with tissue factor (TF), a transmembrane receptor for FVII/VIIa that is present in subendothelial tissue.[212] The TF pathway (extrinsic pathway) requires an exogenous agent (i.e., TF) for activation of the coagulation factors in plasma.[213] The TF:FVIIa complex activates FIX to activated FIX (FIXa) and FX to FXa, leading to the formation of low amounts of thrombin, the central protease of the coagulation cascade. Thrombin activates the cofactors FV and FVIII, activates platelets by cleaving protease-activated receptors, cleaves fibrinogen into fibrin, activates the transglutaminase FXIII that cross-links fibrin and activates FXI of the intrinsic pathway to amplify thrombin generation (Fig. 1.12).[214,215]

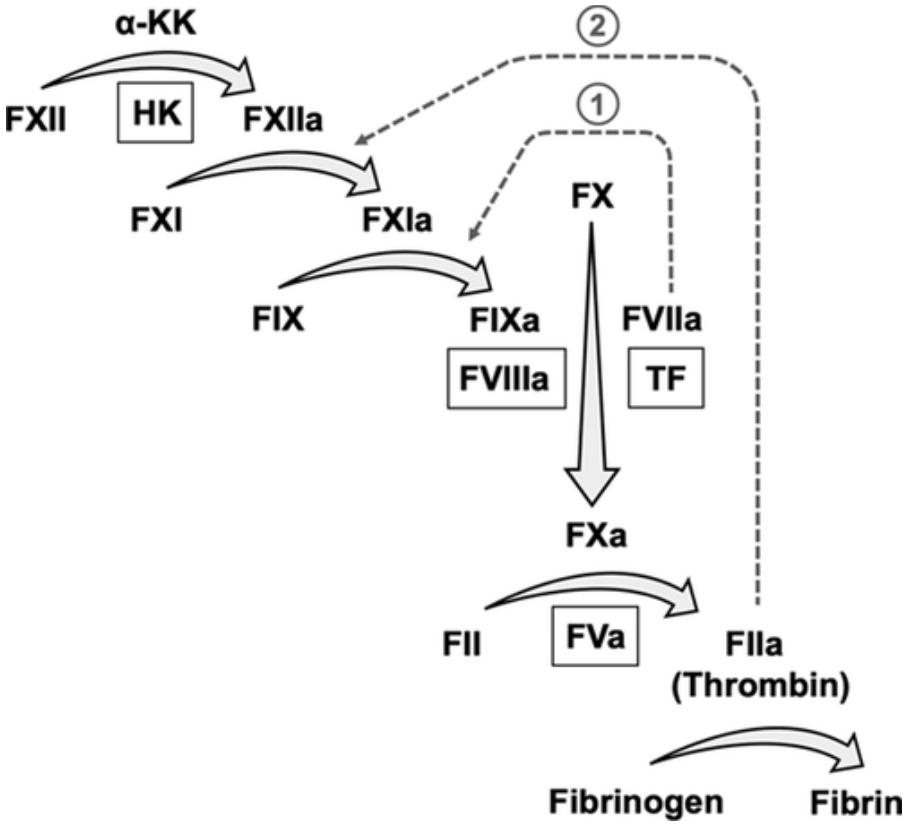

Figure 1.12. Schematic overview of the intrinsic and extrinsic (tissue factor) pathways of coagulation. In the extrinsic pathway, exposure of subendothelial TF complexes with FVIIa to catalyze FXa generation. In the intrinsic pathway, sequential activation of FXII, FXI and FIX leads to formation of the tenase complex (FIXa and cofactor FVIIIa) that also catalyzes FXa generation. FXa in complex with its cofactor FVa forms the prothrombinase complex that catalyzes thrombin generation, catalyzing the formation of insoluble fibrin through cleavage of soluble fibrinogen and activation of the transglutaminase FXIII. Dotted lines represent amplification pathways that involve crosstalk between the extrinsic and intrinsic pathways, which converge at FX (common pathway). αKK indicates α-kallikrein; HK-high molecular weight kininogen; TF-tissue factor. Figure adapted from Grover et al., *Arteriosclerosis, Thrombosis, and Vascular Biology* 2019; 39:331-338. Reprinted with permission.

1.9.2 The intrinsic pathway

The intrinsic pathway is initiated by FXII activation into FXIIa, which cleaves prekallikrein (PK) to generate active kallikrein that in turn feeds back to amplify FXII activation. In addition, FXII can readily be activated by exposure to negatively charge molecules and surfaces, including RNA, DNA and polyphosphate,[216-218] although kallikrein-mediated activation of FXII is 30-fold more efficient than autoactivation of FXII on negative surfaces.[219] FXIIa then activates FXI, which in turn activates FIX, resulting in thrombin generation and fibrin formation via the common pathway.[220] FXI also facilitates clot formation through auxiliary mechanisms outside the well-established intrinsic pathway. FXI can be activated by thrombin to amplify thrombin generation, a process that can be enhanced by platelet polyphosphate by 3,000-fold.[221] FXIa can also activate cofactors V and VIII, FX and inactivate tissue factor pathway inhibitor to further promote thrombin generation (Fig. 1.12).[215,222-226]

1.10 Current and emerging anticoagulants

Millions of patients in the United States use anticoagulation for numerous indications such as in the prevention of stroke in those with atrial fibrillation and for treatment and prevention of venous thrombosis. The history of anticoagulants has been shaped by coumarin and heparin derivatives. For over six decades, vitamin K antagonists such as warfarin were the only available oral anticoagulants for the long-term treatment of coronary artery disease, whose efficacy was demonstrated in the WARIS and ASPECT

studies.[227,228] Warfarin is easy to reverse and has well-established reversal protocols using prothrombin complex.[229] However, several well-known problems with warfarin include the need for frequent Internal Normalized Ratio monitoring,[230,231] numerous food and drug interactions and bleeding risks.[232-234]

Now, new direct oral anticoagulants (DOACs) that specifically inhibit thrombin or activated factor X combine advantages of their progenitor drugs and hence are revolutionizing the landscape of antithrombotic therapy.[235] In 2010, the Food and Drug Administration approved its first DOAC, dabigatran (direct thrombin inhibitor), followed by rivaroxaban (FXa inhibitor) in 2011, apixaban in 2012 and edoxaban in 2015, both are FXa inhibitors. As of 2016, DOAC prescriptions exceeded those for warfarin, with rivaroxaban being the most frequently prescribed DOAC. In spite of this increased use, many clinicians remain reluctant to prescribe DOACs due to bleeding risks and reversibility issues, as routine coagulation assays cannot be used to reliably monitor therapeutic anticoagulation with DOACs,[236,237] and more reversal agents are still being developed.[238]

1.11 FXI as a therapeutic target

1.11.1 FXI deficiency and hemostasis

FXI deficiency (hemophilia C), most often caused by mutations in the F11 gene for making FXI protein, is estimated to affect 1 in 1 million people worldwide, although the

severe deficiency disorder is much more common in people with central and eastern European (Ashkenazi) Jewish ancestry, occurring in about 1 in 450 people.[239,240] The most common feature of FXI deficiency is prolonged bleeding following surgery or trauma, especially involving the oral and nasal cavities or the urinary tract.[241-245] Mild cases of FXI deficiency often do not come to medical attention due to a lack of bleeding symptoms, suggesting that the actual prevalence of the disorder may be higher than reported.

The activated partial thromboplastin time (aPTT) assay, which measures thrombin generation in platelet-poor plasma following intrinsic pathway activation and is a common diagnostic test, has not been found to accurately predict the bleeding phenotype of FXI-deficient patients, presenting a serious dilemma for clinicians and patients when it comes to FXI replacement therapy. Recently, a study demonstrated that using a thrombin generation assay in platelet-rich plasma, in which intrinsic pathway is inhibited (by corn trypsin inhibitor) while the extrinsic pathway is activated by TF, was able to discriminate between control subjects and FXI-deficient individuals, and between FXI-deficient bleeders and non-bleeders.[246] This suggests that FXI does not play a role in hemostasis via the intrinsic pathway, but rather that FXI can initiate coagulation via the extrinsic pathway in the presence of platelets and TF. Other studies have shown that patients deficient in FXII, prekallikrein and high-molecular-weight kininogen do not exhibit bleeding symptoms as do FXI-deficient patients, supporting the role of FXI in the extrinsic, TF-mediated pathway rather than the intrinsic pathway.[242]

1.11.2 FXI as an antithrombotic target

A role for FXI in thrombosis has been postulated due to the fact that an elevated level of FXI is an independent risk factor for deep vein thrombosis, ischemic stroke and myocardial infarction,[247,248] while patients with severe FXI deficiency were reported to exhibit protection from ischemic stroke and venous thromboembolism (VTE).[249,250] Congenital FXI deficiency is not clearly associated with bleeding disorders, indicating that FXI does not seem to be essential for hemostasis.[251] Reducing FXI levels using an antisense oligonucleotide approach in patients undergoing unilateral total knee arthroplasty prevented post-operative VTE, suggesting FXI inhibition or reduction as an effective method of anticoagulation in surgery.[252] Studies have shown that inhibition of FIX activation by FXIa reduced thrombus formation *in vivo*,[253] and inhibiting FXI activation by FXIIa was protective in mouse models of thrombosis and ischemic stroke.[254-256]

1.11.3 FXI as an anti-inflammatory target

Uniquely located at the interface between thrombin generation and FXII activation, FXI supports activation of FXII and PK *in vivo,* potentially as a mechanism driving inflammatory responses. The intrinsic pathway activation promotes bradykinin formation via the kallikrein-kinin system.[257,258] Bradykinin binds to its receptor on endothelial cells and subsequently promotes vascular permeability through endothelial nitric oxide and prostacyclin synthesis.[259] Increased vascular permeability allows extravasation of

coagulation factors that come in contact with TF expressed in the subendothelial space and can initiate coagulation. Inhibition of FXI activation attenuates inflammation while improving survival of mouse and non-human primate sepsis.[260-262] FXI deficiency also protects against atherothrombosis and atherogenesis in mice.[256,263] Together with cytokine production and complement activation, intrinsic pathway activation contributes to the local or systemic inflammation in addition to its role in thrombosis.

1.12 The vascular endothelium

1.12.1 Endothelial homeostatic functions

Endothelial cells (ECs) line the entire circulatory system and embody a wide range of homeostatic functions including fluid filtration (in the kidney glomeruli), blood vessel tone, hemostasis and hormone trafficking.[264] The roles of ECs are carried out by the presence of membrane-bound receptors for numerous molecules including proteins, lipid-transporting particles, metabolites and hormones, as well as by junctional proteins and receptors that regulate cell-cell and cell-ECM interactions.[265] Under physiological conditions, ECs prevent thrombosis by means of anticoagulant and antiplatelet mechanisms (Fig. 1.13).[266-268]

1.12.2 Endothelial antiplatelet agents

Intact and inactive endothelium releases prostacyclin (PGI_2), a product of arachidonic acid metabolism with vasodilating properties and inhibits platelet aggregation by elevating cAMP intracellular levels.[266,267] Prostacyclin synergizes with NO, the most important endothelial vasodilator, and inhibits platelet activation by enhancing production of guanosine monophosphate (GMP), resulting in decreased platelet intracellular calcium level and suppressing $\alpha_{IIb}\beta_3$ binding with fibrinogen. Furthermore, CD-39 (ecto-ADPase) on EC surface hydrolyzes ATP and ADP to generate AMP, attenuating platelet activity.[269]

1.12.3 Endothelial anticoagulant agents

Thrombomodulin is a vasoactive factor highly expressed on the EC surface, exerting potent anticoagulation effect by binding to thrombin to reduce levels of circulating thrombin, and inactivates FVa and VIIIa by potentiating the generation of activated protein C.[270,271] Tissue factor pathway inhibitor (TFPI) is another major endogenous anticoagulant protein, inhibiting TF activation by inhibition of FXa and prevents FVIIa/TF activities.[272] Plasminogen activator inhibitor-1 (PAI-1) is a serine protease inhibitor produced by the endothelium; elevated PAI-1 is a risk factor for thrombosis and atherosclerosis.[273] I recently demonstrated that endothelial PAI-1 binds FXIa and facilitates degradation of FXIa via endocytosis, suggesting dual role of endothelial PAI-1 in regulating thrombosis and inflammation.[274]

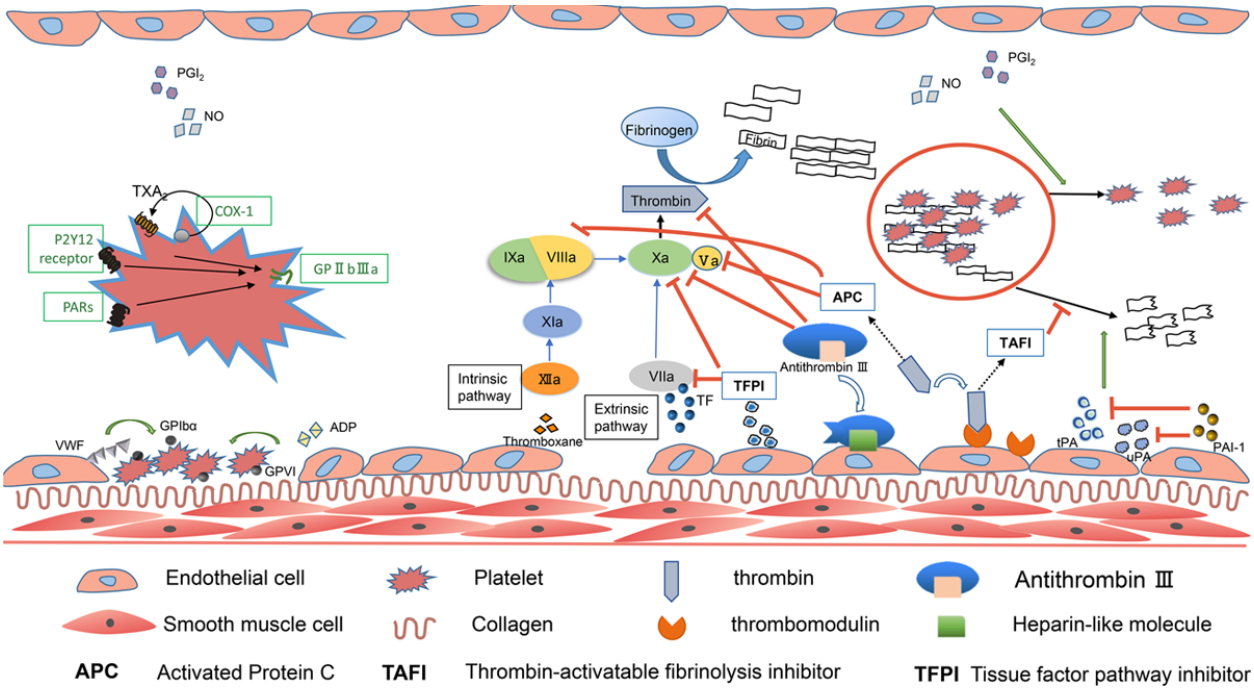

Figure 1.13. Endothelial regulation of thrombosis. Endothelium separates blood platelets and coagulation proteases from exposure to subendothelial ECM components. Endothelial cells secrete and expresses vasoactive factors that modulate platelet reactivity, coagulation, fibrinolysis and vascular tone. APC indicates activated protein C; GP-glycoprotein; NO-nitric oxide; PAI-plasminogen activator inhibitor; TF-tissue factor; tPA-tissue-type plasminogen activator; uPA-urokinase-type plasminogen activator; VWF-von Willebrand factor. Figure adapted from Wang et al., *Arteriosclerosis, Thrombosis, and Vascular Biology* 2018; 38:e90-e95. Reprinted with permission.

1.12.4 Endothelial dysfunction and vascular inflammation

Endothelial dysfunction is characterized by a shift in the actions of ECs toward reduced vasodilation and a proinflammatory and prothrombotic state associated with most forms of cardiovascular disease such as hypertension, coronary artery disease, chronic heart failure, peripheral artery disease, diabetes, chronic kidney failure and some viral infections. Under inflammatory conditions, platelets may interact with ECs even in the absence of any apparent morphological damage to the endothelium. Platelet and leukocyte recruitment are mediated by the major constituents of the endothelial Weibel-Palade bodies, VWF and P-selectin, which are the most active promoters of platelet and leukocyte adhesion. Initial contact between leukocytes, platelets and ECs is mediated by P-selectin (CD62P), E-selectin and P-selectin glycoprotein ligand 1 (PSGL-1).[275-277] P-selectin initiates leukocyte rolling, adhesion and transmigration into inflamed tissue.[278-280] Activated ECs also produce other vasoconstrictive and prothrombotic substances such as TXA_2, fibronectin, thrombospondin, prostaglandins and procoagulant factors such as FV. Chronic inflammation defines the development and progression of atherosclerotic plaques, from the early stages till plaque rupture and atherothrombosis.

1.12.5 Platelet-coagulation-endothelium interactions regulate atherosclerosis

Pathologic stimuli like hypertension, diabetes mellitus, smoking and dyslipidemia drives vascular inflammation and triggers the atherosclerotic process. Atherosclerosis is

characterized by infiltration of inflammatory cells and lipid accumulation in the intima of the arterial wall.[281] Atherothrombosis, a complication of atherosclerosis following exposure of thrombogenic, lipid-rich necrotic core of the ruptured plaque, is the main cause of mortality due to cardiovascular disease.

Platelet and coagulation factors, through complex interactions with activated ECs and inflammatory cells, drive the pathology of atherosclerosis.[280,282] Low-density lipoprotein (LDL) accumulation reduces NO levels, triggers inflammatory pathways,[283,284], enhances endothelin-1 expression and increases secretion of fibronectin, thrombospondin and glycoproteins to reinforce leukocyte and platelet adhesion.[285] ECs also express ADAM-15 that binds platelets through αIIbβ3, promoting platelet activation.[286]

Activated platelets can secrete inflammatory and mitogenic factors leading to EC activation and monocyte recruitment.[287] Activated platelets release chemokines such as platelet factor 4/CXCL4, RANTES/CCL5, CXCL12/SDF-1, monocyte chemoattractant protein (MCP-1), interleukins and TGF-β1 that further promotes the pathology of atherosclerosis.[286,288-294] Furthermore, there is evidence for associated activation of both coagulation and inflammation during atherogenesis. Thrombin,[295,296] tissue factor pathway inhibitor,[297] FVIII,[298] FXa [299], FXII and FXI [263,300] have all been shown to contribute to atherosclerosis plaque development in mice.

1.13 Thesis Overview

In this thesis, I examine the role of platelets and the intrinsic pathway of coagulation in regulating hemostasis, thrombosis and inflammatory disease. The following studies investigate platelet cytoskeletal signaling, molecular mechanisms underlying platelet procoagulant phenotype, developmental differences between neonatal and adult platelets, and the contribution of coagulation factor XI in vascular inflammation and atherosclerosis.

In Chapter 3, I investigated the roles for Rho-specific guanine nucleotide dissociation inhibitors (Rho GDIs) in platelet function, uncovering the expression and co-localization of Rho GDIs relative to Rac1, Cdc42, microtubules and PKC in platelets. I then utilized interactome and pathway analyses to investigate the signaling link between PKC and Rho GTPases, identifying crucial roles for PKC in mediating phosphorylation and spatial regulation of Ly-GDI relative to Rac1 and Cdc42 downstream of the platelet collagen receptor GPVI. Results from this study provided insights into the “lesser-known” Rho GDI functions and how platelet activation events may be spatially organized relative to the dynamic cytoskeleton of activating platelets.

To further support the use of pathway tools in the analysis of omics data set to generate mechanistic hypotheses for platelet studies, in Chapter 4, I utilized a combination of interactome, pathway analysis and other systems biology tools to gain insights into the molecular events underlying platelet function. Particularly, I analyzed proteins that are

functionally modified by phosphorylation upon platelet activation and discovered multiple signaling relations around PKC and MAPKs associated with cytoskeletal dynamics, hemostatic functions and inflammatory responses. Specifically, a MAPK p38-MK2-RTN4-Bcl-xl pathway was identified as a crucial mediator of platelet procoagulant phenotype. This study highlights the values of causal pathway tools in organizing, modeling, and discovering novel signaling routes and targets in platelets and other physiologically relevant cell and tissue systems.

In Chapter 5, I take a step back and investigated developmental differences between neonatal and adult platelets, as neonatal platelets exhibit transient hyporeactivity to agonists compared to adult platelets while not displaying a bleeding tendency. I utilized small-volume, whole blood platelet function assays to assess neonatal platelet GPCR-mediated granule secretion, integrin activation and spreading, as well as platelet thrombin generation and procoagulant phenotype under shear stress. I discovered that neonatal platelets exhibit an enhanced reactivity to ADP, potentially as a compensatory mechanism to maintain neonatal hemostasis. Results from this study provide considerations for diagnosis and treatment of hemostatic disorders as well as the development of platelet transfusion guidelines in the neonatal population.

In Chapter 6, I investigated the contribution of the intrinsic pathway, specifically factor (F) XI in regulating atherosclerosis, a chronic inflammatory process. I treated $Ldlr^{-/-}$ mice with FXI antibody (14E11) and an antisense oligonucleotide (FXI-ASO), concomitantly with high-fat diet (HFD) for eight weeks after HFD was initiated (established disease

model). I demonstrated that FXI inhibition reduced atherosclerotic lesion area when 14E11 and FXI-ASO were administered concomitantly with HFD. Meanwhile, FXI inhibition exhibited modest effects on lesion area in the established disease model, highlighting the importance of prevention and early treatment of atherosclerosis. I then cultured endothelial cells and exposed them to FXIa, demonstrating that FXIa exposure disrupted endothelial junction marker (VE-cadherin) expression and increased endothelial permeability to lipoproteins. Overall, data from this study suggest that interference with the intrinsic coagulation pathway reduces development and progression of atherosclerosis, implicating roles for intrinsic pathway of coagulation in driving vascular inflammation and cardiovascular disease.

Finally, Chapter 7 presents conclusions from these studies and future perspectives to extend my understanding of platelet small GTPases signaling beyond cytoskeletal dynamics to membrane trafficking of endocytosis and exocytosis compartments within platelets and megakaryocytes. The overall goal of the presented work is to elucidate signaling mechanisms of platelet activation underlying hemostasis and vascular inflammation.

Chapter 2. General Methods

2.1 Ethical considerations

Experiments using human donors were performed in accordance with Oregon Health & Science University and Stony Brook University Institutional Review Board-approved protocols. All human adult donors and/or parents of neonates gave full informed consent in accordance with the Declaration of Helsinki prior to blood sample collection. All blood samples were de-identified prior to sample processing. Experiments using animals were performed in accordance with the regulations of the Institutional Animal Care and Usage Committee of Oregon Health & Science University.

2.2 Blood collection

2.2.1 Human adult blood collection

Blood was drawn by venipuncture from healthy adult donors into sodium citrate (0.38% w/v) or 10% acid citrate dextrose (for shear experiments).

2.2.2 Human neonate and cord blood collection

Blood was drawn from healthy, full-term neonates at 24 h of life via heel stick into sodium citrate (0.38% w/v) following a 3 min application of an infant heel warmer.

Samples were collected after obtaining blood for a newborn screen and were obtained by scooping blood from the puncture site. Umbilical cord blood samples were obtained from healthy, full-term neonates immediately after clamping post-Caesarean section delivery and mixed with sodium citrate (0.38% w/v) or citrate phosphate dextrose (for shear experiments).

2.2.3 Mouse blood collection

Whole blood was drawn from the retro-orbital sinus into 5nM final concentration of EDTA in PBS or with sodium citrate (0.32% w/v) for plasma isolation.

2.3 Blood sample preparation

2.3.1 Human washed platelets

Warmed acid-citrate-dextrose (85 mM sodium citrate, 100 mM glucose, 71 mM citric acid, 30°C) was added to the anticoagulated whole blood and then centrifuged at 200 × g for 20 min to separate platelet-rich plasma (PRP). The PRP was further purified by centrifugation in the presence of PGI_2 (0.1 μg/ml) at 1,000 × g for 10 min. Purified platelets were resuspended in modified HEPES/Tyrode buffer (129 mM NaCl, 0.34 mM Na_2HPO_4, 2.9 mM KCl, 12 mM $NaHCO_3$, 20 mM HEPES, 1 mM $MgCl_2$, pH 7.3; supplemented with 5 mM glucose) containing 0.1 μg/ml PGI_2. Platelets were washed

once by centrifugation at 1,000 × g for 10 min and resuspended in HEPES/Tyrode buffer at indicated concentrations.

2.3.2 Human sheared platelets

Platelets, PRP, and whole blood were exposed to constant shear stresses (1, 10, 30, 50, 70 dyn/cm^2) for 4 min in a computer-controlled hemodynamic shearing device (HSD). Samples were collected using a LabView-controlled syringe pump (PSD/8, Hamilton, Reno, NV) connected to the HSD via a 28-ga Polytetrafluoroethylene tube.

2.3.3 Mouse platelet-poor-plasma

Plasma was isolated by centrifuging whole blood (mixed with sodium citrate, 0.32% w/v) at 2,000 × g for 10min at RT and stored at -80°C.

2.5 Static adhesion assay

Glass coverslips or glass-bottom dishes were coated with fibrinogen or poly-l-lysine, washed with phosphate-buffered saline (PBS) and blocked with fatty acid-free bovine-serum albumin (BSA) prior to platelet treatment with vehicle, inhibitors and/or select agonists in solution. Treated platelets were seeded onto immobilized surfaces for 45 min at 37°C, and adherent platelets were fixed with 4% paraformaldehyde. Coverslips were mounted onto glass slides with Fluoromount G, and platelets were imaged using

Kohler-illuminated Nomarski differential interference contrast optics with a Zeiss ×63 oil immersion 1.40 numerical aperture (NA) plan-apochromat lens on a Zeiss Axio Imager M2 microscope.

2.6 Immunofluorescence and superresolution microscopy

2.6.1 Platelets

Following platelet spreading and PFA fixation as above, adherent platelets were permeabilized with blocking solution (1% BSA and 0.1% SDS in PBS) and stained with indicated primary antibodies overnight at 4°C in blocking buffer. Alexa Fluor secondary antibodies or TRITC (Tetramethylrhodamine)-phalloidin were added in blocking buffer for 2 h. Coverslips were mounted with Fluoromount G on glass slides. Platelets were imaged using a Zeiss Axio Imager M2 microscope. Adherent platelets were also imaged using superresolution structured illumination microscopy (SR-SIM) with a Zeiss ×100 oil immersion 1.46 NA lens on a Zeiss Elyra PS.1 microscope.

2.6.2 Platelet annexin V staining

Washed human platelets were pretreated with inhibitors as described and then incubated on fibrinogen-coated coverglass dishes in the presence or absence of bovine thrombin (0.25 U/ml) for 45 min at 37°C. Next, annexin V-Alexa Fluor 488 and $CaCl_2$ were added to platelets for an additional 30 min. Following washing in

HEPES/Tyrode buffer supplemented with $CaCl_2$, platelets were immediately imaged by fluorescence microscopy and DIC optics at ×63 magnification.

2.6.3 Endothelial cells

Human umbilical vein endothelial cells (HUVECs) were grown to confluence on 0.1% gelatin-coated glass coverslips with Vasculife VEGF Endothelial Medium Complete Kit. HUVECs were incubated with vehicle (serum-free media, SFM), purified human FXI, FXIa, α-thrombin, FXIa or thrombin in the presence of the serine-protease-inhibitor PPACK (D-Phenylalanyl-L-prolyl-L-arginine chloromethyl ketone) for 3 h at 37°C in SFM with 10 μM $ZnCl_2$. Treatments with FXI or FXIa were performed in the presence of the potent thrombin inhibitor hirudin in order to prevent any thrombin-mediated effects. HUVECs were then washed with PBS and fixed in 4% PFA for 15 min at RT prior to blocking with 1% BSA and 2% fetal bovine serum in PBS. Primary antibody (VE-Cadherin/CD144) was incubated overnight at 4°C. Slides were then washed with PBS and secondary Alexa Fluor anti-mouse IgG and TRITC-phalloidin were incubated for 2 h at RT in 1% BSA in the dark. Hoechst 33342 was incubated in PBS for 30 min prior to mounting onto glass slides using Fluoromount G. HUVECs were imaged using a Zeiss ×20 Plan-APOCHROMAT 0.8 NA objective on a Zeiss Axio Imager M2 microscope.

2.7 Interactome and neighborhood in silico analyses

High-probability (low false discovery rate) predicted Ly-GDI (ARHGDIB) protein-protein interactions were determined through FpClass queries for molecules with a non-zero feature combination score and visualized as an interactome by GeNets (see https://apps.broadinstitute.org/genets). ChiBE was used to query and visualize the literature-curated protein-protein interaction neighborhood of Ly-GDI (ARHGDIB), MK2 (MAPKAP2) and RTN4 in Pathway Commons. In addition to Pathway Commons data, LyGDI phosphorylation sites were curated from PhosphoSitePlus. The “controls-state-change-of” binary relation type to was used to capture signaling, and “in-complex-with” and “interacts-with” relation types were used to capture protein interactions on the Simple Interaction Format (SIF) network, with length limit 1. These two interaction types were merged for simpler visualization.

2.8 Signaling pathway analysis

CausalPath was utilized to identify pathway fragments that can explain correlated changes in the phosphoproteomic data set from previous literature, by processing the Pathway Commons database using the BioPAX-pattern library, searching for patterns that capture potential binary cause-effect relations between protein activity, abundance and modifications. Then, select subset of the causal relations that fit the given data were rendered with the ChiBE visualization tool, which is available at https://github.com/PathwayCommons/chibe. In addition to Pathway Commons data, manual literature curation was performed for some of the phosphorylation sites that were not covered by Pathway Commons. CasualPath was used in either 1) default

mode or 2) by relaxing site-matching constraints. The site-matching constraint requires the phosphorylation site position to be mentioned in the pathway model and has to match with the site position identified and measured in the phosphoproteomic data set of interest, generating a higher-confidence subgraph of the signaling network and therefore more specific mechanistic information. CausalPath is available at https://github.com/PathwayAndDataAnalysis/causalpath.

2.9 Fluorescence-activated cell sorting

2.9.1 Platelet activation

P-selectin and PAC-1 expression on the platelet surface were detected using FACS. Adult, neonatal, and cord citrated whole blood was diluted with modified HEPES/Tyrode's buffer. Diluted whole blood was then incubated with Abs against P-selectin (APC-CD62P) and activated integrin GPIIb/IIIa (FITC-PAC1) in the presence of select agonists or vehicle control (HEPES/Tyrode's buffer) for 20 min at room temperature (RT). BD Cytofix Buffer was added to each sample and incubated for 5 min. Samples were finally diluted with PBS, measured by FACS, and analyzed using FlowJo software.

2.9.2 Platelet receptor screening

Diluted adult and neonatal whole blood were incubated with anti-PAR4 Abs (14H6 and 5F10), anti-PAR1 blocking Ab (ATAP2), $P2Y_1$ (APR-009), or $P2Y_{12}$ (APR-121) Abs at RT. Next, samples were stained with a polyclonal FITC anti-IgG Ab, followed by measurements on a FACS Canto II system and analyzed using FlowJo. Number of molecules per platelet was extrapolated by comparing the mean fluorescence intensity (MFI) of the sample to the MFI of a calibrator system using beads coated with increasing and accurately known quantities of immunoglobulins IgG.

2.9.3 Platelet activation and phosphatidylserine exposure under shear

Sheared whole blood and platelet-rich plasma (PRP) suspensions were assessed for platelet activation using anti-CD62P (phycoerythrin (PE)-CD62P) and Annexin V (FITC-Annexin V). Unsheared suspensions were used as controls. Whole blood or PRP samples were diluted with platelet buffer and FcR blocking reagent and stained with anti-CD62P for 15 min in the dark at 4°C. Separately, whole blood or PRP samples were diluted with Annexin V buffer and stained with Annexin V for 15 min in the dark at RT. Samples were supplemented with platelet buffer or Annexin V buffer to a final volume of 500 µl at 4°C, scanned using FACS BD Accuri C6 system, and analyzed using Kaluza software. Nonspecific signals were eliminated using PE and APC anti-IgG1κ as controls.

2.9.4 Inflammatory monocytes and platelet-monocyte aggregates

Whole blood was drawn from the mouse retro-orbital sinus into 5 mM final concentration of EDTA. Blood was then incubated with FITC-CD45R/B220, FITC-CD335 and FITC-Ly6G antibodies at RT to exclude B cells, NK cells and granulocytes, respectively, from the analysis. Monocytes were identified using PE-CD11b antibody. Inflammatory monocytes and monocyte-platelet aggregates were quantified using APC-Ly6C and BV421-CD41 antibodies, respectively. Samples were washed with PBS, fixed and stored in 1% PFA until flow cytometry analysis.

2.10 Immunoprecipitation

Washed human platelets (0.5-1 × 10^9/ml) were pretreated with inhibitors for 10 min before stimulation with agonists as indicated at RT. Following stimulation, platelets were lysed with the addition of 0.1% Triton X-100 together with protease and Sigma phosphatase inhibitor cocktail 2 and 3 and sonication. Platelet lysates were precleared with protein L agarose before the addition of antibodies or nonspecific IgG/IgM. Captured proteins were precipitated with protein A/G/L agarose. Agarose beads were washed three times with HEPES/Tyrode (with 0.1% Triton X-100) before elution in Laemmli sample buffer and Western blot analysis for captured proteins.

2.11 Western blotting

2.11.1 In human platelets

Protein samples were resolved by SDS-PAGE and transferred to polyvinylidene difluoride membranes and blotted with indicated antibodies and horseradish peroxidase-conjugated secondary antibodies. Protein was detected using enhanced chemiluminescence.

2.11.2 In mice

One microliter samples of mouse platelet-poor plasma (PPP) were size-fractionated under non-reducing conditions on 7.5% polyacrylamide-SDS gels. Proteins were transferred to nitrocellulose membranes and the blot was developed with biotin-conjugated anti-mouse FXI IgG 14E11. Blots were developed with Strepavidin-HRP and chemiluminescence.

2.12 Dense granule secretion

Human washed platelets (2×10^8/ml) were incubated with inhibitors as indicated or vehicle alone at RT. Platelets were then incubated with orbital shaking in a white flat bottom 96-well plate in the presence of platelet agonist for 30 s at 37°C. Detection reagent Chronolume was added to the wells and sample luminescence was detected using an Infinite M200 Tecan spectrophotometer.

2.13 Atherosclerosis analysis

2.13.1 Total cholesterol and fast performance liquid chromatography

Pooled mouse plasma (based on sex) very-low-density lipoprotein (VLDL), low-density lipoprotein (LDL), and high-density lipoprotein (HDL) were separated using FPLC. Cholesterol levels from plasma and FPLC fractions were determined by colorimetric assays using colorimetric kit.

2.13.2 En face analysis in proximal aortas

Proximal aortas were removed and fixed for 48 h at 4°C with 4% paraformaldehyde (PFA), then stored in saline until *en face* analysis. Images of proximal aortas, cut longitudinally, were obtained and lesion areas were quantified using ImageJ.

2.13.3 Oil-red-O staining in aortic sinus

Frozen sections of the aortic sinus were fixed with 4% PFA for 10 min, incubated with 100% propylene glycol for 10 min and stained with Oil-Red-O for 24 min at 55°C. Sections were then rinsed with 85% propylene glycol for 3 min, followed by 10 s of hematoxylin staining. Sections were mounted with glycerol gelatin mounting media and imaged using Fisherbrand AX800 series compound microscope and Moticam 3.0MP camera with Motic Imaging software.

2.14 Permeability assay

HUVECs were grown to confluence in gelatin-coated upper chambers of Transwell devices (0.4 μm polyester membrane) prior to incubation with purified human, FXIa, α-thrombin, FXIa or thrombin together with PPACK in SFM supplemented with 10 μM $ZnCl_2$ and 0.3% BSA for 3 h at 37°C. Treatments with FXI or FXIa were performed in the presence of the potent thrombin inhibitor hirudin. Evans Blue dye (0.67 mg/ml) in 4% BSA in SFM was added to the upper chamber at RT, and samples were removed from the bottom chamber every 10 min. Samples were then diluted with PBS, and absorbance was measured at 650 nm using a spectrophotometer. In separate experiments, Alexa Fluor 488-labeled acetylated LDL (4 μg/ml) was added to the upper chamber and incubated for 24 h at 37°C. Samples were removed from the bottom chamber, diluted with water in a black-bottom 96-well plate and fluorescence intensity was measured at 495/519 Ex/Em using a spectrophotometer.

2.15 Immunohistochemistry

Five serial cryosections (10μm) of the aortic root, adjacent to sections used to quantify atherosclerosis, were fixed in 4% PFA for 15 min at RT, washed with PBS and permeabilized with 0.1% sodium citrate and 0.1% Triton X-100 for 3 min at RT. Sections were then blocked in Background Buster for 1 h at 37°C and incubated with primary antibody at 4°C overnight. Slides were then washed with PBS and incubated with Alexa

Fluor secondary antibody for 1 h at 37°C. Samples were mounted using Vector Shield containing DAPI and imaged using confocal microscopy.

Chapter 3. Platelet cytoskeletal signaling and function regulated by the Rho-specific guanine nucleotide dissociation inhibitor Ly-GDI

Anh T. P. Ngo,* Marisa L. D. Thierheimer, Özgün Babur, Anne D. Rocheleau, Tao Huang, Jiaqing Pang, Rachel A. Rigg, Annachiara Mitrugno, Dan Theodorescu, Julja Burchard, Xiaolin Nan, Emek Demir, Owen J. T. McCarty, and Joseph E. Aslan

*In this study, I conceived and designed the research, performed experiments, analyzed data, interpreted the results, prepared figures and wrote the manuscript.

This work was originally published by the *American Journal of Physiology: Cell Physiology* 2017; 312(4): C527-C536.

3.1 Abstract

On activation at sites of vascular injury, platelets undergo morphological alterations essential to hemostasis via cytoskeletal reorganizations driven by the Rho GTPases Rac1, Cdc42, and RhoA. Here I investigate roles for Rho-specific guanine nucleotide dissociation inhibitor proteins (RhoGDIs) in platelet function. I find that platelets express two RhoGDI family members, RhoGDI and Ly-GDI. Whereas RhoGDI localizes throughout platelets in a granule-like manner, Ly-GDI shows an asymmetric, polarized localization that largely overlaps with Rac1 and Cdc42 as well as microtubules and protein kinase C (PKC) in platelets adherent to fibrinogen. Antibody interference and

platelet spreading experiments suggest a specific role for Ly-GDI in platelet function. Intracellular signaling studies based on interactome and pathways analyses also support a regulatory role for Ly-GDI, which is phosphorylated at PKC substrate motifs in a PKC-dependent manner in response to the platelet collagen receptor glycoprotein (GP) VI–specific agonist collagen-related peptide. Additionally, PKC inhibition diffuses the polarized organization of Ly-GDI in spread platelets relative to its colocalization with Rac1 and Cdc42. Together, my results suggest a role for Ly-GDI in the localized regulation of Rho GTPases in platelets and hypothesize a link between the PKC and Rho GTPase signaling systems in platelet function.

Graphical Abstract

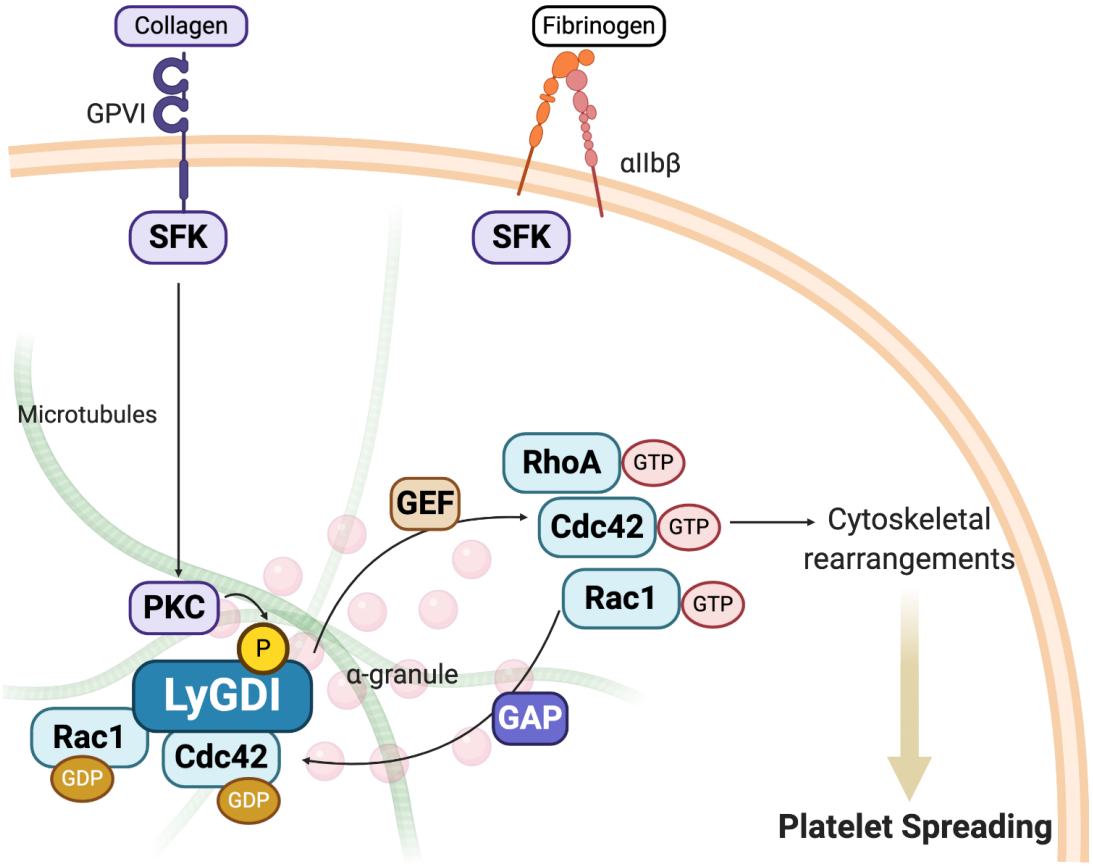

3.2 Introduction

Platelets are anucleate cell fragments of megakaryocytes that are well known as the primary cellular mediators of hemostasis.[301-304] Circulating quiescently in a discoid shape, platelets undergo drastic changes in morphology on detection of vessel damage and aggregate with other platelets to protect the integrity of the vasculature. After their attachment to extracellular matrix proteins, platelets reorganize their cytoskeleton, leading to the formation of actin-rich filopodia, which are later filled in to make sheets of lamellipodia. The actin regulatory Rho GTPase proteins Cdc42, Rac1, and RhoA all play critical roles in platelet responses that ultimately allow for the formation of a hemostatic plug.[12] For instance, Rac1 facilitates the formation of lamellipodia to support platelet spreading as well as thrombus stabilization.[172,173,305,306] Cdc42 also has described roles in filopodia formation, platelet spreading, and granule secretion.[306-309] RhoA mediates actin stress fiber formation, actin contractility, and platelet shape change on activation and is essential for the stabilization of thrombi under shear.[310] In addition, more recently characterized molecules such as RhoG also have been shown to regulate platelet secretion and thrombus formation.[311,312]

The diverse functional outputs of Rho GTPases are mediated by a cycling between guanosine triphosphate (GTP)–bound “active” and guanosine diphosphate (GDP)–bound “inactive” states, as regulated by Rho GTPase-activating proteins (RhoGAPs), which inactivate Rho GTPases by accelerating the hydrolysis of GTP to GDP, and Rho guanine nucleotide exchange factors (RhoGEFs), which facilitate the exchange of GDP

for GTP to drive Rho GTPase activation.[12] In addition to GAPs and GEFs, a set of Rho-specific guanine nucleotide dissociation inhibitor proteins (RhoGDIs) also bind to Rho GTPases to block GDP dissociation from Rho GTPases, maintaining the inactive state while anchoring Rho GTPases in specific intracellular locations, serving as an "invisible hand" in the regulation and coordination of Rho GTPase activities intracellularly.[170] In mammalian cells, Rho GTPase activities are coordinated by ~70 Rho GAP proteins and 60 GEFs, whereas only three RhoGDI genes are expressed in mammalian cells to mediate Rho GTPase sequestration.[307,313] RhoGDI1 (also known as RhoGDIα or ARHGDIA—referred to here as "RhoGDI" in this study) is ubiquitously expressed, interacts with a number of Rho GTPases, and is considered to be the best characterized RhoGDI family member.[314] RhoGDI2 (also known as Ly-GDI, RhoGDIβ, D4-GDI, or ARHGDIB—referred to as "Ly-GDI" in this study) is highly expressed in lymphocytic and hematopoietic cells and is typically found to be more closely associated with the cytoskeleton.[170,315] Loss of RhoGDI activities has multiple functional effects on different cell types, ranging from decreased rates of spreading in mesangial and melanoma cells [316] to increased migration in cancer cells and increased permeability of the pulmonary vasculature,[317] consistent with increased RhoA and Rac activities. RhoGDIs are regulated by a number of modalities, including reversible, posttranslational phosphorylation by Src family kinases, protein kinase C (PKC), and p21-activated kinases.[170,318,319] RhoGDI localization and function is also regulated by prenylation modifications.[319] More recently, reversible lysine acetylation has also been demonstrated to regulate differential aspects of RhoGDI function.[320]

Despite the critical roles of Rho GTPases and their regulation in platelet function, many relevant Rho GTPase regulatory proteins such as RhoGDIs remain uncharacterized for roles in platelet Rho GTPase regulation and platelet function.[12] Here I investigate the expression, localization, and regulation of RhoGDI proteins in human platelets, uncovering the GDI family member Ly-GDI as a putative target of protein kinase C (PKC) in the organized regulation of Rho GTPase proteins in platelets. My data suggest that Ly-GDI may serve as a cytoskeletal-localized regulator of Rac1 and Cdc42 at specific intracellular locations in a PKC-dependent manner, offering Ly-GDI as a novel regulatory protein relevant to developing models of platelet cytoskeletal signaling in hemostatic function and thrombus formation.

3.3 Materials and Methods

3.3.1 Reagents

All reagents were from Sigma-Aldrich except as noted. Prostacyclin (PGI_2) was from Cayman Chemical (Ann Arbor, MI). For static adhesion assays, fluorescence microscopy, and immunoprecipitation, human fibrinogen (FIB3) was from Enzyme Research (South Bend, IN). Anti-Cdc42 (610928), D4-GDI (556498), PKC (610107), and Rac1 (610650) were from BD Biosciences (San Diego, CA). Anti-RhoGDI (sc-360), P-selectin (sc-271267), RhoA (26C4), integrin β_3 (sc-51738), mouse IgGs (sc-2025), rabbit IgGs (sc-2027), and protein A/G PLUS-agarose beads (sc-2003) were from Santa

Cruz Biotechnology (Dallas, TX). Phospho-(Ser) pan-PKC substrate antibody (2261) was from Cell Signaling (Danvers, MA). tetramethylrhodamine (TRITC)-phalloidin and the α-tubulin (T6199) antibody were from Sigma. Integrilin (eptifibatide) was from Merck & Co. (Whitehouse Station, NJ). Alexa Fluor secondary antibodies were from Life Technologies (Carlsbad, CA). Collagen-related peptide (CRP) was from R. Farndale (Cambridge University, Cambridge, UK). Ro 31-8220 and Go 6976 were from Tocris (Bristol, UK). Chariot reagent was from Active Motif (Carlsbad, CA).

3.3.2 Preparation of human washed platelets

Blood was drawn by venipuncture from healthy human donors in accordance with an Oregon Health & Science University IRB-approved protocol into a final concentration of 0.38% sodium citrate as previously described.[321,322] Warmed acid-citrate-dextrose (85 mM sodium citrate, 100 mM glucose, 71 mM citric acid, 30°C) was added to the anticoagulated whole blood and then centrifuged at 200 *g* for 20 min to separate platelet-rich plasma. The platelet-rich plasma was further purified by centrifugation in the presence of PGI_2 (0.1 μg/ml) at 1,000 *g* for 10 min. Purified platelets were resuspended in modified HEPES/Tyrode buffer (129 mM NaCl, 0.34 mM Na_2HPO_4, 2.9 mM KCl, 12 mM $NaHCO_3$, 20 mM HEPES, 1 mM $MgCl_2$, pH 7.3; supplemented with 5 mM glucose) containing 0.1 μg/ml PGI_2. Platelets were washed once by centrifugation at 1,000 *g* for 10 min and resuspended in HEPES/Tyrode buffer at indicated concentrations.

3.3.3 Static adhesion assay

For platelet spreading experiments, 12-mm no. 1.5 glass coverslips (Fisher Scientific or Warner Instruments) or cover glass-bottom dishes (MatTek) were coated with human fibrinogen (50 μg/ml) followed by surface blocking with filtered fatty acid-free BSA (5 mg/ml). Vehicle (0.1% DMSO) or inhibitors (Ro 31-8220, 10 μM; Go 6976 1 μM) were added to platelets in solution (2×10^7/ml) for 10 min before seeding onto immobilized surfaces at 37°C for 45 min followed by washing with PBS. Adherent platelets were fixed with 4% paraformaldehyde (PFA) at room temperature for 10 min before mounting on glass slides with Fluoromount G (Southern Biotech). Platelets were imaged using Kohler-illuminated Nomarski differential interference contrast optics with a Zeiss ×63 oil immersion 1.40 numerical aperture (NA) plan-apochromat lens on a Zeiss Axio Imager M2 microscope using Slidebook 5.5 image acquisition software (Intelligent Imaging Innovations, Denver, CO) as previously described.[13]

3.3.4 Fluorescence microscopy

After platelet spreading and PFA fixation as above, adherent platelets were permeabilized with blocking solution (1% BSA and 0.1% SDS in PBS). Platelets were then stained with indicated primary antibodies overnight at 4°C at a 1:100 dilution in blocking buffer. Alexa Fluor secondary antibodies (1:500) or TRITC-phalloidin (1:500) were added in blocking buffer for 2 h. Coverslips were mounted with Fluoromount G on glass slides. Platelets were imaged using a Zeiss Axio Imager M2 microscope.

Adherent platelets were also imaged using superresolution structured illumination microscopy (SR-SIM) with a Zeiss ×100 oil immersion 1.46 NA lens on a Zeiss Elyra PS.1 microscope as previously described.[322] For two-channel colocalization analyses, immunofluorescence overlap was quantified using an in-house Matlab application to calculate the Pearson's coefficient as previously described.[323] Data are shown as means ± SE. Statistical analyses were performed using the two-tailed Student's *t*-test; *P* values < 0.05 were considered significant.

3.3.5 Immunoprecipitation, Ly-GDI protein capture and Western blotting

Purified platelets (0.5–1 × 10^9/ml) were incubated with the glycoprotein (GP) IIbIIIa inhibitor Integrilin (20 μg/ml) before the addition of vehicle (0.1% DMSO) or Ro 31-8220 for 10 min at room temperature. Platelets were then stimulated with CRP (10 μg/ml) for 10 min at room temperature before the addition of lysis/immunoprecipitation (IP) buffer [10 mM Tris·HCl pH 7.4, 150 mM NaCl, 2 mM EDTA, 1% (vol/vol) Triton X-100] supplemented with phenylmethylsulfonyl (PMSF) and Sigma Phosphatase Inhibitor Cocktail 3. Platelet lysates were precleared with protein A/G Sepharose and then incubated with 2 μg of RhoGDI, D4-GDI antibodies, or nonspecific IgGs overnight at 4°C. Antibody protein complexes were then captured with protein A/G PLUS-agarose beads (2 h, room temperature) and washed three times in IP buffer. RhoGDI and Ly-GDI precipitates were then eluted through the addition Laemmli sample buffer (Bio-Rad, Hercules, CA) containing 200 mM DTT. Rac1–glutathione S-transferase (GST) protein capture assays were performed as previously described.[183] Protein samples were

resolved by SDS-PAGE and transferred to polyvinylidene difluoride membranes and blotted with indicated antibodies and horseradish peroxidase-conjugated secondary antibodies. Protein was detected using enhanced chemiluminescence (Thermo Scientific).

3.3.6 Chariot antibody delivery

Chariot antibody interference experiments were performed following the methods of Diagouraga et al.[324] with minor modifications. Briefly, 2 µg of RhoGDI, Ly-GDI (D4-GDI) primary antibodies, or control IgGs were incubated with Chariot agent (2 mg/ml stock solution, diluted 1:25 with sterile H_2O before use) at room temperature for 45 min. Platelets (6×10^7/ml) were added to the Chariot antibody solution at equal volume. The platelet-Chariot-antibody solution was then incubated at 37°C for 1 h. Samples were diluted with modified Tyrode buffer at equal volume before seeding onto fibrinogen-coated glass coverslips at 37°C for 45 min. Coverslips were then washed with PBS, fixed with 4% PFA, mounted, and visualized by differential interference contrast microscopy to measure and analyze platelet surface areas and adhesion as previously described.[322]

3.3.7 In silico analyses

High-probability (low false discovery rate) predicted Ly-GDI (ARHGDIB) protein-protein interactions were determined through FpClass queries [325] for molecules with a non-

zero feature combination score and visualized as an interactome by GeNets (see https://apps.broadinstitute.org/genets). ChiBE [326] was used to query and visualize the literature-curated interaction neighborhood of Ly-GDI (ARHGDIB) in Pathway Commons [327] and Ly-GDI phosphorylations in PhosphoSitePlus [328]. The "controls-state-change-of" binary relation type to capture signaling and "in-complex-with" and "interacts-with" relation types were used to capture protein interactions, and these two interaction types were merged for simpler visualization.

3.4 Results

3.4.1 Expression of RhoGDI and Ly-GDI in human platelets

The Rho GTPases Rac1, Cdc42, and RhoA have several reported roles in platelet function, yet whether they are associated with or regulated by Rho-specific guanine nucleotide dissociation inhibitor (RhoGDI) proteins in platelets remains unexamined.[12] I first sought to determine whether platelets express RhoGDI family members, including RhoGDI and Ly-GDI. Washed human platelets were prepared from citrated whole blood from healthy donors and lysed directly into Laemmli sample buffer before SDS-PAGE and Western blot (WB) analysis for RhoGDI and Ly-GDI expression. Whole cell lysates of MDA-MB-231 cells, a breast cancer cell line that expresses functional RhoGDI as well as Ly-GDI,[329] served as a positive control for GDI protein expression and immunoreactivity. As seen in Fig. 3.1A, Western blotting determined that human

platelets express RhoGDI as well as Ly-GDI at levels similar to MDA-MB-231 cells relative to the expression of actin, which served as a loading control.

3.4.2 RhoGDI and Ly-GDI specifically distribute in platelets

To examine the expression and intracellular localization of RhoGDI and Ly-GDI proteins in platelets, I next performed immunofluorescence microscopy analyses of platelets adherent to a surface of fibrinogen. Washed human platelets were incubated on fibrinogen-coated coverglass (37°C, 45 min) before fixation, blocking and staining with RhoGDI or Ly-GDI antibodies and TRITC-phalloidin to visualize the platelet actin cytoskeleton. In platelets adherent to fibrinogen, RhoGDI showed a distributed, granular-type staining pattern, while Ly-GDI displayed an uneven or “polarized” localization, often adjacent to or emanating from the centralized platelet granulomere at nascent lamellipodia-like structures (Fig. 3.1B).

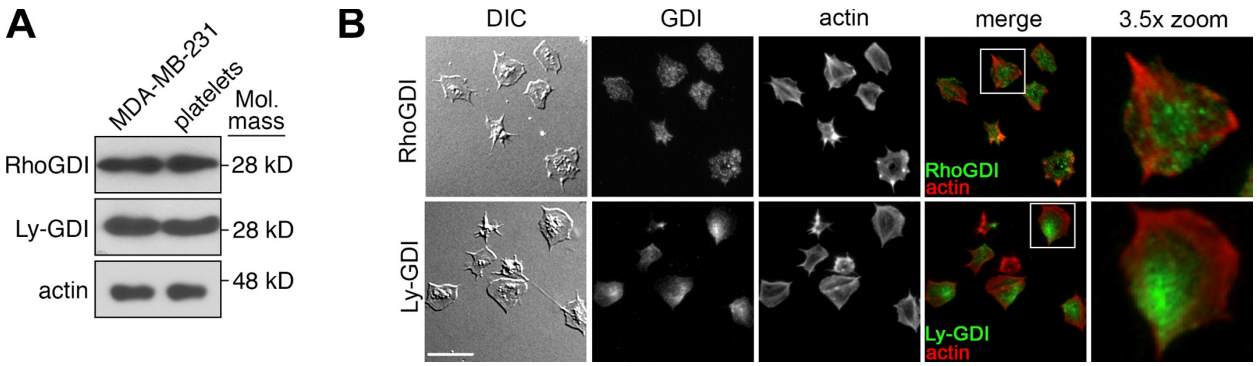

Figure 3.1. Expression and localization of RhoGDI proteins in human platelets. **A**: WB analysis of RhoGDI and Ly-GDI expression in human platelet and MDA-MB-231 cell lysates. Actin serves as a loading control. Positions of 28-kDa and 48-kDa molecular mass markers are indicated with tick marks as shown. *Data were generated by Jiaqing Pang (OHSU).* **B**: platelets were spread on glass coverslips coated with fibrinogen before fixation, blocking, and staining for RhoGDI or Ly-GDI (green) together with actin (red, stained with TRITC-phalloidin) and visualization by immunofluorescence microscopy (scale bar = 10 μm). Representative platelets (white box) from each set of staining are also shown at an enhanced ×3.5 magnification.

3.4.3 Rac1 and Cdc42 colocalize with Ly-GDI in platelets

As GDI proteins bind to Rho GTPases to sequester and release their activities at specific membrane and intracellular compartments,[170,319] I next examined the intracellular localization of RhoGDI or Ly-GDI together with the Rho GTPases Rac1, Cdc42, or RhoA in fibrinogen-bound platelets by immunofluorescence superresolution structured illumination microscopy (SR-SIM). Cdc42 and Rac1 showed minimal overlap with RhoGDI in platelets spread on fibrinogen (Fig. 3.2A). Interestingly, Rac1 and Cdc42 both showed a polarized distribution largely overlapping with Ly-GDI and suggestive of structural elements (Fig. 3.2B) resembling the localization of microtubules in platelets adherent to fibrinogen, as previously described.[330-335] Unlike Cdc42 and Rac1, however, RhoA showed a more evenly distributed staining pattern throughout the platelet cell body that did not overlap with RhoGDI or Ly-GDI (Fig. 3.2, A–C). Pearson's correlation-based colocalization analyses revealed more colocalization between Ly-GDI and Rac1 as well as Ly-GDI and Cdc42 (Fig. 3.2D) relative to RhoGDI and the Rho GTPases (Fig. 3.2D). Pearson's analyses also supported a greater extent of colocalization between Rac1 and GDI proteins in general compared with Cdc42 in a manner reflective of the qualitatively more structured organization of Cdc42 in adherent platelets (Fig. 3.2, C and D). As a functional control to confirm that platelet Ly-GDI can interact with Rho GTPases, I captured Ly-GDI protein from platelet lysates with immobilized Rac1-GST protein. As seen in Fig. 3.2E, GST-Rac1 captured Ly-GDI from resting as well as CRP-stimulated platelet lysates at equivalent levels, consistent with

the role of Ly-GDI in Rho GTPase sequestration. GST protein alone failed to capture any detectable Ly-GDI protein from platelet lysates (Fig. 3.2E).

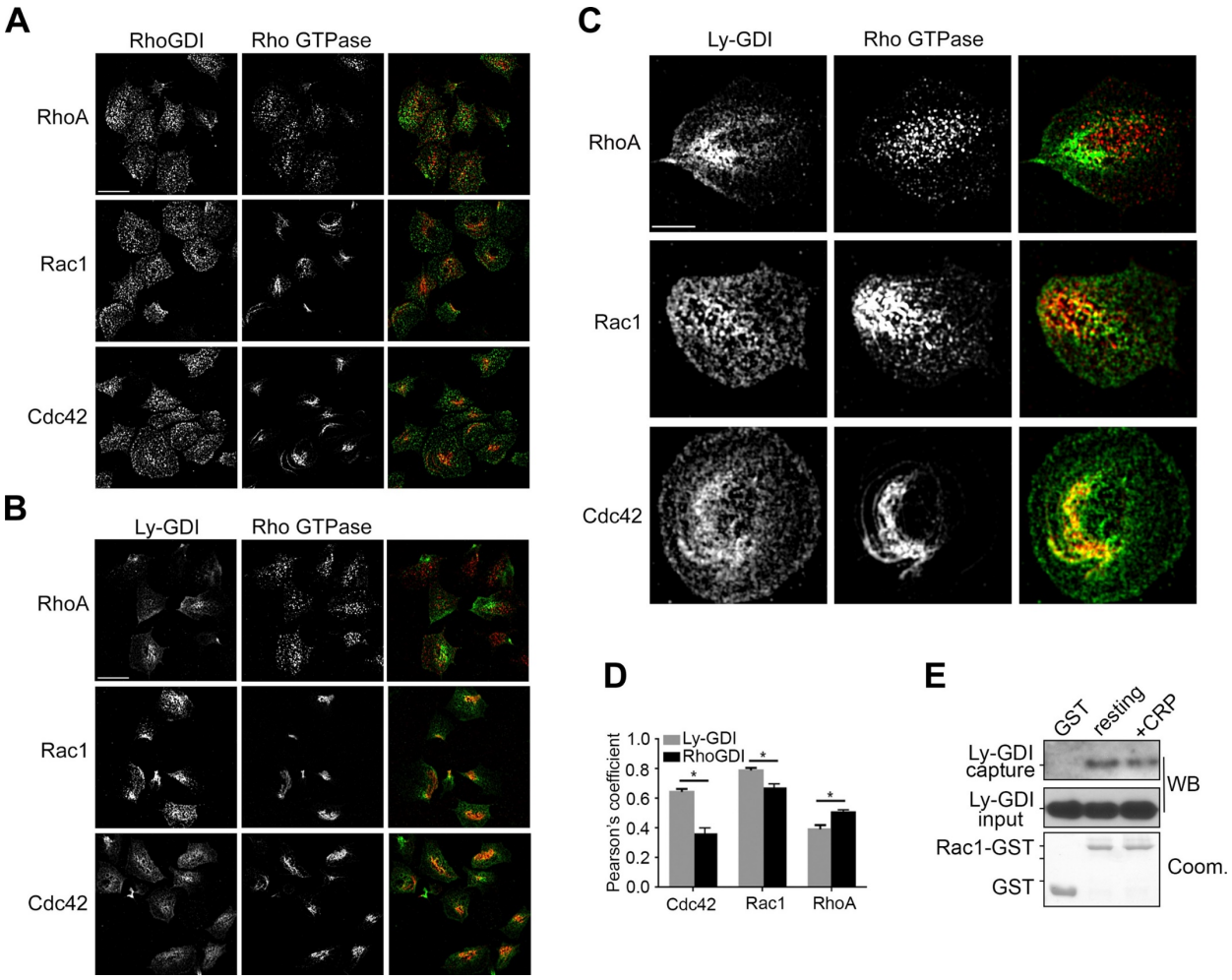

Figure 3.2. Localization of RhoGDI and Ly-GDI with Rac1 and Cdc42 in platelets adherent to fibrinogen.
A and **B**: platelets were spread on glass coverslips coated with fibrinogen before fixation, blocking, and staining for RhoGDI (**A**) or Ly-GDI (green) (**B**) together with Rac1, Cdc42, or RhoA (red) and visualization by SR-SIM (scale bar = 2 μm). **C**: magnified images of individual platelets representative of the colocalization of Ly-GDI (green) and RhoA, Rac1, or Cdc42 (red) (scale bar = 2 μm). **D**: Pearson's correlation of GDI and Rho GTPase overlay demonstrates significantly increased colocalization of Ly-GDI and Rac1 or Cdc42 relative to RhoGDI; determined by Student's t-test, and *P < 0.05. **E**: Ly-GDI protein capture by Rac1-GST and GST alone from resting and CRP-activated platelet lysates analyzed by WB. For WB panels, tick marks indicate position of 28-kDa molecular mass marker. GST protein loading for protein capture shown by PAGE and Coomassie (Coom.) staining. For the Comassie gel, the tick marks indicate position of 28 kDa (bottom), 35-kDa (middle), and 48-kDa (top) molecular mass markers. *Data were generated by Jiaqing Pang (OHSU).*

3.4.4 Ly-GDI colocalizes with polarized cytoskeletal elements in platelets

Recent models of platelet function suggest a polarized role for Rho GTPase activities in platelet attachment, spreading, and secretion during hemostatic plug or thrombus formation,[304,336,337] but cell biological mechanisms to account for polarized Rho GTPase activities have not yet been set forth. Intriguingly, the microtubules of adherent platelets, originating from a specific unwinding and reorganization of the marginal band during activation,[324,338-340] often show a shifted or polarized distribution as platelets spread on surfaces such as fibrinogen.[335] I therefore next examined whether Ly-GDI colocalized with microtubules in platelets. Platelets adherent to fibrinogen were stained for Ly-GDI and α-tubulin and processed for immunofluorescence microscopy. As seen in Fig. 3.3A, the microtubules in platelets adherent to fibrinogen displayed a partially unwound structure shifted in a polarized-like manner. Costaining experiments demonstrated a colocalization of these polarized microtubules together with Ly-GDI (Fig. 3.3A). Superresolution microscopy studies further supported a specific colocalization of Ly-GDI together with specific microtubule structures (Fig. 3.3B). To further investigate the punctate, granular-like staining pattern of RhoGDI, I next examined the colocalization of RhoGDI or Ly-GDI together with the α-granule marker P-selectin. As seen in Fig. 3.3C, Ly-GDI staining showed relatively more overlap with P-selectin compared with RhoGDI. RhoGDI and Ly-GDI showed minimal colocalization with the platelet integrin β_3 (Fig. 3.3D).

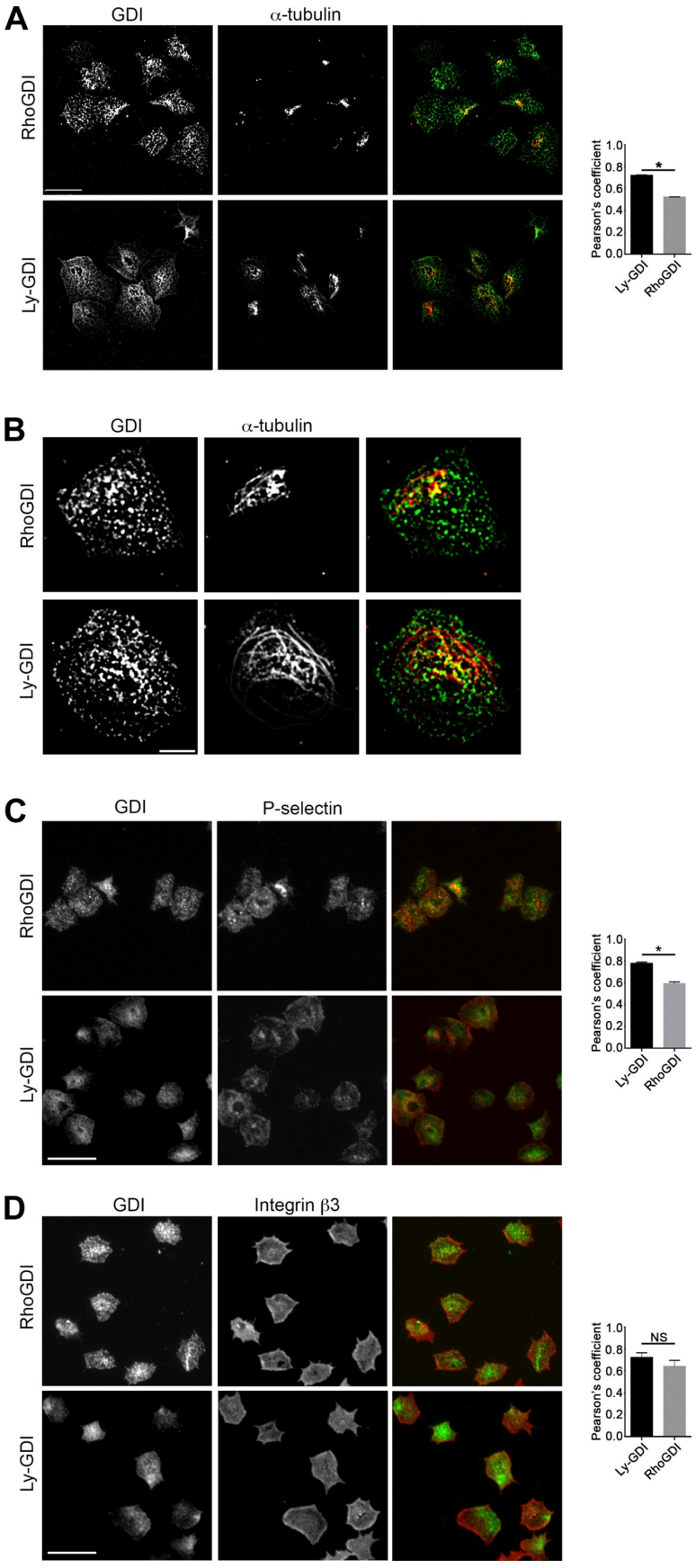

Figure 3.3. Localization of RhoGDIs with structural elements in platelets adherent to fibrinogen.
A: platelets were spread on glass coverslips coated with fibrinogen before fixation, blocking, and staining for RhoGDI or Ly-GDI (green) and α-tubulin (red) and visualization by SR-SIM (scale bar = 2 μm). Pearson's correlation reveals significantly increased colocalization of Ly-GDI and α-tubulin relative to RhoGDI and α-tubulin (indicated by *).
B: magnified images of individual platelets representative of the colocalization RhoGDI or Ly-GDI (green) and α-tubulin (scale bar = 2 μm).
C and **D**: other sets of coverslips were stained for RhoGDI or Ly-GDI (green) together with the platelet α-granule marker P-selectin (red) (**C**) and integrin β3 (red) (**D**) and visualized by conventional fluorescence microscopy (scale bar = 10 μm).

3.4.5 Ly-GDI interference inhibits platelet spreading

The localization of Ly-GDI together with Rac1 and Cdc42 at polarized cytoskeletal elements suggested a role for Ly-GDI in the sequestration, localization, and regulation of Rho GTPase function in platelets. Accordingly, I next sought to examine whether interfering with Ly-GDI or RhoGDI would impact platelet function. To interfere with RhoGDI accessibility and any putative Rho GTPase–associated functions in platelets, a Chariot agent permeabilization protocol [324] was used to introduce antibodies that bind to the NH_2 terminal, Rho GTPase binding domains of RhoGDI or Ly-GDI into live, washed human platelets before spreading on fibrinogen-coated coverslips. As seen in Fig. 3.4, A and B, Chariot-permeabilized platelets treated with nonspecific IgGs or RhoGDI antibodies spread on fibrinogen normally with mean surface areas of 20.7 ± 0.23 μm^2 and 22.7 ± 1.69 μm^2, respectively; in contrast, treatment of platelets with anti-Ly-GDI antibodies dramatically reduced spreading on fibrinogen (9.48 ± 0.71 μm^2). Chariot-permeabilized platelets treated with Ly-GDI antisera also exhibited a reduced binding to fibrinogen (24.7 ± 2.91 bound platelets per field vs. 69.7 ± 15.5 and 65.3 ± 11.7 bound platelets per field for IgG and anti-RhoGDI-treated platelets, respectively).

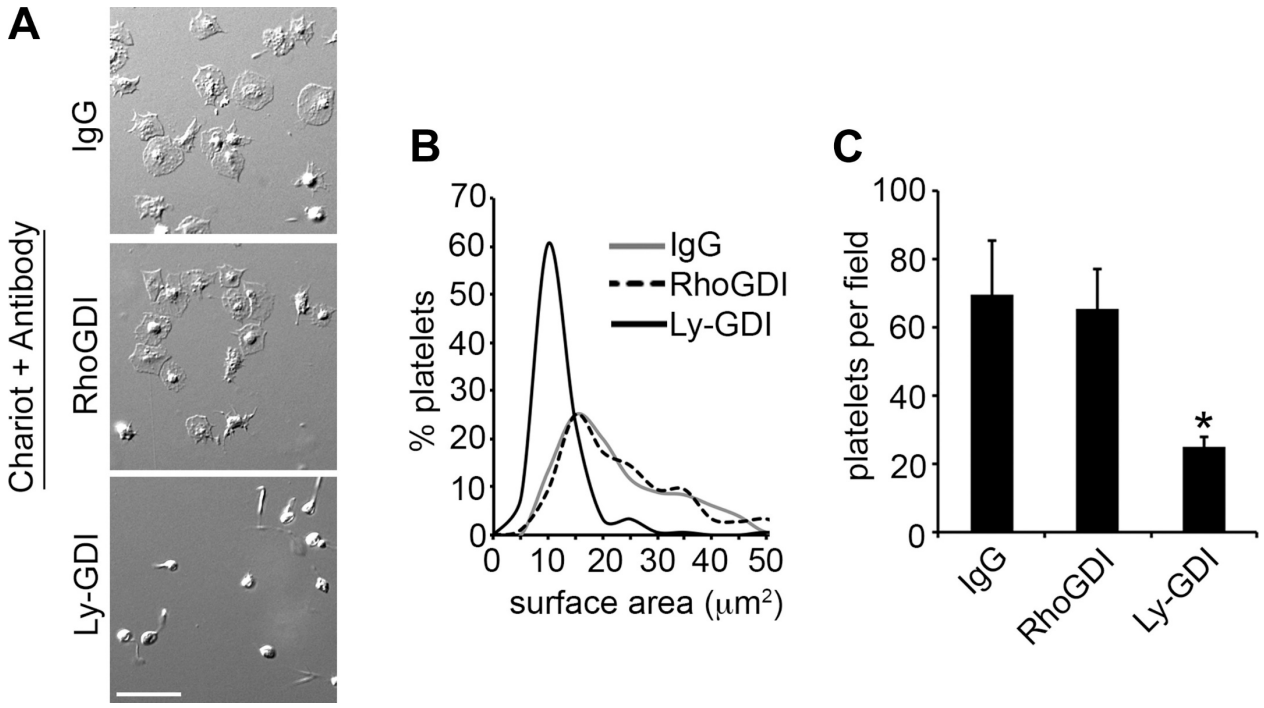

Figure 3.4. Ly-GDI interference inhibits platelet spreading on fibrinogen. Antibodies directed against the NH_2-terminal Rho GTPase binding domains of RhoGDI or Ly-GDI or control IgGs were introduced into washed human platelets using the Chariot system. **A–C**: platelets were spread on fibrinogen-coated coverglass for 45 min before fixation, mounting, and visualization by DIC Nomarski microscopy (**A**) to assess the statistical distribution of surface areas of platelets adherent to fibrinogen (**B**) and to quantify the numbers of adherent platelets per field (**C**). Scale bar = 10 μm.

3.4.6 Ly-GDI phosphorylation in platelet activation

A number of signaling proteins such as the Src family tyrosine kinases and the p21-activated kinases serve regulatory roles in platelets upstream and downstream of Rac1-GTP and Cdc42-GTP formation, respectively.[12,319] However, in platelets, Rac1 and Cdc42 themselves are not typically regulated by phosphorylation, but rely on the phosphorylation of regulatory proteins such as GEFs and GAPs to translate intracellular signals into Rho GTPase functional outputs. To begin to investigate and visualize how Ly-GDI may regulate platelet function mechanistically, I next examined Ly-GDI protein-protein interactions and functional covalent modifications using both predicative and curated bioinformatics tools. An in silico analysis of Ly-GDI (termed “ARHGDIB”) binding partners based on modeled, folded domain structures using FpClass predicted 19 high-probability protein-protein interactions with Rac1, Cdc42, and RhoA as well as several other Rho GTPases and Rho GTPase regulators such as Vav1 (Fig. 3.5A). These and other functional interactions were additionally evident in curated protein interaction data in Pathway Commons, which also suggested roles for Caspase-3 (Fig. 3.5B) as well as specific protein kinases (PKCα, Src) in Ly-GDI regulation (Fig. 3.5, B and C).

To investigate whether RhoGDI and Ly-GDI serve as substrates of these kinases with known roles in Rac1 and Cdc42 regulation in the platelet activation program, I next examined the phosphorylation status of RhoGDI and Ly-GDI in resting and CRP-stimulated platelets by Western blot analysis following Ly-GDI immunoprecipitation.

Washed human platelets were treated with the GPVI-specific agonist CRP for 10 min before lysis into IP buffer and immunocapture with RhoGDI, Ly-GDI or control IgG antisera. After protein A/G agarose precipitation, Western blot analysis revealed that Ly-GDI was readily captured from platelet lysates (Fig. 3.5D). Western blotting with antisera directed against phosphorylated consensus protein kinase C (PKC) (R/KXpSX[R/K]) substrate motifs determined that Ly-GDI was phosphorylated at PKC motifs following stimulation with CRP. Although Ly-GDI has been previously reported to be regulated by tyrosine phosphorylation in other cellular systems to influence physiological processes such as cancer cell metastasis,[341] no tyrosine phosphorylation of platelet Ly-GDI was detectable by IP and Western blot analysis with 4G10 antisera under the conditions of my study (data not shown). Similarly, I did not detect any caspase-mediated proteolysis of Ly-GDI in CRP-activated platelets using antisera that specifically recognize the cleaved form of Ly-GDI (data not shown). While RhoGDI readily precipitated from platelet lysates, no phosphorylation of the platelet RhoGDI protein was detected by Western blot analysis under the conditions described (data not shown).

The detected phosphorylation of Ly-GDI at PKC motifs raised the possibility that PKC may also localize with Ly-GDI to regulate platelet function. Accordingly, I next examined the localization of Ly-GDI together with PKC in platelets adherent to fibrinogen. While PKC showed some colocalization with RhoGDI, Ly-GDI colocalized more significantly with PKC in adherent platelets in a polarized manner as determined by fluorescence microscopy (Fig. 3.5E), SR-SIM (Fig. 3.5F), and Pearson's correlation analyses.

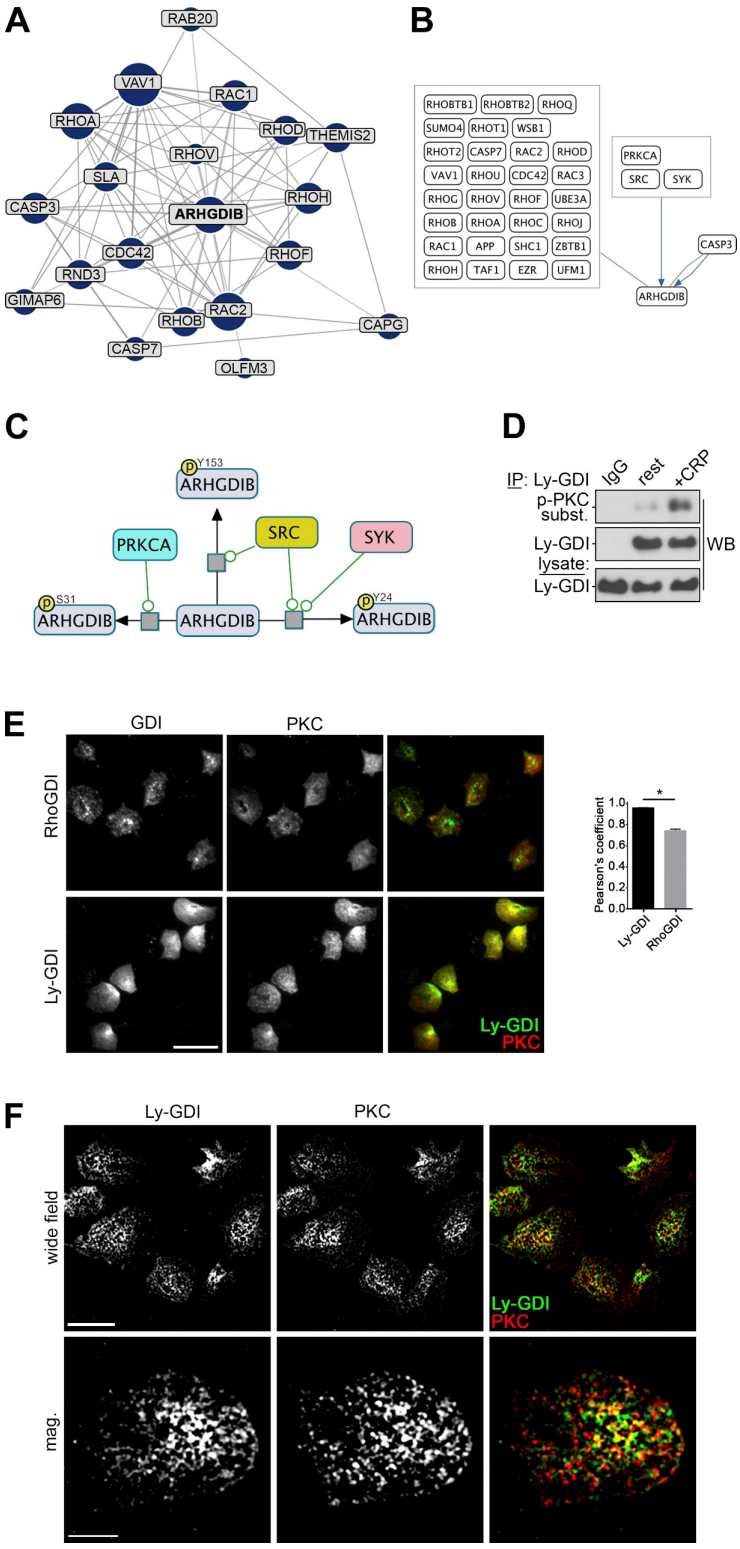

Figure 3.5. Ly-GDI is phosphorylated at PKC substrate motifs following platelet activation and colocalizes with PKC in platelets.
A: FpClass predicted interaction partners for Ly-GDI (ARHGDIB). **B**: Neighborhoods of curated Ly-GDI interaction partners and regulatory proteins. Directed edges (arrows) indicate signaling steps and undirected edges indicate protein interactions. **C**: ChiBE "detailed view" of the specific phosphorylation of Ly-GDI by PKCα (PRKCA) as well as Src and Syk. *Data were generated by Dr. Ozgun Babur (OHSU)*. **D**: platelets were stimulated with CRP or vehicle alone before collection into IP buffer and immunocapture with Ly-GDI antibodies or nonspecific rabbit IgGs. After IP, protein A/G eluates were analyzed for PKC substrate phosphorylation and total Ly-GDI protein capture by WB. For WB panels, tick marks indicate position of 28-kDa molecular mass marker. *Data were generated by Jiaqing Pang (OHSU)*. **E**: platelets were spread on glass coverslips coated with fibrinogen before fixation and staining for RhoGDI or Ly-GDI (green) together with PKC (red) and visualized by conventional fluorescence microscopy (scale bar = 10 μm). Pearson's correlation reveals significantly increased colocalization of Ly-GDI and PKC relative to RhoGDI and PKC (indicated by *). **F**: wide-field (scale bar = 5 μm) and magnified (scale bar = 2 μm) SR-SIM imaging of adherent platelets stained for Ly-GDI (green) and PKC (red).

3.4.7 PKC regulates Ly-GDI phosphorylation and distribution in platelets

The colocalization of Ly-GDI with PKC suggested a role for PKC in regulating Ly-GDI function in the coordination of platelet Rho GTPase activities. To further investigate the regulation of Ly-GDI by PKC, I next examined the phosphorylation of Ly-GDI under PKC-inhibited conditions. Purified platelets were pretreated the pan-PKC inhibitor Ro 31-8220 and the PKCαβ-specific inhibitor Go 6976 or vehicle alone (0.1% DMSO) for 10 min before stimulation with CRP (10 μg/ml, 10 min), lysis into IP buffer, and immunocapture with Ly-GDI or control IgG antisera. Western blot analysis of precipitates revealed that Ly-GDI was readily enriched from platelet lysates under all treatment conditions (Fig. 3.6, A and B) and that PKC substrate phosphorylation of Ly-GDI increased following CRP treatment, but not under PKC-inhibited conditions.

To examine whether PKC influences the intracellular, polarized distribution of Ly-GDI in platelets, I visualized Ly-GDI together with actin in platelets adherent to fibrinogen under control and PKC-inhibited conditions. As seen in Fig. 3.6C, compared with vehicle alone, Ro 31-8220 and Go 6976 treatment partially inhibited platelet spreading on fibrinogen and disorganized the polarized, concentrated localization of Ly-GDI in adherent platelets, as visualized by SR-SIM and measured by the increased Pearson's correlation of Ly-GDI overlap with actin. However, PKC inhibition had no significant effect on the distribution of the Rho GTPases Rac1 and Cdc42, as also determined by SR-SIM and Pearson's correlation of Rho GTPase and Ly-GDI colocalization (Fig. 3.6D). While Ly-GDI showed a less structured and more diffuse distribution in platelets spread on fibrinogen in the presence of Ro 31-8220 and Go 6976 (Fig. 3.6, D and E),

both Rac1 and Cdc42 remained polarized, suggesting a role for PKC in spatially coordinating regulatory interactions between Ly-GDI and Rac1 or Cdc42 in activating platelets.

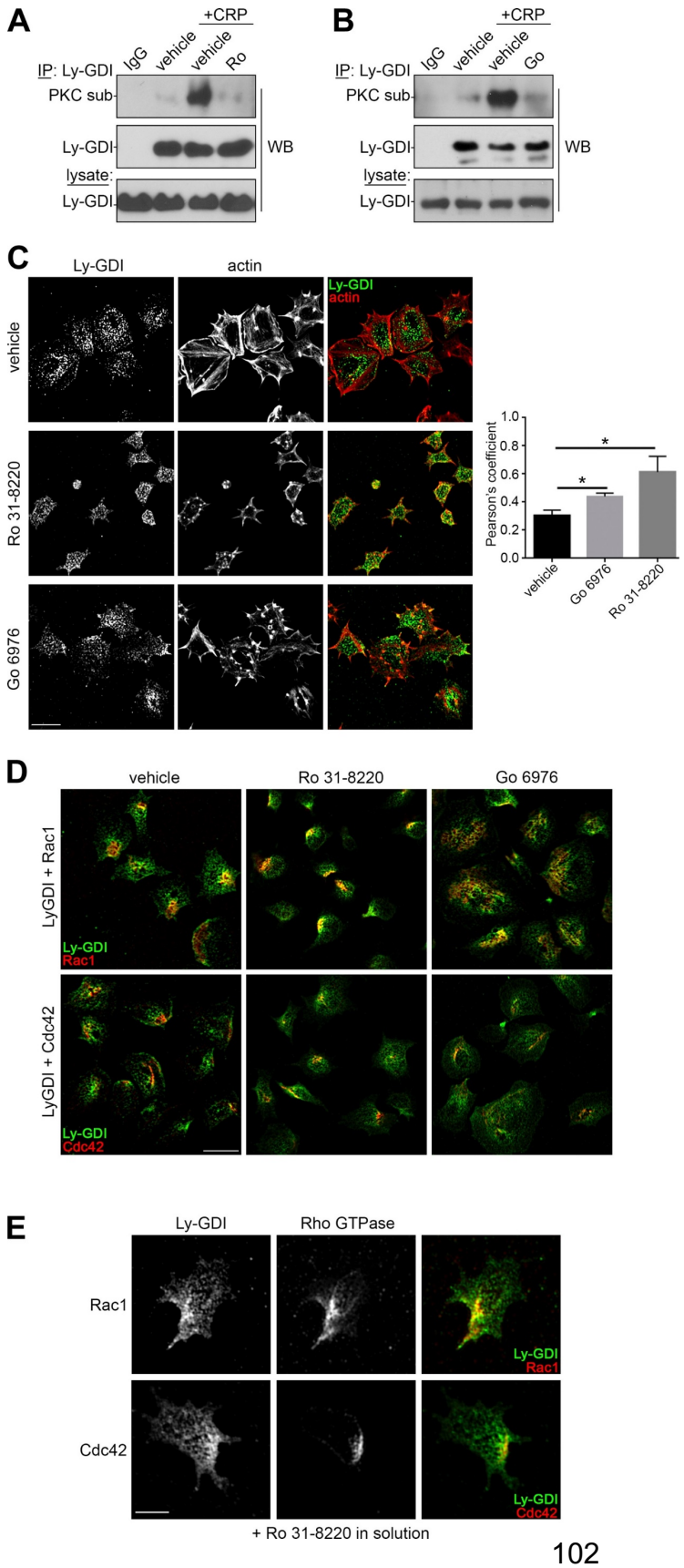

Figure 3.6. PKC inhibition blocks Ly-GDI phosphorylation and disorganizes Ly-GDI localization in adherent platelets.

A and **B**: platelets were pretreated with the PKC inhibitors Ro 31-8220 or Go 6976 or vehicle before stimulation with CRP and IP with Ly-GDI or nonspecific IgG antisera. Eluates were analyzed for PKC substrate phosphorylation and total Ly-GDI protein capture by WB. For WB panels, tick marks indicate position of 28-kDa molecular mass marker. *Data were generated by Jiaqing Pang (OHSU)*. **C**: platelets were spread on glass coverslips coated with fibrinogen before fixation and staining for Ly-GDI (green) together with actin (red) in the presence of Ro 31-8220, Go 6976, or vehicle alone (scale bar = 5 μm). Pearson's correlation of Ly-GDI and actin colocalization serves as a measure of the loss of Ly-GDI polarization. Significance (*P < 0.05) determined by Student's t-test. **D**: other sets of coverslips were stained for Ly-GDI (green) together with Rac1 (red) or Cdc42 (red) as visualized by SR-SIM (scale bar = 5 μm). **E**: representative, magnified SR-SIM visualization of Ly-GDI (green) and Rac1 (red) colocalization and distribution in platelets adherent to fibrinogen (scale bar = 2 μm).

3.5 Discussion

Here I report that platelets express the Rho-specific guanine nucleotide dissociation inhibitor proteins RhoGDI and Ly-GDI and provide data supporting roles for Ly-GDI, a GDI family member commonly found in lymphocytic and hematopoietic cells, in platelet function. I found that while platelets express both RhoGDI and Ly-GDI proteins at similar levels, these GDI proteins show distinct intracellular granular and “polarized” cytoskeletal localizations, respectively, in platelets. Ly-GDI colocalized with the Rho GTPase proteins Rac1 and Cdc42 as well as α-tubulin, consistent with a role in regulating Rho GTPase activities at areas of dynamic cytoskeletal remodeling. Antibody interference experiments also supported a role for Ly-GDI in platelet spreading and Rho GTPase function, as antibodies targeting the NH_2 terminal, Rho GTPase binding domain of Ly-GDI introduced into live, purified platelets inhibited platelet spreading on fibrinogen. Biochemical experiments demonstrated that Ly-GDI is also a target of signaling systems in the platelet activation program, including PKCs, which may promote the phosphorylation of platelet Ly-GDI directly downstream of platelet GPVI engagement or secondarily in response to the release of agonists such as ADP following CRP stimulation. In addition to Rac1 and Cdc42, cytoskeletal-associated Ly-GDI also colocalized with PKC in adherent platelets, and I found that PKC inhibition abrogated Ly-GDI phosphorylation and polarization while leaving Rac1 and Cdc42 polarization intact. Together, my results support roles for Ly-GDI in platelet function and suggest that PKC may orchestrate the regulation of Rac1 and Cdc42 in platelets

through Ly-GDI phosphorylation to spatially coordinate and fine tune Rho GTPase–associated processes during platelet activation (Fig. 3.7).

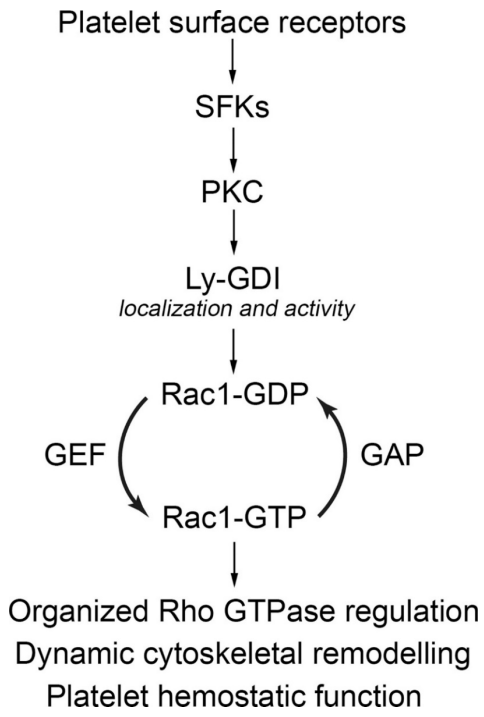

Figure 3.7. Model of hypothesized role of Ly-GDI in platelet function. After the engagement of platelet receptors (GPVI, integrin $\alpha_{IIb}\beta_3$, etc.), Src family kinases (SFKs) drive the protein kinase C (PKC)-mediated phosphorylation, activation, and localization of Ly-GDI to organize Rho GTPase (Rac1, Cdc42, etc.) activities in concert with Rho GTPase-activating proteins (GAPs) and guanine nucleotide exchange factors (GEFs) to direct cytoskeletal remodeling and platelet function.

In mammalian cells, over 20 different functionally diverse Rho GTPase proteins are regulated by ~60 different GAP and GEF proteins; yet only a total of three RhoGDI gene products serve to direct Rho GTPase activities intracellularly.[313,319] In platelets, three Rho GTPase family members, Rac1, Cdc42, and RhoA, play critical roles in platelet function. Moreover, recent studies have identified a role for Rho proteins such as RhoG in regulating platelet physiology.[12,312] While a number of signaling systems such as tyrosine kinases have been shown to regulate Rho GTPase activities in platelets and other cells, the Rho GTPases themselves are not directly regulated by phosphorylation in regards to platelet function. Accordingly, as is the case in other cell types, a number of Rho GTPase regulatory proteins most likely serve as targets of signaling pathways to mediate Rho GTPase activation, organization, and function in platelets. Notably, the Rho GEF Vav, a component of the linker for activation of T cells signalosome and target of early phosphorylation events in platelet activation, has been shown to play a role in regulating platelet Rac1 activation and platelet function.[12,94,342] Other GEFs such as phosphatidylinositol 3,4,5-triphosphate-dependent Rac exchanger, leukemia-associated RhoGEF, TIAM, p21-activated kinase-interacting exchange factor, and GIT proteins have been investigated for roles in platelet function.[12] Studies of GAPs such as IQGAP, ARHGAP17, Nadrin, and oligophrenin-1 have described functions for these proteins in platelets. Yet, despite their interactions with Rho GTPases and a number of other proteins and signaling systems critical to platelet function,[12,170,341,343,344] RhoGDIs have remained largely overlooked in studies of platelet Rho GTPase regulation. Here I find that platelets

express RhoGDI and Ly-GDI and provide data suggesting specific roles for Ly-GDI in platelet function.

In an effort to understand how platelet RhoGDI proteins may be regulated by intracellular signaling systems associated with platelet activation programs, I used a set of bioinformatics tools to determine predicted and known GDI binding partners and modifying enzymes (Fig. 3.5, A–C). PhosphoSitePlus-based Pathways Commons analyses of Ly-GDI regulation noted the regulation of Ly-GDI by PKC. In vitro IP-Western blot analyses demonstrated that Ly-GDI is phosphorylated at PKC consensus sites in activating platelets and that Ly-GDI colocalized with PKC as well as Rac1 and Cdc42 in spreading platelets, potentially linking PKC signaling to platelet Rho GTPase regulation (Fig. 3.5). In other cell types a number of regulatory mechanisms are known to converge on RhoGDIs to effect cellular outputs. For instance, prenylation serves to link RhoGDIs to specific membranes. 14-3-3 protein binding and release has also been proposed to regulate RhoGDI localization and function. Ly-GDI has also been shown to be regulated by proteolytic cleavage.[345] Reversible lysine acetylation as catalyzed by lysine acetyltransferases such as p300 and deacetylase enzymes such as histone deacetylase 6 (HDAC6) and sirtuin (SIRT) proteins have also been shown to modify RhoGDIs to regulate their function.[320] Indeed, my recent characterization of the platelet lysine acetylome identified Ly-GDI as a lysine-acetylated protein in platelets with a putative role in regulating actin-mediated platelet processes.[346,347] Future work is needed to better understand how the phosphorylation and lysine acetylation of Ly-GDI as well as specific Ly-GDI protein-protein interactions regulate platelet function.

Present models of Rho GTPases in platelet cell biological functions account for a temporal sequence of platelet activation events, specifically attachment, secretion, spreading—generally medicated by Rac1 and Cdc42—and early and late contractile events such as shape change and retraction as mediated by RhoA–Rho-associated protein kinase signaling.[12] Although the global, temporal regulation of these events in platelets has been investigated over the past decade, more recent studies suggest that platelet activation is spatially regulated to solicit specific secretory and cytoskeletal outputs within a tightly packed “core” or more loosely associated expanding “shell” of a growing hemostatic plug or thrombus.[304,336] Along these lines, hypotheses of differential Rho GTPase activation within a growing hemostatic plug or thrombus are supported by studies demonstrating that the spatial context of adhesive matrix substrates translates into specific, organized Rac1-dependent intracellular cytoskeletal and secretory platelet responses.[336,337] However, mechanisms regarding how the polarization of such signaling events may come about in platelets have not been proposed. Intriguingly, I find that Ly-GDI localizes in a polarized manner in adherent platelets, in an intracellular area overlapping with microtubules, Rac1, Cdc42, and PKC, proposing that Ly-GDI acts as a putative, spatially defined regulator of Rac1 and Cdc42 activities in platelets. Together with studies showing an organized cross talk of the platelet actin and microtubule cytoskeletons,[331,335,339,348] my findings provide insights into how signaling events may be spatially organized relative to the dynamic cytoskeleton of activating platelets through Ly-GDI in the physiological context of hemostatic plug and thrombus formation (Fig. 3.7).

Chapter 4. Platelet p38-MK2 axis phosphorylates the Bcl-xl sequestering protein RTN4 in establishing and organizing platelet procoagulant activities

Özgün Babur, Anh T. P. Ngo,* Rachel A. Rigg, Jiaqing Pang, Zhoe T. Rub, Ariana E. Buchanan, Annachiara Mitrugno, Larry L. David, Owen J. T. McCarty, Emek Demir, and Joseph E. Aslan

*In this study, I performed experiments, analyzed data, interpreted the results, prepared figures and wrote the manuscript.

This work was originally published by the *American Journal of Physiology: Cell Physiology*, 2018; 314(5): C603-C615.

4.1 Abstract

Upon encountering physiological cues associated with damaged or inflamed endothelium, blood platelets set forth intracellular responses to ultimately support hemostatic plug formation and vascular repair. To gain insights into the molecular events underlying platelet function, I used a combination of interactome, pathway analysis, and other systems biology tools to analyze associations among proteins functionally modified by reversible phosphorylation upon platelet activation. While an interaction analysis mapped out a relative organization of intracellular mediators in

platelet signaling, pathway analysis revealed directional signaling relations around protein kinase C (PKC) isoforms and mitogen-activated protein kinases (MAPKs) associated with platelet cytoskeletal dynamics, inflammatory responses, and hemostatic function. Pathway and causality analysis further suggested that platelets activate a specific p38-MK2 axis to phosphorylate RTN4 (reticulon-4, also known as Nogo), a Bcl-xl sequestration protein and critical regulator of endoplasmic reticulum (ER) physiology. In vitro, I find that platelets drive a p38-MK2-RTN4-Bcl-xl pathway associated with the regulation of the ER and platelet phosphatidylserine exposure. Together, my results support the use of pathway tools in the analysis of omics data sets as a means to help generate novel, mechanistic, and testable hypotheses for platelet studies while uncovering RTN4 as a putative regulator of platelet cell physiological responses.

Graphical Abstract

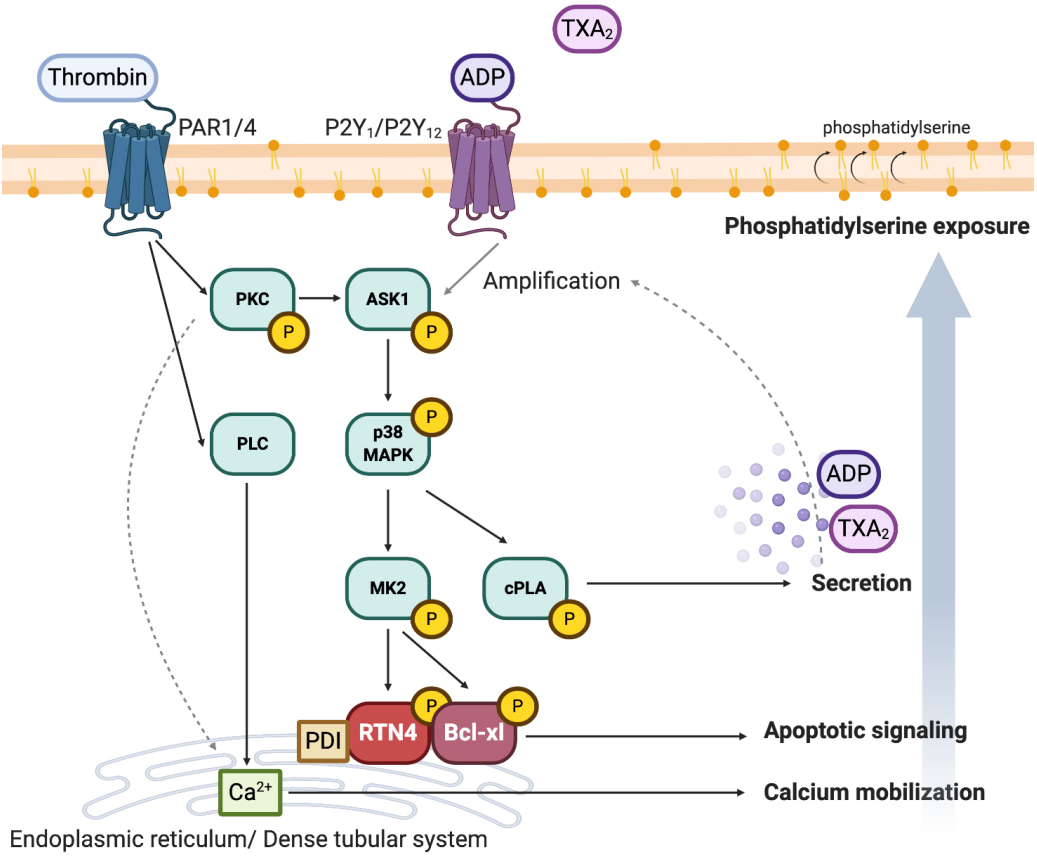

4.2 Introduction

Blood platelets are the primary cellular mediators of hemostasis and contribute to inflammation and thrombosis in vascular disease.[349,350] For over the past 20 years, biochemical and molecular studies of platelets have established critical roles for a number of intracellular signaling systems driving cell biological outputs underlying platelet function.[74,351,352]. Traditionally, mechanistic findings regarding the molecular bases of platelet physiology are built on hypothesis testing around insights afforded from the evolving literature and studies of other molecular regulatory systems generalized over a variety of other cell types. While such endeavors to define the molecular events of platelet regulation continue to be fruitful, they may be, in part, skewed by the bias of investigators or the surreptitious availability of pharmacological agents or genetically manipulated mice and typically neglect to account for how the majority of the >5,000 proteins that constitute the platelet proteome potentially contribute to platelet function.[353-356]

Concurrent with efforts to understand platelet physiology at the molecular level, a range of systems biology and omics-based projects provide an ever-growing variety of increasingly rich data sets associated with platelet physiological function.[353,356,357] Mass spectrometry-driven proteomics experiments have been especially critical in cataloging the expression and modification of platelet proteins under resting, stimulated, and disease conditions.[185,192,357] Surveying the results of platelet proteomics studies, it is immediately apparent that platelets express abundant cytoskeletal,

metabolic, and signaling proteins as well as proteins specific to platelet function and hemostasis.[192,357] More rigorous computational analyses of the platelet proteome focused on mapping physical and functional protein-protein interactions (PPIs) have additionally established that entire (sub)networks of proteins critical to G protein-coupled receptor, intracellular calcium, cyclic nucleotide and phospholipid signaling are also present in platelets and likely critical to platelet function.[353,355-357] Specialized informatics platforms such as PlateletWeb [357] now allow investigators to access and take advantage of a variety of omics data sets aimed at addressing specific questions in the context of platelet physiology; however, other systems modeling tools that take into account how exact protein phosphorylation modifications and other events are causally linked to one another remain underutilized or unavailable in platelet studies.

To better understand the molecular physiology of platelets and the biochemical pathways and systems regulating platelet function, I interrogated a set of platelet proteins functionally modified by reversible tyrosine and serine/threonine phosphorylation using a complementary set of informatics and pathway analysis tools to highlight potentially unrecognized, causal events underlying platelet biology. Using high-detail pathway information from Pathway Commons together with pathway tools such as CausalPath and ChiBE,[326,327] I find that, in addition to noting established signaling steps in platelet function, pathway resources can help to uncover novel, testable, and potentially critical relations underlying the regulation of platelet form and function. In this study, to demonstrate the utility of pathway tools in platelet studies, I present modeling and in vitro experimental findings detailing the sequential p38-MK2 phosphorylation of

the Bcl-xl sequestering protein RTN4 (also termed reticulon-4, RTN-4S, RTN-XS, Nogo, ASY; referred to as RTN4 here going forward) in regulating molecular events in platelets at the level of the endoplasmic reticulum (ER) associated with establishing and organizing platelet procoagulant activities.

4.3 Materials and Methods

4.3.1 Reagents

All reagents were from Sigma-Aldrich except as noted. Human fibrinogen was from Enzyme Research. Antibodies and other labeling agents were sourced as follows: p38 (sc-7972), Nogo/RTN4 (sc-271878), protein disulfide isomerase (PDI) (sc-20132), and mouse IgM (sc-3881) were from Santa Cruz Biotechnology; p-p38 (no. 4511), p-MK2 (no. 3007), MK2 (no. 3042), RXXpS*/T* (no. 9614), and Bcl-xl (no. 2764) were from Cell Signaling; p-Bcl-xl (44-428G) and anti-mouse IgM heavy chain horseradish peroxidase (62-6820) were from ThermoFisher; α-tubulin (T6199) and TRITC-phalloidin (P1951) were from Sigma; goat anti-mouse IgM Alexa Fluor 488 (A21042), goat anti-rabbit IgG Alexa Fluor 546 (A11010), and annexin V-Alexa Fluor 488 (A13201) were from Invitrogen (ThermoFisher Scientific). The P2Y1 antagonist MRS 2179, the P2Y12 antagonist AR-C 66096, the p38 inhibitor SB202190, and the MK2 inhibitor PF3644022 were from Tocris.

4.3.2 Interactome and neighborhood analysis

To generate protein-protein interaction (PPI) networks, I used ChiBE to query Pathway Commons. I used the “paths-between” query on the Simple Interaction Format (SIF) network, selecting “interacts-with” as the relation type, with length limit 1. For the neighborhood analysis of MK2 (MAPKAP2) and RTN4, I queried the Pathway Commons database using ChiBE in SIF mode selecting relation types “controls-state-change-of” and “in-complex-with” using length limit 1.

4.3.3 Pathway analysis

I used CausalPath to identify the pathway fragments that can directly explain correlated changes in the phosphoproteomic data set from Beck et al.[185] CausalPath first processes the Pathway Commons database [327] using the BioPAX-pattern library,[358] searching for graphical patterns that capture potential binary cause-effect relations between protein activity, abundance, and modifications. CausalPath then selects the subset of the causal relations that fit the given data. In addition to Pathway Commons data, I performed a manual literature curation for some of the phosphorylation site effects that were not covered by Pathway Commons. I used CausalPath in two modes: 1) default mode; and 2) by relaxing site-matching constraints. The site-matching constraint requires the phosphorylation site position to be mentioned in the pathway model and to match with the site position identified and measured in the phosphoproteomic data set of interest. CausalPath is available

at https://github.com/PathwayAndDataAnalysis/causalpath. CausalPath result networks are rendered with the ChiBE visualization tool,[326,359] which is available at https://github.com/PathwayCommons/chibe.

4.3.4 Platelet preparation

Washed human platelets were prepared from venous blood drawn from a rotating pool of >20 healthy, adult (>18 yr old) male and female volunteers by venipuncture into 1:10 sodium citrate (3.8%), as previously described.[13,321] Written informed consent was obtained from the subjects and the protocol was approved by Oregon Health & Science University Institutional Review Board. Blood was centrifuged at 200 *g* for 20 min to obtain platelet-rich plasma (PRP), and platelets were isolated from PRP by centrifugation at 1,000 *g* for 10 min in the presence of prostacyclin (0.1 μg/ml). Platelets were resuspended in modified HEPES/Tyrode buffer and washed once via centrifugation before resuspension in modified HEPES/Tyrode buffer. Following platelet preparation, platelet samples from different donors were not mixed or pooled for any of the experiments reported in this study.

4.3.5 Immunoprecipitation

Washed human platelets (5×10^8/ml) were pretreated with inhibitors for 10 min before stimulation with agonists as indicated. Following stimulation, platelets were lysed with the addition of 0.1% Triton X-100 together with protease and Sigma phosphatase

inhibitor cocktail 2 and 3 and sonication. Lysates were precleared with protein L agarose (4°C, 1 h) before the addition of RTN4 antibodies or mouse IgM (2 µg, 4°C, overnight). Captured proteins were precipitated with protein L agarose (Santa Cruz Biotechnology) (4°C, 2 h). Agarose beads were washed three times with HEPES/Tyrode (with 0.1% Triton X-100) before elution in Laemmli sample buffer and Western blot analysis for captured proteins. For Bcl-xl coimmunoprecipitation, platelets were incubated with 2 mM DTBP cross-linker as previously described [360] (30 min, room temperature) before lysis by sonication into 0.1% Triton X-100, immunoprecipitation, and Western blot analysis as previously described.[361] Band densitometry measurements were performed in ImageJ, and data were analyzed by one-way ANOVA with post hoc Tukey's comparison test. $P < 0.05$ was considered statistically significant for all tests. Statistical analyses were performed using GraphPad PRISM (San Diego, CA) as previously described.[361]

4.3.6 Static adhesion assays

Platelet spreading, differential interference contrast (DIC), and super resolution structured illumination microscopy (SR-SIM) microscopy experiments were carried out as previously described.[13] Briefly, for platelet spreading experiments, 12-mm no. 1.5 glass coverslips (Fisher Scientific) or coverglass-bottom dishes (MatTek) were coated with human fibrinogen (50 µg/ml) followed by surface blocking with filtered fatty acid-free BSA (5 mg/ml). Vehicle (0.1% DMSO) or pharmacological inhibitors were added to platelets in solution (2×10^7/ml) for 10 min before seeding onto immobilized surfaces at

37°C for 45 min followed by washing with PBS. Adherent platelets were fixed with 4% paraformaldehyde (PFA) at room temperature for 10 min before mounting on glass slides with Fluoromount G (Southern Biotech). Platelets were imaged using Kohler-illuminated Nomarski DIC optics with a Zeiss ×63 oil immersion 1.40 numerical aperture (NA) plan-apochromat lens on a Zeiss Axio Imager M2 microscope using Slidebook 5.5 image acquisition software (Intelligent Imaging Innovations, Denver, CO) as previously described.[13]

4.3.7 Fluorescence microscopy

Following platelet spreading and PFA fixation as above, adherent platelets were permeabilized with a blocking solution (1% BSA and 0.1% SDS in PBS). Platelets were then stained with indicated primary antibodies overnight at 4°C at a 1:100 dilution in blocking buffer. Alexa Fluor secondary antibodies (1:500) or TRITC-phalloidin (1:500) were added in blocking buffer (2 h). Coverslips were mounted with Fluoromount G on glass slides. Platelets were imaged using a Zeiss Axio Imager M2 microscope. Adherent platelets were also imaged using super resolution structured illumination microscopy (SR-SIM) with a Zeiss ×100 oil immersion 1.46-NA alpha plan-apochromat lens on a Zeiss Elyra PS.1 microscope as previously described.[322]

4.3.8 Annexin V staining of adherent platelets

Following preparation as described above, washed human platelets were pretreated with inhibitors as described and then incubated on fibrinogen-coated coverglass dishes in the presence or absence of bovine thrombin (0.25 U/ml) for 45 min at 37°C. Next, 5 µl annexin V-Alexa Fluor 488 and 2.5 mM $CaCl_2$ were added to the 100 µl platelets for an additional 30 min. Following washing in HEPES/Tyrode buffer supplemented with 2.5 mM $CaCl_2$, platelets were immediately imaged by fluorescence microscopy and DIC optics at ×63 magnification as described above.

4.3.9 Platelet secretion

Platelet secretion was measured using a plate reader-based assay of ATP released from platelet dense granules, measured as the light output generated by an ATP-luciferin-luciferase reaction as previously described.[362] Briefly, human washed platelets (2×10^8/ml) were incubated with inhibitors as indicated or vehicle alone (15 min, 37°C). Platelets were then incubated with orbital shaking in a white flat bottom 96-well plate (Corning Costar, Tewksbury, MA) in the presence of platelet agonist for 30 s at 37°C. Detection reagent Chronolume (Chrono-Log) was added to the wells and sample luminescence was detected using an Infinite M200 spectrophotometer (TECAN, Mannerdorf, Switzerland). A grouped analysis was performed using two-way ANOVA with post hoc Tukey's comparison test in GraphPad PRISM.

4.4 Results

4.4.1 Interactome analysis of the platelet phosphoproteome

Over the past several years, proteomics studies have detailed the expression and functional modification of platelet proteins in a number of contexts.[192,357,363] Recently, a systematic analysis of differentially abundant phosphoproteins in stimulated platelets revealed regulated nodes and functional subnetworks around platelet cytoskeletal dynamics, degranulation, and aggregation as well as more novel nodes suggesting roles for ubiquitin modifications and small GTPase regulatory systems in platelet regulation.[185] To determine whether a protein-protein interaction (PPI) analysis of proteins that undergo significant changes in phosphorylation can likewise provide novel insights into specific mechanistic steps underlying platelet activation, I first carried out a ChiBE-based query of databases associated with Pathway Commons—the largest detailed human pathway database indexing more than 4,000 pathways and 1.3 million genetic and protein associations and biochemical modifications, including site-specific protein phosphorylation events from a number of databases such as PhosphoSitePlus.[364] As seen in Fig. 4.1, a PPI network analysis of dynamically phosphorylated platelet proteins connects a number of established effectors of platelet function, including myosin light chain phosphatase (indicated by gene name PPP1R12A), filamin (FLNA), and protein kinase C (PKC) isoforms (PRKCD, PRKCQ). Other more novel signaling systems of emerging interest to platelet physiological studies were also apparent, including higher density nodes around the ArfGAP AGFG1, the Rac/Cdc42 GEF Cool-1/-PIX (ARHGEF7), and the mitogen-activated protein (MAP) kinase p38 (MAPK14). However, while this PPI analysis begins

to organize some novel nodes and terminal effectors into the logic of platelet regulation, it does not immediately offer directional, mechanistic details for hypothesis-driven studies of platelet function.

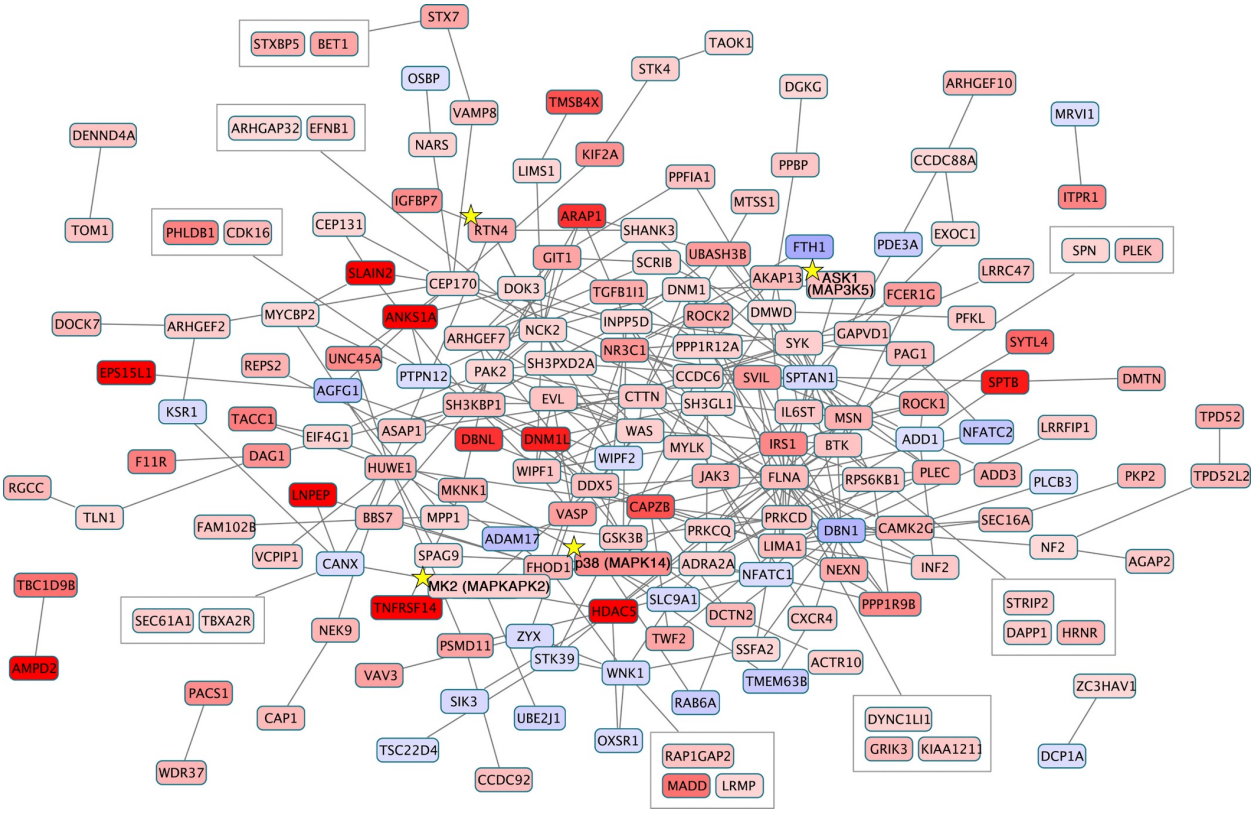

Figure 4.1. Interactome analysis of the regulated platelet phosphoproteome. A protein-protein interaction (PPI) network of dynamically regulated platelet phosphoproteins identified by Beck et al. [185] was generated from an interaction query of Pathway Commons using ChiBE. Node colors indicate the relative intensity of the reported phosphorylation change (red = increase; blue = decrease). Selected proteins of interest to this study, including the MAP kinase p38 (MAPK14), the MAP kinase-activated protein kinase MK2 (MAPKAPK2), and RTN4 are indicated with stars. *Data were generated by Dr. Ozgun Babur (OHSU).*

4.4.2 Pathway and causality analysis of platelet protein phosphorylation

In addition to building interaction networks, more specific pathway analysis tools can offer further mechanistic insights into signaling networks from omics data sets.[327,353,365] I next analyzed the set of platelet proteins modified by phosphorylation described above with CausalPath to identify potential cause-effect relations using an integration of publicly available pathway data provided by Pathway Commons.[327,365] As seen in Fig. 4.2A, a pathway model built from causal enzyme-substrate relationships recapitulated details of pathways in platelet activation downstream of platelet receptors, which feed into PKC, MAPK, and other prominent signaling systems and effectors. Notably, some nodes of this resulting model such as p38 MAPK (MAPK14) and PKC (PRKCD, PRKCQ) are centrally integrated into intracellular signaling networks associated with a diversity of platelet responses. For instance, p38 MAPK is phosphorylated and activated downstream of ASK1 (MAP3K5) activation as well as activities associated with PLCγ3, Syk, and the tyrosine kinase adaptor/scaffold protein Nck2. Following phosphorylation and activation, p38 is predicted to regulate a diverse set of substrates associated with MAPK signaling, intracellular physiology, and platelet hemostatic and procoagulant responses, including the MAP kinase-activated protein kinase MK2 (MAPKAPK2), GSK3β, and ADAM17. In addition to MAPKs and PKC isoforms, platelet activation upregulates the phosphorylation of Syk and Syk effectors associated with ITAM signaling and the LAT and PI3K signalosome (BTK, Vav3, PLCB3, DAPP1). More terminal targets downstream of several signaling systems with roles in platelet activation are also

apparent, including cytoskeletal regulators and elements such as myosin light chain kinase (MYLK), myosin phosphatase (PPP1R12A), cortactin (CTTN), moesin (MSN), zyxin (ZYX), and α-adducin (ADD1) as well as cytoskeletal-associated proteins with uncharacterized roles in platelets, including the centrosomal protein CEP131, Merlin (NF2), WAS/WASL-interacting protein WIPF1, and the actin organizing protein girdin (CCDC88A). Dynamic, feedback-like modifications on receptors and proteins associated with platelet activation as well as immunologic and metabolic processes are also apparent, including phosphorylation of thromboxane A2 receptor (TBXA2R), the disintegrin ADAM17, chemokine receptor (CXCR4), glucocorticoid receptor (NR3C1), insulin receptor substrate (IRS1), IL-6 receptor (IL6ST), and the caspase recruitment adaptor protein CARD9, which connects ITAM and Toll-like receptor (TLR) signaling in myeloid cells.[366] Interestingly, mitochondria-associated proteins, including dynamin-1-like protein (DNM1L) and the neurite outgrowth inhibitor protein RTN4, were also integrated into select pathways. Other proteins with more traditional roles in the nucleus were modified within the pathway context of platelet activation, including NFATC1, NFATC2, and DDX5. Together, this analysis suggested a concerted association between a number of platelet cytoskeletal, secretory, and inflammatory outputs associated with PKC, MAPK, and other signaling systems, offering a means and rationale to build and test novel hypotheses potentially relevant to platelet physiology not immediately apparent by other analyses.

Next, to extract more specific mechanistic information, I included a phosphorylation site matching requirement between detected phosphorylation sites and the sites in the

pathway model, to generate a higher-confidence subgraph of the pathway network in Fig. 4.2A. As seen in Fig. 4.2B, in addition to highlighting cascades terminating in NFATC1, NFATC2, cortactin, and CXCR4 phosphorylation, this analysis predicted a specific MAPK signaling axis (ASK1 Ser_{1033}→p38 Thr_{180},Tyr_{182}→MK2 Thr_{334}) resulting in the phosphorylation of RTN4 Ser_{107}. Together, these models demonstrate that pathway analysis of phosphoproteomics data can predict causal, mechanistic information around regulators and effectors of platelet activation.

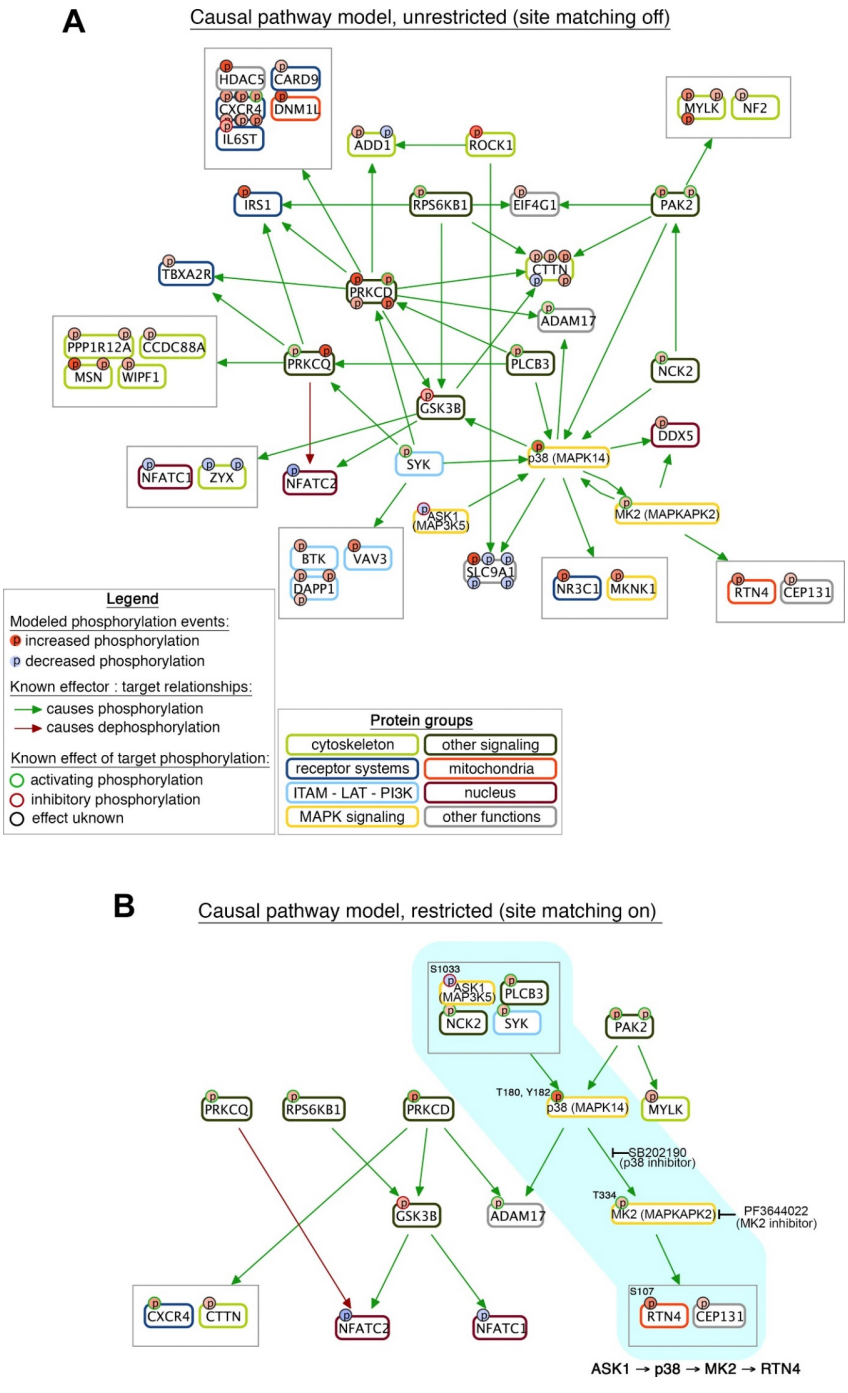

Figure 4.2. Pathway and causality analysis of the activated platelet phosphoproteome. Results from CausalPath identifying pathway fragments and associated changes in platelet protein phosphorylation to show potential cause-effect relations as visualized with ChiBE. The unrestricted model in **(A)** is based on generalized enzyme:substrate relations, independent of phosphorylation site localization details. The stringent model in **(B)** requires the matching of enzymatic events with phosphorylation site details. This model highlights a putative p38→MK2→RTN4 axis associated with platelet activation (light blue background). Nodes represent proteins (conventionally labeled with gene names), and edges represent either causal phosphorylation (green) or dephosphorylation (red) events. Protein phosphorylation sites are shown with smaller "p" circles, where a green border = activating site and red border = inactivating site. The background color of phosphorylation sites indicates their differential measurement from data, red = increase and blue = decrease. The grouped nodes in a compound node indicate that all members have the same graph topology and are grouped for complexity management. Relative targets of the p38 inhibitor (SB202190) and MK2 inhibitor (PF3644022) used in this study are indicated in the context of this model. *Data were generated by Dr. Ozgun Babur (OHSU).*

4.4.3 p38 and MK2 activation and function in platelets

The biology associated with p38 MAPK signaling in platelets is complex, as a variety of agonists and physiological stimuli are well known to upregulate the phosphorylation of p38 and p38 substrates in platelets, yet specific functions for platelet p38 remain unclear.[367] While p38 Thr_{180},Tyr_{182} phosphorylation has been extensively documented in platelets under a number of experimental conditions, limited details are known regarding the phosphoregulation of the p38 substrate MK2 in platelets. As a first step in determining whether the causal pathway model above reflects and predicts signaling relations in platelets, I next examined platelet p38-MK2 activation and signaling in vitro using biochemical and cell biological methods. Washed human platelets (5×10^8/ml) were pretreated with pharmacological inhibitors of p38-associated signaling pathways or vehicle alone (0.1% DMSO) and stimulated with thrombin (0.5 U/ml, 5 min) before lysis in Laemmli sample buffer, separation by SDS-PAGE, and Western blot analysis with p38 Thr_{180},Tyr_{182} and MK2 Thr_{334} phosphospecific antisera. As seen in Fig. 4.3, A and B, thrombin stimulation significantly upregulated p38 as well as MK2 phosphorylation ($P = 0.0036$ and $P = 0.0001$, respectively), as determined by Western blot analysis of platelet lysates with p38 and MK2 phosphorylation site-specific antisera. Pretreatment of platelets with the p38 inhibitor SB202190 (2 μM, previously reported to inhibit p38 activity in platelets [368]) significantly abolished the p38-driven phosphorylation of MK2 Thr_{334} in response to thrombin stimulation with minimal effects on the upstream phosphorylation of p38 itself at Thr_{180},Tyr_{182}. Likewise, pretreatment of platelets with the MK2 inhibitor PF3644022 significantly limited the phosphorylation of

MK2. As seen in Fig. 4.3, A and B, pretreatment with of platelets with PF3644022 also appeared to have some minor although not statistically significant inhibitory effects on p38 phosphorylation in response to thrombin, consistent with previous reports in other cell types suggesting a feedback interaction between MK2 and p38 activation.[369,370] In vivo, in addition to serving as a chemotactic agent that activates platelets at select sites of injury or inflammation in the vasculature, ADP is secreted by platelets and binds to purinergic $P2Y_1$ and $P2Y_{12}$ G protein-coupled receptors.[371] Consequently, ADP amplifies platelet responses in response to physiological agonists such as thrombin downstream of protease-activated receptors (PARs) to support a number of cell biological outputs associated with p38 activation, including “inside-out” activation of integrins, thromboxane generation, procoagulant phosphatidylserine (PS) exposure, thrombin generation, and other platelet functional outputs.[371] Accordingly, I also examined the phosphorylation states of p38 and MK2 in platelets under P2Y1/P2Y12-inhibited conditions. As seen in Fig. 4.3, A and B, combined pretreatment of platelets with the P2Y1/P2Y12 antagonists MRS 2179 (10 μM) and AR-C 66096 (10 μM) significantly inhibited the phosphorylation of p38 as well as MK2 in response to thrombin. Together, these results show that following stimulation with thrombin, platelets phosphorylate MK2 Thr_{334} in a manner dependent on p38 activity as well as purinergic signaling.

Previous studies of platelet MAPKs have hypothesized roles for p38 activity in platelet secretion downstream of phospholipase A (cPLA2) phosphorylation, as p38 inhibition or ASK1 genetic deletion inhibits secretion in response to various platelet

agonists.[368,372,373] To investigate roles for p38 and MK2 in platelet secretion, I pretreated washed human platelets with SB202190, PF3644022, vehicle alone (0.1% DMSO), or the PKC inhibitor Ro 31-8220 before stimulation and measured ATP released from platelet dense granules with an assay of ATP-luciferin-luciferase reactivity. As seen in Fig. 4.3C, PKC and p38 inhibition both significantly impaired platelet secretion in response to thrombin stimulation; however, MK2 inhibition had no significant effect on secretion in response to thrombin (Fig. 4.3C). Roles for p38 activity in platelet cytoskeletal dynamics remain more controversial, as some studies have reported that p38 inhibition interferes with actin regulation in platelets while others conclude that p38 has no major role in the regulation of the platelet cytoskeleton.[374-376] Hence, I next examined the ability of platelets to adhere to and spread on fibrinogen and form actin-rich lamellipodia under basal as well as p38- and MK2-inhibited conditions to assay platelet cytoskeletal function. As seen in Fig. 4.3D, pretreatment of platelets with the lysine acetyltransferase inhibitor C646, a previously described inhibitor of platelet actin cytoskeletal dynamics and lamellipodia formation,[346] readily prevented the spreading of platelets on a surface of fibrinogen. Conversely, inhibition of either p38 or MK2 had no effect on the ability of platelets to adhere to and spread on immobilized fibrinogen and establish phalloidin-positive actin structures, suggesting that p38 as well as MK2 are not critical to events driving platelet cytoskeleton regulation downstream of the fibrinogen receptor integrin $\alpha_{IIb}\beta_3$. Together, these results show that platelets phosphorylate MK2 in a p38-dependent manner and that p38 activity has roles in platelet secretion independent of MK2 activation, likely

through MK2-diverging substrates such as cPLA2 that are associated with eicosanoid metabolism.

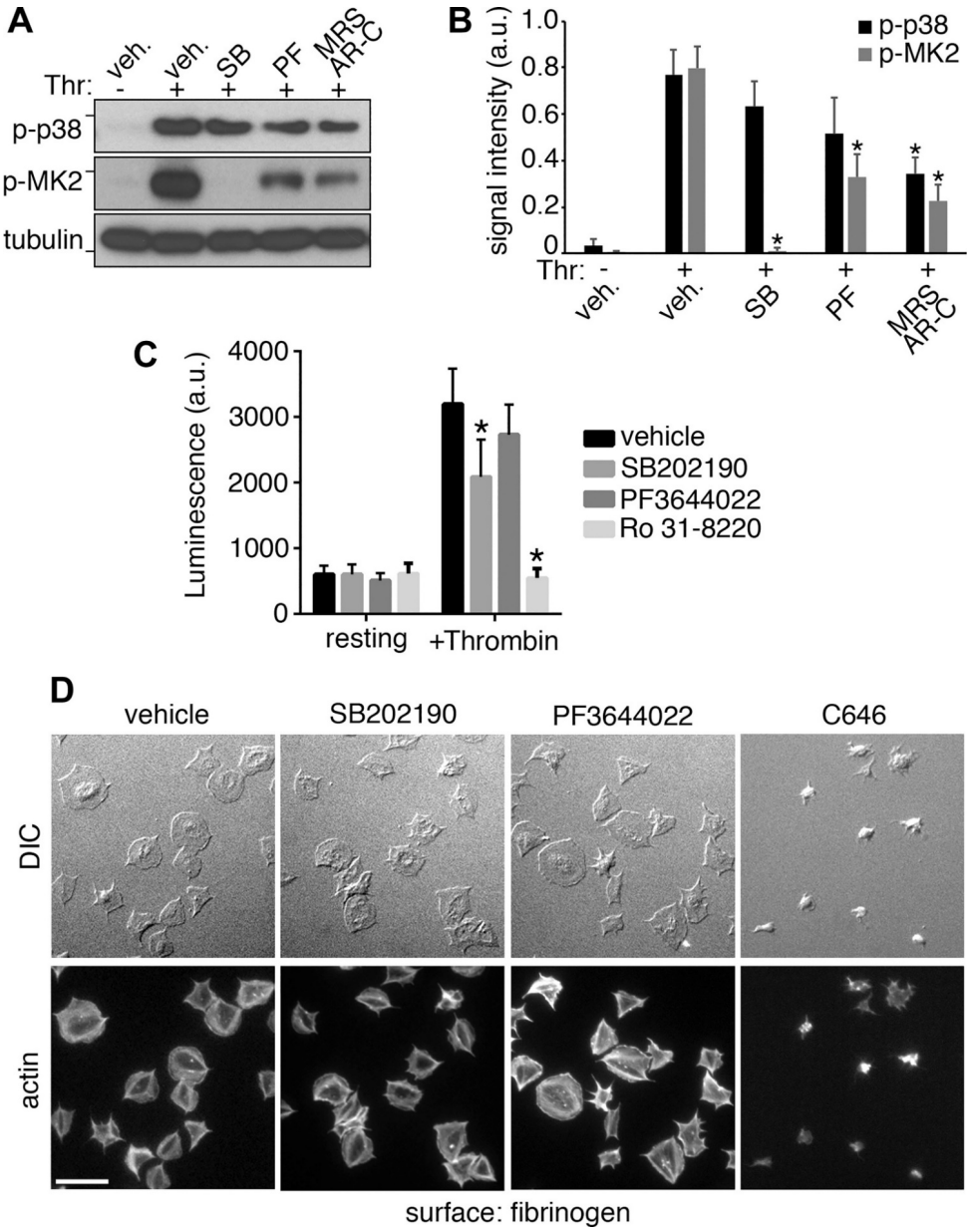

Figure 4.3. p38 and MK2 phosphorylation and function in platelets. **A**: platelets were pretreated with the p38 inhibitor SB202190, MK2 inhibitor PF3644022, a combination of the P2Y1 and P2Y12 antagonists MRS 2179 and AR-C 66096, or vehicle before stimulation with thrombin, lysis into Laemmli sample buffer and WB analysis of phospho-p38 Thr_{180},Tyr_{182} (p-p38) and phospho-MK2 Thr_{334} (p-MK2) immunoreactivity. Total α-tubulin levels serve as a loading control. Tick marks indicate the relative positions of 40-kDa MW (for p-p38) 50-kDa MW (for p-MK2 and α-tubulin). *Data were generated by Jiaqing Pang (OHSU).* **B**: densitometry analysis of p38 (black bars) and MK2 (gray bars) phosphorylation (arbitrary units; AU). *P ≤ 0.05 relative to thrombin stimulated platelets. **C**: platelets were incubated with vehicle, SB 202190, PF 3644022, or Ro 31-8220 before activation with thrombin. Platelet dense granule secretion was measured as function of ATP release generated by an ATP-luciferin-luciferase reaction. Values are mean ± SEM of raw luminescence. *P ≤ 0.05, platelets compared with vehicle in the presence of thrombin. **D**: platelets were treated with SB202190, PF3644022, the lysine acetyltransferase inhibitor C646 or vehicle before incubation on fibrinogen-coated coverglass, fixation, staining and imaging by DIC, and fluorescence microscopy (scale bar = 10 μm).

4.4.4 RTN4 expression, localization and phosphorylation in platelets

Following from functional studies of RTN4 phosphorylation by MK2 in cell line models [377] as well as >350 separate records of RTN4 Ser_{107} phosphorylation from proteomics studies curated in PhosphositePlus,[364] a causality and pathway analysis of differentially phosphorylated platelet proteins [185] through Pathway Commons revealed RTN4 as a specific, putative, and differentially active target of p38→MK2 signaling in platelets (Fig. 4.2). While proteomics studies have detected RTN4 protein in human platelets,[185,192,357] roles for RTN4 in platelet biology remain unknown. In mammalian cells, a number of RTN4 splice variants are expressed in a cell-specific manner [378] to effect specific cell biological functions, including the regulation of ER morphology, cell migration, and cell fate.[379,380] Accordingly, I next examined RTN4 expression in human platelet lysates and immunoprecipitates by Western blotting relative to nucleated MDA-MB-231 human breast adenocarcinoma epithelial cells and human umbilical vein endothelial cells (HUVECs). As seen in Fig. 4.4A, MDA-MB-231 cells, HUVECs, and washed human platelets all express abundant levels of the predominant 55-kDa Nogo-B/RTN4B isoform of RTN4. Following lysis and preclearing with protein L agarose, RTN4-immunoreactive proteins matching the molecular weight of expressed RTN4 isoforms were readily immunoprecipitated from platelets with RTN4 antisera but not with nonspecific mouse IgM (Fig. 4.4A).

To better understand potential roles for RTN4 in platelet function, I next examined the intracellular localization of RTN4 in adherent platelets by super resolution-structured

illumination microscopy (SR-SIM). As seen in Fig. 4.4B, in platelets spread on a surface of fibrinogen, RTN4 displayed a specific, reticular staining pattern similar to that observed in other cell types that partially colocalized with the platelet endoplasmic reticulum (ER) and dense tubular system (DTS) marker protein disulfide isomerase (PDI) (Fig. 4.4B). The addition of thrombin to adhering platelets, which activates phospholipases and mobilizes calcium from the ER downstream of G protein-coupled receptors, condensed the ER-like RTN4 staining pattern together with PDI, suggesting that the RTN4 protein is regulated at the platelet ER in a functional manner in the context of platelet activation (Fig. 4.4B).

To determine if an upregulation of RTN4 Ser_{107} phosphorylation following platelet activation is readily detected by more common biochemical methods, I assayed RTN4 immunoprecipitates from resting and thrombin-stimulated platelets for RXX-phosphoserine motif immunoreactivity by Western blotting. Notably, RTN4 Ser_{107} is found within an acidophilic kinase RXX**S** substrate motif (. . . A_{101}PERQP**S**$_{107}$WDP_{110} . . .) previously described using similar antisera in a number of phosphoproteomics studies from other cell and tissue types.[364] As seen in Fig. 4.4C, RTN4 was readily immunoprecipitated from resting and thrombin-stimulated platelets while nonspecific mouse IgM alone did not precipitate detectable RTN4 beyond background levels. Western blot of RTN4 immunoprecipitates with RXXp**S** motif antisera showed positive, overlapping immunoreactivity for thrombin-stimulated platelets that was not detectable on RTN4 from resting platelets (Fig. 4.4C). To examine whether RTN4 Ser_{107} is phosphorylated in a p38- and MK2-dependent manner in accordance with the site-

matched pathway model from causality analysis above, I also pretreated platelets with the p38 and MK2 inhibitors SB202190 (2 μM) or PF3644022 (2 μM), respectively, before stimulation with thrombin, lysis, RTN4 immunoprecipitation and Western blot analysis. As seen in Fig. 4.4C, pretreatment with SB202190 or PF3644022 completely abrogated RXXp**S** immunoreactivity associated with RTN4 immunoprecipitated from thrombin-stimulated platelets. Together, these results show that platelets express RTN4, which colocalizes to the platelet ER/DTS upon platelet activation, and that RTN4 is phosphorylated in platelet at an RXX**S** motif corresponding to RTN4 Ser_{107} in a p38- and MK2-dependent manner in response to thrombin stimulation.

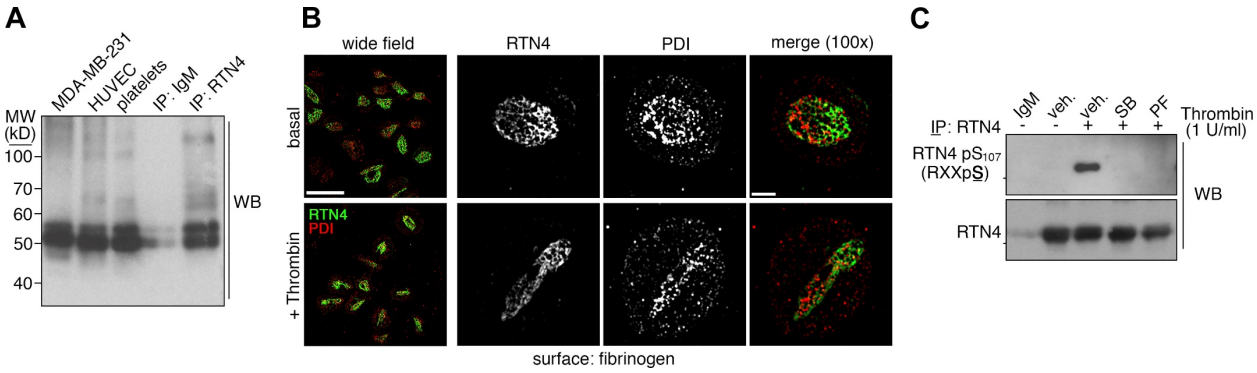

Figure 4.4. RTN4 expression, localization and phosphorylation in platelets. **A**: MDA-MB-231 cell lysates, HUVEC lysates, human platelet lysates, and RTN4 and nonspecific IgM immunoprecipitates from platelets were separated by SDS-PAGE, transferred to nitrocellulose and examined for RTN4 immunoreactivity by WB. Positions of MW markers are indicated. *Data were generated by Jiaqing Pang (OHSU).* **B**: platelets were incubated on fibrinogen-coated coverglass in the absence or presence of 1 U/ml thrombin before fixation, staining for RTN4 (green) and PDI (red), and imaging by SR-SIM at wide field (scale bar = 10 μm) and ×100 (scale bar = 2 μm) magnification. **C**: platelets were pretreated with SB202190, PF3644022 or vehicle before stimulation with thrombin and lysis. RTN4 and nonspecific IgM immunoprecipitates were examined for total RTN4 and RTN4 phospho Ser_{107} (RXXpS) immunoreactivity by WB. Tick marks indicate position of 50-kDa MW marker. *Data were generated by Jiaqing Pang (OHSU).*

4.4.5 Bcl-xl associates with RTN4, p38 and MK2 in platelets

As specific roles for RTN4 as well as MK2 in platelets have not yet been examined, I next queried Pathway Commons for proteins expressed in platelets in the physical and functional vicinities of MK2 and RTN4 to visualize a RTN4 + MK2 neighborhood with ChiBE. As seen in Fig. 4.5A, this neighborhood model places MK2 between p38 and RTN4 and notes that MK2 may change the functional state of a number of downstream targets, including RTN4 [377] as well as Bcl-xl (BCL2L1),[381] a prosurvival Bcl-2 family member well known in the regulation of mitochondria permeabilization, ER mitochondria communication, and apoptosis-related pathways in platelets regulating procoagulant phosphatidylserine exposure.[382] This model also noted that Bcl-xl has previously been described as an RTN4-interacting protein from studies of apoptosis in cell culture.[360] Accordingly, I next examined the interaction of RTN4 and Bcl-xl in platelets by coimmunoprecipitation. As seen in Fig. 4.5B, immunoprecipitation of RTN4 from resting platelet lysates readily captured RTN4 as well as coprecipitating Bcl-xl. Although not identified in platelet proteomics analyses,[185] pathway and neighborhood analyses also noted an interaction between MK2 and Bcl-xl (Fig. 4.5A), as MK2 has been reported to phosphorylate Bcl-xl Ser_{62} in vitro.[381] I next examined the phosphorylation of Bcl-xl Ser_{62} in platelets with phosphospecific antisera, finding that like RTN4, Bcl-xl is also phosphorylated in thrombin-stimulated platelets in a manner significantly inhibited by the inclusion of SB202190 or PF3644022 ($P = 0.0025$ and 0.0038, respectively) (Fig. 4.5C).

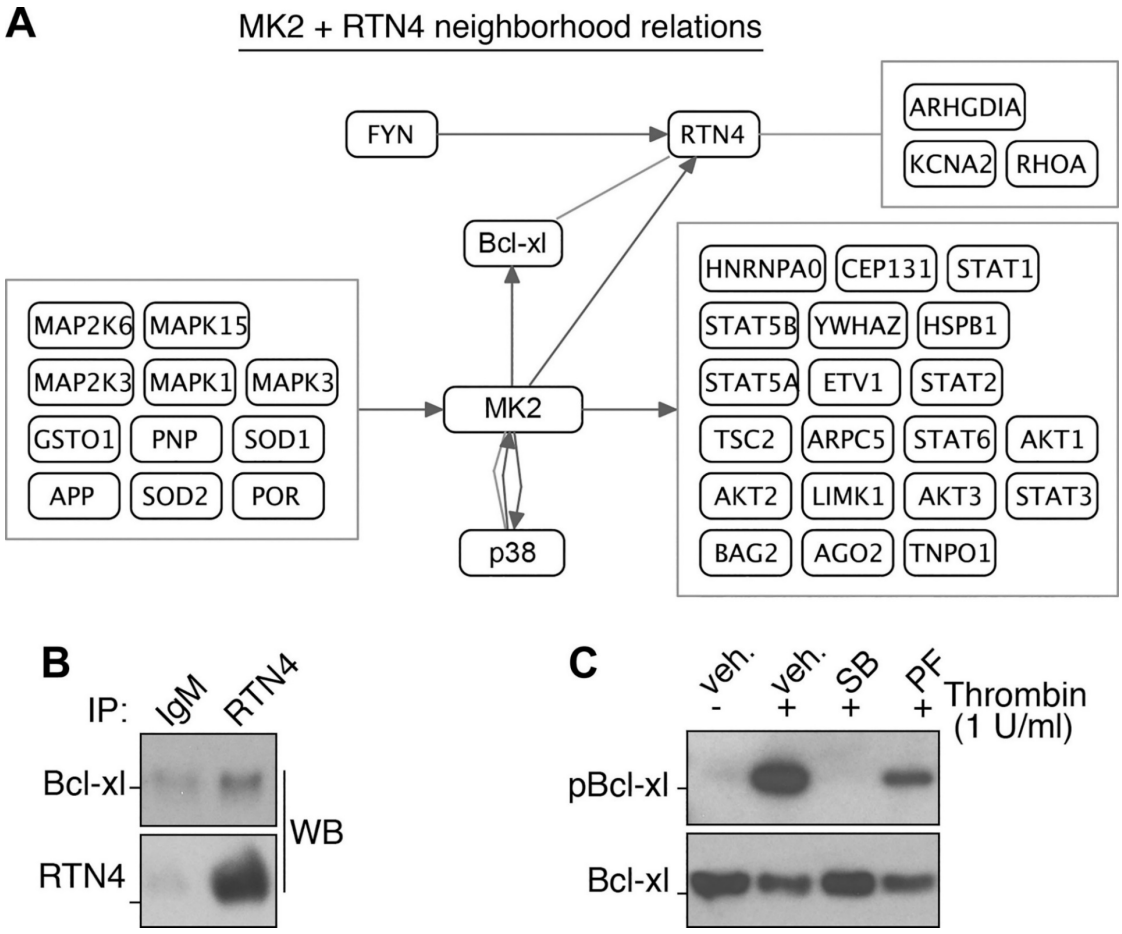

Figure 4.5. Proximity of Bcl-xl to p38, MK2, and RTN4 in platelet function.
A: signaling and protein binding relations in the neighborhood vicinity of MK2 and RTN4 in Pathway Commons, as queried and rendered by ChiBE. Directed relations (arrows) indicate that the source protein controls a state change of the target protein. A state change can be a modification on the protein, on its location, or a change to the complex that the target protein is a member. Undirected edges (connecting lines) indicate that two proteins appear as members in the same complex. *Data were generated by Dr. Ozgun Babur (OHSU).* **B**: platelets were incubated with DTBP cross-linker before lysis and processing for IP. Following IP with RTN4 or control IgM antisera, samples were analyzed for RTN4 capture and Bcl-xl coimmunoprecipitation by WB. Tick marks indicate relative positions of 30- and 50-kDa MW markers for Bcl-xl and RTN4, respectively. **C**: platelets were pretreated with SB202190, PF3644022 or vehicle before stimulation with thrombin. Following lysis into Laemmli sample buffer, samples were examined for Bcl-xl phospho-Ser_{62} (p-Bcl-xl) immunoreactivity by WB Total Bcl-xl levels serve as a control for equal protein loading. Tick marks indicate relative positions of 30-kDa MW. *WB data were generated by Jiaqing Pang (OHSU).*

4.4.6 p38-MK2 regulates the intracellular organization of RTN4 in platelets

Next, to examine the intracellular association or colocalization of RTN4 together with Bcl-xl in platelets, platelets were treated with the p38 and MK2 inhibitors SB202190 or PF3644022, respectively, or vehicle alone (0.1% DMSO) before adhering to fibrinogen in the absence or presence of thrombin and visualization by immunofluorescence SR-SIM (Fig. 4.6A). As seen in Fig. 4.6A, Bcl-xl showed a diffuse localization throughout platelets, partially colocalizing with RTN4-stained reticular structures. Similar to the results above (Fig. 4.4B), thrombin stimulation promoted the condensation of RTN4 together with Bcl-xl in the region of the platelet granulomere (Fig. 4.6A). Strikingly, p38 or MK2 inhibition had profound effects on RTN4 localization and organization under control conditions, as the ER-like RTN4-positive elements in platelets adherent to fibrinogen were severely diffused under p38- as well as MK2-inhibited conditions relative to vehicle alone. Similarly, RTN4 as well as Bcl-xl collapse was dramatically less in response to thrombin in platelets pretreated with SB202190 or PF3644022 (Fig. 4.6A).

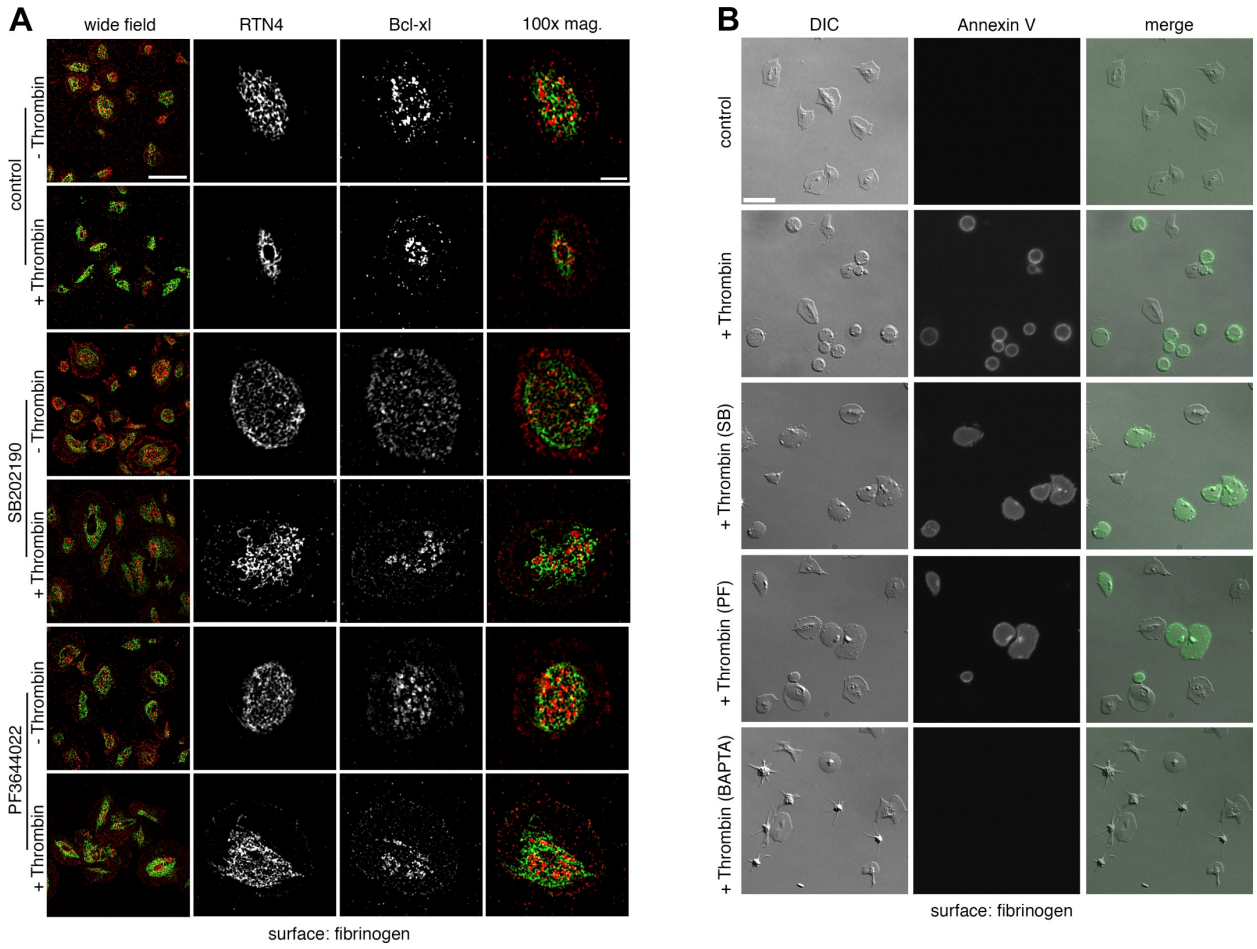

Figure 4.6. p38-MK2-RTN4-Bcl-xl axis in procoagulant platelet function.
A: platelets were pretreated with SB202190, PF3644022 or vehicle before incubation on fibrinogen-coated coverglass in the absence or presence of thrombin. Following fixation in PFA, samples were processed for SR-SIM visualization of RTN4 (green) and Bcl-xl (red) at wide field (×63, scale bar = 10 µm) and ×100 magnification (scale bar = 2 µm). **B**: platelets were pretreated with SB202190, PF3644022, the intracellular calcium chelator BAPTA or vehicle before incubation on fibrinogen-coated cover glass in the absence or presence of thrombin. Following an additional 30 min in the presence of annexin V-Alexa Fluor 488 and 2.5 mM calcium, platelets were visualized for PS exposure and general morphology by DIC and fluorescence microscopy (scale bar = 10 µm). Results are representative of *n* = 3 experiments.

The platelet ER/DTS serves as a reservoir for intracellular calcium mobilization and has critical roles in the initial steps of platelet activation as well as later phases where Bcl-xl-regulated apoptotic pathways promote platelets to take on a procoagulant phenotype through PS exposure.[71,155,383] Previous studies have demonstrated that pharmacological inhibition of p38 activity or knockout of the p38-activating MAP3K ASK1 has no significant effect on intracellular calcium mobilization.[373,374] Despite the striking alterations in RTN4-positive ER morphology under p38- and MK2-inhibited conditions, I similarly detected no alterations in intracellular calcium mobilization in Alexa Fluor 488-Fura-2-loaded platelets in response to thrombin under p38- or MK2-inhibited conditions (data not shown).

I found that calcium-dependent signaling events, specifically the activation of PKC isoforms and PKC substrate phosphorylation, can localize proximal to the platelet ER/DTS in a manner that may have roles in regulating the intracellular spatiality of platelet signaling and activation processes (see Chapter 3). While previous studies have suggested that p38 has no role in regulating phosphatidylserine exposure in response to strong platelet agonists (i.e., dual PAR + glycoprotein VI stimulation), p38 inhibitors have been noted to prevent procoagulant blebbing of platelets adherent to fibrinogen as well as PS exposure in other contexts.[384,385] Moreover, the morphology of procoagulant platelets under MK2-inhibited conditions has not yet been described. I next imaged thrombin-stimulated platelets adherent to fibrinogen for PS exposure through annexin V staining and microscopy. As seen in Fig. 4.6B, treatment of adherent platelets with 0.25 U/ml thrombin for 45 min, followed by the addition of annexin V and

2.5 mM $CaCl_2$, promoted a characteristic rounded or “ballooning”-like morphology [69] and upregulated PS exposure as determined by annexin V stain. Pretreatment of platelets with either SB202190 or PF3644022 limited the number of platelets exhibiting a rounded, PS-positive morphology associated with a procoagulant phenotype, as p38 or MK2 inhibition promoted an increase in PS-positive spread platelets, suggesting either a disruption of intracellular processes that promote procoagulant activity or kinetic delays in platelet proapoptotic signaling. Only background levels of annexin V staining were observed on platelets adherent to fibrinogen in the absence of thrombin stimulation or in the presence of the intracellular calcium chelator BAPTA (Fig. 4.6B). Together with the causal pathway model and other data detailed above, my results suggest that p38 and MK2 target RTN4 as well as Bcl-xl proximal to the platelet ER/DTS to help orchestrate platelet cell biological responses associated with platelet activation.

4.5 Discussion

Over the past decade, proteomics and informatics studies have begun to build a wealth of data associated with platelet biology in experimental and physiological contexts. In general, analyses of omics data associated with platelet physiology rely on PPI-driven tools such as STRING or PlateletWeb that cluster physical and functional protein associations to reveal network-level details underlying platelet function.[357,386] While such analyses are valuable in demonstrating the presence and organization of regulatory (sub)networks in platelets, mechanistic insights are more limited. Here, I use

a cause-effect-oriented pathway analysis approach to interrogate a set of platelet phosphoproteins regulated in response to platelet stimulation, highlighting potentially novel signaling pathways in platelet activation programs. Unlike PPI methods, this approach considers site-specific protein phosphorylation and other events driving the activation (or inhibition) of effectors that, in turn, modify and regulate other target proteins within a signaling pathway model. As an example of the utility of this approach, I identify a novel arm of a MAPK signaling network in platelets and provide mechanistic, biochemical, and cell biological evidence that p38 MAPK targets RTN4 to regulate the cellular physiology of the endoplasmic reticulum in platelet activation programs.

The causal pathway model resulting from my analysis of regulated platelet phosphoproteins noted the MAP kinase p38 (MAPK14) as a putative central, highly connected node in platelet signaling networks. Numerous studies have determined that p38 is phosphorylated and activated in platelets in a variety of contexts, yet specific roles for p38 in platelet function remain enigmatic.[367] Importantly, megakaryocyte/platelet-specific knockout models have recently demonstrated a role for platelet p38 in thrombotic and inflammatory pathologies associated with ischemia and myocardial infarction.[387] Earlier knockout studies of p38 function in platelets were hindered by embryonic lethality; however, heterozygous $p38^{+/-}$ mice exhibited reduced thrombus formation in a ferric chloride-induced model of carotid arterial injury.[388] Likewise, genetic deletion of the p38-activating MAP3K ASK1 (MAP3K5) limits platelet p38 activation, thromboxane generation, secretion, and thrombus formation.[373] Studies taking advantage of specific p38 inhibitors similarly support roles for p38 in

thromboxane generation via phosphorylation and activation of the cytosolic phospholipase cPLA2.[368,389] However, roles for p38 in platelet hemostatic function remain less apparent and controversial.[374,375,390] Using pharmacological inhibitors against p38 and MK2, I provide evidence that p38 has roles in platelet secretion independent of MK2 activation, which regulates cell physiological events at the platelet ER through the phosphorylation of RTN4 and RTN4 interactions with the antiapoptotic Bcl-2 family member Bcl-xl.

While a number of putative p38 substrates are expressed in platelets,[192,357] little is known regarding mechanistic p38 targets in platelet activation programs beyond cPLA2.[391] In addition to cPLA2, the MAP kinase-activated protein kinase MK2 has been assumed to serve as a p38 substrate with roles in platelets via the phosphorylation of the heat shock protein Hsp27;[392-394] however, evidence for MK2 phosphorylation in platelets has only been recently demonstrated.[387] In other cell types, p38 phosphorylates and activates MK2 in response to specific cellular stresses, leading to the phosphorylation of MK2 substrates such as RTN4 and Bcl-xl. Interestingly, RTN4 is also known as a Bcl-xl-interacting and sequestration protein with roles in regulating ER morphology and physiology as well as ER-mitochondria communication underlying apoptotic regulation. In platelets, the endoplasmic reticulum (often referred to as the dense tubular system, or DTS) is highly specialized and interconnected with the platelet open canicular system, microtubule cytoskeleton, and other ultrastructural components. Here I show that in response to thrombin stimulation, platelets upregulate the phosphorylation of RTN4 Ser_{107} as well as Bcl-xl Ser_{62} in a

manner dependent on p38 and MK2 activity that may organize the ER/DTS relative to the mitochondria and other intracellular targets to facilitate localized calcium signaling events that form the basis for platelet activation processes.

Given the requisite roles of RTN4 in regulating ER morphology and physiology in other cell types [395] together with the role of Bcl-xl in mediating platelet PS exposure through apoptosis-related pathways,[384,396] the p38-MK2-RTN4 axis afforded by causal pathway analysis offered an intriguing target for in vitro studies. Following activation with procoagulant stimuli, platelets elevate cytosolic calcium through a variety of mechanisms in a manner requisite for PS exposure and procoagulant activity.[383] However, the signaling mechanisms regulating and driving platelet PS exposure and procoagulant activity are unknown. Here, I show that in addition to preventing RTN4 and Bcl-xl phosphorylation in response to thrombin, inhibition of p38 and MK2 dramatically relaxed and expanded the characteristic reticular staining pattern of RTN4 in adherent platelets and altered the morphology and phosphatidylserine surface distribution of procoagulant platelets. These results suggest that p38 signaling may have specific roles in specifying the proaggretory or procoagulant fates of platelets within the context of a growing thrombus in a manner hypothesized by recent studies.[397,398] Such prohemostatic roles for p38 via MK2 and other targets would help to understand the multifaceted and disparate roles for p38 reported in the literature. In addition to better placing p38 into the context of platelet activation programs, my model and results may also help to better understand the role of p38 signaling in other contexts where RTN4 regulates vascular remodeling,[399] endothelial cell function,[400] pulmonary

hypertension,[401] and a growing list of other physiological and metabolic processes generally rooted in ER-mitochondria communication. Indeed, future efforts to investigate and target other components of the ER-mitochondria axis beyond RTN4 such as mitofusin-2 [402] and PACS-2 [403,404] may also help to advance studies of platelets for basic science and translational efforts.

Beyond roles in organizing platelet signaling in hemostasis, thrombosis, and immunity, p38 provides an interesting target for extending platelet lifetime in storage for transfusion. Indeed, a number of studies have noted that p38 is activated in stored platelets and that p38 inhibition can decrease PS exposure in aging platelets [405] as well as in response to UV treatment.[384] Interestingly, oxidative stress activates ADAM17/TACE (a p38 target noted in my pathway analysis in Fig. 4.2) and induces target receptor shedding in platelets in a p38-dependent fashion, and p38 inhibition has been suggested to increase platelet lifetime.[406] Given the predicted diverging and more specific roles of MK2 downstream of p38 described herein, MK2 inhibition may serve as a more optimal strategy to extend platelet lifetime. Even more specialized RTN4 inhibitors that disrupt ER organization in cancer cells in a manner similar to that observed in platelets with MAPK inhibition in this study may also help to limit platelet PS exposure and extend the viability of platelets in storage.[407]

In addition to the MAPK-RTN4 axis described herein, causal pathway analysis highlighted several other targets and systems of interest to platelet physiological function for future studies (Fig. 4.2). For instance, DAPP1, a recently described

component of the platelet PI3K signalosome, was noted as a functionally phosphorylated target in the context of platelet activation.[408] Furthermore, a number of receptors associated with platelet activation and inflammatory signaling are suggested to be phosphorylated in an “inside-out” signaling-like manner, including thromboxane receptor TBXAR2 as well as the disintegrin ADAM17, chemokine receptor (CXCR4), glucocorticoid receptor (NR3C1), insulin receptor substrate (IRS1), and IL-6 receptor (IL6ST). Along these lines, an ASK1-p38 axis was recently demonstrated to have a role in phosphorylating the P2Y12 receptor to support signaling processes through ADP that sustain Akt activation in platelets.[372] While my work highlights some potential novel signaling steps in platelet regulation for future studies, it should be noted that pathway models such as those generated herein are dependent on several developing factors, including advancing proteomics tools, informatics technologies, data curation methods, and the careful description and cataloging of gene/protein functions. Nonetheless, despite any current limitations, as omics tools and informatics databases continue to mature, causal pathway tools will become an invaluable tool in organizing, modeling, and discovering novel signaling routes and targets in platelets and other physiologically relevant cell and tissue systems.

Chapter 5. Distinct differences in platelet function between neonates and adults: implications for the clinical management of neonatal transfusions

Anh T. P. Ngo,* Jawaad Sheriff, Anne D. Rocheleau, Matthew Bucher, Kendra R. Jones, Anna-Liisa I. Sepp, Lisa E. Malone, Amanda Zigomalas, Alina Maloyan, Wadie F. Bahou, Danny Bluestein, Owen J. T. McCarty, and Kristina M. Haley

*In this study, I conceived and designed the research, performed experiments, analyzed data, interpreted the results, prepared figures and wrote the manuscript.

This work was originally published by *Platelets*, 2020; 31(1): 68-78.

Permission is not required by the publisher for this type of use.

5.1 Abstract

Despite the transient hyporeactivity of neonatal platelets, full-term neonates do not display a bleeding tendency, suggesting potential compensatory mechanisms which allow for balanced and efficient neonatal hemostasis. This study aimed to utilize small-volume, whole blood platelet functional assays to assess the neonatal platelet response downstream of the hemostatic platelet agonists thrombin and adenosine diphosphate (ADP). Thrombin activates platelets via the protease-activated receptors (PARs) 1 and 4, whereas ADP signals via the receptors $P2Y_1$ and $P2Y_{12}$ as a positive feedback

mediator of platelet activation. I observed that neonatal and cord blood-derived platelets exhibited diminished PAR1-mediated granule secretion and integrin activation relative to adult platelets, correlating to reduced PAR1 expression by neonatal platelets. PAR4-mediated granule secretion was blunted in neonatal platelets, correlating to lower PAR4 expression as compared to adult platelets, while PAR4-mediated GPIIb/IIIa activation was similar between neonatal and adult platelets. Under high shear stress, cord blood-derived platelets yielded similar thrombin generation rates but reduced phosphatidylserine expression as compared to adult platelets. Interestingly, I observed enhanced $P2Y_1$/$P2Y_{12}$-mediated dense granule trafficking in neonatal platelets relative to adults, although $P2Y_1$/$P2Y_{12}$ expression in neonatal, cord, and adult platelets were similar, suggesting that neonatal platelets may employ an ADP-mediated positive feedback loop as a potential compensatory mechanism for neonatal platelet hyporeactivity.

Graphical Abstract

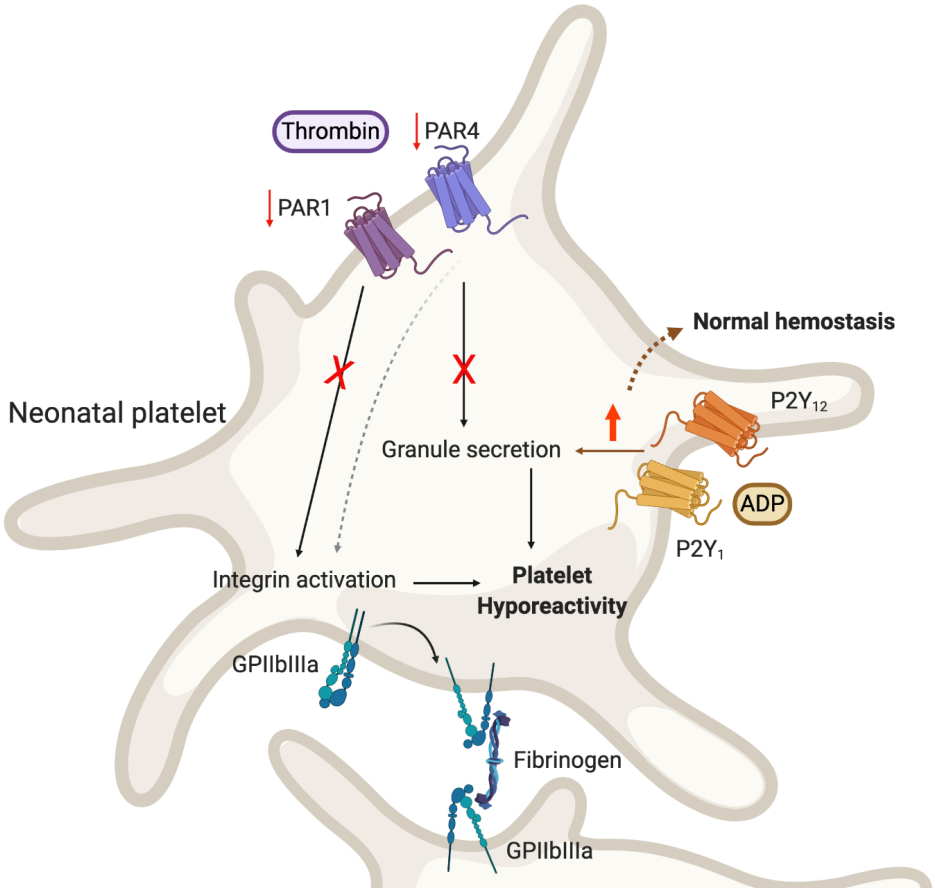

5.2 Introduction

Activation of platelets requires agonist stimulation of several G protein-coupled receptors (GPCRs), resulting in rapid calcium mobilization, α- and dense granule release, cytoskeletal reorganization, thromboxane A2 (TxA2) release, and conformational changes in the glycoprotein (GP) IIb/IIIa complex to facilitate platelet aggregation.[409] Thrombin is the most potent platelet GPCR activator, signaling through protease-activated receptors (PARs), and structural differences between PAR1 and PAR4 result in distinct functional responses in human platelets.[410] The coordinated action of PAR1 and PAR4 leads to intracellular signaling in adult platelets that is critical for the downstream secretion of adenosine diphosphate (ADP) from platelet dense granules.[409,410] ADP release results in a positive feedback loop via the GPCRs $P2Y_1$ and $P2Y_{12}$.[411] The secreted ADP activates $P2Y_1$/$P2Y_{12}$, further potentiating PAR-mediated platelet activation.[362]

As platelet $P2Y_1$/$P2Y_{12}$ receptors are known to synergize with PARs to amplify platelet activation,[362,411] several antiplatelets have been developed targeting these receptors. Clopidogrel was developed as an ADP-receptor antagonist and has been used as a successful antiplatelet therapeutic since the late 1990s; the PAR1 antagonist SCH 530348 (Vorapaxar) was developed as an antiplatelet drug, and while early clinical trials were halted due to increased major bleeding events, this drug received FDA approval in 2014 for use in reducing thrombotic cardiovascular events in patients with a history of myocardial infarction or with peripheral arterial disease.[7] As running

comparable clinical trials is not feasible in the neonatal population, the recommendations for use and dosage for antiplatelet agents are often extrapolated from studies in adults despite the fact that in pediatric patients, and in particular neonates, the hemostatic system is still maturing and the platelet response to thrombin and ADP is ill-defined.[412]

Currently, neonatal platelets are characterized as being hyporesponsive as compared to adult platelets. Several studies have linked neonantal platelet hyporesponsiveness with deficient synthesis of TxA2 [413] and impaired signal transduction downstream of TxA2 receptors,[414] impaired mobilization of intracellular calcium,[415] and decreased PAR1, PAR4,[416] and GPIIb/IIIa expression [417] levels by neonatal platelets as compared to adults. In my previous work evaluating platelet function in healthy neonates, neonatal platelet α-granule secretion and GPIIb/IIIa activation were markedly reduced in response to PAR1 stimulation while still responsive to $P2Y_1$/$P2Y_{12}$ receptor stimulation with ADP.[418] These findings suggest that PAR1-mediated responses are impaired in neonatal platelets; yet, the amplification of platelet activation via ADP feedback loop is still functional. Questions remain with regard to the potential explanation for the impaired neonatal PAR1 response, whether neonatal PAR4 response is also impaired, and the degree of PAR1 and PAR4 crosstalk with $P2Y_1$/$P2Y_{12}$ in mediating neonatal platelet activation.

Understanding the mechanisms underlying neonatal hyporeactivity is requisite in part for pediatric clinical practice to inform decisions on the management of bleeding

complications as well as management or prevention of thrombosis and use of antiplatelet agents, especially in the neonatal intensive care unit. In the present study, I set out to assess the neonatal platelet response downstream of the hemostatic platelet agonists thrombin and ADP utilizing whole-blood functional assays.

5.3 Materials and Methods

5.3.1 Reagents

All reagents were from Sigma-Aldrich except as noted. For static adhesion assays and super-resolution microscopy, anti-CD63 (MX-49) was from Santa Cruz Biotechnology (Dallas, TX, USA). Anti-MRP4 (D1Z3W) was from Cell Signaling (Danvers, MA, USA). Alexa Fluor secondary antibodies (Abs) were from Life Technologies (Carlsbad, CA, USA). ADP and TRAP-6 (SFLLRN) were from Tocris Biosience (Bristol, UK). PAR4 peptide (AYPGKF) was from Abgent (San Diego, CA, USA). For platelet receptor screening, PAR4 Abs (14H6 and 5F10) [419] were a generous gift from Dr. Marvin Nieman (Case Western Reserve University, Cleveland, OH, USA). $P2Y_1$ (APR-009) and $P2Y_{12}$ (APR-012) Abs were from Alomone Labs (Jerusalem, Israel). Flow cytometry Abs for P-selectin (CD62P), PAC-1, and phosphatidylserine (PS) (Annexin V) staining were obtained from BD Biosciences (Franklin Lakes, NJ, USA).

5.3.2 Study population

Full-term neonates were at least 38 weeks of gestational age, with APGAR scores ranging from 7 to 9 at 1 min, and 9 to 10 at 5 min. Neonates were excluded from the study if presenting with a major congenital anomaly, maternal history of diabetes mellitus, maternal history of immune thrombocytopenia, known drug or alcohol exposure, intraventricular hemorrhage, intravenous antibiotics, pre-eclampsia, or chorioamnionitis.

The adult control group consisted of self-reported healthy adults aged 18-50 years. Adults were excluded from the study if presenting with a history of abnormal hemostasis or had taken medication known to affect platelet function in the 2 weeks prior to participation. Prior to blood sample collection, consent was obtained from the adult donors and/or parents in accordance with Oregon Health and Science University and Stony Brook University Institutional Review Board-approved protocols. All blood samples were de-identified prior to sample processing.

5.3.3 Blood collection and preparation

Briefly, blood was drawn by venipuncture from healthy adult donors into sodium citrate (0.38% w/v) or 10% acid citrate dextrose (ACD-A; for shear experiments). Blood was drawn from healthy, full-term neonates at 24 h of life via heel stick into sodium citrate (0.38% w/v) following a 3-min application of an infant heel warmer. Samples were collected after obtaining blood for a newborn screen and were obtained by scooping blood from the puncture site as previously described.[418] Umbilical cord blood samples

were obtained from healthy, full-term neonates immediately after clamping post-Caesarean section delivery and mixed with sodium citrate (0.38% w/v) or citrate phosphate dextrose (for shear experiments).

After collection of cord blood samples, three suspensions were prepared: whole blood, platelet-rich plasma (PRP), and gel-filtered platelets (GFP). For high shear experiments, PRP was prepared by centrifuging whole blood for 4.5 min at 650 × g. GFP samples were prepared by filtering PRP through a column of Sepharose 2B beads into HEPES-buffered modified Tyrode's solution with 1 mM sodium citrate and 0.1% bovine serum albumin ("platelet buffer"), as previously described.[420,421] GFP and PRP were diluted to a final platelet count of 20000/μl in platelet buffer, whereas whole blood was diluted in platelet buffer in a similar proportion to that of the diluted PRP. All suspensions were mixed with 3 mM $CaCl_2$ for 10 min prior to shear experiments. Platelet suspensions were prepared in polypropylene tubes using buffer containing 0.1% bovine serum albumin and placed on a gentle rocker after recalcification to minimize contact activation effects.

5.3.4 Platelet activation in response to biochemical agonists

P-selectin and PAC-1 expression on the platelet surface were detected using fluorescence-activated cell sorting (FACS) as previously described.[418] Briefly, adult, neonatal, and cord citrated whole blood was diluted with modified HEPES/Tyrode's buffer (129 mM NaCl, 12 mM $NaHCO_3$, 2.9 mM KCl, 20 mM HEPES, 1 mM $MgCl_2$, 0.34

mM Na_2HPO_4, pH 7.3; supplemented with 5 mM glucose). Diluted whole blood was then incubated with Abs against P-selectin (Allophycocyanin [APC] CD62P) and activated integrin GPIIb/IIIa (Fluorescein isothiocyanate [FITC] PAC-1) in the presence of select agonists (10 μM ADP, 10 μM TRAP-6, 200 μM AYPGKF) or vehicle control (HEPES/Tyrode's buffer) for 20 min at room temperature (RT). BD Cytofix Buffer was added to each sample and incubated at RT for 5 min. Samples were finally diluted with PBS, measured by FACS, and analyzed using FlowJo software (Ashland, OR). A platelet-size gate was set based on forward (FSC) and side scatter (SSC) to exclude larger white blood cell and red blood cell populations. All samples were subjected to flow cytometry for the same duration, and percentage of P-selectin expression of PAC-1 binding was normalized to the total platelet count (at least 5000 platelets) detected from each sample. Nonspecific signal was eliminated using APC and FITC anti-IgG as controls.

5.3.5 Platelet dense granule secretion

ATP released from platelet dense granules was used as a surrogate marker for ADP secretion and measured as light output generated by an ATP–luciferin–luciferase reaction as previously described.[362] Briefly, adult, neonatal, and cord citrated whole blood was diluted with modified HEPES Tyrode’s buffer prior to incubation with select agonists (10 μM ADP, 10 μM TRAP-6, 200 μM AYPGKF) or vehicle (HEPES/Tyrode’s buffer) for 30 s at 37°C under orbital shaking in a white, flat bottom 96-well plate (Corning Costar, Tewksbury, MA, USA). Detection reagent Chronolume (Chrono-Log

Corporation, Havertown, PA, USA) was added to the wells and sample luminescence was immediately detected using an Infinite M200 spectrophotometer (TECAN, Mannerdorf, Switzerland).

5.3.6 Static adhesion assay and Superresolution-Structured Illumination microscopy

Glass-bottom dishes (MatTek) were coated with poly-l-lysine and washed with PBS. Vehicle (HEPES/Tyrode's buffer) or select agonists (10 μM ADP, 10 μM TRAP-6, 200 μM AYPGKF) were incubated with adult or neonate whole blood for 10 min prior to fixation with 4% paraformaldehyde (PFA) for 10 min and seeded onto immobilized poly-l-lysine for 1 h at RT. Adherent platelets were permeabilized with blocking solution (1% Fraction V BSA and 0.1% SDS in PBS), then stained with indicated primary Abs (anti-CD63 and anti-MRP4 in blocking solution) overnight at 4°C. Alexa Fluor secondary Abs were added in blocking solution for 2 h prior to mounting with Fluoromount G (Southern Biotech, AL, USA). Platelets were imaged using super-resolution structured illumination microscopy (SR-SIM) with a Zeiss 100× oil immersion 1.46 NA lens on a Zeiss Elyra PS.1 microscope.

5.3.7 Platelet receptor screening

Diluted whole blood was incubated with 10 μg/mL anti-PAR4 Abs (14H6 and 5F10), anti-PAR1 blocking Ab (ATAP2), $P2Y_1$ (APR-009), or $P2Y_{12}$ (APR-121) Abs. Next, samples were stained with a polyclonal FITC anti-IgG Ab (Biocytex Kit, Marseille,

France), followed by measurements on a FACS Canto II system (Beckton Dickinson, CA, USA) and analyzed using FlowJo. Number of molecules per platelet was extrapolated by comparing the mean fluorescence intensity (MFI) of the sample to the MFI of a calibrator system using beads coated with increasing and accurately known quantities of immunoglobulins IgG.

5.3.8 Exposure of platelets to shear conditions

GFP, PRP, and whole blood preparations were exposed to constant shear stresses for 4 min in a computer-controlled hemodynamic shearing device (HSD).[422] For thrombin generation measurement, only GFP suspensions were exposed to shear stresses of 1, 10, 30, 50, and 70 dyn/cm^2, and samples were collected every minute using a LabView-controlled syringe pump (PSD/8, Hamilton, Reno, NV) connected to the HSD via a 28-ga polytetrafluoroethylene (PTFE) tube.[423] For flow cytometry measurements, PRP and whole blood suspensions were exposed to high shear stresses of 70 dyn/cm^2 for 4 min, with samples collected prior to and at the end of shear exposure.

5.3.9 Thrombin generation in sheared platelets

Thrombin generation for sheared GFP samples was measured using a modified prothrombinase-based platelet activation state (PAS) assay that uses acetylated prothrombin to measure rate of thrombin generation.[424] PAS absorbance readings were normalized against fully activated GFP, generated by sonicating quiescent GFP at

10 W for 10 s with a Branson Sonifier 150 with a microprobe (Branson, MO, USA) [421] on each day. Normalized PAS values represent the PAS as a fraction of the full activation and allow comparison of data obtained on different days regardless of the full thrombin generation potential for each sample. The change in PAS, ΔPAS, was calculated over the 4-min duration of shear-stress exposure.

5.3.10 Platelet P-selectin expression and PS exposure under shear

Sheared whole blood and PRP suspensions were assessed for platelet activation using anti-CD62P (PE) and Annexin V (FITC). Unsheared suspensions were used as controls. Whole blood or PRP samples were diluted with platelet buffer and FcR blocking reagent (human, Miltenyi Biotec, Auburn, CA) and stained with anti-CD62P for 15 min in the dark at 4ºC. Separately, whole blood or PRP samples were diluted with Annexin V buffer and stained with Annexin V for 15 min in the dark at RT. Samples were supplemented with platelet buffer or Annexin V buffer to a final volume of 500 µl at 4°C, scanned using FACS (BD Accuri C6, BD Biosciences, Franklin Lakes, NJ), and analyzed using Kaluza (Beckman Coulter Life Sciences, Indianapolis, IN). Nonspecific signals were eliminated using PE and APC anti-IgG1κ as controls.

5.3.11 Statistical analysis

Data were analyzed using GraphPad PRISM 4.0 software (San Diego, CA, USA). To determine statistical significance, one-way ANOVA, or two-tailed Student's *t*-test and

Tukey *post-hoc* tests were used for comparison between treatments. Data are represented as mean ± standard error of the mean of at least three independent experiments. For all comparisons, $P < 0.05$ was used to establish significance.

5.4 Results

5.4.1 Measurement of platelet α-granule secretion

Platelet activation initiates α-granule secretion resulting in P-selectin expression on the platelet surface.[412] I first investigated the neonatal hemostatic system by assessing platelet activation and α-granule secretion in the presence of agonists to the PAR1/4 or $P2Y_1/P2Y_{12}$ receptors. Citrated adult, neonate peripheral, and cord whole blood were incubated with an APC-labeled anti-CD62P mAb in the presence of platelet agonists or vehicle prior to fixation and evaluation by flow cytometry. The platelet population was gated from the red blood cell and leukocyte populations based on size (forward scatter-FSC) and granularity (side scatter-SSC) (Fig. 5.1A). Resting platelets were used to determine baseline P-selectin expression levels, with eFluor-labeled anti-CD31 mAbs used as the platelet marker. The same population gates defined using resting platelets were used to determine the degree of platelet activation in stimulated samples (Fig. 5.1A). Baseline levels of platelet activation were equivalent for adult, neonatal, and cord blood samples ($n = 3$).

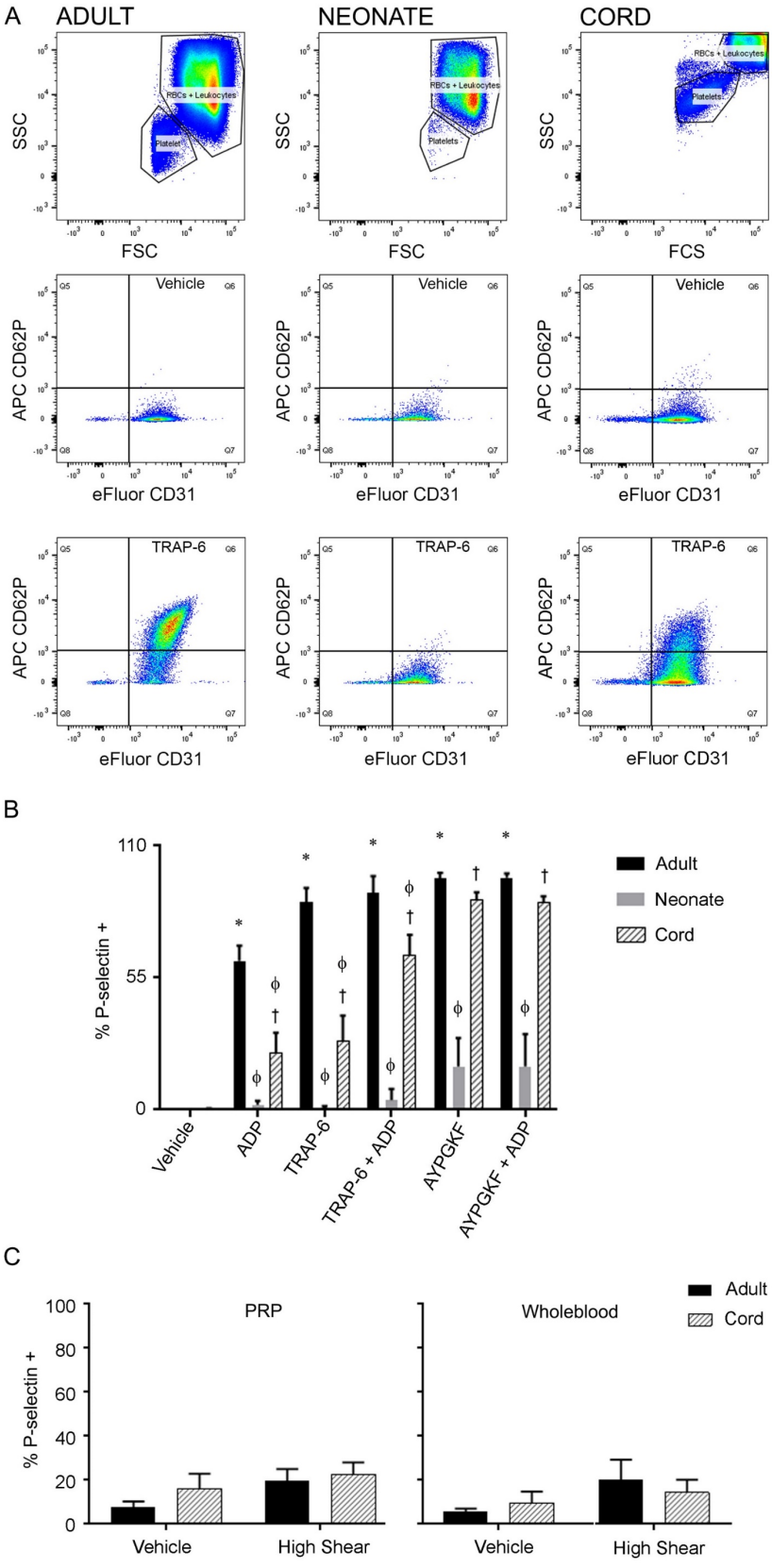

Figure 5.1. Effects of G-protein-coupled receptor agonists on platelet α-granule secretion. **A**: Representative fluorescence intensity of resting and activated platelets in response to HEPES/Tyrode buffer and TRAP-6, respectively, in adult, neonatal peripheral and cord blood. **B**: P-selectin expression in adults, neonatal, and cord blood in response to vehicle or ADP, TRAP-6, AYPGKF or a combination of agonists. **C**: P-selectin expression in PRP and whole blood in response to vehicle or high shear stress of 70 dyn/cm^2. Data are represented as mean ± SEM of at least three independent experiments; *$P < 0.05$ compared to adult vehicle; $^{\dagger}P < 0.05$ compared to cord vehicle; $^{\Phi}P < 0.05$ adults versus neonatal/ cord blood.

Adult platelet P-selectin expression significantly increased in response to the PAR1 agonist TRAP-6, PAR4-agonist AYPGKF, $P2Y_1/P2Y_{12}$-agonist ADP, or a combination of ADP and TRAP-6 or AYPGKF ($P < 0.001$; Fig. 5.1B). I then investigated the response of neonatal peripheral platelets to these agonists, as measured by P-selectin expression levels, and observed no significant increase above baseline in P-selectin expression in response to TRAP-6, AYPGKF, or a combination of ADP and TRAP-6 or AYPGKF. In contrast, cord blood-derived platelet P-selectin expression significantly increased above baseline upon stimulation with TRAP-6, AYPGKF, ADP, or a combination of ADP and TRAP-6 or AYPKGF ($P < 0.001$). However, the degree of α-granule secretion remained blunted as compared to adult platelets for agonists TRAP-6, ADP, or the combination of ADP and TRAP-6 ($P < 0.01$; Fig. 5.1B), while responses to AYPGKF or the combination of AYPGKF and ADP were equivalent for cord and adult platelets.

I then subjected adult and cord blood samples to high shear stress using a HSD. P-selectin expression was monitored in response to 4 min of shear exposure of 70 dyn/cm^2. Platelet activity was defined as the percentage of platelets staining positive for PE-labeled CD62P. In PRP, P-selectin-positive events were similar for both sheared adult and cord blood-derived platelets ($n = 3$, Fig. 5.1C). Similar results were observed in whole blood (Fig. 5.1C), suggesting that cord-derived and adult platelet α-granule secretion in response to shear was similar at the conditions tested.

5.4.2 Measurement of platelet integrin activation

"Inside-out" signaling following platelet activation causes conformational changes that facilitate the conversion of GPIIb/IIIa to a high affinity state for ligand binding, primarily fibrinogen.[425] Conformational changes in GPIIb/IIIa can be quantified by measuring the binding of the Ab PAC-1, which selectively recognizes the active form of GPIIb/IIIa. Citrated adult, neonate, and cord whole blood were incubated with a FITC-labeled PAC-1 mAb in the presence of platelet agonists or vehicle prior to fixation and evaluation by flow cytometry (Fig. 5.2A). I did not observe any differences in PAC-1 binding among all samples at resting conditions (Fig. 5.2B). Adult platelets exhibited a significantly increased level of activated GPIIb/IIIa in response to TRAP-6, AYPGKF, ADP, or the combination of ADP and TRAP-6 or AYPGKF ($P < 0.0001$). Neonatal platelets also exhibited a significant increase in GPIIb/IIIa activation above baseline in response to AYPGKF, ADP, or the combination of ADP and TRAP-6 or AYPKGF ($P < 0.05$). In contrast, neonatal platelet GPIIb/IIIa activation remained blunted in response to TRAP-6 as compared to adult platelets ($P < 0.0001$), while AYPGKF elicited a similar response in neonates as compared to adult platelets. Addition of exogenous ADP in combination with TRAP-6 or AYPGKF neonatal platelets induced the same degree of PAC-1 binding as compared to adult platelets under these conditions (Fig. 5.2B). Cord-derived platelet integrin activation increased significantly in response to AYPGKF, ADP, and ADP in combination with TRAP-6 or AYPGKF ($P < 0.05$), but not in response to TRAP-6 stimulation alone (Fig. 5.2B). Integrin activation in cord blood-derived platelets, while

being slightly lower, remained statistically similar to adult platelets, except in response to TRAP-6 ($P < 0.05$).

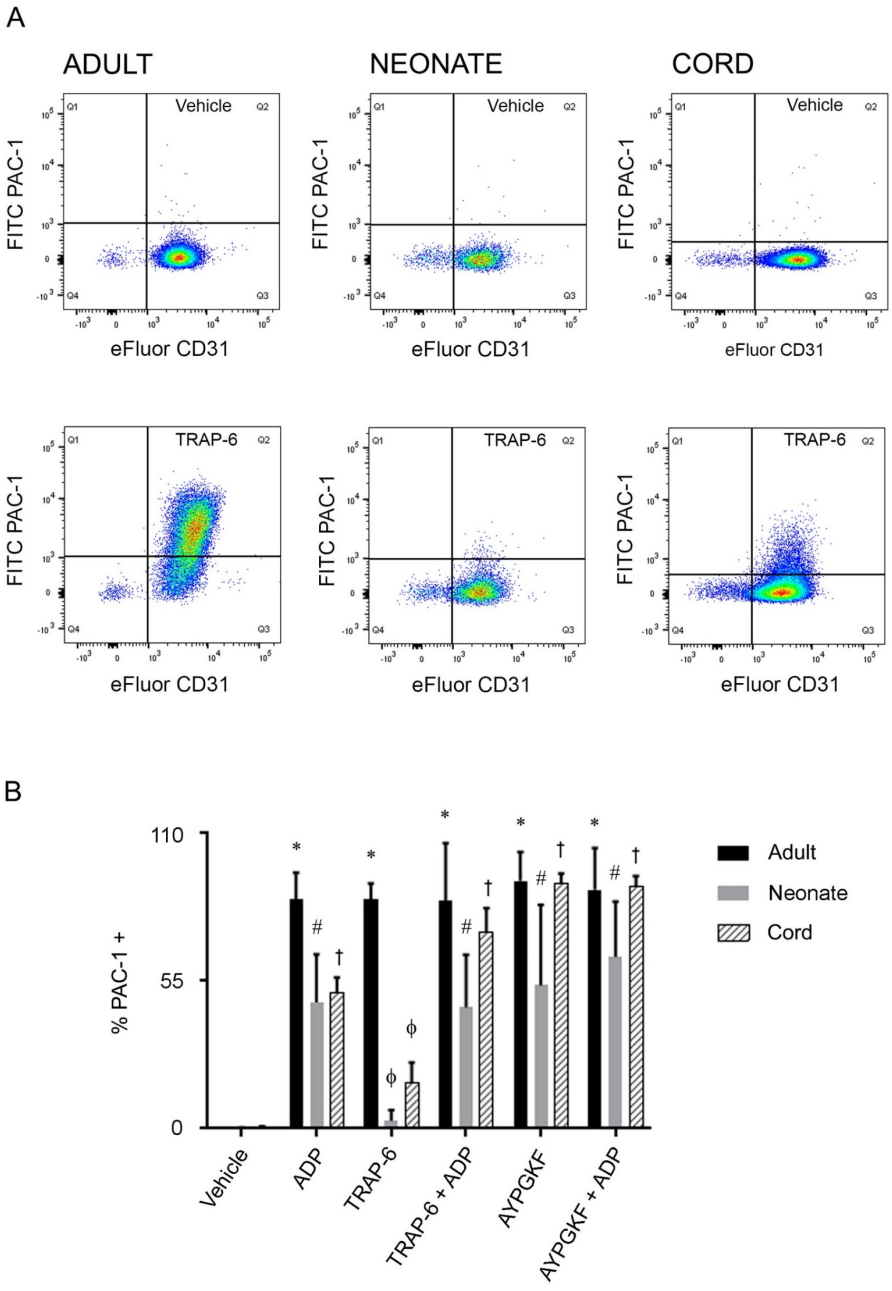

Figure 5.2. Effects of G-protein-coupled receptor stimulation on platelet integrin activation. A: Representative flow cytometry of activated GPIIb/IIIa (FITC PAC-1) and eFluor CD31 fluorescence intensity of resting and TRAP-6-activated adult, neonatal peripheral and cord blood. **B**: PAC-1 expression in resting and stimulated adult, neonatal and cord platelets in response to ADP, TRAP-6, AYPGKF or a combination of agonists. Data are represented as mean ± SEM of at least three independent experiments; $^{*}P < 0.05$ compared to adult vehicle; $^{\#}P < 0.05$ compared to neonatal vehicle; $^{\dagger}P < 0.05$ compared to cord vehicle; $^{\Phi}P < 0.05$ adults versus neonatal/cord blood.

5.4.3 Measurement of platelet dense granule secretion

ADP is stored at high concentrations in platelet dense granules and is secreted upon platelet activation to further amplify platelet activation downstream of the $P2Y_1$ and $P2Y_{12}$ receptors.[118] I next assessed neonatal, cord, and adult blood-derived platelet dense granule secretion by measuring ATP release.[362] Since the constant ratio of ATP:ADP in dense granules is 2:3, ATP can be used as a surrogate marker for ADP secretion. I observed no differences in baseline ATP level among all samples (n = 5, Fig. 5.3A).

Adult platelet dense granule release increased significantly in response to TRAP-6, AYPGKF, or a combination of ADP and TRAP-6 or AYPGKF ($P < 0.0001$) (Fig. 5.3A). A significant increase in dense granule release was observed following stimulation of neonatal platelets with ADP, or the combination of ADP and AYPGKF ($P < 0.01$), but not to TRAP-6, AYPKF alone, or the combination of ADP and TRAP-6. Neonatal platelet dense granule secretion was reduced as compared to adult platelets in response to TRAP-6, AYPGKF, or a combination of ADP and TRAP-6 ($P < 0.001$). Cord blood-derived platelets secreted ATP in response to ADP, or a combination of ADP and TRAP-6 or AYPGKF ($P < 0.0001$), but not to TRAP-6 or AYPGKF alone. Compared to adult platelets, cord blood-derived platelets exhibited a similar degree of dense granule secretion in response to all agonists, except AYPGKF ($P < 0.05$; Fig. 5.3A).

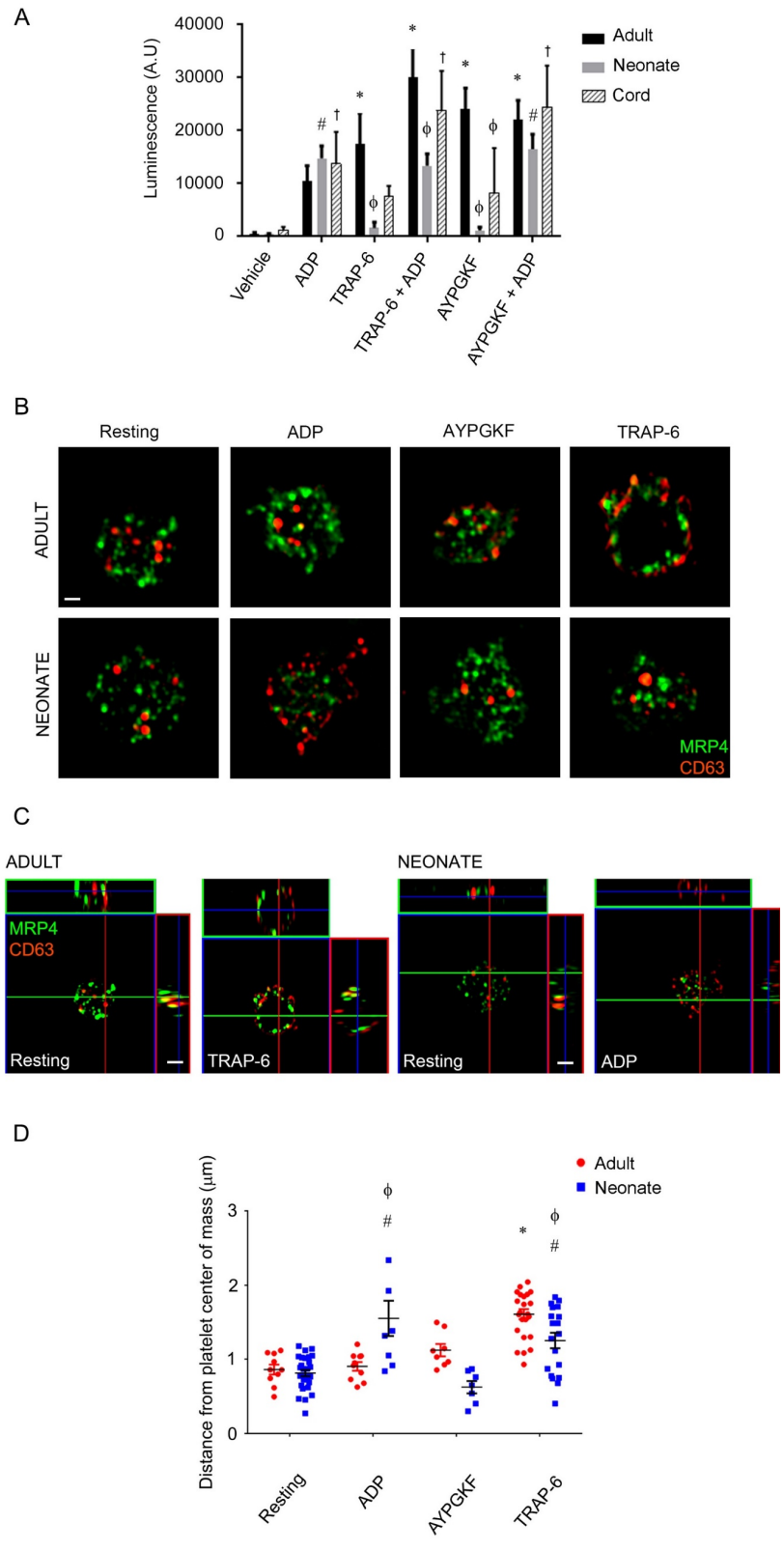

Figure 5.3. Dense granule secretion and distribution of CD63 and MRP-4 in whole blood activated with GPCR agonists.
A: Dense granule secretion from resting and stimulated platelets in adults, neonatal and cord blood. Values are mean ± SEM of raw luminescence ($\times 10^6$) of at least three independent experiments. **B**: Dense granule trafficking using CD63 as dense granule marker (red) and ATP transporter marker MRP4 (green) (scale bar = 1 µm). **C**: Ortho view of platelet CD63 (red) upon stimulation with TRAP-6 (adult) and ADP (neonate) (scale bar = 2 µm). **D**: Images captured in Z-stacks were processed and analyzed using Imaris software to render dense granules using a spot detection algorithm. A center of mass was determined for each platelet. Each data point on the graph represents the distance between a single granule and the center of mass of corresponding platelet. $^{*}P < 0.05$ compared to adult vehicle; $^{\#}P < 0.05$ compared to neonatal vehicle; $^{\dagger}P < 0.05$ compared to cord vehicle; $^{\Phi}P < 0.05$ adults versus neonatal/ cord blood. *Degranulation analyses were performed by Anne Rocheleau (OHSU).*

I then utilized an immunofluorescence approach and SR-SIM to quantify trafficking of platelet dense granules in adult and neonatal platelets, using the dense granule marker CD63 (red) together with a marker for the multidrug resistance protein 4 (MRP4, green), a signaling molecule transporter in platelets. Under resting conditions, I observed punctate, granular-like staining structures (red) for both adult and neonatal platelet dense granules (Fig. 5.3B). TRAP-6 induced translocation of CD63 toward the platelet plasma membrane in adult platelets and to a lesser extent in neonatal platelets (Fig. 5.3B). Interestingly, ADP induced a dramatic translocation of CD63 in neonatal platelets, while no differences were observed in adult platelets (Fig. 5.3B). Stimulation of platelets with the PAR4 agonist AYPGKF elicited a higher expression of dense granule markers at the platelet periphery in adult platelets, while no differences were observed in neonatal platelets (Fig. 5.3B). Ortho images of dense granules along the Z-axis indicate that TRAP-6 elicits degranulation of dense granules in adult platelets, while ADP promotes the greatest degree of degranulation in neonatal platelets, resulting in a decrease in the concentration and dispersion of CD63 observed at the platelet membrane (Fig. 5.3C).

To quantify the translocation of dense granules to the cellular periphery, I next performed an analysis of SR-SIM images using Imaris (Bitplane AG, Zurich, Switzerland). Each dense granule was rendered using a spot detection algorithm, and the platelet center of mass was also determined by the software. In Fig. 5.3D, I show the distance between each dense granule and the platelet center of mass, quantifying the translocation of dense granules within each platelet. In adult platelets, I found that

the distance of granules from the center of the platelet significantly increased in response to TRAP-6 (n = 3, P < 0.0001) but not to ADP or AYPGKF in adults. Neonatal platelet granule movement significantly increased in response to ADP and TRAP-6 (n = 3, P < 0.0009), but not to AYPGKF. As compared to adult platelets, neonatal platelets exhibited significantly higher translocation of dense granules in response to ADP, while a reduced extent of granule movement in response to TRAP-6 (P < 0.05); both adult and neonatal platelet dense granule trafficking were largely unresponsive to stimulation with AYPGKF (Fig. 5.3D).

5.4.4 Quantification of platelet receptors

I next utilized flow cytometry to measure levels of PAR1, PAR4, $P2Y_1$, and $P2Y_{12}$ receptors on adult (n = 6), neonatal peripheral (n = 5), and cord-derived platelets (n = 4). My data confirm that neonatal platelets express significantly lower PAR1 levels than adult platelets and show that neonatal platelets also express significantly lower levels of PAR4 receptors as compared to adult platelets (P < 0.005). The levels of $P2Y_1$ or $P2Y_{12}$ receptors were similar between neonate and adult platelets (Fig. 5.4A). Similarly, the levels of $P2Y_1$ or $P2Y_{12}$ receptors expressed by cord blood-derived platelets were equivalent to those observed as for adult platelets. Yet, PAR1 and PAR4 receptor expression levels on cord blood-derived platelets were significantly lower as compared to adult platelets (P < 0.05, Fig. 5.4A). These data demonstrate that cord and neonate platelets express significantly less PAR1 and PAR4 as compared to adult

platelets, providing a potential mechanism in part for the blunted response to PAR agonists observed for neonate and cord platelets as compared to adult platelets.

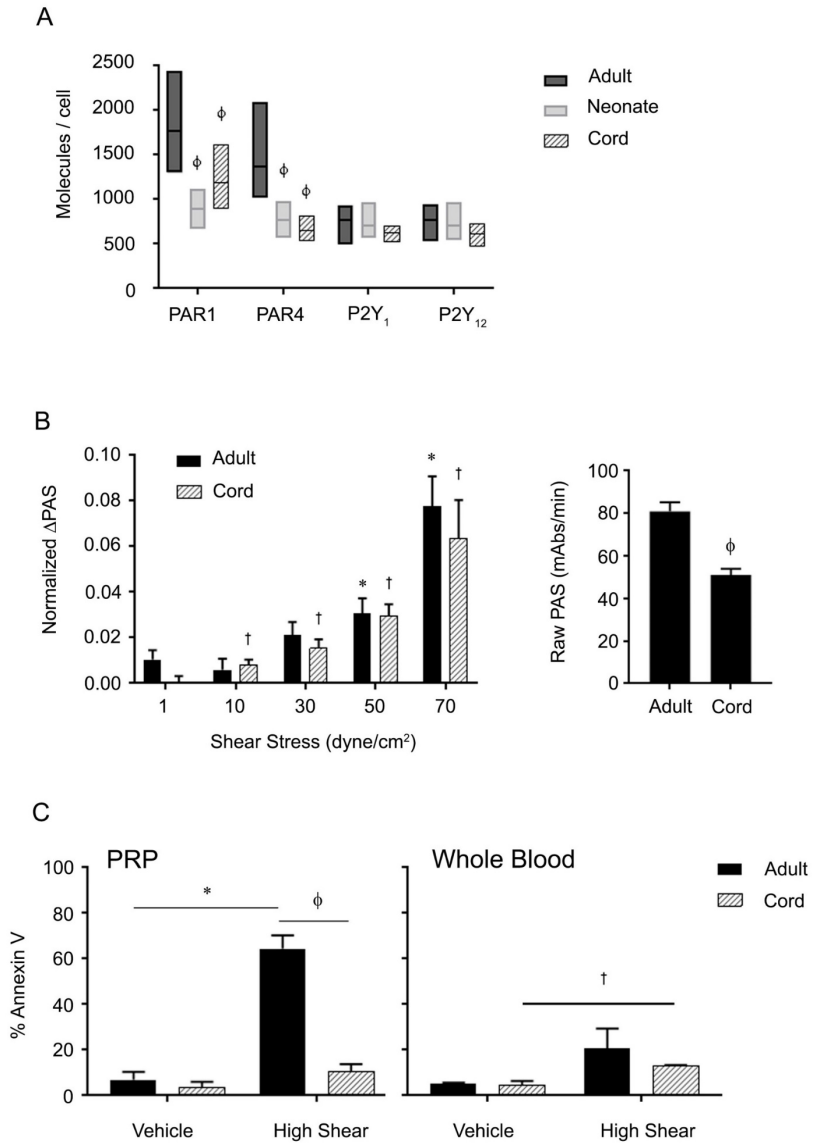

Figure 5.4. Quantitative assessment of select platelet G-protein-coupled receptors and shear-induced platelet activation. A: Protease activated receptors (PARs) 1 and 4, and ADP receptors ($P2Y_1$, $P2Y_{12}$) expression levels in adult platelets, measured by flow cytometry. Data are represented as mean ± SEM of at least three independent experiments; $^{\Phi}P < 0.05$ adults versus neonatal/ cord blood. **B**: Platelet activation state (PAS) was measured every minute for the 4-min duration in adult and cord platelets (left). Change in PAS (ΔPAS) was calculated over the exposure, normalized to the respective 1 dyn/cm^2 control; $^{*}P < 0.05$ versus adults at 1 dyn/cm^2; $^{\dagger}P < 0.05$ versus cord blood at 1 dyn/cm^2. PAS values were normalized with thrombin generation values obtained by sonication of adult and cord-derived platelets (right). $^{\Phi}P < 0.05$ adult versus cord blood. **C**: Sheared whole blood and PRP suspensions were stained for Annexin V (FITC) and subjected to flow cytometry. $^{*}P < 0.05$ versus adult vehicle; $^{\dagger}P < 0.05$ versus cord vehicle; $^{\Phi}P < 0.05$ adult versus cord blood. *Data under shear stress were generated by Dr. Jawaad Sheriff (Stony Brook University).*

5.4.5 Thrombin generation and platelet procoagulant activity under shear

Activated platelets facilitate blood coagulation by flipping of plasma membrane leaflets and exposing procoagulant PS. It has been demonstrated that fluid shear stress significantly enhances agonist-induced PS exposure in platelets.[426] Binding of coagulation factors (F) Xa and Va to PS promotes prothrombinase assembly on the platelet surface and enhances proteolytic activity of FXa to catalyze thrombin generation.[427,428] To quantify thrombin generation, I acetylated human prothrombin such that upon activation by prothrombinase, this species retains the ability to bind to the platelet surface and cleave a chromogenic peptide substrate yet is incapable of cleaving PAR receptors to activate platelets.[424,429] GFP from both adult and cord-derived blood were exposed for 4 min to five levels of constant shear stress (n = 6, Fig. 5.4B, left). Both adult and cord blood-derived platelets (Fig. 5.4B, left) yielded similar increases in PAS, a measure of normalized thrombin generation rate, consistent with prior reports.[430] Adult platelets showed a significant increase in PAS after a 4-min exposure to 50 and 70 dyn/cm^2 as compared to baseline levels at 1 dyn/cm^2. The baseline levels for cord blood-derived platelets were lower, and as a result, a significant PAS increase was observed at all shear-stress levels (Fig. 5.4B). Still, the total thrombin generation rate, a measure of the full platelet activation potential, for adult platelets was 80.73 ± 4.30 mAbs/min (n = 42), but significantly lower at 50.90 ± 2.82 mAbs/min (n = 33, P < 0.05) for cord blood-derived platelets (Fig. 5.4B, right), suggesting that cord blood-derived platelets may be less procoagulant overall.

Negatively charged PS was quantified by measuring Annexin V binding via flow cytometry analysis. In PRP, a significant increase in Annexin V binding was observed in response to shear for adult but not cord-blood derived platelets (n = 3, P < 0.01, Fig. 5.4C). The level of Annexin V binding observed for cord blood-derived platelets following exposure to shear was significantly lower as compared to adult platelets (P < 0.01, Fig. 5.4C). In whole blood, sheared cord blood-derived platelets exhibited a small yet significant increase in Annexin V positive events as compared to the unsheared control (n = 3, P < 0.01), while the dramatic increase in shear-induced Annexin V binding to adult platelets observed in PRP was lost in whole blood (Fig. 5.4C).

5.5 Discussion

Several studies have indicated that neonatal platelets have blunted responses to platelet agonists, decreased granule secretion, reduced fibrinogen binding, and decreased platelet aggregation as compared to adult platelets and that this hyporesponsive phenotype persists for up to several weeks after birth.[412,431,432] Nevertheless, despite my observation that neonatal platelets were less procoagulant in response to shear, bleeding times and platelet function analyzer-100 (PFA-100) closure times under shear in healthy full-term neonates are shorter than in adults, indicating that neonates exhibit more effective primary hemostatic functions.[433] This may be due in part to enhanced neonatal platelet interactions with the vessel wall due to higher hematocrits, higher mean corpuscular volumes, higher vWF concentrations, and the presence of ultra-large vWF multimers in neonatal blood as compared to adults.[432,434,435] Yet, while most healthy newborns do not manifest a bleeding tendency, an increased prevalence of hemostatic disturbances including thrombocytopenia and coagulopathy is observed in premature and sick newborns, which may result in life-threatening bleeding.[432] The potential role of the inherent neonatal platelet hyporeactivity to these hemostatic disturbances has not been fully examined in the clinical management of this population. Understanding the functional phenotype of neonatal platelets may help guide diagnosis and inform treatment options specifically tailored to the neonatal population.

This study focused on the neonatal platelet response downstream of thrombin and ADP as their respective receptors, PAR1/4 and $P2Y_1$/$P2Y_{12}$, are major targets of antiplatelet therapies in the adult population. Of relevance, drug dosing of antiplatelet agents in the neonatal population still largely relies on data extrapolated from adult clinical trials. In agreement with previous reports,[417,418,436,437] despite similar total P-selectin content and GPIIb/IIIa expression, I observed significantly blunted granule secretion and integrin GPIIb/IIIa activation in response to the PAR1 agonist TRAP-6 in cord and peripheral neonatal platelets as compared to adult platelets. These functional differences may be attributed in part to the observation that neonatal platelets express lower levels of PAR1 as compared to adult platelets.[437] A similar narrative of hypofunctional response to PAR4 agonists and correspondingly reduced PAR4 levels was observed for neonatal platelets. Yet, neonatal platelets still exhibit robust GPIIb/IIIa activation and dense granule secretion but not α-granule secretion to ADP, which may be due to different regulatory effects that the actin cytoskeleton exerts on dense granules as compared to α-granules.[438,439] Perhaps this shift in responsiveness from thrombin to ADP provides a selection advantage during development and the trauma of birth. The functional difference and responsiveness of neonatal platelets as compared to adult platelets should be considered when managing bleeding complications through transfusion of adult platelets prophylactically into neonates for fear of potentiating a hypercoagulable, prothrombotic state.

There are several limitations to this study. The sample sizes used in my current study were limited to 3-4 samples per test due to limited availability of neonatal samples,

together with the inherently small volume constraint in heel-stick samples. Moreover, the mode of blood collection differed between neonatal, cord-blood derived, and adult samples. Subsequently, limited conclusions can be drawn from this study with regards to the normal population distribution of neonatal platelet functional responses and comparison of similarities and differences between neonatal, cord blood-derived, and adult platelets. In light of these limitations, I aimed to assess platelet responses to PARs and $P2Y_1$/$P2Y_{12}$ receptor agonists using whole blood assays as compared to cord, neonatal peripheral, and adult peripheral platelets, demonstrating utility and feasibility of my small-volume assays. Neonatal platelets exhibited a hyporeactive phenotype in response to PAR1/4 agonists, indicative of a loss of sensitivity to the potent platelet agonist thrombin. Neonatal platelets may compensate for this to retain their hemostatic function by enhancing their dense granule trafficking and secretion in response to ADP. Understanding the functional differences between neonates and adults and the mechanisms during development is necessary for the diagnosis and treatment of hemostatic disorders in the neonatal population as well as the development of platelet transfusion guidelines.

Chapter 6. Pharmacological Targeting of Coagulation Factor XI Mitigates the Development of Experimental Atherosclerosis

Anh T.P. Ngo,* Kelley R. Jordan, Paul A. Mueller, Matthew W. Hagen, Stéphanie E. Reitsma, Cristina Puy, Alexey S. Revenko, Christina U. Lorentz, Erik I. Tucker, Quifang Cheng, Monica T. Hinds, Sergio Fazio, Brett P. Monia, David Gailani, András Gruber, Hagai Tavori, and Owen J.T. McCarty

*In this study, I conceived and designed the research, performed experiments, analyzed data, interpreted the results, prepared figures and wrote the manuscript.

This work has been accepted for publication in the *Journal of Thrombosis and Haemostasis,* 2021.

6.1 Abstract

Human coagulation factor (F) XI deficiency, a defect of the contact activation system, protects against venous thrombosis, stroke, and heart attack, while FXII, prekallikrein or kininogen deficiencies are asymptomatic. FXI deficiency, inhibition of FXI production, activated FXI (FXIa) inhibitors, and antibodies to FXI that interfere with FXI/FXII interactions reduce experimental thrombosis and inflammation. FXI inhibitors are antithrombotic in patients, and FXI and FXII deficiencies are athero-protective in

apolipoprotein-E-deficient mice. In this study, I the effects of pharmacological targeting of FXI in experimental models of atherogenesis and established atherosclerosis. Low-density lipoprotein receptor-knockout ($Ldlr^{-/-}$) mice were administered high-fat diet (HFD) for 8 weeks; concomitantly FXI was targeted with anti-FXI antibody (14E11) or FXI antisense oligonucleotide (ASO). 14E11 and FXI-ASO reduced atherosclerotic lesion area in proximal aortas when compared to controls, and 14E11 also reduced aortic sinus lesions. In an established disease model, wherein therapy was given after atherosclerosis had developed, $Ldlr^{-/-}$ mice were fed HFD for 8 weeks and then administered 14E11 or FXI-ASO weekly until 16 weeks on HFD. In this established disease model, 14E11 and FXI-ASO reduced atherosclerotic lesion area in proximal aortas, but not in aortic sinus. In cultures of human endothelium, FXIa exposure disrupted VE-Cadherin expression and increased endothelial lipoprotein permeability. Strikingly, I found that 14E11 prevented the disruption of VE-Cadherin expression in aortic sinus lesions observed in the atherogenesis mouse model. In conclusion, pharmacological targeting of FXI reduced atherogenesis in $Ldlr^{-/-}$ mice. Interference with the contact activation system may safely reduce development or progression of atherosclerosis.

Graphical Abstract

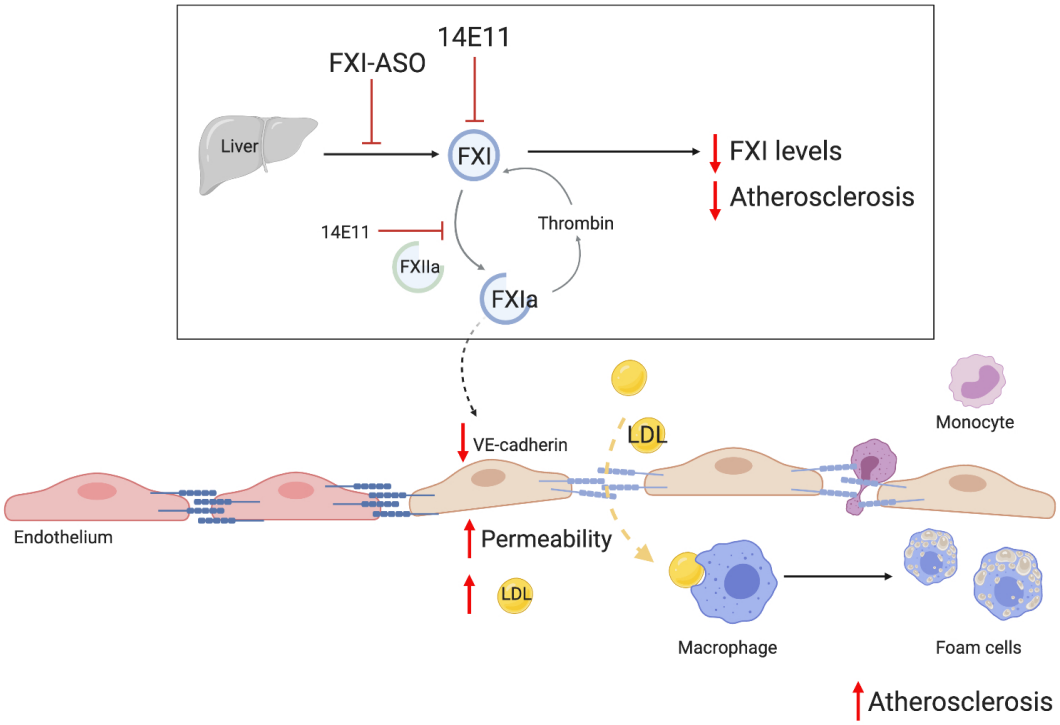

6.2 Introduction

Atherosclerosis is a chronic inflammatory disease, characterized by endothelial dysfunction leading to lipid and calcium accumulation in the subendothelial space, followed by leukocyte recruitment into the subintima.[440] Here, monocytes differentiate into macrophages that internalize modified lipoproteins and become foam cells that form early atherosclerotic lesions.[441,442] Over time, apoptotic foam cells coupled with their defective clearance lead to the formation of a necrotic core, and advanced plaques become vulnerable to erosion and rupture which trigger atherothrombosis that is clinically manifested as myocardial infarction, peripheral artery disease, or ischemic stroke.[443]

Atherosclerosis-associated cardiovascular complications remain the leading cause of morbidity and mortality in the Western world and developing countries.[444] The link between coagulation and atherothrombosis has been demonstrated in numerous animal [2-4] and clinical studies,[5,6] supporting the idea that anticoagulation in addition to antiplatelet therapy [8] may be a form of intervention for atherothrombotic events; however, the role of coagulation in promoting the early steps of atherosclerosis and therefore therapeutic potential of anticoagulants for impeding early onset of atherosclerosis and its progression remains unclear. Evidence now suggests that numerous coagulation components are present in human atherosclerotic lesions, strongly indicative of roles of coagulation activity during early plaque development.[445] Furthermore, there is evidence for associated activation of both coagulation and

inflammation during atherogenesis. Indeed, thrombin,[295,296] tissue factor pathway inhibitor,[297] coagulation factor (F) VIII,[298] and activated FX (FXa) [299] have all been shown to contribute to plaque development in mice. Components of the intrinsic pathway, such as factor XII (FXII) and more recently factor XI (FXI), have also been shown to play a role in atherogenesis in ApoE$^{-/-}$ mice [263,300] through unclear mechanisms.

Factor XI is an interesting therapeutic target due to its unique role at the interface between thrombin generation and FXII activation. Thrombin, initially generated via the tissue factor pathway, can feed back to activate FXI, a process that further amplifies FXI activation and thrombin generation.[222] Recent evidence suggests FXI also supports activation of FXII and plasma prekallikrein (PK) *in vivo*.[262] Activated FXII (FXIIa) then initiates the contact activation system by activation of FXI and PK to ultimately generate thrombin, and promote bradykinin via plasma kallikrein cleavage of high molecular weight kininogen. Bradykinin subsequently induces endothelial nitric oxide and prostacyclin production, which drives vascular permeability, and together with complement activation and cytokine production result in local or systemic inflammation.[257,258] Such bidirectional relationships between FXI-thrombin and FXI-FXIIa provide means by which the role of coagulation FXI extends beyond just thrombin generation, platelet activation and clotting, to include regulation of inflammatory pathways as well.

While the contact activation system does not seem to be essential for hemostasis, as congenital FXI deficiency is not clearly associated with bleeding disorders, high FXI levels are associated with increased risk of MI [446] and marginally associated with risk of stroke.[248] Due to FXI involvement in experimental and human thrombosis,[252,447-449] experimental inflammation,[260,450,451] and atherogenesis but only a supportive role in hemostasis,[452] pharmacological inhibition of FXI levels, activity, or activation by thrombin or FXIIa could attenuate multiple mechanisms that promote atherosclerosis. Since the mechanism of contact activation system in potentially promoting atherogenesis remains unclear, I sought to investigate the role of FXI in atherogenesis and established atherosclerosis through pharmacological reduction of FXI levels by two means in $Ldlr^{-/-}$ mice: administration of the anti-FXI antibody (14E11) or a FXI antisense oligonucleotide (FXI-ASO) that reduces FXI synthesis by the liver. Furthermore, I sought to define the direct relationships between FXI activity and endothelial inflammation and permeability *in vitro*, as compromised endothelial barrier integrity driven by inflammation is a hallmark of the onset of early atherosclerosis.

6.3 Materials and Methods

6.3.1 Factor XI antisense oligonucleotide (ASO) synthesis and dosing

FXI-ASO used in this study was a second-generation ASO, fully phosphorothioate (PS)-modified with a central gap region of 10 PS DNA nucleotides flanked on either end with 5 2'-*O*-methoxyethyl RNA (MOE) nucleotides. Synthesis, purification, and testing of $GalNAc_3$-conjugated FXI-ASO were done as previously described.[453] $GalNAc_3$-conjugation facilitates specific delivery and uptake of FXI-ASO by hepatocytes via high-affinity binding to the hepatocyte-specific asialoglycoprotein receptor. $GalNAc_3$-conjugated FXI-ASO dosage for this study was determined based on previously reported *in vivo* safety assessment, FXI plasma activity assessment and FXI mRNA expression analysis to achieve significant reduction (~95%) in liver FXI mRNA and plasma FXI protein.[453] Plasma was serially collected from mice to analyze the FXI levels following the administration of FXI-ASO.

6.3.2 Factor XI Antibody (14E11) derivation and dosing

Derivation and activity of the murine anti-mouse FXI monoclonal antibody, 14E11, used in this study have been described elsewhere.[255] Briefly, the antibody was generated by immunizing FXI-deficient mice with recombinant mouse FXI. Clone 14E11 was expanded in a CL1000 bioreactor (Integra Biosciences, Hudson, NH) and immunoglobulin G (IgG) was purified by cation exchange and thiophilic agarose chromatography.

Dosage of 14E11 for this study to achieve its maximal effect on prolonged activated partial thromboplastin time (aPTT), used as a marker of pharmacological inhibition of

the contact system activation over the course of the study, was determined based on a dose-finding experiment wherein C57BL/6 mice were injected with a single subcutaneous (SC) dose of 14E11 (4 mg/kg) and aPTT was monitored over a period of 10 days. Whole blood was collected into sodium citrate (0.32% w/v) at days 0, 3, 6, and 10 post-injection. Platelet-poor-plasma (PPP) was isolated by centrifuging whole blood at 2,000×g for 10 min at room temperature (RT). PPP was mixed 1:1 with aPTT reagent and incubated for 3 min at 37°C. $CaCl_2$ (8.3 mM final) was added in equal volume to PPP and aPTT reagent and time to clot formation was measured using KC4 coagulation analyzer (Trinity Biotech, Jamestown, NY). Throughout the study, plasma was serially collected from mice to analyze the FXI levels following the administration of 14E11.

6.3.3 Factor XI Western Blot

One microliter samples of mouse PPP were size-fractionated under non-reducing conditions on 7.5% polyacrylamide-SDS gels. Samples are from saline-treated mice (vehicle, n=3), 14E11-treated mice (n=3), and FXI-ASO-treated mice (n=3). All samples are from animals after 4 weeks or 8 weeks of HFD together with saline, 14E11 or FXI-ASO treatments. Control samples are wild type (WT) mouse plasma, FXI-deficient ($FXI^{-/-}$) mouse plasma and WT mouse plasma supplemented with 14E11 (50-100μg/ml) *ex vivo.* Proteins were transferred to nitrocellulose membranes and the blot was developed with biotin-conjugated anti-mouse FXI IgG 14E11. Blots were developed with Streptavidin-HRP and chemiluminescence.

6.3.5 Mouse model of atherogenesis

All animal care and experimental procedures in this project were performed in accordance with the regulations of the Institutional Animal Care and Usage Committee of Oregon Health & Science University.

Eight-week-old male (n=25) and female (n=25) $Ldlr^{-/-}$ mice on C57BL/6 background (Jackson Laboratory, Bar Harbor, ME) were fed a high-fat diet (HFD) (42% kcal from fat, Envigo, Indianapolis, IN) for 8 weeks while concurrently receiving either vehicle (saline, n=16), 14E11 (4mg/kg, n=16) or FXI-ASO ($GalNAc_3$-conjugated; 7.5mg/kg, SC, n=16) once weekly based on prior safety and dose-finding screening studies in C57BL/6 mice.[260,453]

Treatment of $GalNAc_3$-conjugated FXI-ASO was initiated with 3 SC loading doses the week prior to the study. Eight weeks after HFD together with vehicle, 14E11, or FXI-ASO treatments, mice were euthanized for hematological analysis, whole blood flow cytometry, plasma lipid levels, and atherosclerosis analysis. Plasma was serially collected from mice to analyze the FXI levels following the administration of FXI-ASO.

6.3.6 Mouse model of established atherosclerosis

A separate cohort of eight-week-old male (n=25) and female (n=25) $Ldlr^{-/-}$ mice on C57BL/6 background were fed HFD for 8 weeks prior to being administered vehicle

(saline, n=16), 14E11 (4mg/kg, n=16) or $GalNAc_3$-conjugated FXI-ASO (7.5mg/kg, n=16) once weekly starting at week 8 HFD and continuing to week 16 HFD. During week 7 HFD, plasma was collected and animals were randomized to vehicle, 14E11, and FXI-ASO treatments based on total cholesterol levels (**Fig. 4A**).

Treatment of $GalNAc_3$-conjugated FXI-ASO was initiated with 3 SC loading doses the week prior to the start of injections (at week 7 HFD) (**Fig. 4A**). At week 16 of HFD together with 8 weeks of administration of vehicle, 14E11, or FXI-ASO treatments, mice were euthanized for hematological analysis, whole blood flow cytometry, plasma lipid levels and atherosclerosis analysis.

6.3.7 Hematological Analysis

Whole blood was drawn from the retro-orbital sinus and diluted 1:1 with 10mM EDTA in phosphate-buffered saline (PBS). Complete blood counts were obtained using a Scil Vet ABC hematology analyzer (ScilVet, Viernheim, Germany) within 1h of blood collection.

6.3.8 Atherosclerosis Analysis

The extent of atherosclerosis was determined both by *en face* analysis in proximal aortas and by Oil-red-O (ORO) staining of cross sections from the aortic valves to a

region in the ascending aortic arch, as previously recommended and described.[454,455]

En face analysis

Proximal aortas were removed and fixed for 48h at 4°C with 4% paraformaldehyde (PFA), then stored in saline for at least 24h prior to *en face* analysis. Images of proximal aortas, cut longitudinally, were obtained and lesion areas were quantified using ImageJ. Quantified area includes the aortic root, ascending aorta, aortic arch and 3 cm below aortic arch in the descending aorta region.

Oil-Red-O analysis

The hearts were embedded in optimal cutting temperature compound and stored at -80°C. Cryosections were orientated relative to the disappearance of the aortic valve cusps, and five (10μm) serial sections at 80μm intervals were placed on a single slide. Frozen serial sections of the aortic sinus were fixed with 4% PFA for 10 min at RT, incubated with 100% propylene glycol for 10 min and stained with ORO for 24 min at 55°C. Sections were then rinsed with 85% propylene glycol for 3 min, followed by 10 sec of hematoxylin staining at RT. Sections were mounted with glycerol gelatin mounting media and imaged using Fisherbrand AX800 series compound microscope and Moticam 3.0MP camera with Motic Imaging software. Data were collected from 5 serial sections on a single slide for each mouse heart sample and averaged. ORO areas were quantified using ImageJ. Sections without the presence of 3 aortic valve

leaflets were excluded from the analysis. Atherosclerotic lesions were quantified in a blinded manner by 2 observers.

Cholesterol analysis

PPP was isolated by centrifuging whole blood (mixed with sodium citrate, 0.32% w/v) at 2,000 × g for 10 min at RT and stored at -80°C until further analyses. Pooled plasma (based on sex) very-low-density lipoprotein (VLDL), low-density lipoprotein (LDL), and high-density lipoprotein (HDL) were separated using fast performance liquid chromatography (FPLC). Cholesterol levels from PPP and FPLC fractions were determined by colorimetric assays using colorimetric kit (Cholesterol Reagent Set; Pointe Scientific C7510120, Canton, MI). Samples obtained from blood draws with complications were excluded from the study.

6.3.9 Flow Cytometry

Whole blood was drawn from the retro-orbital sinus into 5nM final concentration of EDTA in PBS. Blood was then incubated with FITC-CD45R/B220 (553087, BD Biosciences, San Jose, CA), FITC-CD335 (560756, BD Biosciences), and FITC-Ly6G (561105, BD Biosciences) antibodies to exclude B cells, NK cells and granulocytes, respectively, from the analysis. Monocytes were identified using PE-CD11b (BD Biosciences) antibody. Inflammatory monocytes and monocyte-platelet aggregates were quantified using APC-Ly6C (56272, BD Biosciences) and BV421-CD41 (133912,

Biolegend, San Diego, CA) antibodies, respectively. Samples were washed with PBS, fixed and stored in 1% PFA until flow cytometry analysis.

6.3.10 Immunohistochemistry

Serial cryosections (10μm) of the aortic root, adjacent to sections used to quantify atherosclerosis, were fixed in 4% PFA for 15 min at RT, washed with PBS and permeabilized with 0.1% sodium citrate and 0.1% Triton X-100 for 3 min at RT. Sections were then blocked in Background Buster (Innovex Biosciences, Richmond, CA) for 1 h at 37°C and incubated with markers of monocytes/macrophages (CD68, Abcam, Cambridge, MA), fibrin (US Biological, Salem, MA) and VE-cadherin (CD144, US Biological) together with CD31 (Abcam) at 4°C overnight. Slides were then washed with PBS and incubated with Alexa Fluor anti-rabbit IgG for 1 h at 37°C. Samples were mounted using VECTASHIELD containing DAPI (Vector Laboratories, Burlingame, CA) and imaged using confocal microscopy.

Area fraction was calculated as percent area threshold positive after using a Phansalkar local autothreshold with radius of 5 pixels using Fiji software. Data were collected from at least 3 sections for each mouse and averaged.

6.3.11 Immunofluorescence

Human umbilical vein endothelial cells (HUVECs, ATCC, Manassas, VA) were grown to confluence on 0.1% gelatin-coated glass coverslips with Vasculife VEGF Endothelial Medium Complete Kit (Lifeline Cell Technology, Frederick, MD). HUVECs were incubated with vehicle (serum-free media, SFM), purified human FXI (30nM, Haematologic Technologies, Essex Junction, VT), FXIa (30nM, Haematologic Technologies), α-thrombin (10nM, Haematologic Technologies), FXIa or thrombin in the presence of the serine-protease-inhibitor PPACK (100μM) for 3h at 37°C in SFM with 10μM $ZnCl_2$. Treatments with FXI or FXIa were performed in the presence of the potent thrombin inhibitor hirudin (25μg/ml) in order to prevent any thrombin-mediated effects. HUVECs were then washed with PBS and fixed in 4% PFA for 15min at RT prior to blocking with 1% bovine serum albumin (BSA) and 2% fetal bovine serum in PBS.

Primary antibodies (VE-Cadherin (CD144), 2μg/ml in 1% BSA, Santa Cruz Biotechnology, Dallas, TX) were incubated overnight at 4°C. Slides were then washed with PBS and secondary Alexa Fluor anti-mouse IgG (4μg/ml, Life Technologies, Carlsbad, CA) and TRITC-phalloidin (1:500 dilution, Sigma-Aldrich, St. Louis, MO) were incubated for 2h at RT in 1% BSA in the dark. Hoechst 33342 (Life Technologies) was incubated in PBS for 30min prior to mounting onto glass slides using Fluoromount G (Southern Biotech, Birmingham, AL). HUVECs were imaged using a Zeiss ×20 Plan-APOCHROMAT 0.8 NA objective on a Zeiss Axio Imager M2 microscope. Representative images were collected from at least 3 field-of-view per experimental condition.

6.3.12 Permeability in Transwell Assay

HUVECs were grown to confluence in gelatin-coated upper chambers of Transwell devices (0.4μm polyester membrane, Corning) prior to incubation with purified human FXI (30nM), FXIa (30nM), α-thrombin (10nM), FXIa or thrombin together with PPACK (100μM) in SFM supplemented with 10μM $ZnCl_2$ and 0.3% BSA for 3h at 37°C. Treatments with FXI or FXIa were performed in the presence of hirudin (25μg/ml) in order to prevent any thrombin-mediated effects. The integrity of the endothelial monolayer prior to the start of experiment was assessed by light microscopy for ~90% confluency. Each experimental condition was performed in duplicates.

To assess HUVEC permeability to BSA following exposure to FXI, FXIa, and α-thrombin, Evans Blue dye (0.67mg/ml) in 4% BSA in SFM was added to the upper chamber at RT, and samples were removed from the bottom chamber every 10min. Samples were then diluted with PBS, and absorbance was measured at 650nm using a spectrophotometer (Tecan).

To assess HUVEC permeability to lipoproteins following exposure to FXI, FXIa, and α-thrombin, Alexa Fluor 488-labeled acetylated LDL (acLDL, 4μg/ml, ThermoFisher Scientific, Waltham, MA) was added to the upper chamber and incubated for 24h at 37°C. Samples were removed from the bottom chamber, diluted with water in a black-bottom 96-well plate and fluorescence intensity was measured at 495/519 Ex/Em using a spectrophotometer (Tecan). A standard curve to transform fluorescence intensity

(arbitrary unit, A.U.) into acLDL concentration (ng/ml) was generated by spiking selected concentrations of acLDL (4, 2, 1, 0.5, 0.25 μg/ml) into 0.3% BSA to measure fluorescence intensity.

6.3.13 Statistical Analyses

Data are presented as mean ± SEM. The Shapiro-Wilk normality test was used to determine whether group data were distributed normally, and Levene's test was used to determine equality of variances. One-way ANOVA with Tukey's post hoc test was used to compare between treatment groups. Kruskal-Wallis with Dunn post hoc test was used to compare between groups when the data did not qualify for parametric statistics. ANOVA with repeated measures were used when comparing animal body weight over time and absorbance of Evan's Blue dye over time in Transwells. $P < 0.05$ was considered significant. All statistical analyses were conducted using GraphPad Prism 8 (San Diego, CA).

6.4 Results

6.4.1 The anti-FXI mAb 14E11 and FXI-ASO reduce FXI levels in mice

Based on my dose-finding experiment, I observed that a single dose of 4 mg/kg 14E11 significantly prolonged mouse clotting time, measured by aPTT assay, by 2.75-fold compared to baseline (Day 0) through day 6 after treatment (Figure 6.1A). Therefore, I chose to inject 14E11 on a weekly basis throughout this study. I then designed

experiments to characterize the effects of the anti-FXI mAb 14E11 and the FXI-ASO on the contact activation system in mice. My data show that weekly administration of both the anti-FXI mAb 14E11 and FXI-ASO reduced FXI levels in mice as measured by Western blot when assessed at 4 weeks HFD (Figure 6.1B) and 8 weeks HFD (Figure 6.1C).

To determine the extent of the observed FXI reduction by 14E11 and FXI-ASO, I supplemented human $FXI^{-/-}$ plasma with increasing concentrations of purified human FXI and subjected the plasma to clotting time assays (aPTT). Prolonged clotting times by 2.75- fold compared to 100% FXI (30nM), similarly to mice injected with 14E11, correlated to ~1-2nM or ~5% concentration of FXI in human plasma (Figure 6.1D). This would suggest that 14E11 and FXI-ASO treatments achieved ~95% reduction in the plasma FXI protein levels in mice. I then used these two distinct tools to determine the effect of pharmacological targeting of FXI on atherogenesis.

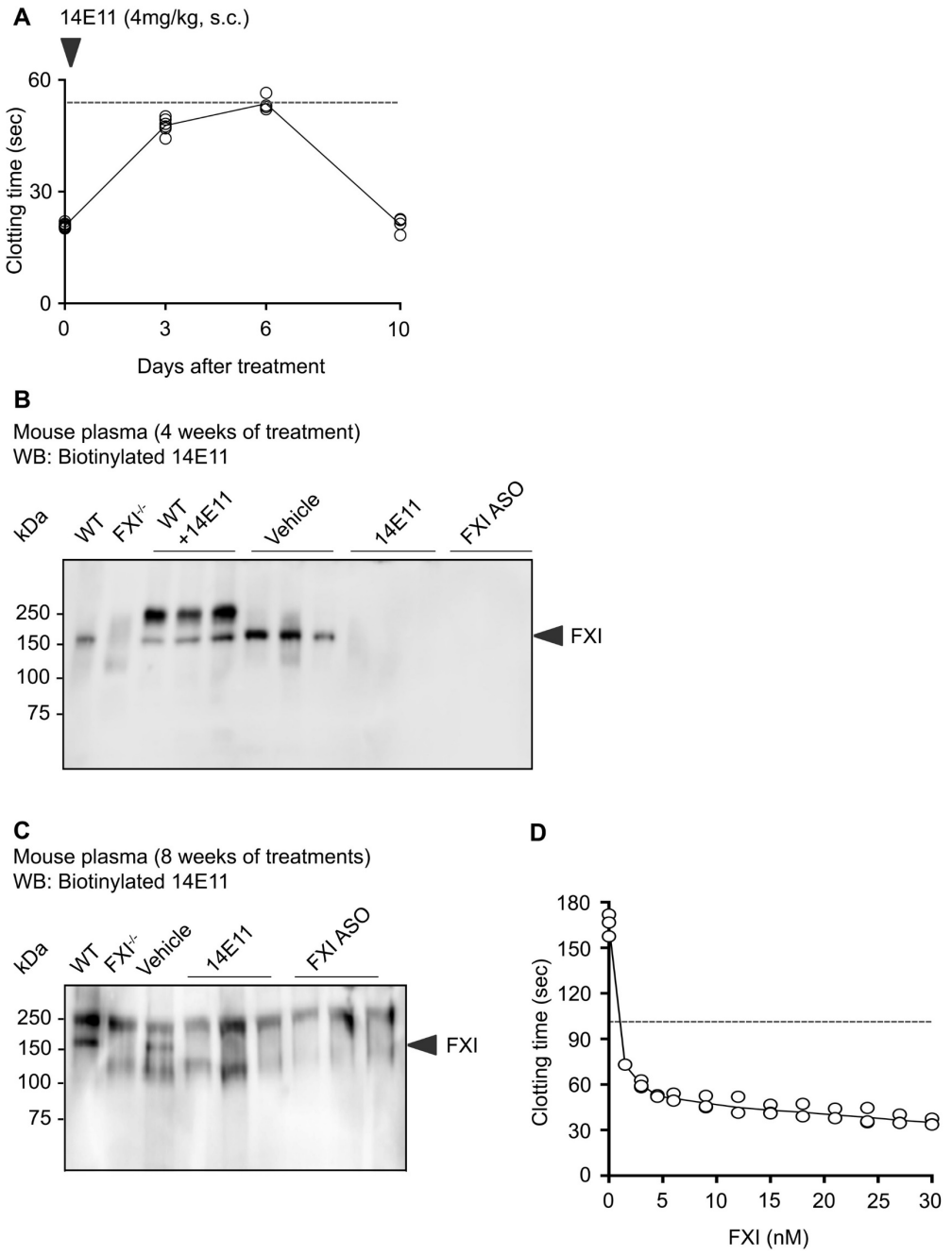

Figure 6.1. The anti-FXI mAb 14E11 and FXI-ASO reduce FXI levels in mice. A: clotting time of C57BL/6 mice injected with a single dose of 14E11, measured by aPTT assay. **B-C:** FXI levels in plasma from Ldlr$^{-/-}$ mice after 4 weeks (**B**) and 8 weeks (**C**) of HFD and treatments with vehicle, 14E11 or FXI-ASO. *Data were generated by Dr. David Gailani (Vanderbilt University).* **D:** clotting time of human FXI$^{-/-}$ plasma supplemented with increasing concentrations of purified human FXI, measured by aPTT assay. *Data were generated by Stéphanie E. Reitsma (OHSU).* Dotted lines indicate 2.75-fold increase in clotting times compared to baseline (Day 0) or 30nM FXI.

6.4.2 Effects of pharmacological targeting of FXI on atherogenesis

Ldlr$^{-/-}$ mice were fed a HFD for 8 weeks to incite atherogenesis; meanwhile select cohorts were concurrently treated for 8 weeks with either 14E11 or FXI-ASO. In proximal aortas of Ldlr$^{-/-}$ mice on HFD, mice treated with 14E11 and FXI-ASO showed 39% and 36% reduction, respectively, in lesion areas as measured by *en face* (5.1±0.3% and 5.3±0.5% aortic arch area, respectively; n=15 for vehicle, n=16 for 14E11 and FXI-ASO; $P<0.005$) compared to vehicle control (8.3±1.0% aortic arch area) (Figure 6.2B). As a secondary measure of atherosclerosis, aortic sinus sections were stained with ORO and counterstained with hematoxylin for the determination of total lesion area and plaque lipid content. Aortic sinus lesion areas and ORO (lipid) areas were normalized to the averaged total aortic sinus area to account for variability in aortic sizes between sections and animals. Compared to vehicle (lesion area=3.9±0.5 $\times 10^4 \mu m^2$, lipid area=3.4±0.4 $\times 10^4 \mu m^2$), 14E11 reduced lesion area by 33% (2.6±0.2 $\times 10^4 \mu m^2$, $P<0.05$) (Figure 6.2C, left) and lipid area by 38% (2.1±0.2 $\times 10^4 \mu m^2$, $P<0.005$) (Figure 6.2C, right). Interestingly, treatment with FXI-ASO indicated a slight but not statistically significant reduction in lesion area (3.3±0.3 $\times 10^4 \mu m^2$) (Figure 6.2C, left) and lipid area (2.6±0.2 $\times 10^4 \mu m^2$) (Figure 6.2C, right) compared to vehicle control (n=12 for vehicle, n=15 for 14E11- and n=12 for FXI-ASO-treated animals).

Eight weeks of HFD led to an increase in body weight (Figure 6.3A) and total plasma cholesterol levels compared to lean animals in all treatment groups (145±9mg/dl baseline, n=6 vs. 1044± 122mg/dl in vehicle-treated males, n=6, 989±53mg/dl in 14E11-

treated males, n=8, 941±62mg/dl in FXI-ASO-treated males, n=8, 786± 39mg/dl in vehicle-treated females, n=8, 685±32mg/dl in 14E11-treated females, n=8, or 803±46mg/dl in FXI-ASO-treated females, n=8) (Figure 6.3B, $P<0.0001$). Similarly, plasma separated by FPLC analyses demonstrated neither 14E11 nor FXI-ASO significantly altered plasma lipoprotein levels compared to vehicle controls in male (Figure 6.3C) and female (Figure 6.3D) mice on 8 weeks of HFD.

Early plaque formation is associated with monocyte influx mostly consisting of the $Ly6C^{high}$ monocytes. Moreover, platelets have been implicated in facilitating monocyte recruitment at sites of atherosclerotic plaque development.[456] I next sought to investigate whether pharmacological targeting of FXI would alter levels of circulating $Ly6C^{high}$ monocytes, as well as platelet activation using monocyte-platelet aggregates as a surrogate marker measured by flow cytometry.

In my model of atherogenesis, there was a significant increase in platelet activation upon HFD, determined as an increase in monocyte-platelet aggregates in animals treated with vehicle (14.1±1.61% total monocytes) compared to baseline (8.7±0.5% total monocytes, $P<0.05$); similar levels were observed in animals treated with 14E11 (14.4±1.5% total monocytes) or FXI-ASO (13.4±1.0% total monocytes) (Figure 6.3E). HFD showed a slight but not significant increase in circulating $Ly6C^{high}$ monocytes as compared to baseline (45.4±2.9% total monocytes in lean animals versus 55.5±3.4% in HFD animals under vehicle conditions); equivalent increases in $Ly6C^{high}$ monocyte

levels were observed for 14E11- and FXI-ASO-treated HFD animals (53.5±3.5% and 57.8±1.5%, respectively) (Figure 6.3F, n=8 for all treatment groups).

Additional hematological analyses showed no differences in levels of platelets, leukocytes, or other relevant hematological components of $Ldlr^{-/-}$ mice treated with 14E11 or FXI-ASO compared to vehicle (Table 1, n=8 for all treatment groups).

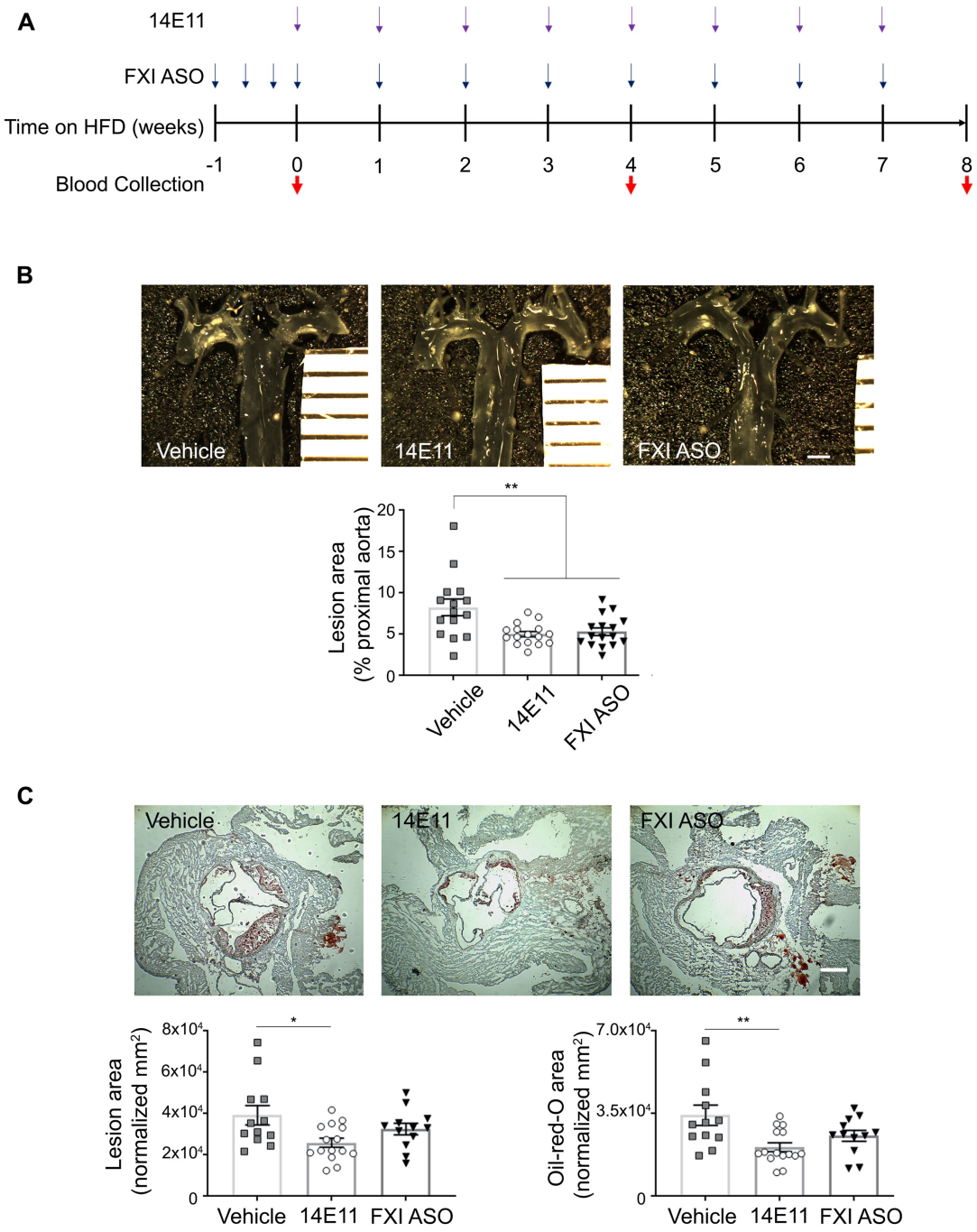

Figure 6.2. Atherosclerosis assessment in 14E11- and FXI-ASO-treated Ldlr-/- mice on 8 weeks HFD. **A:** 14E11 (4mg/kg) and FXI-ASO (7.5 mg/kg) were administered weekly while Ldlr$^{-/-}$ mice were fed HFD for 8 weeks. **B:** Atherosclerotic lesion area in the proximal aortas, quantified under light microscopy. Scale bar = 1mm. **C:** Cross-sections of aortic sinus were obtained and atherosclerotic lesion area was determined by Oil-Red-O staining (red, $\times 10^4$ μm^2). Scale bar = 200μm. Data were analyzed using Kruskal-Wallis with Dunn post hoc test. *P < 0.05; **P < 0.005; ***P < 0.0001. *P<0.05; **P<0.005; ***P<0.0001.

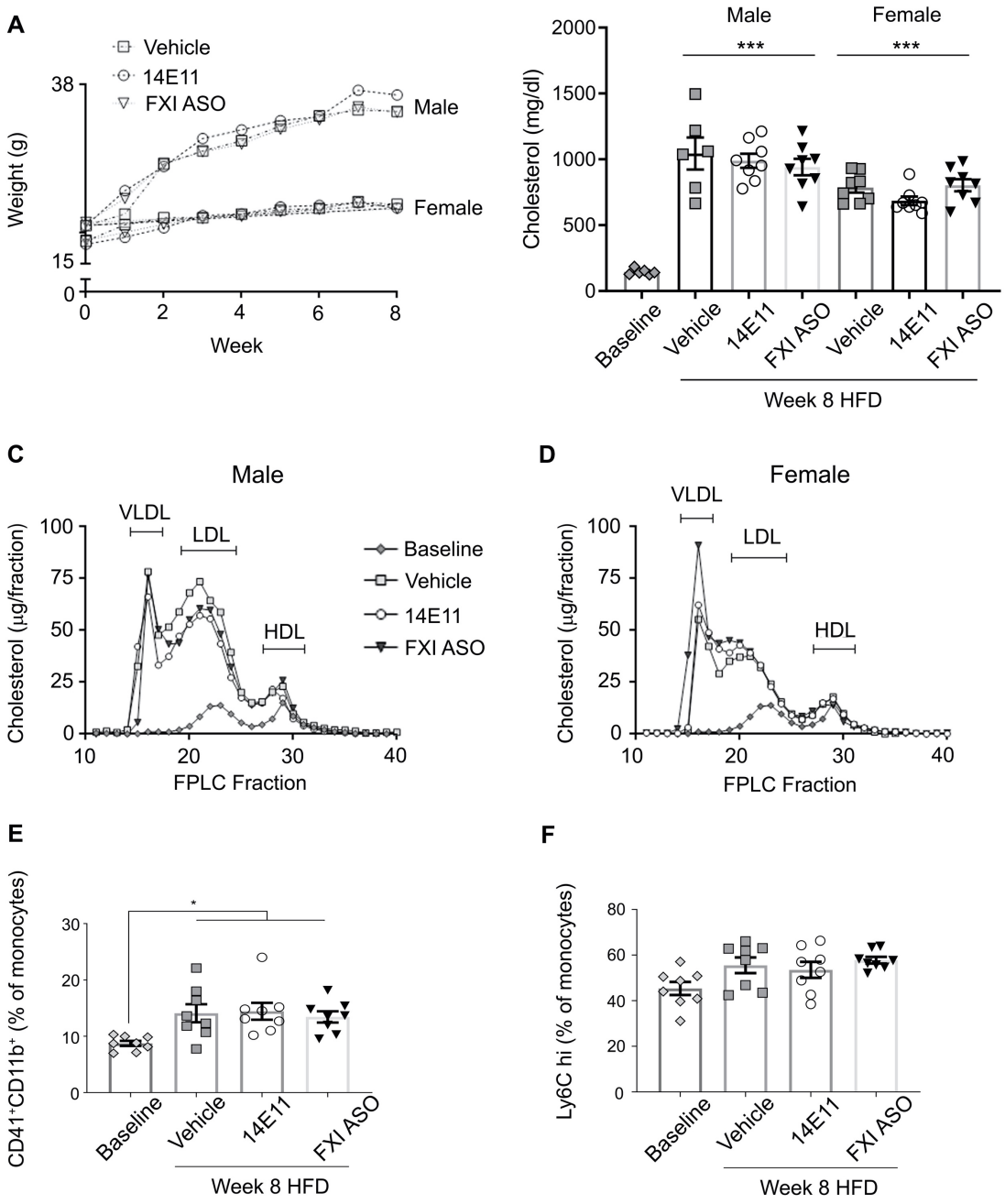

Figure 6.3. Body weight, total cholesterol, and lipid profiles in 14E11- and FXI-ASO-treated Ldlr$^{-/-}$ mice on 8 weeks HFD. A: Animal body weight recorded weekly and **B:** total cholesterol levels (mg/dl) from Ldlr$^{-/-}$ mice (males and females) at baseline and following 8 weeks HFD were measured. **C-D:** Lipid profiles, performed by FPLC for total cholesterol (µg per FPLC fraction) from pooled plasma at 8 weeks HFD. **E:** Monocyte-platelet aggregates and **F:** Ly6C^{high}, shown as % of total monocytes at baseline and 8 weeks HFD in vehicle-, 14E11-, and FXI-ASO-treated animals. Data were analyzed using ANOVA with repeated measures and Kruskal-Wallis with Dunn post hoc test. *P<0.05; ***P<0.0001 vs. baseline.

Table 6.1. Complete blood counts at 8 weeks HFD. Whole blood was drawn from the retro-orbital sinus into EDTA and subjected to hematological analysis within 1 h from collection.

	Vehicle	**14E11**	**FXI-ASO**
WBC (k/μ)	10.9 ± 0.84	11.6 ± 0.68	11.2 ± 1.08
HGB (k/μ)	18.1 ± 0.32	18.2 ± 0.49	18.1 ± 0.31
HCT (k/μ)	59 ± 0.98	59 ± 1.58	59 ± 1.02
RBC (k/μ)	11.7 ± 0.20	11.7 ± 0.31	11.5 ± 0.20
Lymphocyte (k/μ)	6.73 ± 0.41	7.95 ± 0.38	8.15 ± 0.71
Monocyte (k/μ)	0.58 ± 0.05	0.63 ± 0.06	0.53 ± 0.09
Granulocyte (k/μ)	2.70 ± 0.33	3.05 ± 0.28	2.53 ± 0.33
PLT (k/μ)	980 ± 36.8	1031 ± 20.0	1025 ± 46.8
MCV (fl)	50.13 ± 0.13	50.50 ± 0.27	51.13 ± 0.23
MCH (pg)	15.40 ± 0.09	15.55 ± 0.17	15.70 ± 0.12
MCHC (g/dl)	30.7 ± 0.18	30.9 ± 0.17	30.7 ± 0.13
RDW (%)	11.9 ± 0.11	12.2 ± 0.11	12.1 ± 0.18
MPV (fl)	5.28 ± 0.02	5.29 ± 0.04	5.33 ± 0.05

6.4.3 Effects of pharmacological targeting of FXI on atherosclerosis in a model of established disease

To study the effects of pharmacological targeting of FXI on the progression of already existing atherosclerotic plaques, $Ldlr^{-/-}$ mice fed a HFD for 8 weeks were treated with either 14E11 or FXI-ASO starting at week 8 and continuing for an additional 8 weeks while on HFD (Figure 6.4A). *En face* analysis of proximal aortas at week 16 of HFD revealed that compared to saline-treated animals (19.5±1.1% aortic arch area), 14E11 and FXI-ASO treatment for the final 8 weeks caused 23% and 20% reduction, respectively, in lesion area (15.1±1.5% and 15.6±0.7% aortic arch area, respectively) (n=17 for vehicle, n=16 for 14E11- and FXI-ASO-treated animals, $P<0.005$) (Figure 6.4B).

I also determined the effect of delayed 14E11 and FXI-ASO administration on atherosclerotic lesion area in the aortic sinus at 16 weeks of HFD. Compared to saline-treated animals (lesion area=4.9±0.1 $\times 10^4 \mu m^2$, lipid area=4.2±0.1 $\times 10^4 \mu m^2$), treatment with 14E11 and FXI-ASO starting at week 8 HFD did not result in reduced lesion area (4.8±0.2 $\times 10^4 \mu m^2$ and 4.9±0.2 $\times 10^4 \mu m^2$, respectively) (Figure 6.4C) or lipid area (4.1±0.2 $\times 10^4 \mu m^2$ and 4.2±0.1 $\times 10^4 \mu m^2$, respectively) (Figure 6.4C) in the aortic sinus (n=16 for saline, n=14 for 14E11- and n=16 for FXI-ASO-treated animals).

At 16 weeks of HFD, total plasma cholesterol significantly increased compared to week 8 (712±26mg/dl, $P<0.0001$) in untreated animals (Figure 6.4D). Similarly to what was

seen with my 8-week atherogenesis cohort, administration of 14E11 (897±116mg/dl) or FXI-ASO (958±94mg/dl) starting at week 8 HFD did not alter total cholesterol levels compared to vehicle (1114±88mg/dl) (Figure 6.4D, n=49 for week 8 HFD n=17 for vehicle, n=14 for 14E11-, and n=16 for FXI-ASO-treated animals at week 16 HFD).

In this cohort of established atherosclerosis, there was a significant increase in platelet activation compared to week 8 HFD, as quantified as increased monocyte-platelet aggregates in animals treated with vehicle (53.6±6.4% total monocytes) compared to week 8 (14.1±1.6% total monocytes, $P<0.005$); an equivalent increase was observed for 14E11- (46.5±5.9% total monocytes) and FXI-ASO-treated animals (49.8±6.1% total monocytes). Neither treatment had a demonstrable effect on *in vivo* platelet activation compared to vehicle at week 16 HFD (Figure 6.4E, n=8 for baseline, n=15 for vehicle, n=16 for 14E11 and FXI-ASO). Similarly to my atherogenesis cohort, there was a slight but insignificant increase in levels of $Ly6C^{high}$ monocytes compared to week 8 HFD for all treatments (55.5±3.4% total monocytes versus 60.1±5.3% in vehicle- and 62.3± 4.8% in 14E11- and 54.6±5.6% in FXI-ASO-treated animals) (Figure 6.4F).

In addition, 14E11 or FXI-ASO did not alter relevant hematological components at 16 weeks HFD (Table 2, n=16 for all treatment groups).

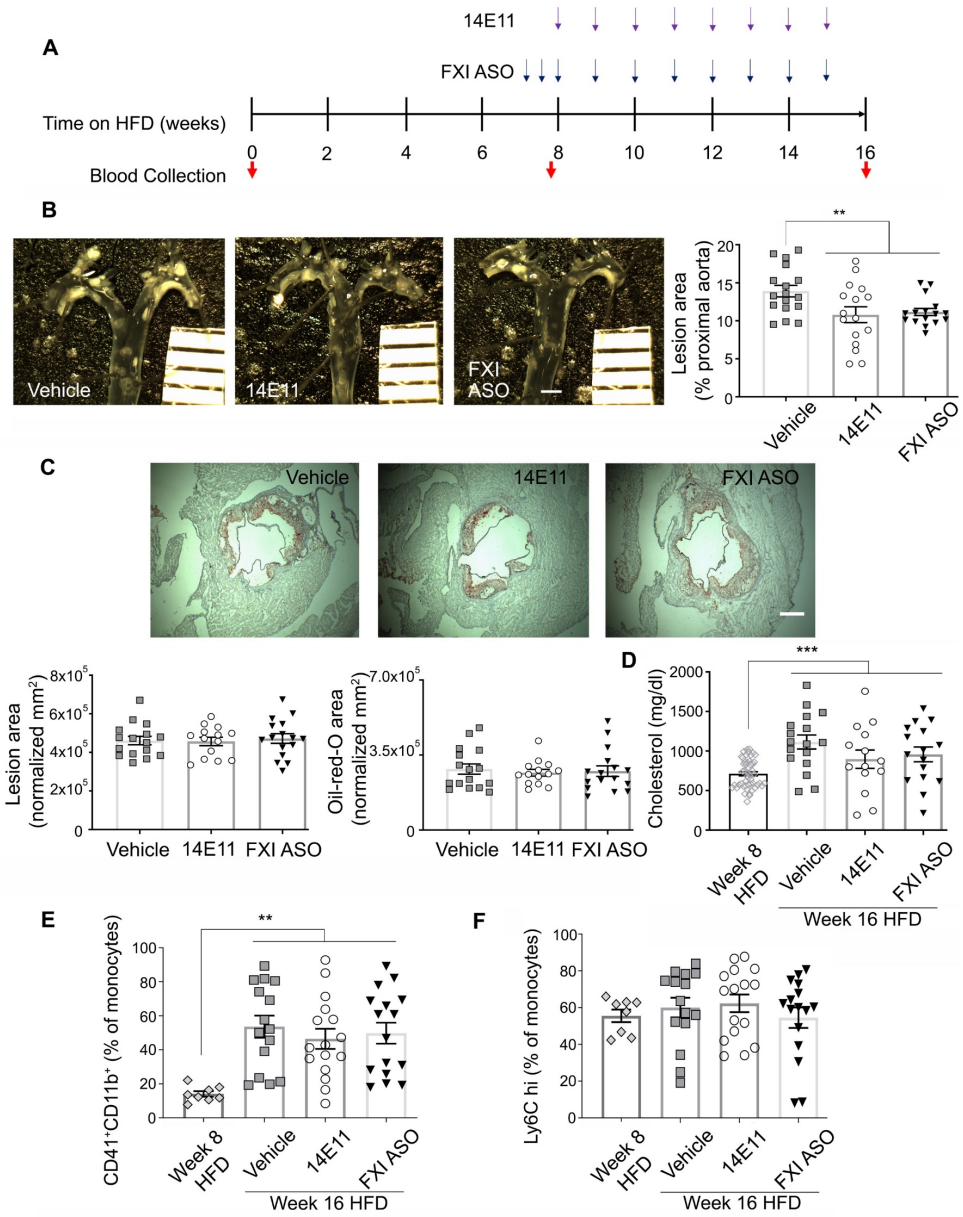

Figure 6.4. Atherosclerosis assessment in 14E11- and FXI-ASO-treated Ldlr$^{-/-}$ mice on 16 weeks HFD. A: At 8 weeks HFD, hyperlipidemic Ldlr$^{-/-}$ mice were randomized and administered 14E11 (4mg/kg) and FXI-ASO (7.5 mg/kg) weekly until 16 weeks HFD. **B:** Atherosclerotic lesion area in the proximal aortas, quantified under light microscopy. Scale bar = 1mm. **D:** Cross-sections of aortic sinus were obtained and atherosclerotic lesion area was determined by Oil-Red-O staining (red, $\times 10^5$ μm^2). Scale bar = 200μm. **D:** Total plasma cholesterol at week 8 before randomization into treatment groups and 16 weeks HFD in Ldlr$^{-/-}$ mice. **E:** Monocyte-platelet aggregates and **F:** Ly6C^{high}, shown as % of total monocytes at 8 weeks HFD before treatments and 8 weeks HFD in vehicle-, 14E11-, and FXI-ASO-treated animals. Data were analyzed using Kruskal-Wallis with Dunn post hoc test. ***P*<0.005. ****P*<0.0001.

Table 6.2. Complete blood counts at 16 weeks of HFD. Whole blood was drawn from the retro-orbital sinus into EDTA and subjected to hematological analysis within 1 h from collection.

	Vehicle	14E11	FXI-ASO
WBC (k/μ)	9.5 ± 0.26	11.2 ± 0.53	9.8 ± 0.53
HGB (k/μ)	16.3 ± 0.18	16.2 ± 0.24	16.3 ± 0.24
HCT (k/μ)	50.9 ± 0.63	51.4 ± 0.78	51.3 ± 0.77
RBC (k/μ)	10.2 ± 0.14	10.3 ± 0.15	10.1 ± 0.16
Lymphocyte (k/μ)	6.6 ± 0.2	7.58 ± 0.31	7.36 ± 0.28
Monocyte (k/μ)	0.51 ± 0.02	0.69 ± 0.06	0.54 ± 0.03
Granulocyte (k/μ)	2.36 ± 0.08	2.86 ± 0.27	2.13 ± 0.11
PLT (k/μ)	1147 ± 20	1078 ± 49	1191 ± 66
MCV (fl)	50.12 ± 0.12	50 ± 0.20	50.75 ± 0.23
MCH (pg)	16.11 ± 0.05	15.72 ± 0.09	16.13 ± 0.08
MCHC (g/dl)	32.1 ± 0.08	31.5 ± 0.08	31.8 ± 0.12
RDW (%)	12.4 ± 0.05	12.4± 0.09	12.5 ± 0.11
MPV (fl)	5.33 ± 0.01	5.37 ± 0.03	5.33 ± 0.04

6.4.4 Effects of pharmacological targeting of FXI on atherosclerotic lesion macrophage accumulation

Since I did not observe any difference in circulating levels of inflammatory Ly6C^{hi} monocytes upon 14E11 and FXI-ASO administration, I then investigated whether infiltration of monocytes and accumulation of lesion macrophages in the aortic sinus were altered upon FXI inhibition.

When either 14E11 or FXI-ASO was administered concomitantly with HFD, higher expression of the macrophage marker CD68, normalized to atherosclerotic lesion area, was observed in Ldlr$^{-/-}$ mice treated with 14E11 (33.3 ± 0.99% lesion area, $P < 0.001$) but not FXI-ASO (29.2 ± 1.42% lesion area) as compared to vehicle control (25.6 ± 1.05% lesion area). This was due to the fact that 14E11 reduced aortic lesion area compared to vehicle control (Figure 6.5A, n=11 for saline, n=15 for 14E11 and n=11 for FXI-ASO).

In the established atherosclerosis model, a similar trend was observed, wherein CD68 levels did not differ between treatment groups (30.88 ± 0.84% in vehicle-, 30.38 ± 1.00% in 14E11- and 31.38 ± 0.96% lesion area) (Figure 6.5B, n=17 for vehicle, n=16 for 14E11 and n=14 for FXI-ASO). These results suggest that infiltration of monocytes into lesion area was not altered due to FXI inhibition in Ldlr$^{-/-}$ mice.

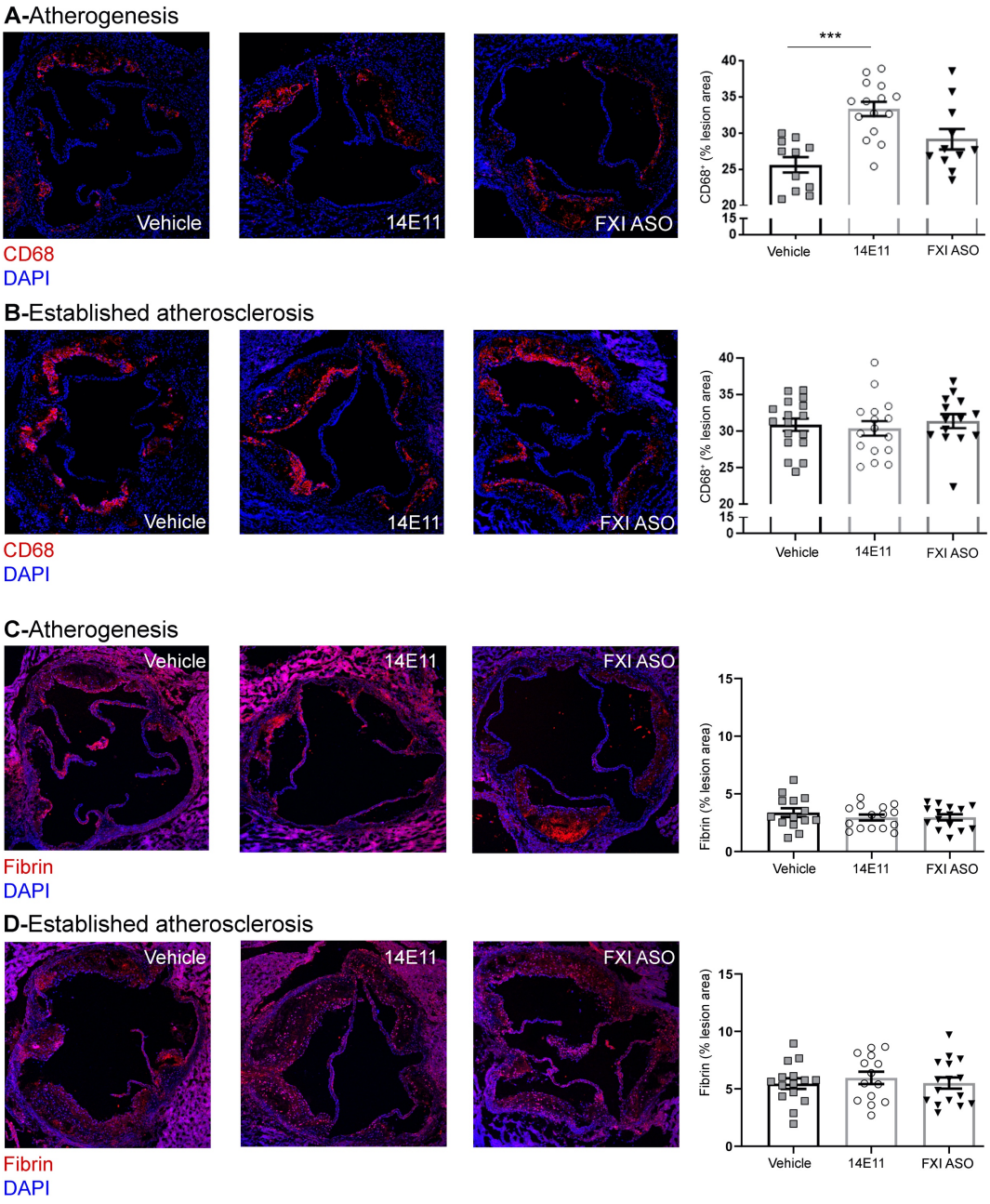

Figure 6.5. Macrophage accumulation and fibrin deposition into atherosclerotic lesions in 14E11- and FXI-ASO-treated Ldlr$^{-/-}$ mice. A-B: Cross-sections of aortic sinus were obtained and macrophage accumulation was determined by CD68 staining (red) together with nuclei (blue) in the atherogenesis model (**A**) and established atherosclerosis model (**B**). **C-D**: Cross-sections of aortic sinus were obtained and fibrin deposition was determined by fibrin staining (red) together with nuclei (blue) in the atherogenesis model (**C**) and established atherosclerosis model (**D**). Area fraction was calculated as percent lesion area threshold positive after using a Phansalkar local autothreshold with radius of 5 px using Fiji software. Data were analyzed using Kruskal-Wallis with Dunn post hoc test. *P<0.05. Scale bar = 200μm

6.4.5 Effects of pharmacological targeting of FXI on atherosclerotic lesion fibrin deposition

Histologically, fibrin(ogen) is a prominent component of progressive lesions, particularly the lesions that appear to be precursor of fibrous plaques. Fibrin(ogen) provides a scaffold for migration and proliferation of smooth muscle cells into the intima.[457] Fibrin and fibrinogen degradation product are byproducts of thrombin breakdown, and their presence in atherosclerotic lesions as well as circulating levels have been shown to add significant risk discrimination for incident of cardiovascular events.[458] I therefore investigated whether pharmacological inhibition and reduction of FXI altered fibrin deposition in aortic sinus lesions.

In the atherogenesis model, fibrin deposition did not differ between treatment groups (3.38 ± 0.38% in vehicle-, 2.95 ± 0.26% in 14E11- and 2.97 ± 0.26% lesion area in FXI-ASO-treated animals) (Figure 6.5C, n=14 for saline, n=15 for 14E11 and FXI-ASO). A similar trend was observed in the model of established atherosclerosis (5.46 ± 0.46% in vehicle-, 5.96 ± 0.54% in 14E11- and 5.51 ± 0.49% lesion area in FXI-ASO-treated animals) (Figure 6.5D, n=15 for vehicle, n=14 for 14E11 and n=16 for FXI-ASO). These results suggest that fibrin deposition into lesion area was not altered by FXI inhibition in $Ldlr^{-/-}$ mice.

6.4.6 Role of FXIa activity on endothelial cell barrier integrity

One of the hallmarks of atherosclerosis is endothelial dysfunction, characterized by disruption in endothelial barrier integrity manifesting as down-regulation of endothelial junction markers and consequently enhanced endothelial permeability to macromolecules and infiltration of white blood cells into the subendothelial space. I sought to qualitatively determine whether the enzymatic activity of FXIa affects the expression of endothelial transmembrane adhesion molecules controlling cellular junctions; I focused my experiments on VE-Cadherin (CD144) expression *in vitro*.

In HUVECs under vehicle conditions, a continuous, undisrupted pattern of VE-Cadherin was observed. Incubation of ECs with FXIa (in the presence of hirudin) or α-thrombin disrupted the surface expression pattern of VE-Cadherin (Figure 6.6). In contrast, the zymogen FXI had no effect on VE-Cadherin expression pattern on HUVECs, similar to vehicle control (Figure 6.6). In the presence of PPACK, which binds irreversibly to the active site of serine proteases and therefore inhibits catalytic activities of FXIa and α-thrombin, no change in VE-Cadherin expression pattern on HUVECs was observed (Figure 6.6). Together, these results suggest that the enzymatic activity of FXIa induces endothelial cell-cell junction weakening and compromised barrier integrity.

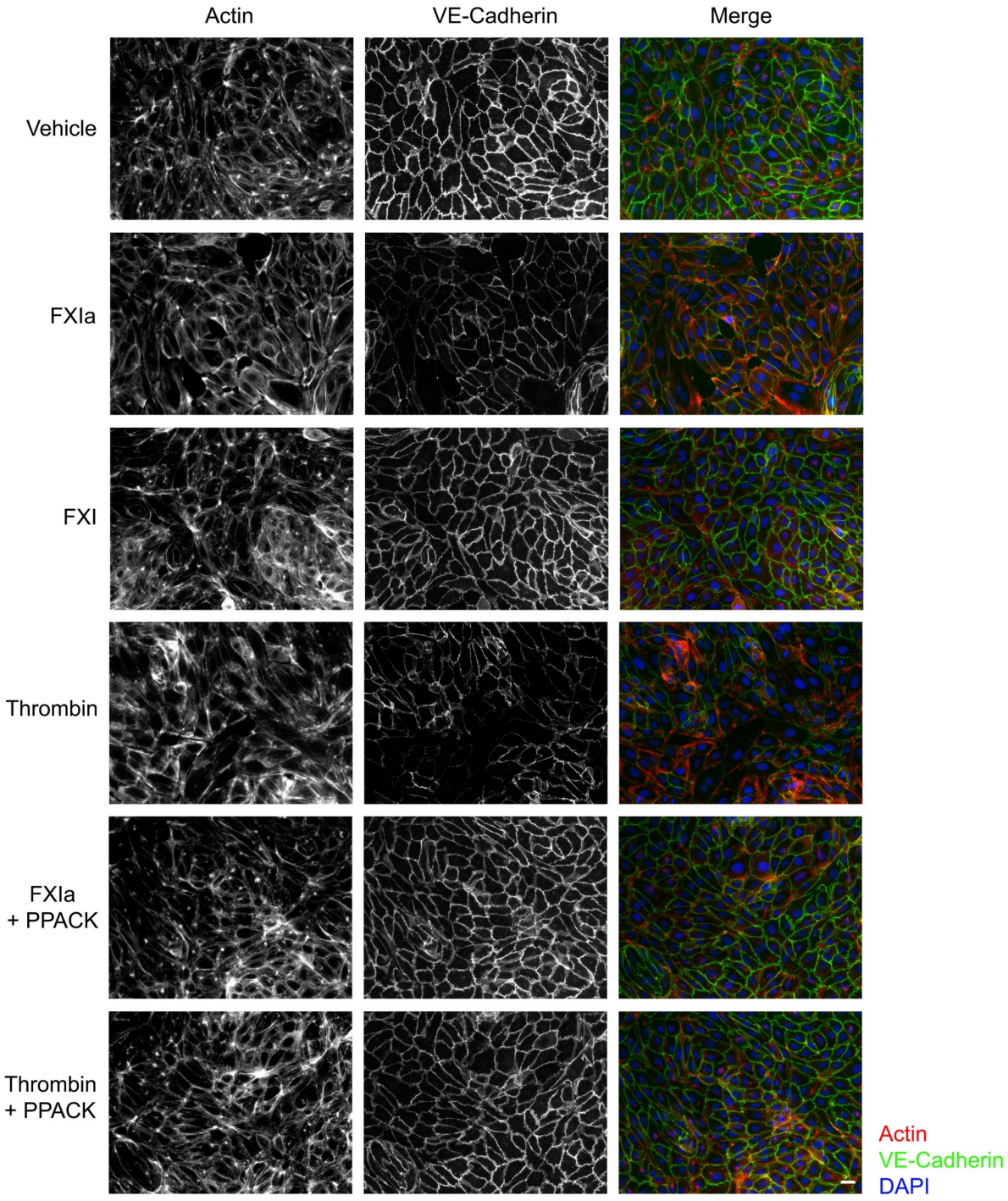

Figure 6.6. VE-Cadherin expression on the surface of endothelial cells following exposure to FXIa. HUVECs were seeded onto gelatin-coated glass coverslips and grown to confluence in a 24-well plate prior to exposure to vehicle, FXIa (30nM), FXI (30nM), α-thrombin (10nM), or FXIa or thrombin in the presence of PPACK. Cells were fixed and stained for VE-Cadherin (green), together with actin (red), nuclei (blue) and visualized by immunofluorescence microscopy. Scale bar = 50μm.

6.4.7 Role of FXIa activity on endothelial cell permeability

Since VE-Cadherin is known to play an essential role in maintaining endothelial cell permeability, I next designed experiments to determine whether the enzymatic activity of FXIa increased endothelial cell permeability.

Incubation of ECs with FXIa caused a significant increase in the leakage of Evans Blue dye, quantified as an increase in absorbance at 650nm over time from the lower chamber of Transwells ($P<0.05$; Figure 6.7A). A similar effect was observed for α-thrombin. Inhibition of the active site of FXIa and α-thrombin with PPACK prevented Evans Blue dye leakage ($P<0.05$; Figure 6.7A).

Furthermore, exposure of endothelial cells to FXIa also resulted in an increased rate of acLDL transport across the endothelial monolayer towards the lower chamber of Transwells ($P<0.005$; Figure 6.7B). Inhibition of FXIa activity with PPACK prevented the transmission of acLDL across the endothelial monolayer (Figure 6.7B). Together, these experiments suggest that structural changes in HUVECs upon exposure to FXIa correlates to an increase in endothelial permeability to lipoproteins, mediated by the enzymatic activity of FXIa.

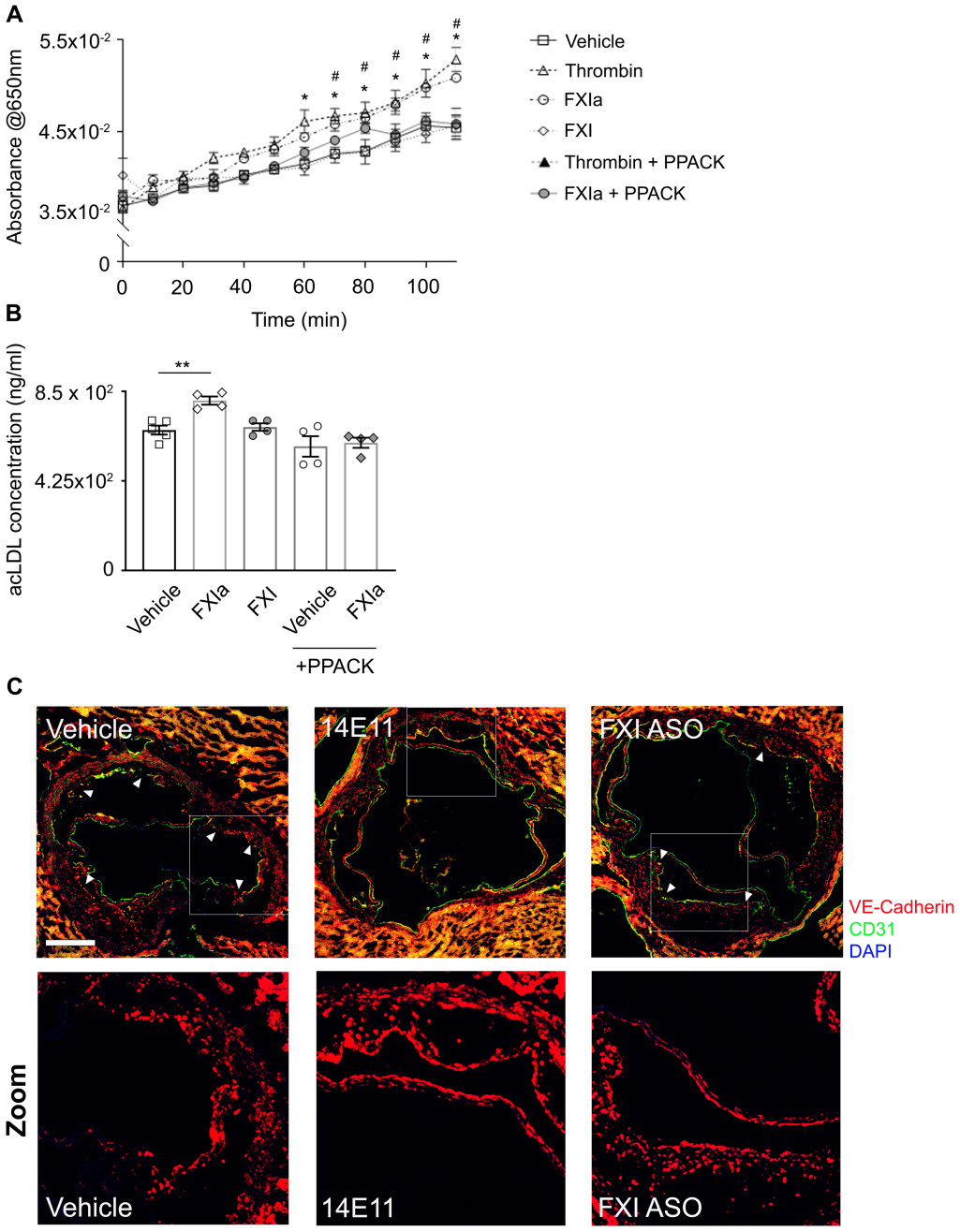

Figure 6.7. Endothelial permeability to lipoproteins *in vitro* and aortic lesion VE-Cadherin expression *in vivo*. A: Absorbance of labeled BSA from the lower chamber. **B:** acLDL was added in 0.3% BSA to the upper chamber and media from the lower chamber was collected at 24 h post-incubation. acLDL concentration (ng/ml) was calculated based on standard curve. **C:** Lesion endothelial barrier integrity was determined by VE-Cadherin (red) and CD31 (green) staining together with nuclei (blue). Scale bar = 200μm. White arrows indicate regions with disrupted VE-Cadherin staining pattern. White boxes highlight regions chosen for Zoomed images. Data were analyzed using One-way ANOVA with Tukey's post hoc tests to compare treatment groups. **P*<0.05 Thrombin vs. vehicle. #*P*<0.05 FXIa vs. vehicle. ***P*<0.005 FXIa vs. vehicle.

6.4.8 Effects of pharmacological targeting of FXI on lesion VE-Cadherin expression in Ldlr$^{-/-}$ mice

I then qualitatively investigated whether the disruption of VE-Cadherin expression, induced by FXIa, in cultured human endothelial cells observed *in vitro* would correlate to disrupted VE-Cadherin expression in the aortic sinus lesions *in vivo* in the atherogenesis mouse model. I performed immunohistochemistry staining for VE-Cadherin and the endothelial marker CD31 in aortic sections of Ldlr$^{-/-}$ mice.

Vehicle-treated animals exhibited lesions with marked disruption in VE-Cadherin expression along the luminal side of atherosclerotic plaques. FXI-ASO-treated animals also exhibited lesions with some degree of disruption in VE-Cadherin staining pattern. Strikingly, 14E11-treated animals exhibited continuous and undisrupted VE-Cadherin expression on the lesion luminal surface (Figure 6.7C). Altogether, these results suggest, as a proof-of-concept, that FXI activity may contribute to atherosclerosis development and progression through enhancing endothelial permeability to macromolecules.

6.5 Discussion

Almost all coagulation factors, including FXI of the contact activation complex, are present in human atherosclerotic plaques, raising the possibility of a causal link between thrombin generation and atherosclerosis.[445] The role of FXI in atherogenesis remains ambiguous as compared to its role in thrombosis in acutely ruptured plaques and inflammation.[256,260,451] Therefore, I investigated whether FXI promotes atherosclerosis development and plays a role in already established atherosclerosis in $Ldlr^{-/-}$ mice by targeting FXI with 14E11 or FXI-ASO. Previously, Ganor et al. was the first to investigate whether lack of FXI affects atherogenesis using ApoE/FXI double knockout mice.[263] Herein, my study utilized a pharmacological approach to inhibit and reduce FXI levels in a mouse atherosclerosis model. A significant reduction in atherosclerotic lesions was observed in the proximal aortas of 14E11- and FXI-ASO-treated animals when 14E11 and FXI-ASO were administered at the start of HFD, or in my model of established disease. Similar to FXI-deficiency in $ApoE^{-/-}$ mice,[263] lowering FXI levels had no effect on plasma cholesterol levels or lipoprotein distribution, suggesting that the effects of 14E11 or FXI-ASO were not mediated by changing the lipid profile of $Ldlr^{-/-}$ mice.

In the aortic sinus, 14E11-treated animals exhibited significant lesion area reduction relative to vehicle at 8 weeks HFD; however, this effect is no longer observed in the sinus when 14E11 was administered once lesions have already developed. On the contrary, *en face* analysis shows a significant lesion area reduction in the proximal

aortas, regardless of when FXI inhibition was administered relative to HFD. This suggests that there exist selective modulations at multiple vascular sites that regulate site-specific atherosclerosis development and therefore influence pharmacological effects of FXI inhibition. For instance, hemodynamic factors can prime endothelial gene expression at particular vascular locations and therefore regulate lipoprotein oxidation and adhesion of inflammatory cells,[459] as an example of atherogenic mechanisms beyond the scope of my study. Furthermore, FXI-ASO did not alter atherosclerotic lesion area in the aortic sinus in either atherosclerosis models. The difference may be explained by the slow onset of action of ASO-s as compared to the antibody-mediated clearance of FXI by 14E11, as initiation of the pathological process may have happened by the time pharmacological activity of FXI-ASO became significant.[453] My study also highlights notable differences between rodents and primates, as far as FXI is concerned, including the presence of a non-circulating FXI reserve associated with the endothelium in mice,[460] and the observation presented herein that 14E11 rapidly clears FXI in mice, all of which may affect the translational relevance of the experiments in mice.

Several studies have implicated the involvement of FXI in certain forms of inflammation and infections,[260,262,450,451] which prompted us to investigate platelet activation and Ly6C^{high} inflammatory monocyte levels, together with the accumulation of CD68^{+} macrophages in aortic sinus lesions as surrogate markers for systemic and local lesion inflammation, respectively. 14E11 and FXI-ASO treatments had no effect on platelet activation or Ly6C^{high} monocyte levels in whole blood, and macrophage accumulation

was not altered in aortic lesions upon FXI inhibition. Targeting FXI also did not affect complete blood counts compared to vehicle-treated mice. These findings indicate that FXI does not seem to play a role in regulating systemic inflammatory responses or the local plaque inflammatory state in experimental atherogenesis, in contrast to the observed role for FXII in these processes. For instance, although the role of FXII in vascular inflammation remains controversial, it has been shown that ApoE/FXII double knockout mice exhibit reduced lesion area, and that FXII functions as a strong inducer of pro-inflammatory cytokine release by T-cells and macrophages in those mice.[300] Since $Ldlr^{-/-}$ mouse model largely depends on hepatic receptor defect to induce hypercholesterolemia, while deficiencies in ApoE in hepatocytes, macrophages and other cells also contribute to hyperlipidemia in $ApoE^{-/-}$ mice, future studies using pharmacological approaches to target FXI in $ApoE^{-/-}$ mice may yield further insights into the role of FXI in atherogenesis.

Lastly, my *in vitro* data indicating that FXIa exposure to endothelial cells induces permeability to lipoproteins, together with the fact that reducing FXI levels with 14E11 reversed the hallmark distribution of VE-Cadherin expression observed in vehicle-treated $Ldlr^{-/-}$ mice suggest that FXIa-induced vascular permeability may contribute to the pathology of atherosclerosis by altering endothelial junctional regulation. This further supports the hypothesis that FXI activation and activity exerts inflammatory effects on the endothelium that may promote infiltration of macromolecules into the subendothelial space, which may in part facilitate atherogenesis. Altogether, my data implicate the

importance of early intervention in order to gain athero-protective benefits when targeting FXI.

Currently, antiplatelet agents and anticoagulants remain the cornerstone for primary and secondary prevention of cardiovascular diseases, despite the fact that risk of bleeding often outweighs benefits, especially in the case of combination therapies.[9,10,461-463] Since the role of the contact activation system, specifically FXI, appears to be limited in hemostasis,[464] interference with contact activation of FXI or FXI production may help prevent or slow down the development of atherosclerosis without an associated major risk of bleeding. My results obtained from experiments using 14E11- and FXI-ASO-treated $Ldlr^{-/-}$ mice suggest athero-protective benefits of contact system inhibition by lowering FXI levels. It may well be that targeting FXI, along with the use of cholesterol-lowering drugs, could yield additive benefits in inhibiting the progression of atherosclerosis.

Chapter 7. Conclusions and Future Directions

7.1 Conclusions

The studies outlined in this thesis explore platelet signaling mechanisms underlying hemostasis and vascular inflammation with the goal of improving rational design and development of antiplatelet and anticoagulant therapies. Platelet activation is associated with major changes in the actin cytoskeleton driven by small GTPases. The first chapter investigated the spatial and functional regulation of Rho GTPases by RhoGDIs, uncovering signaling mechanism of PKC in regulating platelet cytoskeletal dynamics. The second chapter further explored signaling pathways related to PKC and MAPK p38 associated with platelet cytoskeletal dynamics, procoagulant activity and inflammatory response, as little is known regarding p38 targets in platelet activation. Utilizing causal pathway tools, I modeled, organized and discovered new PKC and MAPK signaling routes that may be potential therapeutic targets in platelets activation. My next chapter was motivated by developmental differences between adult and neonatal platelets that manifested in neonatal platelet hyporeactivity to agonists. I investigated neonatal platelet response downstream of GPCRs, discovering neonatal platelets exhibiting enhanced sensitivity to the secondary mediator ADP. My study highlights distinct functional neonatal platelet phenotype that must be considered in the management of neonatal platelet transfusion with adult platelets. My last chapter examined the role of factor (F) XI of the intrinsic pathway in driving early development of atherosclerosis. I

found that reducing FXI level in atherogenic Ldlr$^{-/-}$ mice reduced atherosclerotic lesion area, potentially via inhibition of FXI modulation on endothelial permeability.

In this chapter, I summarize the results and describe future work to investigate signaling mechanisms underlying membrane trafficking orchestrated by Rab-GTPases as an elaboration of existing roles for small GTPases in platelet hemostatic function.

7.2 Summary

7.2.1 Platelet Rho GTPase-driven cytoskeletal function regulated by PKC

I observed that platelets express two RhoGDI members, RhoGDI and Ly-GDI that have not been characterized before in the context of platelet activation. I found that RhoGDI and Ly-GDI had distinct localization throughout platelets, with Ly-GDI exhibiting polarized localization that overlaps with Rho GTPases Rac1 and Cdc42, together with microtubules and PKC. Biochemical assays demonstrated that Ly-GDI is phosphorylated in a PKC-dependent manner downstream of GPVI, orchestrating the co-localization of Ly-GDI with Rac1 and Cdc42 along platelet microtubules. Such spatial organization of Rho GTPases and RhoGDIs by PKC signaling fine tunes Rho GTPase-driven hemostatic response upon platelet activation.

7.2.2 Platelet procoagulant phenotype regulated by MAPK signaling

Utilizing a combination of interactome, pathway analysis and systems biology tools, I investigated signaling relations around PKC and MAPK associated with cytoskeletal dynamics, hemostatic function and inflammatory responses. Pathway and causality analysis identified MAPK p38 as a putative central, highly connected node in the platelet signaling network. Using biochemical assays, I confirmed and further detailed sequential p38-MK2 phosphorylation of RTN4 and sequestration of Bcl-xl to organize platelet procoagulant activity at the endoplasmic reticulum level. This study demonstrates utility of omics tools to generate testable hypothesis and discover new signaling mechanisms and therapeutic targets in platelets and other cell and tissue systems.

7.2.3 Distinct differences in platelet function between adults and neonates

I utilized small-volume, whole blood functional assays to investigate neonatal platelet response downstream of GPCRs. I demonstrated that neonatal and cord blood-derived platelet exhibited diminished response to protease-activated receptor stimulation yet enhanced sensitivity to ADP, a secondary mediator important for amplification of platelet activation. Neonatal platelets may employ ADP-mediated feedback activation loop as a compensatory mechanism for hyporeactivity downstream of PARs. This study highlights the distinct functional phenotypes between adults and neonates that may come to relevance in the management of neonatal bleeding complications through transfusion of adult platelets into neonates.

7.2.4 Pharmacological targeting of coagulation factor XI mitigates atherosclerosis

I investigated the effects of FXI inhibition and reduction in experimental models of atherogenesis and established atherosclerosis. Early treatment of FXI antibody (14E11) or FXI antisense oligonucleotide (FXI-ASO) reduced atherosclerosis in the proximal aortas of $Ldlr^{-/-}$ mice, and 14E11 also reduced lesion area in the aortic sinus. Delayed FXI inhibition (established atherosclerosis model) still demonstrated reduced lesion area in the proximal aortas, yet no effect in the aortic sinus of $Ldlr^{-/-}$ mice. Cultured endothelial cells exposed to activated FXI showed enhanced permeability to lipoprotein, suggesting that pharmacological targeting of FXI reduced atherogenesis potentially by modulating endothelial barrier function. This study provided a rationale for interference with the contact activation system as a safer approach to target development and progression of atherosclerosis and potentially other inflammatory diseases.

7.3 Future Directions

7.3.1 Platelet membrane trafficking

Trafficking of vesicles is essential for granule biogenesis and maturation and facilitates exocytosis and endocytosis processes crucial for platelet activity.[465-467] It has become increasingly apparent that small GTPases play crucial roles in the regulation of membrane vesicle trafficking. I previously explored Rho GTPase signaling pathways underlying platelet cytoskeletal dynamics in Chapters 3 and 4, which are tightly

interconnected processes with vesicle trafficking in orchestrating platelet hemostatic function. Recent work utilizing biochemical, phosphoproteomics and systems analysis approaches has highlighted over 40 unmapped proteins associated with Rab GTPases, the most abundant family of small GTPases comprising of almost 70 human members that are master regulators of vesicle trafficking within exocytosis and endocytosis pathways.[169] Rab GTPases are regulated by phosphorylation events upon platelet stimulation,[169,468] yet the functional significance of such regulation by immunomodulatory kinases is unknown. Studies characterizing the functionality of Rabs remain limited and therefore reflecting the lack of pharmacological or molecular tools to target Rabs within platelets. Utilizing similar approaches as in Chapters 3 and 4, I hypothesize that the roles of yet-to-be-characterized Rab GTPases in platelets may in part overlap with Rho GTPases and therefore provide further insights into signaling pathways and crosstalk underlying platelet hemostatic function.

7.3.2 Small GTPases in platelet membrane trafficking

Rab GTPases

Human platelets contain 40 Rab members that function to provide specific membrane identity and ensuring that cargoes are trafficked correctly to cellular compartments.[192,469] Rabs exist in both soluble and membrane-bound forms. When activated, GTP-Rabs can interact with numerous effectors, adaptor, motor proteins, kinases and phosphatases to regulate trafficking events (Fig. 7.1).[469,470] Studies in

mice lacking Rab27A and Rab27B, the most highly expressed Rab member, show that these Rab GTPases are important for dense granule secretion and biogenesis.[471-473] GTP-loaded Rab27B and Rab27A have been shown to interact with SNARE tethering factor Munc13-4 in platelets.[474,475] Other studies have shown the actin motor protein, myosin Va, can interact with Rab27.[476] Rab8 has been shown to regulate dense granule secretion, and Rab4 has been found to associate with α-granules and facilitate VWF secretion from α-granules.[477,478] Many other Rabs have been found based on proteomic expression in platelets and their association with exocytotic vesicles such as Rab3, Rab26 and Rab37, yet functional roles of these Rab proteins remain uncharacterized within the platelet activation program.[469]

Investigating the spatial localization of Rabs relative to their effectors, adaptors, GAPs, GEFs and GDIs that participate in vesicle tethering and how they regulate SNARE-mediated fusion of vesicles with the cell membrane would yield insights into subcellular communications between Rabs during platelet secretion. This can be achieved using biochemical assays utilizing immunofluorescence and immunoprecipitation approaches in platelets, or in megakaryocytes using live-cell imaging and FRET-based assays to asses spatio-temporal regulation of Rab trafficking throughout the subcellular compartments.

Internalized cargo is trafficked through Rab4 (early endosomes) positive compartments prior to being targeted to Rab11 (recycling endosomes) and α-granules compartments in platelets (Fig. 7.1). Rab7A is often associated with vesicle transport to the lysosomes,

while Rab7B controls endosomal transport to the Golgi complex. So far, proteomic data only supports the expression of Rab7A in platelets,[169,479] whose function still remains to be determined. In megakaryocytes, Rab1B plays a role in early vesicle transport from the ER to the Golgi complex and subsequent α-granules.[480] Rats lacking Rab38 have no dense granules within megakaryocytes and platelets. Rab32 and Rab38 differentially regulate dense granule biogenesis and trafficking to immature Rab7A positive late endosomes.[481,482] Rab10 and Rab14 are highly expressed in platelets while their trafficking roles remain unknown.[470] Other uncharacterized Rabs and their regulators in platelets include the GEFs Rab3A-interacting protein (regulates Rab8), Rabex-5 (regulates Rab5A) and the GAPs RabGAP1 (regulates Rab6), RabGAP1-like (regulates Rab22A) and Rab3GAP1 (regulates Rab3).[192] I hypothesize that each Rab isoform exhibits specific subcellular localization and distinct regulators and effectors within platelets with some redundancy. Investigating how Rabs communicate with each other to specify functions and territories within platelets would aid in the differentiation between signaling mechanisms applicable to all Rab-regulated pathways versus Rab isoform-specific pathways. Knockout and knockdown animal models of various Rab isoforms will further help to reveal the common and unique functions of each Rab isoforms in the context of hemostasis, thrombosis and vascular inflammation.

Overall, I propose to utilize platelet biochemical assays and phosphoproteomics methods to characterize Rab spatio-temporal organization and profile signaling mechanisms regulating Rab GTPases within platelets. Together with literature-guided

causal interference tools, I can narrow down site-specific signaling relations of Rabs and their regulators and potential crosstalk with Rho GTPases during platelet endocytosis, granule biogenesis and secretion following receptor stimulation.

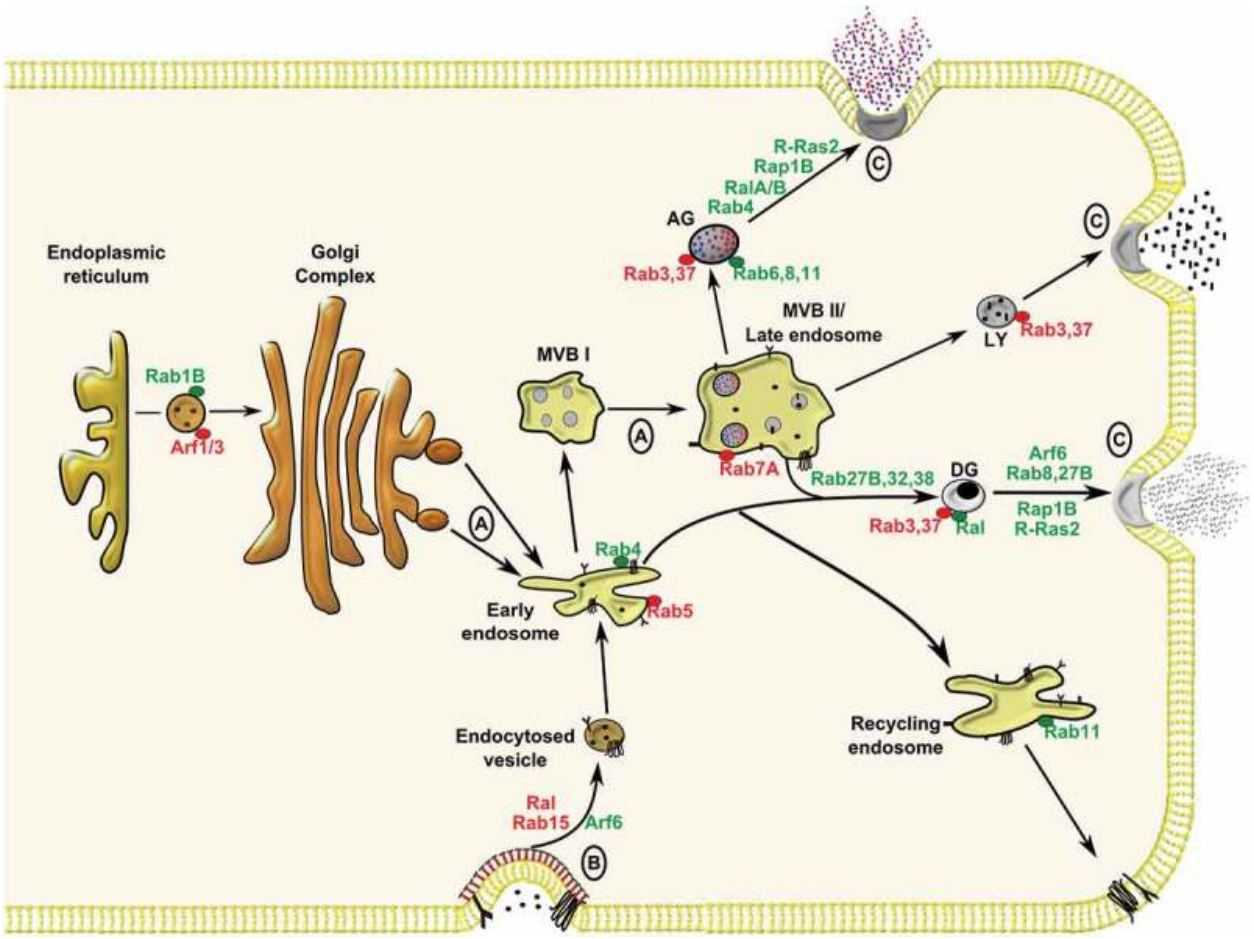

Figure 7.1. Membrane trafficking pathways within megakaryocytes and platelets involving Rab, Arf and Ras GTPases. A: Granule biogenesis. B: Endocytosis pathways. C: Exocytosis. Granule biogenesis and endocytosis culminate in cargo packaging into early endosomes before sorting in immature MVB to mature endosomes or lysosomes. Following biogenesis, AG, LY and DG mature within platelets before exocytosis upon platelet activation. AG indicates α-granule; LY-lysosome; DG-dense granules; MVB-multi-vesicular bodies. Trafficking roles for megakaryocytes/platelets GTPases are highlighted in green. Roles for GTPases inferred from other cell systems are in red. Figure adapted from Walsh et al., *Platelets* 2019; 30(1):31-40. Reprinted with permission.

Other small GTPases in membrane trafficking

The ADP-ribosylation factor (Arf) family of small GTPases include six members (Arfs 1-6) that form part of a larger family containing over 20 proteins.[483] Arfs are regulated functionally and spatially by GEFs and GAPs, but they exhibit distinct myristoylation at the N terminus that brings Arf in close contact with the cell membrane for biological activity.[484] GTP-Arf effectors include proteins involved in endocytosis, membrane tethers, lipid enzymes and scaffold proteins, but GTP-Arf can also interact with effectors to regulate trafficking events.[485] Arf family also plays important role in cytoskeletal remodeling, similarly to Rho GTPases.[486] I hypothesize that there exists tightly regulated crosstalk between Rabs, Arfs and Rho GTPases in regulating platelet hemostatic function. Immunofluorescence and super-resolution microscopy approaches investigating spatial localization of these small GTPases relative to each other, to all granular compartments and to the platelet cytoskeleton would yield insights into the orchestration of platelet membrane trafficking driven by Arf upon platelet activation.

The Ras sarcoma (Ras) GTPases are the second largest family of the Ras superfamily, consisting of 36 members associated with cell proliferation, differentiation and survival.[487] Mutations in four genes associated with Ras signaling result in Noonan Syndrome with a bleeding diathesis.[488,489] Rap1 (A and B) are the most abundantly expressed Ras GTPases in platelets and play crucial roles in platelet adhesion, secretion and integrin activation.[490,491] The Ras-like (Ral) GTPases (A and B) have been implicated as regulators of vesicle trafficking.[492] Ral is associated with dense

granules and can be activated by various platelet agonists in a calcium-dependent manner.[493,494] Ral activity is regulated by Ras GTPases, including Rap1, and RalGAP that regulates Ral-GTP hydrolysis.[495] Interestingly, murine platelets deficient in RalA or RalB have no defect in dense granule secretion, and RalA/B double knock-out platelets have only mild defect that does not alter aggregation and thrombus formation.[496] I hypothesize that the potential crosstalk and redundant trafficking roles for Ral, Ras and other small GTPases in platelets can be explored using pathway analysis to generate signaling models from omics datasets and testable hypotheses for future platelet studies.

7.3.2 Clinical significance

Platelet proteomic datasets have provided expression data on an array of small GTPases, whose functional relevance to platelet signaling and activity remains to be determined.[192,470,497] Combination of causal pathway analysis and other omics tools will aid in the identification of specific targets underlying exocytic and endocytic processes in platelets. Understanding the mechanistic basis of endocytosis in megakaryocytes and platelets will expand the potential clinical use of *in vitro*-grown platelets for transfusion applications. Several groups have reported progress towards production of platelets derived from *in vitro*-grown megakaryocytes.[498]
Such *in vitro*-grown megakaryocytes are cultured in media with virtually all of proteins normally endocytosed or pinocytosed by megakaryocytes; therefore, supplementation of missing proteins into the media can restore platelet storage pool deficiencies. *In vitro*-

grown platelets may eventually displace donor-derived platelets for transfusion, and new insights into endocytosis and membrane trafficking of megakaryocytes and platelets will enhance the variety of clinical settings where modified *in vitro-grown* platelets could be uniquely useful, such as in modulating tissue regeneration and cancer metastasis.

References

1 Lozano R, Naghavi M, Foreman K, Lim S, Shibuya K, Aboyans V, Abraham J, Adair T, Aggarwal R, Ahn SY, et al. Global and regional mortality from 235 causes of death for 20 age groups in 1990 and 2010: a systematic analysis for the Global Burden of Disease Study 2010. *Lancet*. 2012; **380**: 2095-128.

2 Posthuma JJ, Posma JJN, van Oerle R, Leenders P, van Gorp RH, Jaminon AMG, Mackman N, Heitmeier S, Schurgers LJ, Ten Cate H, Spronk HMH. Targeting Coagulation Factor Xa Promotes Regression of Advanced Atherosclerosis in Apolipoprotein-E Deficient Mice. *Sci Rep*. 2019; **9**: 3909.

3 Liu X, Ma J, Ma L, Liu F, Zhang C, Zhang Y, Ni M. Overexpression of tissue factor induced atherothrombosis in apolipoprotein E-/- mice via both enhanced plaque thrombogenicity and plaque instability. *J Mol Cell Cardiol*. 2019; **127**: 1-10.

4 Borissoff JI, Otten JJ, Heeneman S, Leenders P, van Oerle R, Soehnlein O, Loubele ST, Hamulyak K, Hackeng TM, Daemen MJ, Degen JL, Weiler H, Esmon CT, van Ryn J, Biessen EA, Spronk HM, ten Cate H. Genetic and pharmacological modifications of thrombin formation in apolipoprotein e-deficient mice determine atherosclerosis severity and atherothrombosis onset in a neutrophil-dependent manner. *PLoS One*. 2013; **8**: e55784.

5 Mega JL, Braunwald E, Wiviott SD, Bassand JP, Bhatt DL, Bode C, Burton P, Cohen M, Cook-Bruns N, Fox KA, Goto S, Murphy SA, Plotnikov AN, Schneider D, Sun X, Verheugt FW, Gibson CM, Investigators AAT. Rivaroxaban in patients with a recent acute coronary syndrome. *N Engl J Med*. 2012; **366**: 9-19.

6 Eikelboom JW, Connolly SJ, Bosch J, Dagenais GR, Hart RG, Shestakovska O, Diaz R, Alings M, Lonn EM, Anand SS, et al. Rivaroxaban with or without Aspirin in Stable Cardiovascular Disease. *N Engl J Med*. 2017; **377**: 1319-30.

7 Becker RC, Moliterno DJ, Jennings LK, Pieper KS, Pei J, Niederman A, Ziada KM, Berman G, Strony J, Joseph D, Mahaffey KW, Van de Werf F, Veltri E, Harrington RA, Investigators T-P. Safety and tolerability of SCH 530348 in patients undergoing non-urgent percutaneous coronary intervention: a randomised, double-blind, placebo-controlled phase II study. *Lancet*. 2009; **373**: 919-28.

8 Mertens L, Eyskens B, Boshoff D, Gewillig M. Safety and efficacy of clopidogrel in children with heart disease. *J Pediatr*. 2008; **153**: 61-4.

9 An J, Niu F, Lang DT, Jazdzewski KP, Le PT, Rashid N, Meissner B, Mendes R, Dills DG, Aranda G, Bruno A. Stroke and Bleeding Risk Associated With Antithrombotic

Therapy for Patients With Nonvalvular Atrial Fibrillation in Clinical Practice. *J Am Heart Assoc*. 2015; **4**.

10 Pasea L, Chung SC, Pujades-Rodriguez M, Shah AD, Alvarez-Madrazo S, Allan V, Teo JT, Bean D, Sofat R, Dobson R, Banerjee A, Patel RS, Timmis A, Denaxas S, Hemingway H. Bleeding in cardiac patients prescribed antithrombotic drugs: electronic health record phenotyping algorithms, incidence, trends and prognosis. *BMC Med*. 2019; **17**: 206.

11 van der Meijden PEJ, Heemskerk JWM. Platelet biology and functions: new concepts and clinical perspectives. *Nat Rev Cardiol*. 2019; **16**: 166-79.

12 Aslan JE, McCarty OJ. Rho GTPases in platelet function. *J Thromb Haemost*. 2013; **11**: 35-46.

13 Aslan JE, Itakura A, Gertz JM, McCarty OJ. Platelet shape change and spreading. *Methods Mol Biol*. 2012; **788**: 91-100.

14 Ruggeri ZM, Mendolicchio GL. Adhesion mechanisms in platelet function. *Circ Res*. 2007; **100**: 1673-85.

15 Andrews RK, Gardiner EE, Shen Y, Whisstock JC, Berndt MC. Glycoprotein Ib-IX-V. *Int J Biochem Cell Biol*. 2003; **35**: 1170-4.

16 Bergmeier W, Piffath CL, Goerge T, Cifuni SM, Ruggeri ZM, Ware J, Wagner DD. The role of platelet adhesion receptor GPIbalpha far exceeds that of its main ligand, von Willebrand factor, in arterial thrombosis. *Proc Natl Acad Sci U S A*. 2006; **103**: 16900-5.

17 Farndale RW, Sixma JJ, Barnes MJ, de Groot PG. The role of collagen in thrombosis and hemostasis. *J Thromb Haemost*. 2004; **2**: 561-73.

18 Mazzucato M, Spessotto P, Masotti A, De Appollonia L, Cozzi MR, Yoshioka A, Perris R, Colombatti A, De Marco L. Identification of domains responsible for von Willebrand factor type VI collagen interaction mediating platelet adhesion under high flow. *J Biol Chem*. 1999; **274**: 3033-41.

19 van der Plas RM, Gomes L, Marquart JA, Vink T, Meijers JC, de Groot PG, Sixma JJ, Huizinga EG. Binding of von Willebrand factor to collagen type III: role of specific amino acids in the collagen binding domain of vWF and effects of neighboring domains. *Thromb Haemost*. 2000; **84**: 1005-11.

20 Garland KS, Reitsma SE, Shirai T, Zilberman-Rudenko J, Tucker EI, Gailani D, Gruber A, McCarty OJT, Puy C. Removal of the C-Terminal Domains of ADAMTS13 by Activated Coagulation Factor XI induces Platelet Adhesion on Endothelial Cells under Flow Conditions. *Front Med (Lausanne)*. 2017; **4**: 232.

21 Arya M, Anvari B, Romo GM, Cruz MA, Dong JF, McIntire LV, Moake JL, Lopez JA. Ultralarge multimers of von Willebrand factor form spontaneous high-strength bonds with the platelet glycoprotein Ib-IX complex: studies using optical tweezers. *Blood*. 2002; **99**: 3971-7.

22 Savage B, Almus-Jacobs F, Ruggeri ZM. Specific synergy of multiple substrate-receptor interactions in platelet thrombus formation under flow. *Cell*. 1998; **94**: 657-66.

23 Ruggeri ZM, Bader R, de Marco L. Glanzmann thrombasthenia: deficient binding of von Willebrand factor to thrombin-stimulated platelets. *Proc Natl Acad Sci U S A*. 1982; **79**: 6038-41.

24 Dejana E, Lampugnani MG, Giorgi M, Gaboli M, Federici AB, Ruggeri ZM, Marchisio PC. Von Willebrand factor promotes endothelial cell adhesion via an Arg-Gly-Asp-dependent mechanism. *J Cell Biol*. 1989; **109**: 367-75.

25 Takamatsu J, Horne MK, 3rd, Gralnick HR. Identification of the thrombin receptor on human platelets by chemical crosslinking. *J Clin Invest*. 1986; **77**: 362-8.

26 Yamamoto N, Greco NJ, Barnard MR, Tanoue K, Yamazaki H, Jamieson GA, Michelson AD. Glycoprotein Ib (GPIb)-dependent and GPIb-independent pathways of thrombin-induced platelet activation. *Blood*. 1991; **77**: 1740-8.

27 Bradford HN, Dela Cadena RA, Kunapuli SP, Dong JF, Lopez JA, Colman RW. Human kininogens regulate thrombin binding to platelets through the glycoprotein Ib-IX-V complex. *Blood*. 1997; **90**: 1508-15.

28 Bradford HN, Pixley RA, Colman RW. Human factor XII binding to the glycoprotein Ib-IX-V complex inhibits thrombin-induced platelet aggregation. *J Biol Chem*. 2000; **275**: 22756-63.

29 Baglia FA, Badellino KO, Li CQ, Lopez JA, Walsh PN. Factor XI binding to the platelet glycoprotein Ib-IX-V complex promotes factor XI activation by thrombin. *J Biol Chem*. 2002; **277**: 1662-8.

30 Jurk K, Clemetson KJ, de Groot PG, Brodde MF, Steiner M, Savion N, Varon D, Sixma JJ, Van Aken H, Kehrel BE. Thrombospondin-1 mediates platelet adhesion at high shear via glycoprotein Ib (GPIb): an alternative/backup mechanism to von Willebrand factor. *FASEB J*. 2003; **17**: 1490-2.

31 Wang Y, Sakuma M, Chen Z, Ustinov V, Shi C, Croce K, Zago AC, Lopez J, Andre P, Plow E, Simon DI. Leukocyte engagement of platelet glycoprotein Ibalpha via the integrin Mac-1 is critical for the biological response to vascular injury. *Circulation*. 2005; **112**: 2993-3000.

32 Romo GM, Dong JF, Schade AJ, Gardiner EE, Kansas GS, Li CQ, McIntire LV, Berndt MC, Lopez JA. The glycoprotein Ib-IX-V complex is a platelet counterreceptor for P-selectin. *J Exp Med*. 1999; **190**: 803-14.

33 Moroi M, Jung SM, Shinmyozu K, Tomiyama Y, Ordinas A, Diaz-Ricart M. Analysis of platelet adhesion to a collagen-coated surface under flow conditions: the involvement of glycoprotein VI in the platelet adhesion. *Blood*. 1996; **88**: 2081-92.

34 Tandon NN, Kralisz U, Jamieson GA. Identification of glycoprotein IV (CD36) as a primary receptor for platelet-collagen adhesion. *J Biol Chem*. 1989; **264**: 7576-83.

35 Diaz-Ricart M, Tandon NN, Carretero M, Ordinas A, Bastida E, Jamieson GA. Platelets lacking functional CD36 (glycoprotein IV) show reduced adhesion to collagen in flowing whole blood. *Blood*. 1993; **82**: 491-6.

36 Emsley J, Knight CG, Farndale RW, Barnes MJ, Liddington RC. Structural basis of collagen recognition by integrin alpha2beta1. *Cell*. 2000; **101**: 47-56.

37 Chiang TM, Rinaldy A, Kang AH. Cloning, characterization, and functional studies of a nonintegrin platelet receptor for type I collagen. *J Clin Invest*. 1997; **100**: 514-21.

38 Savage B, Ruggeri ZM. Selective recognition of adhesive sites in surface-bound fibrinogen by glycoprotein IIb-IIIa on nonactivated platelets. *J Biol Chem*. 1991; **266**: 11227-33.

39 Knight CG, Morton LF, Onley DJ, Peachey AR, Ichinohe T, Okuma M, Farndale RW, Barnes MJ. Collagen-platelet interaction: Gly-Pro-Hyp is uniquely specific for platelet Gp VI and mediates platelet activation by collagen. *Cardiovasc Res*. 1999; **41**: 450-7.

40 Massberg S, Gawaz M, Gruner S, Schulte V, Konrad I, Zohlnhofer D, Heinzmann U, Nieswandt B. A crucial role of glycoprotein VI for platelet recruitment to the injured arterial wall in vivo. *J Exp Med*. 2003; **197**: 41-9.

41 Kato K, Kanaji T, Russell S, Kunicki TJ, Furihata K, Kanaji S, Marchese P, Reininger A, Ruggeri ZM, Ware J. The contribution of glycoprotein VI to stable platelet adhesion and thrombus formation illustrated by targeted gene deletion. *Blood*. 2003; **102**: 1701-7.

42 Moroi M, Jung SM, Okuma M, Shinmyozu K. A patient with platelets deficient in glycoprotein VI that lack both collagen-induced aggregation and adhesion. *J Clin Invest*. 1989; **84**: 1440-5.

43 Kehrel B, Balleisen L, Kokott R, Mesters R, Stenzinger W, Clemetson KJ, van de Loo J. Deficiency of intact thrombospondin and membrane glycoprotein Ia in platelets

with defective collagen-induced aggregation and spontaneous loss of disorder. *Blood*. 1988; **71**: 1074-8.

44 Ginsberg MH, Xiaoping D, O'Toole TE, Loftus JC, Plow EF. Platelet integrins. *Thromb Haemost*. 1993; **70**: 87-93.

45 Cho J, Mosher DF. Impact of fibronectin assembly on platelet thrombus formation in response to type I collagen and von Willebrand factor. *Blood*. 2006; **108**: 2229-36.

46 Cho J, Mosher DF. Role of fibronectin assembly in platelet thrombus formation. *J Thromb Haemost*. 2006; **4**: 1461-9.

47 Ni H, Yuen PS, Papalia JM, Trevithick JE, Sakai T, Fassler R, Hynes RO, Wagner DD. Plasma fibronectin promotes thrombus growth and stability in injured arterioles. *Proc Natl Acad Sci U S A*. 2003; **100**: 2415-9.

48 Savage B, Saldivar E, Ruggeri ZM. Initiation of platelet adhesion by arrest onto fibrinogen or translocation on von Willebrand factor. *Cell*. 1996; **84**: 289-97.

49 Hantgan RR, Hindriks G, Taylor RG, Sixma JJ, de Groot PG. Glycoprotein Ib, von Willebrand factor, and glycoprotein IIb:IIIa are all involved in platelet adhesion to fibrin in flowing whole blood. *Blood*. 1990; **76**: 345-53.

50 Nigatu A, Sime W, Gorfu G, Geberhiwot T, Anduren I, Ingerpuu S, Doi M, Tryggvason K, Hjemdahl P, Patarroyo M. Megakaryocytic cells synthesize and platelets secrete alpha5-laminins, and the endothelial laminin isoform laminin 10 (alpha5beta1gamma1) strongly promotes adhesion but not activation of platelets. *Thromb Haemost*. 2006; **95**: 85-93.

51 Inoue O, Suzuki-Inoue K, McCarty OJ, Moroi M, Ruggeri ZM, Kunicki TJ, Ozaki Y, Watson SP. Laminin stimulates spreading of platelets through integrin alpha6beta1-dependent activation of GPVI. *Blood*. 2006; **107**: 1405-12.

52 Lakshmanan HHS, Melrose AR, Sepp AI, Mitrugno A, Ngo ATP, Khader A, Thompson R, Sallee D, Pang J, Mangin PH, Jandrot-Perrus M, Aslan JE, McCarty OJT. The basement membrane protein nidogen-1 supports platelet adhesion and activation. *Platelets*. 2020: 1-5.

53 Wencel-Drake JD, Painter RG, Zimmerman TS, Ginsberg MH. Ultrastructural localization of human platelet thrombospondin, fibrinogen, fibronectin, and von Willebrand factor in frozen thin section. *Blood*. 1985; **65**: 929-38.

54 Kyriakides TR, Zhu YH, Smith LT, Bain SD, Yang Z, Lin MT, Danielson KG, Iozzo RV, LaMarca M, McKinney CE, Ginns EI, Bornstein P. Mice that lack thrombospondin 2 display connective tissue abnormalities that are associated with disordered collagen fibrillogenesis, an increased vascular density, and a bleeding diathesis. *J Cell Biol*. 1998; **140**: 419-30.

55 Kyriakides TR, Rojnuckarin P, Reidy MA, Hankenson KD, Papayannopoulou T, Kaushansky K, Bornstein P. Megakaryocytes require thrombospondin-2 for normal platelet formation and function. *Blood*. 2003; **101**: 3915-23.

56 Podor TJ, Campbell S, Chindemi P, Foulon DM, Farrell DH, Walton PD, Weitz JI, Peterson CB. Incorporation of vitronectin into fibrin clots. Evidence for a binding interaction between vitronectin and gamma A/gamma' fibrinogen. *J Biol Chem*. 2002; **277**: 7520-8.

57 Konstantinides S, Schafer K, Thinnes T, Loskutoff DJ. Plasminogen activator inhibitor-1 and its cofactor vitronectin stabilize arterial thrombi after vascular injury in mice. *Circulation*. 2001; **103**: 576-83.

58 Wu YP, Bloemendal HJ, Voest EE, Logtenberg T, de Groot PG, Gebbink MF, de Boer HC. Fibrin-incorporated vitronectin is involved in platelet adhesion and thrombus formation through homotypic interactions with platelet-associated vitronectin. *Blood*. 2004; **104**: 1034-41.

59 Ruggeri ZM, Dent JA, Saldivar E. Contribution of distinct adhesive interactions to platelet aggregation in flowing blood. *Blood*. 1999; **94**: 172-8.

60 Ni H, Denis CV, Subbarao S, Degen JL, Sato TN, Hynes RO, Wagner DD. Persistence of platelet thrombus formation in arterioles of mice lacking both von Willebrand factor and fibrinogen. *J Clin Invest*. 2000; **106**: 385-92.

61 Machesky LM, Insall RH. Signaling to actin dynamics. *J Cell Biol*. 1999; **146**: 267-72.

62 Harper MT, Poole AW. Diverse functions of protein kinase C isoforms in platelet activation and thrombus formation. *J Thromb Haemost*. 2010; **8**: 454-62.

63 Janmey PA. Phosphoinositides and calcium as regulators of cellular actin assembly and disassembly. *Annu Rev Physiol*. 1994; **56**: 169-91.

64 Adelstein RS, Conti MA, Daniel JL, Anderson W, Jr. The interaction of platelet actin, myosin and myosin light chain kinase. *Ciba Found Symp*. 1975; **35**: 101-9.

65 Wentworth JK, Pula G, Poole AW. Vasodilator-stimulated phosphoprotein (VASP) is phosphorylated on Ser157 by protein kinase C-dependent and -independent mechanisms in thrombin-stimulated human platelets. *Biochem J*. 2006; **393**: 555-64.

66 Agbani EO, van den Bosch MT, Brown E, Williams CM, Mattheij NJ, Cosemans JM, Collins PW, Heemskerk JW, Hers I, Poole AW. Coordinated Membrane Ballooning and Procoagulant Spreading in Human Platelets. *Circulation*. 2015; **132**: 1414-24.

67 Mattheij NJ, Gilio K, van Kruchten R, Jobe SM, Wieschhaus AJ, Chishti AH, Collins P, Heemskerk JW, Cosemans JM. Dual mechanism of integrin alphaIIbbeta3 closure in procoagulant platelets. *J Biol Chem*. 2013; **288**: 13325-36.

68 Mattheij NJ, Swieringa F, Mastenbroek TG, Berny-Lang MA, May F, Baaten CC, van der Meijden PE, Henskens YM, Beckers EA, Suylen DP, Nolte MW, Hackeng TM, McCarty OJ, Heemskerk JW, Cosemans JM. Coated platelets function in platelet-dependent fibrin formation via integrin alphaIIbbeta3 and transglutaminase factor XIII. *Haematologica*. 2016; **101**: 427-36.

69 Agbani EO, Hers I, Poole AW. Temporal contribution of the platelet body and balloon to thrombin generation. *Haematologica*. 2017; **102**: e379-e81.

70 Remenyi G, Szasz R, Friese P, Dale GL. Role of mitochondrial permeability transition pore in coated-platelet formation. *Arterioscler Thromb Vasc Biol*. 2005; **25**: 467-71.

71 Varga-Szabo D, Braun A, Nieswandt B. Calcium signaling in platelets. *J Thromb Haemost*. 2009; **7**: 1057-66.

72 Varga-Szabo D, Braun A, Nieswandt B. STIM and Orai in platelet function. *Cell Calcium*. 2011; **50**: 270-8.

73 Harper MT, Poole AW. Chloride channels are necessary for full platelet phosphatidylserine exposure and procoagulant activity. *Cell Death Dis*. 2013; **4**: e969.

74 Li Z, Delaney MK, O'Brien KA, Du X. Signaling during platelet adhesion and activation. *Arterioscler Thromb Vasc Biol*. 2010; **30**: 2341-9.

75 Kim J, Zhang CZ, Zhang X, Springer TA. A mechanically stabilized receptor-ligand flex-bond important in the vasculature. *Nature*. 2010; **466**: 992-5.

76 Du X. Signaling and regulation of the platelet glycoprotein Ib-IX-V complex. *Curr Opin Hematol*. 2007; **14**: 262-9.

77 Mu FT, Cranmer SL, Andrews RK, Berndt MC. Functional association of phosphoinositide-3-kinase with platelet glycoprotein Ibalpha, the major ligand-binding subunit of the glycoprotein Ib-IX-V complex. *J Thromb Haemost*. 2010; **8**: 324-30.

78 Mazzucato M, Pradella P, Cozzi MR, De Marco L, Ruggeri ZM. Sequential cytoplasmic calcium signals in a 2-stage platelet activation process induced by the glycoprotein Ibalpha mechanoreceptor. *Blood*. 2002; **100**: 2793-800.

79 Kasirer-Friede A, Cozzi MR, Mazzucato M, De Marco L, Ruggeri ZM, Shattil SJ. Signaling through GP Ib-IX-V activates alpha IIb beta 3 independently of other receptors. *Blood*. 2004; **103**: 3403-11.

80 Yin H, Stojanovic A, Hay N, Du X. The role of Akt in the signaling pathway of the glycoprotein Ib-IX induced platelet activation. *Blood*. 2008; **111**: 658-65.

81 Li Z, Xi X, Du X. A mitogen-activated protein kinase-dependent signaling pathway in the activation of platelet integrin alpha IIbbeta3. *J Biol Chem*. 2001; **276**: 42226-32.

82 Li Z, Xi X, Gu M, Feil R, Ye RD, Eigenthaler M, Hofmann F, Du X. A stimulatory role for cGMP-dependent protein kinase in platelet activation. *Cell*. 2003; **112**: 77-86.

83 Li Z, Zhang G, Feil R, Han J, Du X. Sequential activation of p38 and ERK pathways by cGMP-dependent protein kinase leading to activation of the platelet integrin alphaIIb beta3. *Blood*. 2006; **107**: 965-72.

84 Riba R, Oberprieler NG, Roberts W, Naseem KM. Von Willebrand factor activates endothelial nitric oxide synthase in blood platelets by a glycoprotein Ib-dependent mechanism. *J Thromb Haemost*. 2006; **4**: 2636-44.

85 Wu Y, Suzuki-Inoue K, Satoh K, Asazuma N, Yatomi Y, Berndt MC, Ozaki Y. Role of Fc receptor gamma-chain in platelet glycoprotein Ib-mediated signaling. *Blood*. 2001; **97**: 3836-45.

86 Sullam PM, Hyun WC, Szollosi J, Dong J, Foss WM, Lopez JA. Physical proximity and functional interplay of the glycoprotein Ib-IX-V complex and the Fc receptor FcgammaRIIA on the platelet plasma membrane. *J Biol Chem*. 1998; **273**: 5331-6.

87 Liu J, Fitzgerald ME, Berndt MC, Jackson CW, Gartner TK. Bruton tyrosine kinase is essential for botrocetin/VWF-induced signaling and GPIb-dependent thrombus formation in vivo. *Blood*. 2006; **108**: 2596-603.

88 Liu J, Pestina TI, Berndt MC, Jackson CW, Gartner TK. Botrocetin/VWF-induced signaling through GPIb-IX-V produces TxA2 in an alphaIIbbeta3- and aggregation-independent manner. *Blood*. 2005; **106**: 2750-6.

89 Clemetson KJ, Clemetson JM. Platelet collagen receptors. *Thromb Haemost*. 2001; **86**: 189-97.

90 Tsuji M, Ezumi Y, Arai M, Takayama H. A novel association of Fc receptor gamma-chain with glycoprotein VI and their co-expression as a collagen receptor in human platelets. *J Biol Chem*. 1997; **272**: 23528-31.

91 Reth M. Antigen receptor tail clue. *Nature*. 1989; **338**: 383-4.

92 Ezumi Y, Shindoh K, Tsuji M, Takayama H. Physical and functional association of the Src family kinases Fyn and Lyn with the collagen receptor glycoprotein VI-Fc receptor gamma chain complex on human platelets. *J Exp Med*. 1998; **188**: 267-76.

93 Quek LS, Pasquet JM, Hers I, Cornall R, Knight G, Barnes M, Hibbs ML, Dunn AR, Lowell CA, Watson SP. Fyn and Lyn phosphorylate the Fc receptor gamma chain downstream of glycoprotein VI in murine platelets, and Lyn regulates a novel feedback pathway. *Blood*. 2000; **96**: 4246-53.

94 Watson SP, Auger JM, McCarty OJ, Pearce AC. GPVI and integrin alphaIIb beta3 signaling in platelets. *J Thromb Haemost*. 2005; **3**: 1752-62.

95 Nieswandt B, Watson SP. Platelet-collagen interaction: is GPVI the central receptor? *Blood*. 2003; **102**: 449-61.

96 Pasquet JM, Bobe R, Gross B, Gratacap MP, Tomlinson MG, Payrastre B, Watson SP. A collagen-related peptide regulates phospholipase Cgamma2 via phosphatidylinositol 3-kinase in human platelets. *Biochem J*. 1999; **342 (Pt 1)**: 171-7.

97 Watanabe N, Nakajima H, Suzuki H, Oda A, Matsubara Y, Moroi M, Terauchi Y, Kadowaki T, Suzuki H, Koyasu S, Ikeda Y, Handa M. Functional phenotype of phosphoinositide 3-kinase p85alpha-null platelets characterized by an impaired response to GP VI stimulation. *Blood*. 2003; **102**: 541-8.

98 Gilio K, Munnix IC, Mangin P, Cosemans JM, Feijge MA, van der Meijden PE, Olieslagers S, Chrzanowska-Wodnicka MB, Lillian R, Schoenwaelder S, Koyasu S, Sage SO, Jackson SP, Heemskerk JW. Non-redundant roles of phosphoinositide 3-kinase isoforms alpha and beta in glycoprotein VI-induced platelet signaling and thrombus formation. *J Biol Chem*. 2009; **284**: 33750-62.

99 Christou CM, Pearce AC, Watson AA, Mistry AR, Pollitt AY, Fenton-May AE, Johnson LA, Jackson DG, Watson SP, O'Callaghan CA. Renal cells activate the platelet receptor CLEC-2 through podoplanin. *Biochem J*. 2008; **411**: 133-40.

100 Suzuki-Inoue K, Kato Y, Inoue O, Kaneko MK, Mishima K, Yatomi Y, Yamazaki Y, Narimatsu H, Ozaki Y. Involvement of the snake toxin receptor CLEC-2, in podoplanin-mediated platelet activation, by cancer cells. *J Biol Chem*. 2007; **282**: 25993-6001.

101 Shin Y, Morita T. Rhodocytin, a functional novel platelet agonist belonging to the heterodimeric C-type lectin family, induces platelet aggregation independently of glycoprotein Ib. *Biochem Biophys Res Commun*. 1998; **245**: 741-5.

102 Manne BK, Getz TM, Hughes CE, Alshehri O, Dangelmaier C, Naik UP, Watson SP, Kunapuli SP. Fucoidan is a novel platelet agonist for the C-type lectin-like receptor 2 (CLEC-2). *J Biol Chem*. 2013; **288**: 7717-26.

103 Pollitt AY, Grygielska B, Leblond B, Desire L, Eble JA, Watson SP. Phosphorylation of CLEC-2 is dependent on lipid rafts, actin polymerization, secondary mediators, and Rac. *Blood*. 2010; **115**: 2938-46.

104 Inoue O, Hokamura K, Shirai T, Osada M, Tsukiji N, Hatakeyama K, Umemura K, Asada Y, Suzuki-Inoue K, Ozaki Y. Vascular Smooth Muscle Cells Stimulate Platelets and Facilitate Thrombus Formation through Platelet CLEC-2: Implications in Atherothrombosis. *PLoS One*. 2015; **10**: e0139357.

105 May F, Hagedorn I, Pleines I, Bender M, Vogtle T, Eble J, Elvers M, Nieswandt B. CLEC-2 is an essential platelet-activating receptor in hemostasis and thrombosis. *Blood*. 2009; **114**: 3464-72.

106 Hitchcock JR, Cook CN, Bobat S, Ross EA, Flores-Langarica A, Lol KL, Khan M, Dominguez-Medina CC, Lax S, Carvalho-Gaspar M, et al. Inflammation drives thrombosis after Salmonella infection via CLEC-2 on platelets. *J Clin Invest*. 2015; **125**: 4429-46.

107 Bender M, May F, Lorenz V, Thielmann I, Hagedorn I, Finney BA, Vogtle T, Remer K, Braun A, Bosl M, Watson SP, Nieswandt B. Combined in vivo depletion of glycoprotein VI and C-type lectin-like receptor 2 severely compromises hemostasis and abrogates arterial thrombosis in mice. *Arterioscler Thromb Vasc Biol*. 2013; **33**: 926-34.

108 Suzuki-Inoue K. CLEC-2/podoplanin and thromboinflammation. *Blood*. 2017; **129**: 1896-8.

109 Rosenfeld SI, Looney RJ, Leddy JP, Phipps DC, Abraham GN, Anderson CL. Human platelet Fc receptor for immunoglobulin G. Identification as a 40,000-molecular-weight membrane protein shared by monocytes. *J Clin Invest*. 1985; **76**: 2317-22.

110 Karas SP, Rosse WF, Kurlander RJ. Characterization of the IgG-Fc receptor on human platelets. *Blood*. 1982; **60**: 1277-82.

111 Tomiyama Y, Kunicki TJ, Zipf TF, Ford SB, Aster RH. Response of human platelets to activating monoclonal antibodies: importance of Fc gamma RII (CD32) phenotype and level of expression. *Blood*. 1992; **80**: 2261-8.

112 McKenzie SE, Taylor SM, Malladi P, Yuhan H, Cassel DL, Chien P, Schwartz E, Schreiber AD, Surrey S, Reilly MP. The role of the human Fc receptor Fc gamma RIIA in the immune clearance of platelets: a transgenic mouse model. *J Immunol*. 1999; **162**: 4311-8.

113 Gratacap MP, Herault JP, Viala C, Ragab A, Savi P, Herbert JM, Chap H, Plantavid M, Payrastre B. FcgammaRIIA requires a Gi-dependent pathway for an efficient stimulation of phosphoinositide 3-kinase, calcium mobilization, and platelet aggregation. *Blood*. 2000; **96**: 3439-46.

114 Pain S, Falet H, Saci A, Bachelot-Loza C, Rendu F. Tyrosine phosphorylation and association of FcgammaRII and p72(Syk) are not limited to the FcgammaRII signalling pathway. *Cell Signal*. 2000; **12**: 165-71.

115 Gratacap MP, Payrastre B, Viala C, Mauco G, Plantavid M, Chap H. Phosphatidylinositol 3,4,5-trisphosphate-dependent stimulation of phospholipase C-gamma2 is an early key event in FcgammaRIIA-mediated activation of human platelets. *J Biol Chem*. 1998; **273**: 24314-21.

116 Yanaga F, Poole A, Asselin J, Blake R, Schieven GL, Clark EA, Law CL, Watson SP. Syk interacts with tyrosine-phosphorylated proteins in human platelets activated by collagen and cross-linking of the Fc gamma-IIA receptor. *Biochem J*. 1995; **311 (Pt 2)**: 471-8.

117 Blake RA, Asselin J, Walker T, Watson SP. Fc gamma receptor II stimulated formation of inositol phosphates in human platelets is blocked by tyrosine kinase inhibitors and associated with tyrosine phosphorylation of the receptor. *FEBS Lett*. 1994; **342**: 15-8.

118 Offermanns S. Activation of platelet function through G protein-coupled receptors. *Circ Res*. 2006; **99**: 1293-304.

119 Stephens LR, Eguinoa A, Erdjument-Bromage H, Lui M, Cooke F, Coadwell J, Smrcka AS, Thelen M, Cadwallader K, Tempst P, Hawkins PT. The G beta gamma sensitivity of a PI3K is dependent upon a tightly associated adaptor, p101. *Cell*. 1997; **89**: 105-14.

120 Coughlin SR. How the protease thrombin talks to cells. *Proc Natl Acad Sci U S A*. 1999; **96**: 11023-7.

121 Kahn ML, Zheng YW, Huang W, Bigornia V, Zeng D, Moff S, Farese RV, Jr., Tam C, Coughlin SR. A dual thrombin receptor system for platelet activation. *Nature*. 1998; **394**: 690-4.

122 Knezevic I, Borg C, Le Breton GC. Identification of Gq as one of the G-proteins which copurify with human platelet thromboxane A2/prostaglandin H2 receptors. *J Biol Chem*. 1993; **268**: 26011-7.

123 Djellas Y, Manganello JM, Antonakis K, Le Breton GC. Identification of Galpha13 as one of the G-proteins that couple to human platelet thromboxane A2 receptors. *J Biol Chem*. 1999; **274**: 14325-30.

124 Ohlmann P, Laugwitz KL, Nurnberg B, Spicher K, Schultz G, Cazenave JP, Gachet C. The human platelet ADP receptor activates Gi2 proteins. *Biochem J*. 1995; **312 (Pt 3)**: 775-9.

125 Yang J, Wu J, Kowalska MA, Dalvi A, Prevost N, O'Brien PJ, Manning D, Poncz M, Lucki I, Blendy JA, Brass LF. Loss of signaling through the G protein, Gz, results in abnormal platelet activation and altered responses to psychoactive drugs. *Proc Natl Acad Sci U S A*. 2000; **97**: 9984-9.

126 Offermanns S, Toombs CF, Hu YH, Simon MI. Defective platelet activation in G alpha(q)-deficient mice. *Nature*. 1997; **389**: 183-6.

127 Kim S, Foster C, Lecchi A, Quinton TM, Prosser DM, Jin J, Cattaneo M, Kunapuli SP. Protease-activated receptors 1 and 4 do not stimulate G(i) signaling pathways in the absence of secreted ADP and cause human platelet aggregation independently of G(i) signaling. *Blood*. 2002; **99**: 3629-36.

128 Paul BZ, Jin J, Kunapuli SP. Molecular mechanism of thromboxane A(2)-induced platelet aggregation. Essential role for p2t(ac) and alpha(2a) receptors. *J Biol Chem*. 1999; **274**: 29108-14.

129 Li Z, Zhang G, Le Breton GC, Gao X, Malik AB, Du X. Two waves of platelet secretion induced by thromboxane A2 receptor and a critical role for phosphoinositide 3-kinases. *J Biol Chem*. 2003; **278**: 30725-31.

130 Offermanns S, Laugwitz KL, Spicher K, Schultz G. G proteins of the G12 family are activated via thromboxane A2 and thrombin receptors in human platelets. *Proc Natl Acad Sci U S A*. 1994; **91**: 504-8.

131 Moers A, Nieswandt B, Massberg S, Wettschureck N, Gruner S, Konrad I, Schulte V, Aktas B, Gratacap MP, Simon MI, Gawaz M, Offermanns S. G13 is an essential mediator of platelet activation in hemostasis and thrombosis. *Nat Med*. 2003; **9**: 1418-22.

132 Klages B, Brandt U, Simon MI, Schultz G, Offermanns S. Activation of G12/G13 results in shape change and Rho/Rho-kinase-mediated myosin light chain phosphorylation in mouse platelets. *J Cell Biol*. 1999; **144**: 745-54.

133 Gong H, Shen B, Flevaris P, Chow C, Lam SC, Voyno-Yasenetskaya TA, Kozasa T, Du X. G protein subunit Galpha13 binds to integrin alphaIIbbeta3 and mediates integrin "outside-in" signaling. *Science*. 2010; **327**: 340-3.

134 Wolberg AS. Thrombin generation and fibrin clot structure. *Blood Rev*. 2007; **21**: 131-42.

135 Wright JH, Minot GR. The Viscous Metamorphosis of the Blood Platelets. *J Exp Med*. 1917; **26**: 395-409.

136 Feinstein MB, Fraser C. Human platelet secretion and aggregation induced by calcium ionophores. Inhibition by PGE1 and dibutyryl cyclic AMP. *J Gen Physiol*. 1975; **66**: 561-81.

137 Wallach DF, Surgenor DM, Steele BB. Calcium-lipid complexes in human platelets. *Blood*. 1958; **13**: 589-98.

138 Hathaway DR, Adelstein RS. Human platelet myosin light chain kinase requires the calcium-binding protein calmodulin for activity. *Proc Natl Acad Sci U S A*. 1979; **76**: 1653-7.

139 McCarty OJ, Zhao Y, Andrew N, Machesky LM, Staunton D, Frampton J, Watson SP. Evaluation of the role of platelet integrins in fibronectin-dependent spreading and adhesion. *J Thromb Haemost*. 2004; **2**: 1823-33.

140 Ren Q, Ye S, Whiteheart SW. The platelet release reaction: just when you thought platelet secretion was simple. *Curr Opin Hematol*. 2008; **15**: 537-41.

141 Reed GL, Fitzgerald ML, Polgar J. Molecular mechanisms of platelet exocytosis: insights into the "secrete" life of thrombocytes. *Blood*. 2000; **96**: 3334-42.

142 Blair P, Flaumenhaft R. Platelet alpha-granules: basic biology and clinical correlates. *Blood Rev*. 2009; **23**: 177-89.

143 Konopatskaya O, Gilio K, Harper MT, Zhao Y, Cosemans JM, Karim ZA, Whiteheart SW, Molkentin JD, Verkade P, Watson SP, Heemskerk JW, Poole AW. PKCalpha regulates platelet granule secretion and thrombus formation in mice. *J Clin Invest*. 2009; **119**: 399-407.

144 Li Z, Zhang G, Liu J, Stojanovic A, Ruan C, Lowell CA, Du X. An important role of the SRC family kinase Lyn in stimulating platelet granule secretion. *J Biol Chem*. 2010; **285**: 12559-70.

145 Kovacsovics TJ, Bachelot C, Toker A, Vlahos CJ, Duckworth B, Cantley LC, Hartwig JH. Phosphoinositide 3-kinase inhibition spares actin assembly in activating platelets but reverses platelet aggregation. *J Biol Chem*. 1995; **270**: 11358-66.

146 Woulfe D, Jiang H, Morgans A, Monks R, Birnbaum M, Brass LF. Defects in secretion, aggregation, and thrombus formation in platelets from mice lacking Akt2. *J Clin Invest*. 2004; **113**: 441-50.

147 Stojanovic A, Marjanovic JA, Brovkovych VM, Peng X, Hay N, Skidgel RA, Du X. A phosphoinositide 3-kinase-AKT-nitric oxide-cGMP signaling pathway in stimulating platelet secretion and aggregation. *J Biol Chem*. 2006; **281**: 16333-9.

148 Li Z, Zhang G, Marjanovic JA, Ruan C, Du X. A platelet secretion pathway mediated by cGMP-dependent protein kinase. *J Biol Chem*. 2004; **279**: 42469-75.

149 Flevaris P, Li Z, Zhang G, Zheng Y, Liu J, Du X. Two distinct roles of mitogen-activated protein kinases in platelets and a novel Rac1-MAPK-dependent integrin outside-in retractile signaling pathway. *Blood*. 2009; **113**: 893-901.

150 Shattil SJ, Kim C, Ginsberg MH. The final steps of integrin activation: the end game. *Nat Rev Mol Cell Biol*. 2010; **11**: 288-300.

151 French DL, Seligsohn U. Platelet glycoprotein IIb/IIIa receptors and Glanzmann's thrombasthenia. *Arterioscler Thromb Vasc Biol*. 2000; **20**: 607-10.

152 Timpl R, Dziadek M, Fujiwara S, Nowack H, Wick G. Nidogen: a new, self-aggregating basement membrane protein. *Eur J Biochem*. 1983; **137**: 455-65.

153 Joo SJ. Mechanisms of Platelet Activation and Integrin alphaIIbeta3. *Korean Circ J*. 2012; **42**: 295-301.

154 Coller BS, Shattil SJ. The GPIIb/IIIa (integrin alphaIIbbeta3) odyssey: a technology-driven saga of a receptor with twists, turns, and even a bend. *Blood*. 2008; **112**: 3011-25.

155 Obydennyy SI, Sveshnikova AN, Ataullakhanov FI, Panteleev MA. Dynamics of calcium spiking, mitochondrial collapse and phosphatidylserine exposure in platelet subpopulations during activation. *J Thromb Haemost*. 2016; **14**: 1867-81.

156 Heemskerk JW, Hoyland J, Mason WT, Sage SO. Spiking in cytosolic calcium concentration in single fibrinogen-bound fura-2-loaded human platelets. *Biochem J*. 1992; **283 (Pt 2)**: 379-83.

157 Mazzucato M, Cozzi MR, Battiston M, Jandrot-Perrus M, Mongiat M, Marchese P, Kunicki TJ, Ruggeri ZM, De Marco L. Distinct spatio-temporal Ca2+ signaling elicited by integrin alpha2beta1 and glycoprotein VI under flow. *Blood*. 2009; **114**: 2793-801.

158 Leisner TM, Wencel-Drake JD, Wang W, Lam SC. Bidirectional transmembrane modulation of integrin alphaIIbbeta3 conformations. *J Biol Chem*. 1999; **274**: 12945-9.

159 Obergfell A, Eto K, Mocsai A, Buensuceso C, Moores SL, Brugge JS, Lowell CA, Shattil SJ. Coordinate interactions of Csk, Src, and Syk kinases with [alpha]IIb[beta]3 initiate integrin signaling to the cytoskeleton. *J Cell Biol*. 2002; **157**: 265-75.

160 Law DA, DeGuzman FR, Heiser P, Ministri-Madrid K, Killeen N, Phillips DR. Integrin cytoplasmic tyrosine motif is required for outside-in alphaIIbbeta3 signalling and platelet function. *Nature*. 1999; **401**: 808-11.

161 Anthis NJ, Haling JR, Oxley CL, Memo M, Wegener KL, Lim CJ, Ginsberg MH, Campbell ID. Beta integrin tyrosine phosphorylation is a conserved mechanism for regulating talin-induced integrin activation. *J Biol Chem*. 2009; **284**: 36700-10.

162 Xi X, Flevaris P, Stojanovic A, Chishti A, Phillips DR, Lam SC, Du X. Tyrosine phosphorylation of the integrin beta 3 subunit regulates beta 3 cleavage by calpain. *J Biol Chem*. 2006; **281**: 29426-30.

163 Arthur WT, Petch LA, Burridge K. Integrin engagement suppresses RhoA activity via a c-Src-dependent mechanism. *Curr Biol*. 2000; **10**: 719-22.

164 Flevaris P, Stojanovic A, Gong H, Chishti A, Welch E, Du X. A molecular switch that controls cell spreading and retraction. *J Cell Biol*. 2007; **179**: 553-65.

165 Boylan B, Gao C, Rathore V, Gill JC, Newman DK, Newman PJ. Identification of FcgammaRIIa as the ITAM-bearing receptor mediating alphaIIbbeta3 outside-in integrin signaling in human platelets. *Blood*. 2008; **112**: 2780-6.

166 Durrant TN, van den Bosch MT, Hers I. Integrin alphaIIbbeta3 outside-in signaling. *Blood*. 2017; **130**: 1607-19.

167 Hitchcock IS, Fox NE, Prevost N, Sear K, Shattil SJ, Kaushansky K. Roles of focal adhesion kinase (FAK) in megakaryopoiesis and platelet function: studies using a megakaryocyte lineage specific FAK knockout. *Blood*. 2008; **111**: 596-604.

168 Kasirer-Friede A, Kang J, Kahner B, Ye F, Ginsberg MH, Shattil SJ. ADAP interactions with talin and kindlin promote platelet integrin alphaIIbbeta3 activation and stable fibrinogen binding. *Blood*. 2014; **123**: 3156-65.

169 Babur O, Melrose A, Cunliffe J, Klimek J, Pang J, Sepp AL, Zilberman-Rudenko J, Tassi Yunga S, Zheng T, Parra-Izquierdo I, Minnier J, McCarty O, Demir E, Reddy A, Wilmarth P, David LL, Aslan JE. Phosphoproteomic quantitation and causal analysis reveal pathways in GPVI/ITAM-mediated platelet activation programs. *Blood*. 2020.

170 Garcia-Mata R, Boulter E, Burridge K. The 'invisible hand': regulation of RHO GTPases by RHOGDIs. *Nat Rev Mol Cell Biol*. 2011; **12**: 493-504.

171 Aslan JE. Platelet Rho GTPase regulation in physiology and disease. *Platelets*. 2019; **30**: 17-22.

172 Pleines I, Elvers M, Strehl A, Pozgajova M, Varga-Szabo D, May F, Chrostek-Grashoff A, Brakebusch C, Nieswandt B. Rac1 is essential for phospholipase C-gamma2 activation in platelets. *Pflugers Arch*. 2009; **457**: 1173-85.

173 McCarty OJ, Larson MK, Auger JM, Kalia N, Atkinson BT, Pearce AC, Ruf S, Henderson RB, Tybulewicz VL, Machesky LM, Watson SP. Rac1 is essential for platelet lamellipodia formation and aggregate stability under flow. *J Biol Chem*. 2005; **280**: 39474-84.

174 Akbar H, Duan X, Saleem S, Davis AK, Zheng Y. RhoA and Rac1 GTPases Differentially Regulate Agonist-Receptor Mediated Reactive Oxygen Species Generation in Platelets. *PLoS One*. 2016; **11**: e0163227.

175 Martens L, Van Damme P, Van Damme J, Staes A, Timmerman E, Ghesquiere B, Thomas GR, Vandekerckhove J, Gevaert K. The human platelet proteome mapped by peptide-centric proteomics: a functional protein profile. *Proteomics*. 2005; **5**: 3193-204.

176 Rowley JW, Oler AJ, Tolley ND, Hunter BN, Low EN, Nix DA, Yost CC, Zimmerman GA, Weyrich AS. Genome-wide RNA-seq analysis of human and mouse platelet transcriptomes. *Blood*. 2011; **118**: e101-11.

177 Ridley AJ, Hall A. The small GTP-binding protein rho regulates the assembly of focal adhesions and actin stress fibers in response to growth factors. *Cell*. 1992; **70**: 389-99.

178 Riento K, Ridley AJ. Rocks: multifunctional kinases in cell behaviour. *Nat Rev Mol Cell Biol*. 2003; **4**: 446-56.

179 van Horck FP, Ahmadian MR, Haeusler LC, Moolenaar WH, Kranenburg O. Characterization of p190RhoGEF, a RhoA-specific guanine nucleotide exchange factor that interacts with microtubules. *J Biol Chem*. 2001; **276**: 4948-56.

180 Tsai HJ, Huang CL, Chang YW, Huang DY, Lin CC, Cooper JA, Cheng JC, Tseng CP. Disabled-2 is required for efficient hemostasis and platelet activation by thrombin in mice. *Arterioscler Thromb Vasc Biol*. 2014; **34**: 2404-12.

181 Kim S, Cipolla L, Guidetti G, Okigaki M, Jin J, Torti M, Kunapuli SP. Distinct role of Pyk2 in mediating thromboxane generation downstream of both G12/13 and integrin alphaIIbbeta3 in platelets. *J Biol Chem*. 2013; **288**: 18194-203.

182 Xiang B, Zhang G, Ye S, Zhang R, Huang C, Liu J, Tao M, Ruan C, Smyth SS, Whiteheart SW, Li Z. Characterization of a Novel Integrin Binding Protein, VPS33B, Which Is Important for Platelet Activation and In Vivo Thrombosis and Hemostasis. *Circulation*. 2015; **132**: 2334-44.

183 Aslan JE, Baker SM, Loren CP, Haley KM, Itakura A, Pang J, Greenberg DL, David LL, Manser E, Chernoff J, McCarty OJ. The PAK system links Rho GTPase signaling to thrombin-mediated platelet activation. *Am J Physiol Cell Physiol*. 2013; **305**: C519-28.

184 Paul DS, Casari C, Wu C, Piatt R, Pasala S, Campbell RA, Poe KO, Ghalloussi D, Lee RH, Rotty JD, Cooley BC, Machlus KR, Italiano JE, Jr., Weyrich AS, Bear JE, Bergmeier W. Deletion of the Arp2/3 complex in megakaryocytes leads to microthrombocytopenia in mice. *Blood Adv*. 2017; **1**: 1398-408.

185 Beck F, Geiger J, Gambaryan S, Solari FA, Dell'Aica M, Loroch S, Mattheij NJ, Mindukshev I, Potz O, Jurk K, Burkhart JM, Fufezan C, Heemskerk JW, Walter U, Zahedi RP, Sickmann A. Temporal quantitative phosphoproteomics of ADP stimulation reveals novel central nodes in platelet activation and inhibition. *Blood*. 2017; **129**: e1-e12.

186 Goggs R, Williams CM, Mellor H, Poole AW. Platelet Rho GTPases-a focus on novel players, roles and relationships. *Biochem J*. 2015; **466**: 431-42.

187 Pan D, Amison RT, Riffo-Vasquez Y, Spina D, Cleary SJ, Wakelam MJ, Page CP, Pitchford SC, Welch HC. P-Rex and Vav Rac-GEFs in platelets control leukocyte recruitment to sites of inflammation. *Blood*. 2015; **125**: 1146-58.

188 Nagy Z, Wynne K, von Kriegsheim A, Gambaryan S, Smolenski A. Cyclic Nucleotide-dependent Protein Kinases Target ARHGAP17 and ARHGEF6 Complexes in Platelets. *J Biol Chem*. 2015; **290**: 29974-83.

189 Elvers M, Beck S, Fotinos A, Ziegler M, Gawaz M. The GRAF family member oligophrenin1 is a RhoGAP with BAR domain and regulates Rho GTPases in platelets. *Cardiovasc Res*. 2012; **94**: 526-36.

190 Liu M, Bi F, Zhou X, Zheng Y. Rho GTPase regulation by miRNAs and covalent modifications. *Trends Cell Biol*. 2012; **22**: 365-73.

191 Croft DR, Olson MF. Transcriptional regulation of Rho GTPase signaling. *Transcription*. 2011; **2**: 211-5.

192 Burkhart JM, Vaudel M, Gambaryan S, Radau S, Walter U, Martens L, Geiger J, Sickmann A, Zahedi RP. The first comprehensive and quantitative analysis of human platelet protein composition allows the comparative analysis of structural and functional pathways. *Blood*. 2012; **120**: e73-82.

193 Kalantzi KI, Tsoumani ME, Goudevenos IA, Tselepis AD. Pharmacodynamic properties of antiplatelet agents: current knowledge and future perspectives. *Expert Rev Clin Pharmacol*. 2012; **5**: 319-36.

194 Amsterdam EA, Wenger NK, Brindis RG, Casey DE, Jr., Ganiats TG, Holmes DR, Jr., Jaffe AS, Jneid H, Kelly RF, Kontos MC, Levine GN, Liebson PR, Mukherjee D, Peterson ED, Sabatine MS, Smalling RW, Zieman SJ. 2014 AHA/ACC Guideline for the Management of Patients with Non-ST-Elevation Acute Coronary Syndromes: a report of the American College of Cardiology/American Heart Association Task Force on Practice Guidelines. *J Am Coll Cardiol*. 2014; **64**: e139-e228.

195 Chew DP, Bhatt DL, Sapp S, Topol EJ. Increased mortality with oral platelet glycoprotein IIb/IIIa antagonists: a meta-analysis of phase III multicenter randomized trials. *Circulation*. 2001; **103**: 201-6.

196 Cannon CP, McCabe CH, Wilcox RG, Langer A, Caspi A, Berink P, Lopez-Sendon J, Toman J, Charlesworth A, Anders RJ, Alexander JC, Skene A, Braunwald E. Oral glycoprotein IIb/IIIa inhibition with orbofiban in patients with unstable coronary syndromes (OPUS-TIMI 16) trial. *Circulation*. 2000; **102**: 149-56.

197 Morrow DA, Braunwald E, Bonaca MP, Ameriso SF, Dalby AJ, Fish MP, Fox KA, Lipka LJ, Liu X, Nicolau JC, et al. Vorapaxar in the secondary prevention of atherothrombotic events. *N Engl J Med*. 2012; **366**: 1404-13.

198 Tricoci P, Huang Z, Held C, Moliterno DJ, Armstrong PW, Van de Werf F, White HD, Aylward PE, Wallentin L, Chen E, et al. Thrombin-receptor antagonist vorapaxar in acute coronary syndromes. *N Engl J Med*. 2012; **366**: 20-33.

199 Li H, Lockyer S, Concepcion A, Gong X, Takizawa H, Guertin M, Matsumoto Y, Kambayashi J, Tandon NN, Liu Y. The Fab fragment of a novel anti-GPVI monoclonal antibody, OM4, reduces in vivo thrombosis without bleeding risk in rats. *Arterioscler Thromb Vasc Biol*. 2007; **27**: 1199-205.

200 Horii K, Okuda D, Morita T, Mizuno H. Structural characterization of EMS16, an antagonist of collagen receptor (GPIa/IIa) from the venom of Echis multisquamatus. *Biochemistry*. 2003; **42**: 12497-502.

201 Akbar H, Duan X, Piatt R, Saleem S, Davis AK, Tandon NN, Bergmeier W, Zheng Y. Small molecule targeting the Rac1-NOX2 interaction prevents collagen-related peptide and thrombin-induced reactive oxygen species generation and platelet activation. *J Thromb Haemost*. 2018; **16**: 2083-96.

202 Bosco EE, Kumar S, Marchioni F, Biesiada J, Kordos M, Szczur K, Meller J, Seibel W, Mizrahi A, Pick E, Filippi MD, Zheng Y. Rational design of small molecule inhibitors targeting the Rac GTPase-p67(phox) signaling axis in inflammation. *Chem Biol*. 2012; **19**: 228-42.

203 Koupenova M, Clancy L, Corkrey HA, Freedman JE. Circulating Platelets as Mediators of Immunity, Inflammation, and Thrombosis. *Circ Res*. 2018; **122**: 337-51.

204 Henn V, Slupsky JR, Grafe M, Anagnostopoulos I, Forster R, Muller-Berghaus G, Kroczek RA. CD40 ligand on activated platelets triggers an inflammatory reaction of endothelial cells. *Nature*. 1998; **391**: 591-4.

205 Khlgatian M, Nassar H, Chou HH, Gibson FC, 3rd, Genco CA. Fimbria-dependent activation of cell adhesion molecule expression in Porphyromonas gingivalis-infected endothelial cells. *Infect Immun*. 2002; **70**: 257-67.

206 Puhlmann M, Weinreich DM, Farma JM, Carroll NM, Turner EM, Alexander HR, Jr. Interleukin-1beta induced vascular permeability is dependent on induction of endothelial tissue factor (TF) activity. *J Transl Med*. 2005; **3**: 37.

207 Koupenova M, Vitseva O, MacKay CR, Beaulieu LM, Benjamin EJ, Mick E, Kurt-Jones EA, Ravid K, Freedman JE. Platelet-TLR7 mediates host survival and platelet count during viral infection in the absence of platelet-dependent thrombosis. *Blood*. 2014; **124**: 791-802.

208 Semple JW, Italiano JE, Jr., Freedman J. Platelets and the immune continuum. *Nat Rev Immunol*. 2011; **11**: 264-74.

209 Crawford A, Angelosanto JM, Nadwodny KL, Blackburn SD, Wherry EJ. A role for the chemokine RANTES in regulating CD8 T cell responses during chronic viral infection. *PLoS Pathog*. 2011; **7**: e1002098.

210 Furie B, Furie BC. The molecular basis of blood coagulation. *Cell*. 1988; **53**: 505-18.

211 Heemskerk JW, Bevers EM, Lindhout T. Platelet activation and blood coagulation. *Thromb Haemost*. 2002; **88**: 186-93.

212 Grover SP, Mackman N. Tissue Factor: An Essential Mediator of Hemostasis and Trigger of Thrombosis. *Arterioscler Thromb Vasc Biol*. 2018; **38**: 709-25.

213 Parry GC, Erlich JH, Carmeliet P, Luther T, Mackman N. Low levels of tissue factor are compatible with development and hemostasis in mice. *J Clin Invest*. 1998; **101**: 560-9.

214 Owens AP, 3rd, Mackman N. Tissue factor and thrombosis: The clot starts here. *Thromb Haemost*. 2010; **104**: 432-9.

215 Palta S, Saroa R, Palta A. Overview of the coagulation system. *Indian J Anaesth*. 2014; **58**: 515-23.

216 Smith SA, Mutch NJ, Baskar D, Rohloff P, Docampo R, Morrissey JH. Polyphosphate modulates blood coagulation and fibrinolysis. *Proc Natl Acad Sci U S A*. 2006; **103**: 903-8.

217 Kannemeier C, Shibamiya A, Nakazawa F, Trusheim H, Ruppert C, Markart P, Song Y, Tzima E, Kennerknecht E, Niepmann M, von Bruehl ML, Sedding D, Massberg S, Gunther A, Engelmann B, Preissner KT. Extracellular RNA constitutes a natural procoagulant cofactor in blood coagulation. *Proc Natl Acad Sci U S A*. 2007; **104**: 6388-93.

218 Noubouossie DF, Whelihan MF, Yu YB, Sparkenbaugh E, Pawlinski R, Monroe DM, Key NS. In vitro activation of coagulation by human neutrophil DNA and histone proteins but not neutrophil extracellular traps. *Blood*. 2017; **129**: 1021-9.

219 Wiggins RC, Cochrane CC. The autoactivation of rabbit Hageman factor. *J Exp Med*. 1979; **150**: 1122-33.

220 Mackman N, Tilley RE, Key NS. Role of the extrinsic pathway of blood coagulation in hemostasis and thrombosis. *Arterioscler Thromb Vasc Biol*. 2007; **27**: 1687-93.

221 Choi SH, Smith SA, Morrissey JH. Polyphosphate is a cofactor for the activation of factor XI by thrombin. *Blood*. 2011; **118**: 6963-70.

222 Kravtsov DV, Matafonov A, Tucker EI, Sun MF, Walsh PN, Gruber A, Gailani D. Factor XI contributes to thrombin generation in the absence of factor XII. *Blood*. 2009; **114**: 452-8.

223 von dem Borne PA, Meijers JC, Bouma BN. Feedback activation of factor XI by thrombin in plasma results in additional formation of thrombin that protects fibrin clots from fibrinolysis. *Blood*. 1995; **86**: 3035-42.

224 Gailani D, Broze GJ, Jr. Factor XI activation in a revised model of blood coagulation. *Science*. 1991; **253**: 909-12.

225 Mast AE. Tissue Factor Pathway Inhibitor: Multiple Anticoagulant Activities for a Single Protein. *Arterioscler Thromb Vasc Biol*. 2016; **36**: 9-14.

226 Puy C, Tucker EI, Wong ZC, Gailani D, Smith SA, Choi SH, Morrissey JH, Gruber A, McCarty OJ. Factor XII promotes blood coagulation independent of factor XI in the presence of long-chain polyphosphates. *J Thromb Haemost*. 2013; **11**: 1341-52.

227 Smith P, Arnesen H, Holme I. The effect of warfarin on mortality and reinfarction after myocardial infarction. *N Engl J Med*. 1990; **323**: 147-52.

228 Effect of long-term oral anticoagulant treatment on mortality and cardiovascular morbidity after myocardial infarction. Anticoagulants in the Secondary Prevention of Events in Coronary Thrombosis (ASPECT) Research Group. *Lancet*. 1994; **343**: 499-503.

229 Guyatt GH, Akl EA, Crowther M, Gutterman DD, Schuunemann HJ, American College of Chest Physicians Antithrombotic T, Prevention of Thrombosis P. Executive summary: Antithrombotic Therapy and Prevention of Thrombosis, 9th ed: American College of Chest Physicians Evidence-Based Clinical Practice Guidelines. *Chest*. 2012; **141**: 7S-47S.

230 Giugliano RP, Ruff CT, Braunwald E, Murphy SA, Wiviott SD, Halperin JL, Waldo AL, Ezekowitz MD, Weitz JI, Spinar J, et al. Edoxaban versus warfarin in patients with atrial fibrillation. *N Engl J Med*. 2013; **369**: 2093-104.

231 Connolly SJ, Ezekowitz MD, Yusuf S, Eikelboom J, Oldgren J, Parekh A, Pogue J, Reilly PA, Themeles E, Varrone J, et al. Dabigatran versus warfarin in patients with atrial fibrillation. *N Engl J Med*. 2009; **361**: 1139-51.

232 Wells PS, Holbrook AM, Crowther NR, Hirsh J. Interactions of warfarin with drugs and food. *Ann Intern Med*. 1994; **121**: 676-83.

233 Hylek EM, Evans-Molina C, Shea C, Henault LE, Regan S. Major hemorrhage and tolerability of warfarin in the first year of therapy among elderly patients with atrial fibrillation. *Circulation*. 2007; **115**: 2689-96.

234 Gage BF, Birman-Deych E, Kerzner R, Radford MJ, Nilasena DS, Rich MW. Incidence of intracranial hemorrhage in patients with atrial fibrillation who are prone to fall. *Am J Med*. 2005; **118**: 612-7.

235 Kirley K, Qato DM, Kornfield R, Stafford RS, Alexander GC. National trends in oral anticoagulant use in the United States, 2007 to 2011. *Circ Cardiovasc Qual Outcomes*. 2012; **5**: 615-21.

236 Francart SJ, Hawes EM, Deal AM, Adcock DM, Gosselin R, Jeanneret C, Friedman KD, Moll S. Performance of coagulation tests in patients on therapeutic doses of rivaroxaban. A cross-sectional pharmacodynamic study based on peak and trough plasma levels. *Thromb Haemost*. 2014; **111**: 1133-40.

237 Cuker A, Siegal DM, Crowther MA, Garcia DA. Laboratory measurement of the anticoagulant activity of the non-vitamin K oral anticoagulants. *J Am Coll Cardiol*. 2014; **64**: 1128-39.

238 Joppa SA, Salciccioli J, Adamski J, Patel S, Wysokinski W, McBane R, Al-Saffar F, Esser H, Shamoun F. A Practical Review of the Emerging Direct Anticoagulants, Laboratory Monitoring, and Reversal Agents. *J Clin Med*. 2018; **7**.

239 Duga S, Salomon O. Congenital factor XI deficiency: an update. *Semin Thromb Hemost*. 2013; **39**: 621-31.

240 Duga S, Salomon O. Factor XI Deficiency. *Semin Thromb Hemost*. 2009; **35**: 416-25.

241 He R, Chen D, He S. Factor XI: hemostasis, thrombosis, and antithrombosis. *Thromb Res*. 2012; **129**: 541-50.

242 Puy C, Rigg RA, McCarty OJ. The hemostatic role of factor XI. *Thromb Res*. 2016; **141 Suppl 2**: S8-S11.

243 Wheeler AP, Gailani D. Why factor XI deficiency is a clinical concern. *Expert Rev Hematol*. 2016; **9**: 629-37.

244 Yankol Y, Mecit N, Kanmaz T, Acarli K, Kalayoglu M. Acquired factor XI deficiency: a rare complication after liver transplantation. *Transplant Proc*. 2015; **47**: 179-81.

245 Emsley J, McEwan PA, Gailani D. Structure and function of factor XI. *Blood*. 2010; **115**: 2569-77.

246 Pike GN, Cumming AM, Hay CR, Bolton-Maggs PH, Burthem J. Sample conditions determine the ability of thrombin generation parameters to identify bleeding phenotype in FXI deficiency. *Blood*. 2015; **126**: 397-405.

247 Meijers JC, Tekelenburg WL, Bouma BN, Bertina RM, Rosendaal FR. High levels of coagulation factor XI as a risk factor for venous thrombosis. *N Engl J Med*. 2000; **342**: 696-701.

248 Yang DT, Flanders MM, Kim H, Rodgers GM. Elevated factor XI activity levels are associated with an increased odds ratio for cerebrovascular events. *Am J Clin Pathol*. 2006; **126**: 411-5.

249 Salomon O, Steinberg DM, Zucker M, Varon D, Zivelin A, Seligsohn U. Patients with severe factor XI deficiency have a reduced incidence of deep-vein thrombosis. *Thromb Haemost*. 2011; **105**: 269-73.

250 Salomon O, Steinberg DM, Koren-Morag N, Tanne D, Seligsohn U. Reduced incidence of ischemic stroke in patients with severe factor XI deficiency. *Blood*. 2008; **111**: 4113-7.

251 Schmaier AH. Physiologic activities of the contact activation system. *Thromb Res*. 2014; **133 Suppl 1**: S41-4.

252 Buller HR, Bethune C, Bhanot S, Gailani D, Monia BP, Raskob GE, Segers A, Verhamme P, Weitz JI, Investigators F-AT. Factor XI antisense oligonucleotide for prevention of venous thrombosis. *N Engl J Med*. 2015; **372**: 232-40.

253 Tucker EI, Marzec UM, White TC, Hurst S, Rugonyi S, McCarty OJ, Gailani D, Gruber A, Hanson SR. Prevention of vascular graft occlusion and thrombus-associated thrombin generation by inhibition of factor XI. *Blood*. 2009; **113**: 936-44.

254 Leung PY, Hurst S, Berny-Lang MA, Verbout NG, Gailani D, Tucker EI, Wang RK, McCarty OJ, Gruber A. Inhibition of Factor XII-Mediated Activation of Factor XI Provides Protection Against Experimental Acute Ischemic Stroke in Mice. *Transl Stroke Res*. 2012; **3**: 381-9.

255 Cheng Q, Tucker EI, Pine MS, Sisler I, Matafonov A, Sun MF, White-Adams TC, Smith SA, Hanson SR, McCarty OJ, Renne T, Gruber A, Gailani D. A role for factor XIIa-mediated factor XI activation in thrombus formation in vivo. *Blood*. 2010; **116**: 3981-9.

256 van Montfoort ML, Kuijpers MJ, Knaup VL, Bhanot S, Monia BP, Roelofs JJ, Heemskerk JW, Meijers JC. Factor XI regulates pathological thrombus formation on acutely ruptured atherosclerotic plaques. *Arterioscler Thromb Vasc Biol*. 2014; **34**: 1668-73.

257 Hofman Z, de Maat S, Hack CE, Maas C. Bradykinin: Inflammatory Product of the Coagulation System. *Clin Rev Allergy Immunol*. 2016; **51**: 152-61.

258 Colman RW, Schmaier AH. Contact system: a vascular biology modulator with anticoagulant, profibrinolytic, antiadhesive, and proinflammatory attributes. *Blood*. 1997; **90**: 3819-43.

259 Wu Y. Contact pathway of coagulation and inflammation. *Thromb J*. 2015; **13**: 17.

260 Tucker EI, Verbout NG, Leung PY, Hurst S, McCarty OJ, Gailani D, Gruber A. Inhibition of factor XI activation attenuates inflammation and coagulopathy while improving the survival of mouse polymicrobial sepsis. *Blood*. 2012; **119**: 4762-8.

261 Silasi R, Keshari RS, Lupu C, et al. Inhibition of contact-mediated activation of factor XI protects baboons against S aureus-induced organ damage and death. Blood Adv. 2019;3(4):658-669. *Blood Adv*. 2020; **4**: 3741.

262 Silasi R, Keshari RS, Lupu C, Van Rensburg WJ, Chaaban H, Regmi G, Shamanaev A, Shatzel JJ, Puy C, Lorentz CU, Tucker EI, Gailani D, Gruber A, McCarty OJT, Lupu F. Inhibition of contact-mediated activation of factor XI protects baboons against S aureus-induced organ damage and death. *Blood Adv*. 2019; **3**: 658-69.

263 Shnerb Ganor R, Harats D, Schiby G, Gailani D, Levkovitz H, Avivi C, Tamarin I, Shaish A, Salomon O. Factor XI Deficiency Protects Against Atherogenesis in Apolipoprotein E/Factor XI Double Knockout Mice. *Arterioscler Thromb Vasc Biol*. 2016; **36**: 475-81.

264 Galley HF, Webster NR. Physiology of the endothelium. *Br J Anaesth*. 2004; **93**: 105-13.

265 Cines DB, Pollak ES, Buck CA, Loscalzo J, Zimmerman GA, McEver RP, Pober JS, Wick TM, Konkle BA, Schwartz BS, Barnathan ES, McCrae KR, Hug BA, Schmidt AM, Stern DM. Endothelial cells in physiology and in the pathophysiology of vascular disorders. *Blood*. 1998; **91**: 3527-61.

266 Jin RC, Voetsch B, Loscalzo J. Endogenous mechanisms of inhibition of platelet function. *Microcirculation*. 2005; **12**: 247-58.

267 Moncada S. Adventures in vascular biology: a tale of two mediators. *Philos Trans R Soc Lond B Biol Sci*. 2006; **361**: 735-59.

268 Wang M, Hao H, Leeper NJ, Zhu L, Early Career C. Thrombotic Regulation From the Endothelial Cell Perspectives. *Arterioscler Thromb Vasc Biol*. 2018; **38**: e90-e5.

269 Marcus AJ, Broekman MJ, Drosopoulos JH, Olson KE, Islam N, Pinsky DJ, Levi R. Role of CD39 (NTPDase-1) in thromboregulation, cerebroprotection, and cardioprotection. *Semin Thromb Hemost*. 2005; **31**: 234-46.

270 Conway EM. A Nuclear Attack on Thrombosis and Inflammation. *Arterioscler Thromb Vasc Biol*. 2016; **36**: 221-3.

271 Adams TE, Huntington JA. Thrombin-cofactor interactions: structural insights into regulatory mechanisms. *Arterioscler Thromb Vasc Biol*. 2006; **26**: 1738-45.

272 Girard TJ, Tuley E, Broze GJ, Jr. TFPIbeta is the GPI-anchored TFPI isoform on human endothelial cells and placental microsomes. *Blood*. 2012; **119**: 1256-62.

273 Vaughan DE. PAI-1 and atherothrombosis. *J Thromb Haemost*. 2005; **3**: 1879-83.

274 Puy C, Ngo ATP, Pang J, Keshari RS, Hagen MW, Hinds MT, Gailani D, Gruber A, Lupu F, McCarty OJT. Endothelial PAI-1 (Plasminogen Activator Inhibitor-1) Blocks the Intrinsic Pathway of Coagulation, Inducing the Clearance and Degradation of FXIa (Activated Factor XI). *Arterioscler Thromb Vasc Biol*. 2019; **39**: 1390-401.

275 Frenette PS, Johnson RC, Hynes RO, Wagner DD. Platelets roll on stimulated endothelium in vivo: an interaction mediated by endothelial P-selectin. *Proc Natl Acad Sci U S A*. 1995; **92**: 7450-4.

276 Frenette PS, Moyna C, Hartwell DW, Lol JB, Hynes RO, Wagner DD. Platelet-endothelial interactions in inflamed mesenteric venules. *Blood*. 1998; **91**: 1318-24.

277 Frenette PS, Denis CV, Weiss L, Jurk K, Subbarao S, Kehrel B, Hartwig JH, Vestweber D, Wagner DD. P-Selectin glycoprotein ligand 1 (PSGL-1) is expressed on platelets and can mediate platelet-endothelial interactions in vivo. *J Exp Med*. 2000; **191**: 1413-22.

278 Boilard E, Nigrovic PA, Larabee K, Watts GF, Coblyn JS, Weinblatt ME, Massarotti EM, Remold-O'Donnell E, Farndale RW, Ware J, Lee DM. Platelets amplify inflammation in arthritis via collagen-dependent microparticle production. *Science*. 2010; **327**: 580-3.

279 Hara T, Shimizu K, Ogawa F, Yanaba K, Iwata Y, Muroi E, Takenaka M, Komura K, Hasegawa M, Fujimoto M, Sato S. Platelets control leukocyte recruitment in a murine model of cutaneous arthus reaction. *Am J Pathol*. 2010; **176**: 259-69.

280 Smyth SS, McEver RP, Weyrich AS, Morrell CN, Hoffman MR, Arepally GM, French PA, Dauerman HL, Becker RC, Platelet Colloquium P. Platelet functions beyond hemostasis. *J Thromb Haemost*. 2009; **7**: 1759-66.

281 Hansson GK. Inflammation, atherosclerosis, and coronary artery disease. *N Engl J Med*. 2005; **352**: 1685-95.

282 May AE, Seizer P, Gawaz M. Platelets: inflammatory firebugs of vascular walls. *Arterioscler Thromb Vasc Biol*. 2008; **28**: s5-10.

283 Lusis AJ. Atherosclerosis. *Nature*. 2000; **407**: 233-41.

284 Willerson JT, Kereiakes DJ. Endothelial dysfunction. *Circulation*. 2003; **108**: 2060-1.

285 Badrnya S, Butler LM, Soderberg-Naucler C, Volf I, Assinger A. Platelets directly enhance neutrophil transmigration in response to oxidised low-density lipoprotein. *Thromb Haemost*. 2012; **108**: 719-29.

286 Langer H, May AE, Bultmann A, Gawaz M. ADAM 15 is an adhesion receptor for platelet GPIIb-IIIa and induces platelet activation. *Thromb Haemost*. 2005; **94**: 555-61.

287 Gawaz M, Langer H, May AE. Platelets in inflammation and atherogenesis. *J Clin Invest*. 2005; **115**: 3378-84.

288 Scheuerer B, Ernst M, Durrbaum-Landmann I, Fleischer J, Grage-Griebenow E, Brandt E, Flad HD, Petersen F. The CXC-chemokine platelet factor 4 promotes monocyte survival and induces monocyte differentiation into macrophages. *Blood*. 2000; **95**: 1158-66.

289 Sachais BS, Kuo A, Nassar T, Morgan J, Kariko K, Williams KJ, Feldman M, Aviram M, Shah N, Jarett L, Poncz M, Cines DB, Higazi AA. Platelet factor 4 binds to low-density lipoprotein receptors and disrupts the endocytic machinery, resulting in retention of low-density lipoprotein on the cell surface. *Blood*. 2002; **99**: 3613-22.

290 Nassar T, Sachais BS, Akkawi S, Kowalska MA, Bdeir K, Leitersdorf E, Hiss E, Ziporen L, Aviram M, Cines D, Poncz M, Higazi AA. Platelet factor 4 enhances the binding of oxidized low-density lipoprotein to vascular wall cells. *J Biol Chem*. 2003; **278**: 6187-93.

291 von Hundelshausen P, Weber KS, Huo Y, Proudfoot AE, Nelson PJ, Ley K, Weber C. RANTES deposition by platelets triggers monocyte arrest on inflamed and atherosclerotic endothelium. *Circulation*. 2001; **103**: 1772-7.

292 von Hundelshausen P, Koenen RR, Sack M, Mause SF, Adriaens W, Proudfoot AE, Hackeng TM, Weber C. Heterophilic interactions of platelet factor 4 and RANTES promote monocyte arrest on endothelium. *Blood*. 2005; **105**: 924-30.

293 Lu B, Rutledge BJ, Gu L, Fiorillo J, Lukacs NW, Kunkel SL, North R, Gerard C, Rollins BJ. Abnormalities in monocyte recruitment and cytokine expression in monocyte chemoattractant protein 1-deficient mice. *J Exp Med*. 1998; **187**: 601-8.

294 Hawrylowicz CM, Howells GL, Feldmann M. Platelet-derived interleukin 1 induces human endothelial adhesion molecule expression and cytokine production. *J Exp Med*. 1991; **174**: 785-90.

295 Bea F, Kreuzer J, Preusch M, Schaab S, Isermann B, Rosenfeld ME, Katus H, Blessing E. Melagatran reduces advanced atherosclerotic lesion size and may promote plaque stability in apolipoprotein E-deficient mice. *Arterioscler Thromb Vasc Biol*. 2006; **26**: 2787-92.

296 Lee IO, Kratz MT, Schirmer SH, Baumhakel M, Bohm M. The effects of direct thrombin inhibition with dabigatran on plaque formation and endothelial function in apolipoprotein E-deficient mice. *J Pharmacol Exp Ther*. 2012; **343**: 253-7.

297 Westrick RJ, Bodary PF, Xu Z, Shen YC, Broze GJ, Eitzman DT. Deficiency of tissue factor pathway inhibitor promotes atherosclerosis and thrombosis in mice. *Circulation*. 2001; **103**: 3044-6.

298 Khallou-Laschet J, Caligiuri G, Tupin E, Gaston AT, Poirier B, Groyer E, Urbain D, Maisnier-Patin S, Sarkar R, Kaveri SV, Lacroix-Desmazes S, Nicoletti A. Role of the intrinsic coagulation pathway in atherogenesis assessed in hemophilic apolipoprotein E knockout mice. *Arterioscler Thromb Vasc Biol*. 2005; **25**: e123-6.

299 Hara T, Fukuda D, Tanaka K, Higashikuni Y, Hirata Y, Nishimoto S, Yagi S, Yamada H, Soeki T, Wakatsuki T, Shimabukuro M, Sata M. Rivaroxaban, a novel oral anticoagulant, attenuates atherosclerotic plaque progression and destabilization in ApoE-deficient mice. *Atherosclerosis*. 2015; **242**: 639-46.

300 Vorlova S, Koch M, Manthey HD, Cochain C, Busch M, Chaudhari SM, Stegner D, Yepes M, Lorenz K, Nolte MW, Nieswandt B, Zernecke A. Coagulation factor XII induces pro-inflammatory cytokine responses in macrophages and promotes atherosclerosis in mice. *Thromb Haemost*. 2017; **117**: 176-87.

301 Clemetson KJ. Platelets and primary haemostasis. *Thromb Res*. 2012; **129**: 220-4.

302 Furie B, Furie BC. Thrombus formation in vivo. *J Clin Invest*. 2005; **115**: 3355-62.

303 Stalker TJ, Traxler EA, Wu J, Wannemacher KM, Cermignano SL, Voronov R, Diamond SL, Brass LF. Hierarchical organization in the hemostatic response and its relationship to the platelet-signaling network. *Blood*. 2013; **121**: 1875-85.

304 Welsh JD, Stalker TJ, Voronov R, Muthard RW, Tomaiuolo M, Diamond SL, Brass LF. A systems approach to hemostasis: 1. The interdependence of thrombus architecture and agonist movements in the gaps between platelets. *Blood*. 2014; **124**: 1808-15.

305 Akbar H, Kim J, Funk K, Cancelas JA, Shang X, Chen L, Johnson JF, Williams DA, Zheng Y. Genetic and pharmacologic evidence that Rac1 GTPase is involved in regulation of platelet secretion and aggregation. *J Thromb Haemost*. 2007; **5**: 1747-55.

306 Pleines I, Dutting S, Cherpokova D, Eckly A, Meyer I, Morowski M, Krohne G, Schulze H, Gachet C, Debili N, Brakebusch C, Nieswandt B. Defective tubulin organization and proplatelet formation in murine megakaryocytes lacking Rac1 and Cdc42. *Blood*. 2013; **122**: 3178-87.

307 Pleines I, Eckly A, Elvers M, Hagedorn I, Eliautou S, Bender M, Wu X, Lanza F, Gachet C, Brakebusch C, Nieswandt B. Multiple alterations of platelet functions dominated by increased secretion in mice lacking Cdc42 in platelets. *Blood*. 2010; **115**: 3364-73.

308 Aslan JE, McCarty OJ. Rac and Cdc42 team up for platelets. *Blood*. 2013; **122**: 3096-7.

309 Akbar H, Shang X, Perveen R, Berryman M, Funk K, Johnson JF, Tandon NN, Zheng Y. Gene targeting implicates Cdc42 GTPase in GPVI and non-GPVI mediated platelet filopodia formation, secretion and aggregation. *PLoS One*. 2011; **6**: e22117.

310 Pleines I, Hagedorn I, Gupta S, May F, Chakarova L, van Hengel J, Offermanns S, Krohne G, Kleinschnitz C, Brakebusch C, Nieswandt B. Megakaryocyte-specific RhoA deficiency causes macrothrombocytopenia and defective platelet activation in hemostasis and thrombosis. *Blood*. 2012; **119**: 1054-63.

311 Kim S, Dangelmaier C, Bhavanasi D, Meng S, Wang H, Goldfinger LE, Kunapuli SP. RhoG protein regulates glycoprotein VI-Fc receptor gamma-chain complex-mediated platelet activation and thrombus formation. *J Biol Chem*. 2013; **288**: 34230-8.

312 Goggs R, Harper MT, Pope RJ, Savage JS, Williams CM, Mundell SJ, Heesom KJ, Bass M, Mellor H, Poole AW. RhoG protein regulates platelet granule secretion and thrombus formation in mice. *J Biol Chem*. 2013; **288**: 34217-29.

313 Heasman SJ, Ridley AJ. Mammalian Rho GTPases: new insights into their functions from in vivo studies. *Nat Rev Mol Cell Biol*. 2008; **9**: 690-701.

314 Boulter E, Garcia-Mata R, Guilluy C, Dubash A, Rossi G, Brennwald PJ, Burridge K. Regulation of Rho GTPase crosstalk, degradation and activity by RhoGDI1. *Nat Cell Biol*. 2010; **12**: 477-83.

315 Dovas A, Couchman JR. RhoGDI: multiple functions in the regulation of Rho family GTPase activities. *Biochem J*. 2005; **390**: 1-9.

316 Bielek H, Anselmo A, Dermardirossian C. Morphological and proliferative abnormalities in renal mesangial cells lacking RhoGDI. *Cell Signal*. 2009; **21**: 1974-83.

317 Gorovoy M, Neamu R, Niu J, Vogel S, Predescu D, Miyoshi J, Takai Y, Kini V, Mehta D, Malik AB, Voyno-Yasenetskaya T. RhoGDI-1 modulation of the activity of monomeric RhoGTPase RhoA regulates endothelial barrier function in mouse lungs. *Circ Res*. 2007; **101**: 50-8.

318 Griner EM, Churchill ME, Brautigan DL, Theodorescu D. PKCalpha phosphorylation of RhoGDI2 at Ser31 disrupts interactions with Rac1 and decreases GDI activity. *Oncogene*. 2013; **32**: 1010-7.

319 Hodge RG, Ridley AJ. Regulating Rho GTPases and their regulators. *Nat Rev Mol Cell Biol*. 2016; **17**: 496-510.

320 Kuhlmann N, Wroblowski S, Knyphausen P, de Boor S, Brenig J, Zienert AY, Meyer-Teschendorf K, Praefcke GJ, Nolte H, Kruger M, Schacherl M, Baumann U, James LC, Chin JW, Lammers M. Structural and Mechanistic Insights into the Regulation of the Fundamental Rho Regulator RhoGDIalpha by Lysine Acetylation. *J Biol Chem*. 2016; **291**: 5484-99.

321 Aslan JE, Tormoen GW, Loren CP, Pang J, McCarty OJ. S6K1 and mTOR regulate Rac1-driven platelet activation and aggregation. *Blood*. 2011; **118**: 3129-36.

322 Aslan JE, Itakura A, Haley KM, Tormoen GW, Loren CP, Baker SM, Pang J, Chernoff J, McCarty OJ. p21 activated kinase signaling coordinates glycoprotein receptor VI-mediated platelet aggregation, lamellipodia formation, and aggregate stability under shear. *Arterioscler Thromb Vasc Biol*. 2013; **33**: 1544-51.

323 Itakura A, Aslan JE, Kusanto BT, Phillips KG, Porter JE, Newton PK, Nan X, Insall RH, Chernoff J, McCarty OJ. p21-Activated kinase (PAK) regulates cytoskeletal reorganization and directional migration in human neutrophils. *PLoS One*. 2013; **8**: e73063.

324 Diagouraga B, Grichine A, Fertin A, Wang J, Khochbin S, Sadoul K. Motor-driven marginal band coiling promotes cell shape change during platelet activation. *J Cell Biol*. 2014; **204**: 177-85.

325 Kotlyar M, Pastrello C, Pivetta F, Lo Sardo A, Cumbaa C, Li H, Naranian T, Niu Y, Ding Z, Vafaee F, Broackes-Carter F, Petschnigg J, Mills GB, Jurisicova A, Stagljar I, Maestro R, Jurisica I. In silico prediction of physical protein interactions and characterization of interactome orphans. *Nat Methods*. 2015; **12**: 79-84.

326 Babur O, Dogrusoz U, Cakir M, Aksoy BA, Schultz N, Sander C, Demir E. Integrating biological pathways and genomic profiles with ChiBE 2. *BMC Genomics*. 2014; **15**: 642.

327 Cerami EG, Gross BE, Demir E, Rodchenkov I, Babur O, Anwar N, Schultz N, Bader GD, Sander C. Pathway Commons, a web resource for biological pathway data. *Nucleic Acids Res*. 2011; **39**: D685-90.

328 Hornbeck PV, Kornhauser JM, Tkachev S, Zhang B, Skrzypek E, Murray B, Latham V, Sullivan M. PhosphoSitePlus: a comprehensive resource for investigating the

structure and function of experimentally determined post-translational modifications in man and mouse. *Nucleic Acids Res*. 2012; **40**: D261-70.

329 Zhang Y, Zhang B. D4-GDI, a Rho GTPase regulator, promotes breast cancer cell invasiveness. *Cancer Res*. 2006; **66**: 5592-8.

330 Stritt S, Wolf K, Lorenz V, Vogtle T, Gupta S, Bosl MR, Nieswandt B. Rap1-GTP-interacting adaptor molecule (RIAM) is dispensable for platelet integrin activation and function in mice. *Blood*. 2015; **125**: 219-22.

331 Severin S, Gaits-Iacovoni F, Allart S, Gratacap MP, Payrastre B. A confocal-based morphometric analysis shows a functional crosstalk between the actin filament system and microtubules in thrombin-stimulated platelets. *J Thromb Haemost*. 2013; **11**: 183-6.

332 Sadoul K, Wang J, Diagouraga B, Vitte AL, Buchou T, Rossini T, Polack B, Xi X, Matthias P, Khochbin S. HDAC6 controls the kinetics of platelet activation. *Blood*. 2012; **120**: 4215-8.

333 Kita A, Sakurai Y, Myers DR, Rounsevell R, Huang JN, Seok TJ, Yu K, Wu MC, Fletcher DA, Lam WA. Microenvironmental geometry guides platelet adhesion and spreading: a quantitative analysis at the single cell level. *PLoS One*. 2011; **6**: e26437.

334 Kahr WH, Lo RW, Li L, Pluthero FG, Christensen H, Ni R, Vaezzadeh N, Hawkins CE, Weyrich AS, Di Paola J, Landolt-Marticorena C, Gross PL. Abnormal megakaryocyte development and platelet function in Nbeal2(-/-) mice. *Blood*. 2013; **122**: 3349-58.

335 Bender M, Stritt S, Nurden P, van Eeuwijk JM, Zieger B, Kentouche K, Schulze H, Morbach H, Stegner D, Heinze KG, Dutting S, Gupta S, Witke W, Falet H, Fischer A, Hartwig JH, Nieswandt B. Megakaryocyte-specific Profilin1-deficiency alters microtubule stability and causes a Wiskott-Aldrich syndrome-like platelet defect. *Nat Commun*. 2014; **5**: 4746.

336 Sakurai Y, Fitch-Tewfik JL, Qiu Y, Ahn B, Myers DR, Tran R, Fay ME, Ding L, Spearman PW, Michelson AD, Flaumenhaft R, Lam WA. Platelet geometry sensing spatially regulates alpha-granule secretion to enable matrix self-deposition. *Blood*. 2015; **126**: 531-8.

337 Qiu Y, Brown AC, Myers DR, Sakurai Y, Mannino RG, Tran R, Ahn B, Hardy ET, Kee MF, Kumar S, Bao G, Barker TH, Lam WA. Platelet mechanosensing of substrate stiffness during clot formation mediates adhesion, spreading, and activation. *Proc Natl Acad Sci U S A*. 2014; **111**: 14430-5.

338 Sadoul K. Tubulin acetylation a valuable accessory of the platelet cytoskeleton. Focus on "Histone deacetylase 6-mediated deacetylation of alpha-tubulin coordinates

cytoskeletal and signaling events during platelet activation". *Am J Physiol Cell Physiol*. 2013; **305**: C1211-3.

339 Sadoul K. New explanations for old observations: marginal band coiling during platelet activation. *J Thromb Haemost*. 2015; **13**: 333-46.

340 Aslan JE, Phillips KG, Healy LD, Itakura A, Pang J, McCarty OJ. Histone deacetylase 6-mediated deacetylation of alpha-tubulin coordinates cytoskeletal and signaling events during platelet activation. *Am J Physiol Cell Physiol*. 2013; **305**: C1230-9.

341 Wu Y, Moissoglu K, Wang H, Wang X, Frierson HF, Schwartz MA, Theodorescu D. Src phosphorylation of RhoGDI2 regulates its metastasis suppressor function. *Proc Natl Acad Sci U S A*. 2009; **106**: 5807-12.

342 Pearce AC, Wilde JI, Doody GM, Best D, Inoue O, Vigorito E, Tybulewicz VL, Turner M, Watson SP. Vav1, but not Vav2, contributes to platelet aggregation by CRP and thrombin, but neither is required for regulation of phospholipase C. *Blood*. 2002; **100**: 3561-9.

343 Ahmed M, Sottnik JL, Dancik GM, Sahu D, Hansel DE, Theodorescu D, Schwartz MA. An Osteopontin/CD44 Axis in RhoGDI2-Mediated Metastasis Suppression. *Cancer Cell*. 2016; **30**: 432-43.

344 Groysman M, Hornstein I, Alcover A, Katzav S. Vav1 and Ly-GDI two regulators of Rho GTPases, function cooperatively as signal transducers in T cell antigen receptor-induced pathways. *J Biol Chem*. 2002; **277**: 50121-30.

345 Essmann F, Wieder T, Otto A, Muller EC, Dorken B, Daniel PT. GDP dissociation inhibitor D4-GDI (Rho-GDI 2), but not the homologous rho-GDI 1, is cleaved by caspase-3 during drug-induced apoptosis. *Biochem J*. 2000; **346 Pt 3**: 777-83.

346 Aslan JE, Rigg RA, Nowak MS, Loren CP, Baker-Groberg SM, Pang J, David LL, McCarty OJ. Lysine acetyltransfer supports platelet function. *J Thromb Haemost*. 2015; **13**: 1908-17.

347 Aslan JE, David LL, McCarty OJ. Data detailing the platelet acetyl-lysine proteome. *Data Brief*. 2015; **5**: 368-71.

348 Cerecedo D, Cisneros B, Suarez-Sanchez R, Hernandez-Gonzalez E, Galvan I. beta-Dystroglycan modulates the interplay between actin and microtubules in human-adhered platelets. *Br J Haematol*. 2008; **141**: 517-28.

349 Mancuso ME, Santagostino E. Platelets: much more than bricks in a breached wall. *Br J Haematol*. 2017; **178**: 209-19.

350 Gremmel T, Frelinger AL, 3rd, Michelson AD. Platelet Physiology. *Semin Thromb Hemost*. 2016; **42**: 191-204.

351 Estevez B, Du X. New Concepts and Mechanisms of Platelet Activation Signaling. *Physiology (Bethesda)*. 2017; **32**: 162-77.

352 Andre P. Intracellular signaling as a potential target for antiplatelet therapy. *Handb Exp Pharmacol*. 2012: 339-67.

353 Wright B, Stanley RG, Kaiser WJ, Gibbins JM. The integration of proteomics and systems approaches to map regulatory mechanisms underpinning platelet function. *Proteomics Clin Appl*. 2013; **7**: 144-54.

354 Ruegg C, Tissot JD, Farmer P, Mariotti A. Omics meets hypothesis-driven research. Partnership for innovative discoveries in vascular biology and angiogenesis. *Thromb Haemost*. 2008; **100**: 738-46.

355 Gnatenko DV, Perrotta PL, Bahou WF. Proteomic approaches to dissect platelet function: Half the story. *Blood*. 2006; **108**: 3983-91.

356 Burkhart JM, Gambaryan S, Watson SP, Jurk K, Walter U, Sickmann A, Heemskerk JW, Zahedi RP. What can proteomics tell us about platelets? *Circ Res*. 2014; **114**: 1204-19.

357 Boyanova D, Nilla S, Birschmann I, Dandekar T, Dittrich M. PlateletWeb: a systems biologic analysis of signaling networks in human platelets. *Blood*. 2012; **119**: e22-34.

358 Babur O, Aksoy BA, Rodchenkov I, Sumer SO, Sander C, Demir E. Pattern search in BioPAX models. *Bioinformatics*. 2014; **30**: 139-40.

359 Babur O, Dogrusoz U, Demir E, Sander C. ChiBE: interactive visualization and manipulation of BioPAX pathway models. *Bioinformatics*. 2010; **26**: 429-31.

360 Tagami S, Eguchi Y, Kinoshita M, Takeda M, Tsujimoto Y. A novel protein, RTN-XS, interacts with both Bcl-XL and Bcl-2 on endoplasmic reticulum and reduces their anti-apoptotic activity. *Oncogene*. 2000; **19**: 5736-46.

361 Rigg RA, Healy LD, Nowak MS, Mallet J, Thierheimer ML, Pang J, McCarty OJ, Aslan JE. Heat shock protein 70 regulates platelet integrin activation, granule secretion and aggregation. *Am J Physiol Cell Physiol*. 2016; **310**: C568-75.

362 Mitrugno A, Rigg RA, Laschober NB, Ngo ATP, Pang J, Williams CD, Aslan JE, McCarty OJT. Potentiation of TRAP-6-induced platelet dense granule release by blockade of P2Y12 signaling with MRS2395. *Platelets*. 2018; **29**: 383-94.

363 Jupe S, Akkerman JW, Soranzo N, Ouwehand WH. Reactome - a curated knowledgebase of biological pathways: megakaryocytes and platelets. *J Thromb Haemost*. 2012; **10**: 2399-402.

364 Hornbeck PV, Zhang B, Murray B, Kornhauser JM, Latham V, Skrzypek E. PhosphoSitePlus, 2014: mutations, PTMs and recalibrations. *Nucleic Acids Res*. 2015; **43**: D512-20.

365 Demir E, Babur O, Rodchenkov I, Aksoy BA, Fukuda KI, Gross B, Sumer OS, Bader GD, Sander C. Using biological pathway data with paxtools. *PLoS Comput Biol*. 2013; **9**: e1003194.

366 Hara H, Ishihara C, Takeuchi A, Imanishi T, Xue L, Morris SW, Inui M, Takai T, Shibuya A, Saijo S, Iwakura Y, Ohno N, Koseki H, Yoshida H, Penninger JM, Saito T. The adaptor protein CARD9 is essential for the activation of myeloid cells through ITAM-associated and Toll-like receptors. *Nat Immunol*. 2007; **8**: 619-29.

367 Adam F, Kauskot A, Rosa JP, Bryckaert M. Mitogen-activated protein kinases in hemostasis and thrombosis. *J Thromb Haemost*. 2008; **6**: 2007-16.

368 Kramer RM, Roberts EF, Um SL, Borsch-Haubold AG, Watson SP, Fisher MJ, Jakubowski JA. p38 mitogen-activated protein kinase phosphorylates cytosolic phospholipase A2 (cPLA2) in thrombin-stimulated platelets. Evidence that proline-directed phosphorylation is not required for mobilization of arachidonic acid by cPLA2. *J Biol Chem*. 1996; **271**: 27723-9.

369 Lalaoui N, Hanggi K, Brumatti G, Chau D, Nguyen NN, Vasilikos L, Spilgies LM, Heckmann DA, Ma C, Ghisi M, et al. Targeting p38 or MK2 Enhances the Anti-Leukemic Activity of Smac-Mimetics. *Cancer Cell*. 2016; **30**: 499-500.

370 Tollenaere MAX, Villumsen BH, Blasius M, Nielsen JC, Wagner SA, Bartek J, Beli P, Mailand N, Bekker-Jensen S. p38- and MK2-dependent signalling promotes stress-induced centriolar satellite remodelling via 14-3-3-dependent sequestration of CEP131/AZI1. *Nat Commun*. 2015; **6**: 10075.

371 Jin J, Quinton TM, Zhang J, Rittenhouse SE, Kunapuli SP. Adenosine diphosphate (ADP)-induced thromboxane A(2) generation in human platelets requires coordinated signaling through integrin alpha(IIb)beta(3) and ADP receptors. *Blood*. 2002; **99**: 193-8.

372 Kamiyama M, Shirai T, Tamura S, Suzuki-Inoue K, Ehata S, Takahashi K, Miyazono K, Hayakawa Y, Sato T, Takeda K, Naguro I, Ichijo H. ASK1 facilitates tumor metastasis through phosphorylation of an ADP receptor P2Y12 in platelets. *Cell Death Differ*. 2017; **24**: 2066-76.

373 Naik MU, Patel P, Derstine R, Turaga R, Chen X, Golla K, Neeves KB, Ichijo H, Naik UP. Ask1 regulates murine platelet granule secretion, thromboxane A2 generation, and thrombus formation. *Blood*. 2017; **129**: 1197-209.

374 Begonja AJ, Geiger J, Rukoyatkina N, Rauchfuss S, Gambaryan S, Walter U. Thrombin stimulation of p38 MAP kinase in human platelets is mediated by ADP and thromboxane A2 and inhibited by cGMP/cGMP-dependent protein kinase. *Blood*. 2007; **109**: 616-8.

375 Mazharian A, Roger S, Berrou E, Adam F, Kauskot A, Nurden P, Jandrot-Perrus M, Bryckaert M. Protease-activating receptor-4 induces full platelet spreading on a fibrinogen matrix: involvement of ERK2 and p38 and Ca2+ mobilization. *J Biol Chem*. 2007; **282**: 5478-87.

376 Saklatvala J, Rawlinson L, Waller RJ, Sarsfield S, Lee JC, Morton LF, Barnes MJ, Farndale RW. Role for p38 mitogen-activated protein kinase in platelet aggregation caused by collagen or a thromboxane analogue. *J Biol Chem*. 1996; **271**: 6586-9.

377 Rousseau S, Peggie M, Campbell DG, Nebreda AR, Cohen P. Nogo-B is a new physiological substrate for MAPKAP-K2. *Biochem J*. 2005; **391**: 433-40.

378 Oertle T, Huber C, van der Putten H, Schwab ME. Genomic structure and functional characterisation of the promoters of human and mouse nogo/rtn4. *J Mol Biol*. 2003; **325**: 299-323.

379 Oertle T, Schwab ME. Nogo and its paRTNers. *Trends Cell Biol*. 2003; **13**: 187-94.

380 Teng FY, Tang BL. Cell autonomous function of Nogo and reticulons: The emerging story at the endoplasmic reticulum. *J Cell Physiol*. 2008; **216**: 303-8.

381 Wang J, Beauchemin M, Bertrand R. Phospho-Bcl-x(L)(Ser62) plays a key role at DNA damage-induced G(2) checkpoint. *Cell Cycle*. 2012; **11**: 2159-69.

382 Schoenwaelder SM, Jarman KE, Gardiner EE, Hua M, Qiao J, White MJ, Josefsson EC, Alwis I, Ono A, Willcox A, Andrews RK, Mason KD, Salem HH, Huang DC, Kile BT, Roberts AW, Jackson SP. Bcl-xL-inhibitory BH3 mimetics can induce a transient thrombocytopathy that undermines the hemostatic function of platelets. *Blood*. 2011; **118**: 1663-74.

383 Schoenwaelder SM, Yuan Y, Josefsson EC, White MJ, Yao Y, Mason KD, O'Reilly LA, Henley KJ, Ono A, Hsiao S, Willcox A, Roberts AW, Huang DC, Salem HH, Kile BT, Jackson SP. Two distinct pathways regulate platelet phosphatidylserine exposure and procoagulant function. *Blood*. 2009; **114**: 663-6.

384 Chen Z, Schubert P, Bakkour S, Culibrk B, Busch MP, Devine DV. p38 mitogen-activated protein kinase regulates mitochondrial function and microvesicle release in

riboflavin- and ultraviolet light-treated apheresis platelet concentrates. *Transfusion*. 2017; **57**: 1199-207.

385 Siljander P, Farndale RW, Feijge MA, Comfurius P, Kos S, Bevers EM, Heemskerk JW. Platelet adhesion enhances the glycoprotein VI-dependent procoagulant response: Involvement of p38 MAP kinase and calpain. *Arterioscler Thromb Vasc Biol*. 2001; **21**: 618-27.

386 Szklarczyk D, Franceschini A, Wyder S, Forslund K, Heller D, Huerta-Cepas J, Simonovic M, Roth A, Santos A, Tsafou KP, Kuhn M, Bork P, Jensen LJ, von Mering C. STRING v10: protein-protein interaction networks, integrated over the tree of life. *Nucleic Acids Res*. 2015; **43**: D447-52.

387 Shi P, Zhang L, Zhang M, Yang W, Wang K, Zhang J, Otsu K, Huang G, Fan X, Liu J. Platelet-Specific p38alpha Deficiency Improved Cardiac Function After Myocardial Infarction in Mice. *Arterioscler Thromb Vasc Biol*. 2017; **37**: e185-e96.

388 Sakurai K, Matsuo Y, Sudo T, Takuwa Y, Kimura S, Kasuya Y. Role of p38 mitogen-activated protein kinase in thrombus formation. *J Recept Signal Transduct Res*. 2004; **24**: 283-96.

389 Borsch-Haubold AG, Ghomashchi F, Pasquet S, Goedert M, Cohen P, Gelb MH, Watson SP. Phosphorylation of cytosolic phospholipase A2 in platelets is mediated by multiple stress-activated protein kinase pathways. *Eur J Biochem*. 1999; **265**: 195-203.

390 Kuliopulos A, Mohanlal R, Covic L. Effect of selective inhibition of the p38 MAP kinase pathway on platelet aggregation. *Thromb Haemost*. 2004; **92**: 1387-93.

391 Cuadrado A, Nebreda AR. Mechanisms and functions of p38 MAPK signalling. *Biochem J*. 2010; **429**: 403-17.

392 Butt E, Immler D, Meyer HE, Kotlyarov A, Laass K, Gaestel M. Heat shock protein 27 is a substrate of cGMP-dependent protein kinase in intact human platelets: phosphorylation-induced actin polymerization caused by HSP27 mutants. *J Biol Chem*. 2001; **276**: 7108-13.

393 Kato H, Takai S, Matsushima-Nishiwaki R, Adachi S, Minamitani C, Otsuka T, Tokuda H, Akamatsu S, Doi T, Ogura S, Kozawa O. HSP27 phosphorylation is correlated with ADP-induced platelet granule secretion. *Arch Biochem Biophys*. 2008; **475**: 80-6.

394 Polanowska-Grabowska R, Gear AR. Heat-shock proteins and platelet function. *Platelets*. 2000; **11**: 6-22.

395 Jozsef L, Tashiro K, Kuo A, Park EJ, Skoura A, Albinsson S, Rivera-Molina F, Harrison KD, Iwakiri Y, Toomre D, Sessa WC. Reticulon 4 is necessary for endoplasmic

reticulum tubulation, STIM1-Orai1 coupling, and store-operated calcium entry. *J Biol Chem*. 2014; **289**: 9380-95.

396 Rukoyatkina N, Mindukshev I, Walter U, Gambaryan S. Dual role of the p38 MAPK/cPLA2 pathway in the regulation of platelet apoptosis induced by ABT-737 and strong platelet agonists. *Cell Death Dis*. 2013; **4**: e931.

397 Munnix IC, Kuijpers MJ, Auger J, Thomassen CM, Panizzi P, van Zandvoort MA, Rosing J, Bock PE, Watson SP, Heemskerk JW. Segregation of platelet aggregatory and procoagulant microdomains in thrombus formation: regulation by transient integrin activation. *Arterioscler Thromb Vasc Biol*. 2007; **27**: 2484-90.

398 Stalker TJ, Welsh JD, Tomaiuolo M, Wu J, Colace TV, Diamond SL, Brass LF. A systems approach to hemostasis: 3. Thrombus consolidation regulates intrathrombus solute transport and local thrombin activity. *Blood*. 2014; **124**: 1824-31.

399 Acevedo L, Yu J, Erdjument-Bromage H, Miao RQ, Kim JE, Fulton D, Tempst P, Strittmatter SM, Sessa WC. A new role for Nogo as a regulator of vascular remodeling. *Nat Med*. 2004; **10**: 382-8.

400 Miao RQ, Gao Y, Harrison KD, Prendergast J, Acevedo LM, Yu J, Hu F, Strittmatter SM, Sessa WC. Identification of a receptor necessary for Nogo-B stimulated chemotaxis and morphogenesis of endothelial cells. *Proc Natl Acad Sci U S A*. 2006; **103**: 10997-1002.

401 Sutendra G, Dromparis P, Wright P, Bonnet S, Haromy A, Hao Z, McMurtry MS, Michalak M, Vance JE, Sessa WC, Michelakis ED. The role of Nogo and the mitochondria-endoplasmic reticulum unit in pulmonary hypertension. *Sci Transl Med*. 2011; **3**: 88ra55.

402 de Brito OM, Scorrano L. Mitofusin 2 tethers endoplasmic reticulum to mitochondria. *Nature*. 2008; **456**: 605-10.

403 Aslan JE, Thomas G. Death by committee: organellar trafficking and communication in apoptosis. *Traffic*. 2009; **10**: 1390-404.

404 Simmen T, Aslan JE, Blagoveshchenskaya AD, Thomas L, Wan L, Xiang Y, Feliciangeli SF, Hung CH, Crump CM, Thomas G. PACS-2 controls endoplasmic reticulum-mitochondria communication and Bid-mediated apoptosis. *EMBO J*. 2005; **24**: 717-29.

405 Canault M, Duerschmied D, Brill A, Stefanini L, Schatzberg D, Cifuni SM, Bergmeier W, Wagner DD. p38 mitogen-activated protein kinase activation during platelet storage: consequences for platelet recovery and hemostatic function in vivo. *Blood*. 2010; **115**: 1835-42.

406 Brill A, Chauhan AK, Canault M, Walsh MT, Bergmeier W, Wagner DD. Oxidative stress activates ADAM17/TACE and induces its target receptor shedding in platelets in a p38-dependent fashion. *Cardiovasc Res*. 2009; **84**: 137-44.

407 Bateman LA, Nguyen TB, Roberts AM, Miyamoto DK, Ku WM, Huffman TR, Petri Y, Heslin MJ, Contreras CM, Skibola CF, Olzmann JA, Nomura DK. Chemoproteomics-enabled covalent ligand screen reveals a cysteine hotspot in reticulon 4 that impairs ER morphology and cancer pathogenicity. *Chem Commun (Camb)*. 2017; **53**: 7234-7.

408 Durrant TN, Hutchinson JL, Heesom KJ, Anderson KE, Stephens LR, Hawkins PT, Marshall AJ, Moore SF, Hers I. In-depth PtdIns(3,4,5)P3 signalosome analysis identifies DAPP1 as a negative regulator of GPVI-driven platelet function. *Blood Adv*. 2017; **1**: 918-32.

409 Stalker TJ, Newman DK, Ma P, Wannemacher KM, Brass LF. Platelet signaling. *Handb Exp Pharmacol*. 2012: 59-85.

410 Covic L, Gresser AL, Kuliopulos A. Biphasic kinetics of activation and signaling for PAR1 and PAR4 thrombin receptors in platelets. *Biochemistry*. 2000; **39**: 5458-67.

411 Dorsam RT, Kunapuli SP. Central role of the P2Y12 receptor in platelet activation. *J Clin Invest*. 2004; **113**: 340-5.

412 Haley KM, Recht M, McCarty OJ. Neonatal platelets: mediators of primary hemostasis in the developing hemostatic system. *Pediatr Res*. 2014; **76**: 230-7.

413 Israels SJ, Daniels M, McMillan EM. Deficient collagen-induced activation in the newborn platelet. *Pediatr Res*. 1990; **27**: 337-43.

414 Israels SJ, Cheang T, Roberston C, McMillan-Ward EM, McNicol A. Impaired signal transduction in neonatal platelets. *Pediatr Res*. 1999; **45**: 687-91.

415 Gelman B, Setty BN, Chen D, Amin-Hanjani S, Stuart MJ. Impaired mobilization of intracellular calcium in neonatal platelets. *Pediatr Res*. 1996; **39**: 692-6.

416 Schlagenhauf A, Schweintzger S, Birner-Gruenberger R, Leschnik B, Muntean W. Newborn platelets: lower levels of protease-activated receptors cause hypoaggregability to thrombin. *Platelets*. 2010; **21**: 641-7.

417 Sitaru AG, Holzhauer S, Speer CP, Singer D, Obergfell A, Walter U, Grossmann R. Neonatal platelets from cord blood and peripheral blood. *Platelets*. 2005; **16**: 203-10.

418 Baker-Groberg SM, Lattimore S, Recht M, McCarty OJ, Haley KM. Assessment of neonatal platelet adhesion, activation, and aggregation. *J Thromb Haemost*. 2016; **14**: 815-27.

419 Mumaw MM, de la Fuente M, Arachiche A, Wahl JK, 3rd, Nieman MT. Development and characterization of monoclonal antibodies against Protease Activated Receptor 4 (PAR4). *Thromb Res*. 2015; **135**: 1165-71.

420 Schulz-Heik K, Ramachandran J, Bluestein D, Jesty J. The extent of platelet activation under shear depends on platelet count: differential expression of anionic phospholipid and factor Va. *Pathophysiol Haemost Thromb*. 2005; **34**: 255-62.

421 Sheriff J, Bluestein D, Girdhar G, Jesty J. High-shear stress sensitizes platelets to subsequent low-shear conditions. *Ann Biomed Eng*. 2010; **38**: 1442-50.

422 Xenos M, Girdhar G, Alemu Y, Jesty J, Slepian M, Einav S, Bluestein D. Device Thrombogenicity Emulator (DTE)--design optimization methodology for cardiovascular devices: a study in two bileaflet MHV designs. *J Biomech*. 2010; **43**: 2400-9.

423 Sheriff J, Soares JS, Xenos M, Jesty J, Slepian MJ, Bluestein D. Evaluation of shear-induced platelet activation models under constant and dynamic shear stress loading conditions relevant to devices. *Ann Biomed Eng*. 2013; **41**: 1279-96.

424 Jesty J, Bluestein D. Acetylated prothrombin as a substrate in the measurement of the procoagulant activity of platelets: elimination of the feedback activation of platelets by thrombin. *Anal Biochem*. 1999; **272**: 64-70.

425 Fullard JF. The role of the platelet glycoprotein IIb/IIIa in thrombosis and haemostasis. *Curr Pharm Des*. 2004; **10**: 1567-76.

426 Delaney MK, Liu J, Kim K, Shen B, Stojanovic-Terpo A, Zheng Y, Cho J, Du X. Agonist-induced platelet procoagulant activity requires shear and a Rac1-dependent signaling mechanism. *Blood*. 2014; **124**: 1957-67.

427 Sims PJ, Wiedmer T, Esmon CT, Weiss HJ, Shattil SJ. Assembly of the platelet prothrombinase complex is linked to vesiculation of the platelet plasma membrane. Studies in Scott syndrome: an isolated defect in platelet procoagulant activity. *J Biol Chem*. 1989; **264**: 17049-57.

428 Swords NA, Mann KG. The assembly of the prothrombinase complex on adherent platelets. *Arterioscler Thromb*. 1993; **13**: 1602-12.

429 Jesty J, Yin W, Perrotta P, Bluestein D. Platelet activation in a circulating flow loop: combined effects of shear stress and exposure time. *Platelets*. 2003; **14**: 143-9.

430 Bernhard H, Rosenkranz A, Petritsch M, Kofeler H, Rehak T, Novak M, Muntean W. Phospholipid content, expression and support of thrombin generation of neonatal platelets. *Acta Paediatr*. 2009; **98**: 251-5.

431 Mankin P, Maragos J, Akhand M, Saving KL. Imparied platelet--dense granule release in neonates. *J Pediatr Hematol Oncol*. 2000; **22**: 143-7.

432 Sola-Visner M. Platelets in the neonatal period: developmental differences in platelet production, function, and hemostasis and the potential impact of therapies. *Hematology Am Soc Hematol Educ Program*. 2012; **2012**: 506-11.

433 Roschitz B, Sudi K, Kostenberger M, Muntean W. Shorter PFA-100 closure times in neonates than in adults: role of red cells, white cells, platelets and von Willebrand factor. *Acta Paediatr*. 2001; **90**: 664-70.

434 Andrew M, Paes B, Johnston M. Development of the hemostatic system in the neonate and young infant. *Am J Pediatr Hematol Oncol*. 1990; **12**: 95-104.

435 Weinstein MJ, Blanchard R, Moake JL, Vosburgh E, Moise K. Fetal and neonatal von Willebrand factor (vWF) is unusually large and similar to the vWF in patients with thrombotic thrombocytopenic purpura. *Br J Haematol*. 1989; **72**: 68-72.

436 Rajasekhar D, Kestin AS, Bednarek FJ, Ellis PA, Barnard MR, Michelson AD. Neonatal platelets are less reactive than adult platelets to physiological agonists in whole blood. *Thromb Haemost*. 1994; **72**: 957-63.

437 Schlagenhauf A, Schweintzger S, Birner-Grunberger R, Leschnik B, Muntean W. Comparative evaluation of PAR1, GPIb-IX-V, and integrin alphaIIbbeta3 levels in cord and adult platelets. *Hamostaseologie*. 2010; **30 Suppl 1**: S164-7.

438 Flaumenhaft R, Dilks JR, Rozenvayn N, Monahan-Earley RA, Feng D, Dvorak AM. The actin cytoskeleton differentially regulates platelet alpha-granule and dense-granule secretion. *Blood*. 2005; **105**: 3879-87.

439 Akkerman JW, Gorter G, Kloprogge E. Kinetic analysis of alpha-granule secretion by platelets. A methodological report. *Thromb Res*. 1982; **27**: 59-64.

440 van der Valk FM, Bekkering S, Kroon J, Yeang C, Van den Bossche J, van Buul JD, Ravandi A, Nederveen AJ, Verberne HJ, Scipione C, Nieuwdorp M, Joosten LA, Netea MG, Koschinsky ML, Witztum JL, Tsimikas S, Riksen NP, Stroes ES. Oxidized Phospholipids on Lipoprotein(a) Elicit Arterial Wall Inflammation and an Inflammatory Monocyte Response in Humans. *Circulation*. 2016; **134**: 611-24.

441 Ley K, Miller YI, Hedrick CC. Monocyte and macrophage dynamics during atherogenesis. *Arterioscler Thromb Vasc Biol*. 2011; **31**: 1506-16.

442 Libby P. Inflammation in atherosclerosis. *Nature*. 2002; **420**: 868-74.

443 Viles-Gonzalez JF, Fuster V, Badimon JJ. Atherothrombosis: a widespread disease with unpredictable and life-threatening consequences. *Eur Heart J*. 2004; **25**: 1197-207.

444 Leys D. Atherothrombosis: a major health burden. *Cerebrovasc Dis*. 2001; **11 Suppl 2**: 1-4.

445 Borissoff JI, Heeneman S, Kilinc E, Kassak P, Van Oerle R, Winckers K, Govers-Riemslag JW, Hamulyak K, Hackeng TM, Daemen MJ, ten Cate H, Spronk HM. Early atherosclerosis exhibits an enhanced procoagulant state. *Circulation*. 2010; **122**: 821-30.

446 Siegerink B, Rosendaal FR, Algra A. Antigen levels of coagulation factor XII, coagulation factor XI and prekallikrein, and the risk of myocardial infarction and ischemic stroke in young women. *J Thromb Haemost*. 2014; **12**: 606-13.

447 Chan JC, Ganopolsky JG, Cornelissen I, Suckow MA, Sandoval-Cooper MJ, Brown EC, Noria F, Gailani D, Rosen ED, Ploplis VA, Castellino FJ. The characterization of mice with a targeted combined deficiency of protein c and factor XI. *Am J Pathol*. 2001; **158**: 469-79.

448 Wang X, Cheng Q, Xu L, Feuerstein GZ, Hsu MY, Smith PL, Seiffert DA, Schumacher WA, Ogletree ML, Gailani D. Effects of factor IX or factor XI deficiency on ferric chloride-induced carotid artery occlusion in mice. *J Thromb Haemost*. 2005; **3**: 695-702.

449 Buller HR, Gailani D, Weitz JI. Factor XI antisense oligonucleotide for venous thrombosis. *N Engl J Med*. 2015; **372**: 1672.

450 Tucker EI, Gailani D, Hurst S, Cheng Q, Hanson SR, Gruber A. Survival advantage of coagulation factor XI-deficient mice during peritoneal sepsis. *J Infect Dis*. 2008; **198**: 271-4.

451 Bane CE, Jr., Ivanov I, Matafonov A, Boyd KL, Cheng Q, Sherwood ER, Tucker EI, Smiley ST, McCarty OJ, Gruber A, Gailani D. Factor XI Deficiency Alters the Cytokine Response and Activation of Contact Proteases during Polymicrobial Sepsis in Mice. *PLoS One*. 2016; **11**: e0152968.

452 Asakai R, Chung DW, Davie EW, Seligsohn U. Factor XI deficiency in Ashkenazi Jews in Israel. *N Engl J Med*. 1991; **325**: 153-8.

453 Prakash TP, Graham MJ, Yu J, Carty R, Low A, Chappell A, Schmidt K, Zhao C, Aghajan M, Murray HF, et al. Targeted delivery of antisense oligonucleotides to hepatocytes using triantennary N-acetyl galactosamine improves potency 10-fold in mice. *Nucleic Acids Res*. 2014; **42**: 8796-807.

454 Daugherty A, Tall AR, Daemen M, Falk E, Fisher EA, Garcia-Cardena G, Lusis AJ, Owens AP, 3rd, Rosenfeld ME, Virmani R, American Heart Association Council on Arteriosclerosis T, Vascular B, Council on Basic Cardiovascular S. Recommendation on Design, Execution, and Reporting of Animal Atherosclerosis Studies: A Scientific Statement From the American Heart Association. *Circ Res*. 2017; **121**: e53-e79.

455 Mueller PA, Zhu L, Tavori H, Huynh K, Giunzioni I, Stafford JM, Linton MF, Fazio S. Deletion of Macrophage Low-Density Lipoprotein Receptor-Related Protein 1 (LRP1) Accelerates Atherosclerosis Regression and Increases C-C Chemokine Receptor Type 7 (CCR7) Expression in Plaque Macrophages. *Circulation*. 2018; **138**: 1850-63.

456 McCarty OJ, Conley RB, Shentu W, Tormoen GW, Zha D, Xie A, Qi Y, Zhao Y, Carr C, Belcik T, Keene DR, de Groot PG, Lindner JR. Molecular imaging of activated von Willebrand factor to detect high-risk atherosclerotic phenotype. *JACC Cardiovasc Imaging*. 2010; **3**: 947-55.

457 Smith EB. Fibrin deposition and fibrin degradation products in atherosclerotic plaques. *Thromb Res*. 1994; **75**: 329-35.

458 Eapen DJ, Manocha P, Patel RS, Hammadah M, Veledar E, Wassel C, Nanjundappa RA, Sikora S, Malayter D, Wilson PW, Sperling L, Quyyumi AA, Epstein SE. Aggregate risk score based on markers of inflammation, cell stress, and coagulation is an independent predictor of adverse cardiovascular outcomes. *J Am Coll Cardiol*. 2013; **62**: 329-37.

459 VanderLaan PA, Reardon CA, Getz GS. Site specificity of atherosclerosis: site-selective responses to atherosclerotic modulators. *Arterioscler Thromb Vasc Biol*. 2004; **24**: 12-22.

460 Mohammed BM, Cheng Q, Matafonov A, Verhamme IM, Emsley J, McCrae KR, McCarty OJT, Gruber A, Gailani D. A non-circulating pool of factor XI associated with glycosaminoglycans in mice. *J Thromb Haemost*. 2019; **17**: 1449-60.

461 Burger W, Chemnitius JM, Kneissl GD, Rucker G. Low-dose aspirin for secondary cardiovascular prevention - cardiovascular risks after its perioperative withdrawal versus bleeding risks with its continuation - review and meta-analysis. *J Intern Med*. 2005; **257**: 399-414.

462 Reddy SK, Turley RS, Barbas AS, Steel JL, Tsung A, Marsh JW, Clary BM, Geller DA. Post-operative pharmacologic thromboprophylaxis after major hepatectomy: does peripheral venous thromboembolism prevention outweigh bleeding risks? *J Gastrointest Surg*. 2011; **15**: 1602-10.

463 Whitlock EP, Burda BU, Williams SB, Guirguis-Blake JM, Evans CV. Bleeding Risks With Aspirin Use for Primary Prevention in Adults: A Systematic Review for the U.S. Preventive Services Task Force. *Ann Intern Med*. 2016; **164**: 826-35.

464 Nourse J, Danckwardt S. A novel rationale for targeting FXI: Insights from the hemostatic microRNA targetome for emerging anticoagulant strategies. *Pharmacol Ther*. 2020: 107676.

465 Furie B, Furie BC. Mechanisms of thrombus formation. *N Engl J Med*. 2008; **359**: 938-49.

466 Ruggeri ZM. Mechanisms initiating platelet thrombus formation. *Thromb Haemost*. 1997; **78**: 611-6.

467 Sharda A, Flaumenhaft R. The life cycle of platelet granules. *F1000Res*. 2018; **7**: 236.

468 Karniguian A, Zahraoui A, Tavitian A. Identification of small GTP-binding rab proteins in human platelets: thrombin-induced phosphorylation of rab3B, rab6, and rab8 proteins. *Proc Natl Acad Sci U S A*. 1993; **90**: 7647-51.

469 Stenmark H. Rab GTPases as coordinators of vesicle traffic. *Nat Rev Mol Cell Biol*. 2009; **10**: 513-25.

470 Gillingham AK, Sinka R, Torres IL, Lilley KS, Munro S. Toward a comprehensive map of the effectors of rab GTPases. *Dev Cell*. 2014; **31**: 358-73.

471 Barral DC, Ramalho JS, Anders R, Hume AN, Knapton HJ, Tolmachova T, Collinson LM, Goulding D, Authi KS, Seabra MC. Functional redundancy of Rab27 proteins and the pathogenesis of Griscelli syndrome. *J Clin Invest*. 2002; **110**: 247-57.

472 Novak EK, Gautam R, Reddington M, Collinson LM, Copeland NG, Jenkins NA, McGarry MP, Swank RT. The regulation of platelet-dense granules by Rab27a in the ashen mouse, a model of Hermansky-Pudlak and Griscelli syndromes, is granule-specific and dependent on genetic background. *Blood*. 2002; **100**: 128-35.

473 Tolmachova T, Abrink M, Futter CE, Authi KS, Seabra MC. Rab27b regulates number and secretion of platelet dense granules. *Proc Natl Acad Sci U S A*. 2007; **104**: 5872-7.

474 Shirakawa R, Higashi T, Tabuchi A, Yoshioka A, Nishioka H, Fukuda M, Kita T, Horiuchi H. Munc13-4 is a GTP-Rab27-binding protein regulating dense core granule secretion in platelets. *J Biol Chem*. 2004; **279**: 10730-7.

475 Feldmann J, Callebaut I, Raposo G, Certain S, Bacq D, Dumont C, Lambert N, Ouachee-Chardin M, Chedeville G, Tamary H, Minard-Colin V, Vilmer E, Blanche S, Le Deist F, Fischer A, de Saint Basile G. Munc13-4 is essential for cytolytic granules fusion and is mutated in a form of familial hemophagocytic lymphohistiocytosis (FHL3). *Cell*. 2003; **115**: 461-73.

476 Harper MT, van den Bosch MT, Hers I, Poole AW. Absence of platelet phenotype in mice lacking the motor protein myosin Va. *PLoS One*. 2013; **8**: e53239.

477 Hampson A, O'Connor A, Smolenski A. Synaptotagmin-like protein 4 and Rab8 interact and increase dense granule release in platelets. *J Thromb Haemost*. 2013; **11**: 161-8.

478 Shirakawa R, Yoshioka A, Horiuchi H, Nishioka H, Tabuchi A, Kita T. Small GTPase Rab4 regulates Ca2+-induced alpha-granule secretion in platelets. *J Biol Chem*. 2000; **275**: 33844-9.

479 Guerra F, Bucci C. Multiple Roles of the Small GTPase Rab7. *Cells*. 2016; **5**.

480 Jalagadugula G, Goldfinger LE, Mao G, Lambert MP, Rao AK. Defective RAB1B-related megakaryocytic ER-to-Golgi transport in RUNX1 haplodeficiency: impact on von Willebrand factor. *Blood Adv*. 2018; **2**: 797-806.

481 Ninkovic I, White JG, Rangel-Filho A, Datta YH. The role of Rab38 in platelet dense granule defects. *J Thromb Haemost*. 2008; **6**: 2143-51.

482 Ambrosio AL, Boyle JA, Di Pietro SM. Mechanism of platelet dense granule biogenesis: study of cargo transport and function of Rab32 and Rab38 in a model system. *Blood*. 2012; **120**: 4072-81.

483 Donaldson JG, Jackson CL. ARF family G proteins and their regulators: roles in membrane transport, development and disease. *Nat Rev Mol Cell Biol*. 2011; **12**: 362-75.

484 Antonny B, Beraud-Dufour S, Chardin P, Chabre M. N-terminal hydrophobic residues of the G-protein ADP-ribosylation factor-1 insert into membrane phospholipids upon GDP to GTP exchange. *Biochemistry*. 1997; **36**: 4675-84.

485 Jackson CL, Bouvet S. Arfs at a glance. *J Cell Sci*. 2014; **127**: 4103-9.

486 D'Souza-Schorey C, Chavrier P. ARF proteins: roles in membrane traffic and beyond. *Nat Rev Mol Cell Biol*. 2006; **7**: 347-58.

487 Schubbert S, Shannon K, Bollag G. Hyperactive Ras in developmental disorders and cancer. *Nat Rev Cancer*. 2007; **7**: 295-308.

488 Tidyman WE, Rauen KA. The RASopathies: developmental syndromes of Ras/MAPK pathway dysregulation. *Curr Opin Genet Dev*. 2009; **19**: 230-6.

489 Perez Botero J, Ho TP, Rodriguez V, Khan SP, Pruthi RK, Patnaik MM. Coagulation abnormalities and haemostatic surgical outcomes in 142 patients with Noonan syndrome. *Haemophilia*. 2017; **23**: e237-e40.

490 Zhang G, Xiang B, Ye S, Chrzanowska-Wodnicka M, Morris AJ, Gartner TK, Whiteheart SW, White GC, 2nd, Smyth SS, Li Z. Distinct roles for Rap1b protein in

platelet secretion and integrin alphaIIbbeta3 outside-in signaling. *J Biol Chem*. 2011; **286**: 39466-77.

491 Stefanini L, Bergmeier W. RAP GTPases and platelet integrin signaling. *Platelets*. 2019; **30**: 41-7.

492 Peschard P, McCarthy A, Leblanc-Dominguez V, Yeo M, Guichard S, Stamp G, Marshall CJ. Genetic deletion of RALA and RALB small GTPases reveals redundant functions in development and tumorigenesis. *Curr Biol*. 2012; **22**: 2063-8.

493 Mark BL, Jilkina O, Bhullar RP. Association of Ral GTP-binding protein with human platelet dense granules. *Biochem Biophys Res Commun*. 1996; **225**: 40-6.

494 Wolthuis RM, Franke B, van Triest M, Bauer B, Cool RH, Camonis JH, Akkerman JW, Bos JL. Activation of the small GTPase Ral in platelets. *Mol Cell Biol*. 1998; **18**: 2486-91.

495 Kim MS, Pinto SM, Getnet D, Nirujogi RS, Manda SS, Chaerkady R, Madugundu AK, Kelkar DS, Isserlin R, Jain S, et al. A draft map of the human proteome. *Nature*. 2014; **509**: 575-81.

496 Wersall A, Williams CM, Brown E, Iannitti T, Williams N, Poole AW. Mouse Platelet Ral GTPases Control P-Selectin Surface Expression, Regulating Platelet-Leukocyte Interaction. *Arterioscler Thromb Vasc Biol*. 2018; **38**: 787-800.

497 Walsh TG, Li Y, Wersall A, Poole AW. Small GTPases in platelet membrane trafficking. *Platelets*. 2019; **30**: 31-40.

498 Jarocha D, Vo KK, Lyde RB, Hayes V, Camire RM, Poncz M. Enhancing functional platelet release in vivo from in vitro-grown megakaryocytes using small molecule inhibitors. *Blood Adv*. 2018; **2**: 597-606.

Biographical Sketch

Anh Tran Phuong Ngo was born on April 9, 1994 in Ho Chi Minh City, Viet Nam.

Anh attended Tran Dai Nghia High School until 8th grade, when she decided to travel to Long Island, New York to pursue her dream of studying abroad. She graduated from City Christian High School in Portland, Oregon, and enrolled at Warner Pacific University (WPU) in 2011. She was awarded the WPU Trustee's Scholarship from 2011-2015, received the Freshman Achievement Award in 2012, Outstanding Achievement in Science and Mathematics Award in 2015 and was on the WPU Dean's list throughout her undergraduate studies. She became involved in research thanked to Dr. Elizabeth DuPriest (now a Professor of Biology at WPU). Anh was a research assistant at Oregon Health & Science University (OHSU)/ Portland Veterans Affairs Medical Center from 2014-2016, working in the lab of Dr. Susan Bagby and was mentored by Dr. Elizabeth DuPriest. In December of 2015, she graduated Summa cum Laude and earned her Bachelor of Science degree in Biological Science, with a minor in Chemistry.

Anh continued her higher education at Oregon Health & Science University (OHSU), joining the lab of Dr. Owen McCarty in the Department of Biomedical Engineering in January of 2016. Anh's research has centered on understanding signaling mechanisms and the interplay between platelets, coagulation and the endothelium in regulating hemostasis, thrombosis and cardiovascular diseases. During her graduate studies at OHSU, she was awarded the Graduate Student Research Award in Cell Biology and Chemistry from Sigma Xi (2016), the Career Development Award from Biomedical Engineering Society (2017), the Young Investigator Award from the International Society on Thrombosis and Haemostasis (2018), and the N.L. Tartar Trust Fellowship from OHSU (2019). Anh has presented her research in peer-reviewed journals and at conferences throughout the United States and Europe.

Following graduation from OHSU, Anh plans to continue her career in scientific discovery through academic research. Anh is excited for her next journey as a Postdoctoral Fellow at the Children's Hospital of Philadelphia/ University of Pennsylvania. She is also looking forward to visiting her family back in Viet Nam, waking up to the sound of roosters, lots of Vietnamese street food, and most importantly, being in the arms of those whom she loves most.

Anh's current publications, presentations, teaching and mentoring experiences are listed below.

Publications

Peer-reviewed

1. **Ngo AT**, Thierheimer ML, Pang J, Babur O, Rocheleau AD, Rigg RA, Mitrugno A, Huang T, Nan X, Burchard J, Demir E, McCarty OJT,* Aslan JE.* Assessment of roles for the Rho-specific guanine nucleotide dissociation inhibitor (RhoGDI) Ly-GDI in platelet function. *American Journal of Physiology: Cell Physiology* 2017; 312(4):C527-C536. *co-senior authors (Selected as the *AJP:Cell* Image of the Week). PMID: 28148498.

2. Mitrugno A, Sylman JL, **Ngo AT**, Pang J, Sears RC, Williams CD, McCarty OJ. Aspirin therapy reduces the ability of platelets to promote colon and pancreatic cancer cell proliferation: implications for the oncoprotein c-MYC. *American Journal of Physiology: Cell Physiology* 2017; 312(2):C176-C189. (Selected as the *AJP:Cell* Image of the Week; Featured in *AJP* News). PMID: 27903583.

3. Mitrugno A, Rigg RA, Laschober NB, **Ngo AT**, Pang J, Williams CD, Aslan JE, McCarty OJ. Potentiation of TRAP-6-induced platelet dense granule release by blockade of $P2Y_{12}$ signaling with MRS2395. *Platelets* 2018; 29(4):383-394. PMID: 28523947.

4. Rocheleau AD, Khader A, **Ngo AT**, Boehnlein C, McDavitt C, Lattimore S, Recht M, McCarty OJ, Haley KM. Pilot study of novel lab methodology and testing of platelet function in adolescent women with heavy menstrual bleeding. *Pediatric Research* 2018; 83(3):693-701. PMID: 29166373.

5. Rigg RA, Healy LD, Chu TT, **Ngo AT**, Mitrugno A, Zilberman-Rudenko J, Aslan JE, Hinds MT, Vecchiarelli LD, Morgan TK, Gruber A, Temple KJ, Lindsley CW, Duvernay MT, Hamm HE, McCarty OJ. Protease-activated receptor 4 (PAR4) activity promotes platelet granule release and platelet-leukocyte interactions. *Platelets* 2019; 30(1):126-135. PMID: 30560697.

6. Babur O,* **Ngo AT**,* Rigg RA, Pang J, Rub ZT, Buchanan AE, Mitrugno A, LL David, McCarty OJ, Demir E, Aslan JE. Platelet procoagulant phenotype is modulated by a p38 - MK2 axis regulating RTN4/Nogo proximal to the endoplasmic reticulum: utility of pathway analysis. *American Journal of Physiology: Cell Physiology* 2018; 314(5):C603-C615.*equally contributing first authors (*AJP:Cell* Image of the Week). PMID: 29412690.

7. **Ngo AT**, Sheriff J, Rocheleau AD, Bucher M, Jones KR, Sepp AI, Malone LE, Zigomalas A, Maloyan A, Bahou WF, Bluestein D, McCarty OJ, Haley KM. Assessment of neonatal, cord, and adult platelet granule trafficking and secretion. *Platelets* 2020; 31(1):67-68. PMID: 30810440.

8. Rocheleau AD, Melrose AR, Cunliffe JM, Klimek J, Babur O, Tassi Yunga S, **Ngo AT**, Pang J, David J, McCarty OJ, Aslan JE. Identification, quantification and systems

analysis of cytosolic protein N-ϵ lysine methylation in anucleate blood platelets. *Proteomics* 2019; 19(11):e1900001. PMID: 30977292.

9. Puy C, **Ngo AT**, Pang J, Keshari RS, Hagen MW, Hinds MT, Gailani D, Gruber A, Lupu F, McCarty OJ. Endothelial plasminogen activator inhibitor-1 blocks the intrinsic pathway of coagulation, inducing the clearance and degradation of factor XIa. *Arterioscler Thromb & Vasc Biol* 2019; 39(7): 1390-1401. PMID: 31242030.

10. Shirai T, Revenko AS, Tibbits J, **Ngo AT**, Mitrugno A, Healy LD, Johnson J, Tucker EI, Hinds MT, Coussens LM, McCarty OJ, Monia BP, Gruber A. Hepatic thrombopoietin gene silencing reduces platelet count and breast cancer progression in transgenic MMTV-PyMT mice. *Blood Advances* 2019; 3(20):3080-3091. PMID: 31648335.

11. Lakshmanan H, Melrose AR, Sepp A-L, Mitrugno A, **Ngo AT**, Khader A, Thompson R, Sallee D, Pang J, Mangin PH, Jandrot-Perrus M, Aslan JE, McCarty OJT. The basement membrane protein nidogen-1 supports platelet adhesion and activation. *Platelets* 2020; 1-5. PMID: 32233694.

12. **Ngo AT**, Jordan KR, Mueller PA, Puy C, Reitsma SE, Hagen MW, Revenko AS, Lorentz CU, Tucker EI, Cheng Q, Hinds MT, Fazio S, Monia BP, Gailani D, Gruber A, Tavori H, McCarty OJT. Pharmacological targeting of coagulation Factor XI mitigates the development of experimental atherosclerosis in low-density lipoprotein receptor-deficient mice. Accepted to *Journal of Thrombosis and Haemostasis* 2021.

13. **Ngo AT**,* Parra-Izquierdo I,* Aslan JE, McCarty OJT. Rho GTPase regulation of reactive oxygen species generation and signaling in platelet function and disease. *equally contributing first authors. Accepted to *Small GTPases* 2021.

Reviews, Editorials and Book Chapters

1. **Ngo AT**, Aslan JE, McCarty OJ. Bleeding TAPs out. *Journal of Thrombosis and Haemostasis* 2019; 17(2):247-249. PMID: 30549218.

2. **Ngo AT**, McCarty OJ, Aslan JE. TRPing out platelet calcium – TRPM7 modulates calcium mobilization and platelet function via PLC interactions. *Arterioscler Thromb & Vasc Biol* 2018; 38(2):285-286. PMID: 29367228.

3. **Ngo AT**, Jongen S, Shatzel JJ, McCarty OJT. Platelet integrin activation surfs the calcium waves. *Platelets* 2020; 1-3. PMID: 32441552.

Under Review

1. Kim HJ, Rames M, Yunga ST, Armstrong R, Morita M, **Ngo AT**, McCarty OJT, Civitci F, Morgan TK, Ngo T. Irreversible alteration of extracellular vesicle and cell-free

messenger RNA profiles in human plasma associated with *ex vivo* platelet activation. Submitted to *Scientific Reports.*

Recent Abstracts

1. **Ngo AT**, Puy C, Pang J, Tucker EI, Lorentz CU, Verbout NG, Jordan K, Mueller P, Revenko AS, Monia BP, Gruber A, McCarty OJT, Tavori H. Inhibition of coagulation factor XI suppresses progression of atherosclerosis. *American Heart Association Scientific Meeting*. Philadelphia, USA. Nov 2019. [Oral Presentation]

2. **Ngo AT**, Puy C, Pang J, Tucker E, Lorentz C, Verbout N, Gruber A, Howard C, Tavori H, McCarty OJT. Role of Coagulation Factor XI in Regulating Endothelial Cell Barrier Function. *Arterioslerosis, Thrombosis, and Vascular Biology.* Boston, USA. May 2019. [Poster]

3. **Ngo AT**, Sheriff J, Jones KR, Rocheleau AD, Mitrugno A, Aslan JE, Worthington S, Cox A, Recht M, Nieman M, Malone LE, Zigomalas A, Bahou WF, Bluestein D, McCarty OJT, Haley KM. Assessment of Neonatal Platelet Granule Trafficking and Shear-Induced Platelet Activation in Neonatal Peripheral and Cord Blood. *International Society on Thrombosis and Haemostasis*. Dublin, Ireland. July 2018. [Poster]

4. **Ngo AT**, Puy C, Tucker E, Gailani D, Gruber A, McCarty OJT. FXIa binds and Forms a Complex with Plasminogen Activator Inhibitor-1 that Inhibits Its Activity and Induces Internalization and Degradation by Endothelial Cells. *International Society on Thrombosis and Haemostasis*. Dublin, Ireland. July 2018. [Poster]

5. **Ngo AT**, Puy C, Tucker E, Gailani D, Gruber A, McCarty OJT. Novel approach for visualizing the binding of FXIa on endothelial cell surface and FXIa trafficking following endothelial cell-induced internalization. *Biomedical Engineering Society*. Phoenix, USA. Oct 2017. [Poster]

6. **Ngo AT**, Mitrugno A, Rocheleau A, Baker S, Khader A, Aslan JE, Lattimore S, Recht M, Haley KM, Nan X, McCarty OJT. Assessment of platelet dense granule trafficking, P2Y1/P2Y12, and protease-activated receptors interactions in neonates utilizing whole blood, small volume assays. *Biomedical Engineering Society*. Phoenix, USA. Oct 2017. [Oral Presentation]

7. McCarty OJT, Aslan JE, Babur O, Buchanan A, **Ngo AT**, Pang J, Rigg R, Mitrugno A, David L, Demir E. Pathway analysis reveals a p38 MAP kinase-MAPKAPK2/Nogo axis regulating intracellular calcium dynamics in procoagulant platelets. *Biomedical Engineering Society*. Phoenix, USA. Oct 2017. [Oral Presentation]

8. **Ngo AT**, Thierheimer MLD, Babur O, Rocheleau AD, Huang T, Rigg RA, Mitrugno A, Burchard J, Nan X, Demir E, McCarty OJT, Aslan JE. A spatial system approach to indentifying roles for the Rho-specific guanine nucleotide dissociation inhibitor (RhoGDI)

LyGDI in platelet function. *International Society on Thrombosis and Haemostasis*. Berlin, Germany. Jul 2017. [Poster]

9. **Ngo AT**, Thierheimer ML, Pang J, Babur O, Rocheleau AD, Rigg RA, Mitrugno A, Huang T, Nan X, Burchard J, Demir E, McCarty OJ, Aslan JE. Identification of roles for the Rho-specific guanine nucleotide dissociation inhibitor (RhoGDI) Ly-GDI in platelet function. *Arterioslerosis, Thrombosis, and Vascular Biology*. Minnesota, USA. May 2017. [Poster]

10. **Ngo AT**, Celebic A, Quackenbush A, Cowin B, DuPriest E, Bagby SP. Is Reduced Adiponectin mRNA Associated with Alterations in Transcription Factor ATF3 in Adipose Tissue of Nutritionally Programmed Microswine Offspring? *Annual Murdock College Science Research Conference*. Washington, USA. Nov 2014. [Oral Presentation]

Invited Lectures

1. Lecturer. Program in Molecular and Cellular Bioscience Journal Club 606. Oregon Health & Science University. Fall 2018.

2. Lecturer. Biomedical Engineering Course 608 - Grant Writing. Oregon Health & Science University. 2018-2020.

3. Lecturer. Murdock Scholar Undergraduate Research Program – Applying to graduate school. Oregon Health & Science University. 2017-2019.

4. Lecturer. *The role of platelets in hemostasis and thrombosis*. Warner Pacific College, Portland, OR. Spring 2016.

Research Mentees

1. Zhoe T. Rub (2017-2018): currently a first-year medical student at Chicago Medical School, Chicago, IL.

2. Kendra R. Jones (2017-2018): currently a M.S. student in Bioengineering at the University of Colorado Denver, Denver, CO.

3. Anna-Liisa I. Sepp (2017-2018): currently a first year M.S/Ph.D. student at Columbia University, New York, NY.

4. Tiffany T. Chu (2016-2017): currently a first-year graduate student at Johns Hopkins University, Baltimore, MD in Chemical & Biomolecular Engineering.

5. Marisa L.D. Thierheimer (2016-2017): currently a research associate at Gilead Sciences, Foster City, CA.